Title
Elucidating the Post-Endocytic Sorting Mechanism of the Beta-2 Adrenergic Receptor

Author
Temkin, Paul

Publication Date
2011

Peer reviewed|Thesis/dissertation

Elucidating the Post-Endocytic Sorting Mechanism of the Beta-2 Adrenergic Receptor

by

Paul Temkin

DISSERTATION

Submitted in partial satisfaction of the requirements for the degree of

DOCTOR OF PHILOSOPHY

in

Cell Biology

in the

GRADUATE DIVISION

of the

UNIVERSITY OF CALIFORNIA, SAN FRANCISCO

[redacted]

Dedication and Acknowledgements

The text of this dissertation includes a reprint of the following articles: “SNX27 mediates PDZ-directed sorting from endosomes to the plasma membrane” (JCB 190(4) 2010), “Sequence-dependent sorting of recycling proteins by actin-stabilized endosomal microdomains” (Cell 143(5) 2010) and “SNX27 mediates retromer tubule entry and endosome-to-plasma membrane trafficking of signalling receptors” (NCB 13(6) 2011).

The coauthor Mark von Zastrow directed and supervised the research that forms the basis for the dissertation. P. Temkin provided the experimentation and manuscript preparation of the greater majority of the following dissertation, which constitutes a substantial and comparable contribution to that of other dissertations in the greater Pharmacology and Cell Biology fields. Collaborative contributions from others are specified on the title pages of the relevant chapters.

- Mark von Zastrow, M.D., Ph.D.

As a graduate student, it should not be surprising that in my 6 years in San Francisco I’ve spent the majority of my time in the von Zastrow lab. I would like to thank all the members of the Z-lab past and present for making work feel like a home and not an island prison (For all my days in San Francisco I still have not gone to Alcatraz). I will remember fondly all the good times that we had together at “work”. There is not a bad egg amongst the group of Aaron Marley, Joy Yu, Ben Lauffer, Elaine Lau, James

Hislop, Michael Tanowitz, Sarah Kotowski, Anastasia Henry, Minjong Park, Jin Tomshine, Guillermo Yudowski, Manoj Puthenveedu, Vu Dang, Peter Hein, Alison Leaf, Kate Varandas, and Roshanak Irannejad. Each one of these people has inspired me in different ways. In particular, I need to thank James Hislop for the scientific mentorship he provided. My long term bay-mates Sarah Kotowski, Anastasia Henry, and Guillermo Yudowski helped make a "fun"ctional work environment and gave constant friendship throughout the successes and failures.

Dr. Mark von Zastrow set the tone for this excellent lab. His scientific excitement and broad interests made working for him intellectually stimulating. In addition to being an excitable scientist, Mark is an excellent guy, whose passion for the wellbeing of his lab-members was only be surpassed by his passion for pizza. I thank him for giving me the freedom to explore science while providing me enough support to prevent me from falling into the abyss.

I had first-rate scientific mentorship and partnerships from people outside our lab throughout graduate school. I thank my committee members Keith Mostov and Jonathan Weissman for their insights on my project. Each of my various colaborators has taught me a great deal about the enterprise of science. In particular I thank Andrew Krutchinksy, Nevan Krogan, Cristina Melero, and Peter Capraro for their insights and collaboration. Lastly, I thank Henry Bourne who taught me so much about writing while providing uniquely brilliant and often salacious insight.

Throughout graduate school I had an excellent network of friends and family whom I can't thank enough for their support. I would like to thank all the members of

the UCSF community who made it a pleasure to live, play, and occasionally work in beautiful San Francisco. My classmates have been foremost in this group, leading inspiring lives that include travel as well as high impact publications. In particular I need to thank Mike "the king bolete" Nehil and Andrew "Kramer" Houk for their friendship throughout grad school. I met many great people through soccer, and I thank members of Sciencaurus Rex, Pecan Sandies, Casual Encounters, Troll Toll, Agency, Silent F, 1st years, etc. for their friendship. I also thank people from Peace Corps Ghana, whom readjusted to life in the US with me.

My family has always provided me with a nurturing environment, in which I could succeed. I thank my mom, Nancy Temkin, for the support she has given and for being an understanding ear, as she too is an academic. Her husband Peter Hendrickson and his family have been welcome additions to the family, as well as pleasant distractions from science. My brother Elliott has been with me through most of this graduate endeavor. It has been a pleasure living with him in San Francisco, as a Temkin annex. He provides a constant energy and excitement for life that can't be suppressed, though it can be slowed to the point where he falls asleep at the bar.

Perhaps one of my greatest pleasures in graduate school has been developing a relationship with Manisha Ray. She has been a constant commiserator throughout this journey. Graduate school wouldn't have been nearly as much fun without her. I look forward to seeing our relationship continue to grow.

Finally, I dedicate this dissertation to my father, Richard Temkin, who passed away too soon.

Abstract

Elucidating the Post-Endocytic Sorting Mechanism of the Beta-2 Adrenergic Receptor

by

Paul Temkin

This thesis addresses the endosomal sorting of the β_2 adrenergic receptor (B2AR), a "typical" (family A) member of the large superfamily of seven-transmembrane signaling receptors, the G-protein coupled receptors (GPCRs). The introductory chapter provides background on the general importance of sorting in the cell, how sorting affects signaling receptors, models for protein sorting, a primer on sequence based sorting, and a brief explanation of the scientific approach I took in my thesis work. The 2nd chapter details findings on the role of ubiquitin and the ESCRT machinery in sorting of B2AR. We find that direct receptor ubiquitination plays no role in endosomal sorting of B2AR to the lysosome. Chapter 3 explores the role of actin in maintaining a subset of endosomal tubules which are important for B2AR recycling. In chapter 4, a direct interactor of the B2AR sorting sequence, SNX27, is identified and its role in recycling of B2AR is chronicled. Chapter 5 introduces the retromer complex as the endosomal sorting location for B2AR. Further, it elucidates the connectivity of SNX27 to the retromer and demonstrates a role for SNX27 in receptor entry into the retromer tubule. Lastly, Chapter 6 explores the results presented in the previous chapters, attempts to reconcile them with the "big picture," and suggests avenues for future study.

Table of contents

List of Tables

Chapter 5

Appendices

List of Figures

Chapter 1

Chapter 2

Chapter 3

Chapter 4

Chapter 6

Chapter 1:

Introduction

1.1 Overview

This thesis addresses the endosomal sorting of the β_2 adrenergic receptor (B2AR), a "typical" (family A) member of the large superfamily of seven-transmembrane signaling receptors, the G-protein coupled receptors (GPCRs). The introduction chapter provides background on the general importance of sorting in the cell, how sorting affects signaling receptors, models for protein sorting, a primer on sequence based sorting, and a brief explanation of the scientific approach I took in my thesis work. The 2nd chapter details findings on the role of ubiquitin and the ESCRT machinery in sorting of B2AR. Chapter 3 explores the role of actin in maintaining a subset of endosomal tubules which are important for B2AR recycling. In chapter 4, a direct interactor of the B2AR sorting sequence, SNX27, is identified and its role in recycling of B2AR is chronicled. Chapter 5 introduces the retromer complex as the endosomal sorting location for B2AR. Further, it elucidates the connectivity of SNX27 to the retromer and demonstrates a role for SNX27 in receptor entry into the retromer tubule. Lastly, Chapter 6 explores the results presented in the previous chapters, attempts to reconcile them with the "big picture," and suggests avenues for future study.

1.2 The importance of cargo sorting

A couple of haiku to wet the reader's appetite…ENJOY!

membranes of the cell *organelle's proteins*

have unique composition… *defining identity…*

lone identity *functionality*

The cell is a complicated place. Tightly packed membrane-bound organelle allow for a cadre of processes to occur in relative isolation. Each membrane bound packet is capable of supporting a different microenvironment, suitable to the processes of that organelle. For example, the lysosome must be maintained at a low pH in order for the degradative enzymes, which define the organelle function, to be active. Alternatively, the pH of the early endosome, which also serves as a way station for these destructive enzymes, must be high enough to prevent enzymatic activity, less this hidden destructive capacity detract from its function as a sorting station.

Organelle composition can differ in many ways. For example, varying ion and small molecule concentrations allows for the activity of enzymes to be controlled in different compartments. These differences, and many others, are determined by the composition of specific membrane proteins present in particular organelles. Accordingly, membrane protein composition si thought to be a primary determinant of organelle identity. Perturbing this biochemical organization can destroy organelle identity and lead to pathological dysfunction. An example is Dent's disease, where mutations in the chloride channel CLC-5 prevent endosome acidification. This in turn prevents proper endosomal

trafficking of low-molecular weight protein, manifesting as proteinuria when the kidney cannot reabsorb protein properly (Devuyst 2004). In order to maintain function of the cell and organism, organelle identity must be maintained.

Lipid composition also plays a key role in defining an organelle. However, protein and lipid composition are intertwined in such a complex manner that it is hard to say which controls the other. Proteins are needed to produce or modify many of the lipids that are required to identify cellular compartments. One lipid that is modified to define organelle identity is phosphatidylinositol (PI). The cell utilizes a host of inositol kinases and phosphatases to control the phosphorylation state at distinct positions of the inositol head group. Differentially phosphorylated forms of PI can be recognized by protein domains, such as the phox homology (PX), pleckstrin homology (PH), and FYVE domains. Proteins containing these domains are then recruited to the membrane and can, in turn, recruit or regulate various lipid-modifying enzymes. Thus, whether one focuses on the role of proteins in specifying the lipid environment, or lipids in determining the protein environment, protein localization is an essential determinant of organelle identity. In essence, proteins do the work that define the organelle.

Most organelles (with mitochondria and endoplasmic reticulum being partial exceptions) do not produce their own proteins. Instead they rely on proteins that are produced and modified elsewhere. Protein sorting is required to insure that these proteins arrive at the intended destination. Aberrant localization of key proteins to the wrong organelle results in an organelle that either contains components that don't belong there (new function) or an organelles that is missing components (loss of function). Both of

these scenarios can be deleterious to the cell and can have drastic consequences for the whole organism.

1.3 An overview of GPCR signaling and sorting

Protein sorting not only plays a key role in establishing organelle identity but serves critical functions in adaptive cellular responses. This is particularly evident in the regulation of receptor-mediated signal transduction. Studies of the epidermal growth factor (EGF) receptor tyrosine kinase provided an early example, of receptor endocytosis and trafficking to lysosomes, as a means for achieving adaptive down-regulation of signaling (Babst, Odorizzi et al. 2000; Gruenberg and Stenmark 2004; Grandal and Madshus 2008). My thesis work has focused on the membrane trafficking of seven transmembrane signaling receptors, which are traditionally called GPCRs.

GPCRs comprise the largest and most versatile class of signaling receptors, with approximately 800 distinct receptors accounting for 2% of the human coding genome. Characteristic of this class of signaling receptors include a conserved 7 transmembrane structure and, in general, the ability to couple to intracellular G-proteins. As signaling receptors, their primary role is to transduce signal from the extracellular milieu across the membrane and initiate intercellular signaling cascades. As a result of this, GPCRs play integral roles in many physiologically essential processes such as smell, taste, vision, and regulating heart rate. Due to the essential role of these receptors, manipulating GPCR signaling pathways through specific agonists and antagonists has been a cornerstone of the pharmaceutical industry. Indeed, compounds that stimulate or suppress GPCR signaling represent 40-50% of drugs currently sold for clinical use, and perhaps a greater fraction of those used illicitly for recreational purposes (Allen and Roth 2011).

The vast majority of GPCRs are activated by extracellular ligands. This requires them to be present in the plasma membrane in order to initiate an appropriate cellular signaling response. Several human diseases result from GPCR mutations that prevent proper surface localization (Castro-Fernandez, Maya-Nunez et al. 2005). GPCRs are remarkable for the specificity and diversity of stimuli that activate them. While some GPCRs are activated other means, such as by absorption of light or by specific proteolytic cleavage, receptor activation is typically mediated by similar conformational changes in the GPCR. These conformational changes result in shifting of transmembrane domains to reveal intracellular guanine-nucleotide exchange factor (GEF) activity of the GPCR (Rosenbaum, Rasmussen et al. 2009; Rasmussen, Devree et al. 2011). This GEF activity promotes dissociation of guanosine diphosphate (GDP) bound to the α subunit of the receptor-coupled heterotrimeric G-protein and replacement of this nucleotide with guanosine triphosphate (GTP) that is present in excess in the cytoplasm. The GTP bound form of Gα has lower affinity for receptor and the Gβγ subcomplex. These G-proteins go on to initiate signaling cascades while the receptor is then free to catalyze the activation of further G-proteins (reviewed (Oldham and Hamm 2008)).

Different GPCRs couple to distinct heterotrimeric G-proteins, though they are often a bit promiscuous. There are 21 different Gα, 6 Gβ and 5 Gγ produced in humans (Downes and Gautam 1999). This complexity results in receptor and tissue specific signaling outcomes. Gα breaks down roughly into 4 categories. Two classes of Gα regulate cyclic adenosine monophosphate formation (cAMP) by activating or suppressing the function of adenylyl cyclase enzymes; Gαs/olf-type subunits generally activate adenylyl cyclase increasing cellular cAMP while Gαi/o-type subunits inhibit it, lowering cellular cAMP

concentrations. Gαq/11-type subunits generally activate phospholipase C-β, which cleaves phosphatidylinositol 4,5-biphosphate (PIP2) into inositol (1,4,5) trisphosphate (IP3) and diacylglycerol (DAG). IP3 acts at the the endoplasmic reticulum (ER) to release Ca^{2+} from the ER, while DAG diffuses along the plasma membrane activating Protein Kinase C (PKC). Lastly the $G\alpha_{12/13}$ class can activate small GTPases involved in cytoskeletal remodeling. The use of second messengers in GPCR signaling (cAMP, DAG, IP3, Ca^{2+}) allows GPCRs to initiate a plethora of other cascades leading to complex signaling outputs that are easily integrated with other signaling pathways. At the same time, Gβ/γ subcomplexes liberated by GPT binding to the Gα subunit can mediate other signaling actionsm such as activating GIRK type potassium channels or inhibiting voltage-gated calcium channels.

This GPCR induced signaling continues until the GPCR is shut-off and the heterotrimeric G-protein is returned to its inactive GDP bound state. Though the Gα has intrinsic GTPase activity, it is greatly sped up by regulator of G-protein signaling (RGS) molecules which act as GTPase activating proteins (GAPs). While GPCRs can be effectively shut down pharmacologically by addition of an antagonist that competes for agonist binding, or of an inverse agonist which stabilizes the inactive form of the receptor, there is also active cellular machinery controlling physiological signal termination. One mechanism involves G-protein receptor kinases (GRKs) recruited to the active GPCR phosphorylating serine and threonine residues on the receptor's cytoplasmic surface. Classically, these phosphorylation events are thought to terminate signaling in two ways. First, phosphorylation of receptors inhibits binding of the heterotrimeric G-protein, preventing further GTP exchange. Secondly, phosphorylation

promotes recruitment of β-arrestins that function as regulated endocytic adaptor proteins. They stimulate clathrin-coated pit-mediated removal of the receptor from the cell surface through interaction with clathrin and the clathrin-associated adaptor protein AP2.

Clathrin-mediated endocytosis of the signaling receptor can control signaling sensitivity and duration (Grandal and Madshus 2008; Hanyaloglu and von Zastrow 2008), and can modify signal selectivity between distinct effectors (Sorkin and Goh 2009). Once in the endosome it is traditionally believed the receptor is separated from agonist and the effectors of its signaling pathways. Therefore, it is generally believed that endocytosed receptor does not utilize the canonical G-protein mediated signaling pathway. Recent evidence suggests that in addition to these signal-terminating activities, arrestins can initiate distinct (G-protein independent) signaling. Some form(s) of signaling can occur from internalized receptors. However, specific mechanisms of GPCR signaling from such endosomal receptors are still not clear (Purvanov, Koval et al. 2010; Feinstein, Wehbi et al. 2011; Hupalowska and Miaczynska 2011).

Once the cell has internalized the GPCR, it is generally considered desensitized with regard to G-protein signaling because subsequent addition of ligand is unable to stimulate as robust of a response. This is due to the decreased number of functional surface receptors. Internalized receptors can either be recycled to the plasma membrane, effectively "resensitizing" the cell, or shunted to the lysosome for degradation, resulting in long term attenuation of the cellular response akin to down regulation of the EGF receptor (reviewed (Hanyaloglu and von Zastrow 2008)). These sorting fates thus result in effectively opposite effects on cellular responsiveness. Different GPCR family members have distinct post-endocytic sorting fates, even when co-expressed in the same

cells and delivered to the same early endosomes (Tsao and von Zastrow 2000; Puthenveedu, Lauffer et al. 2010). It is this critical sorting decision that is the primary focus of my thesis. In particular, I studied the endosomal sorting of B2AR, focusing on receptor trafficking through the recycling pathway. I chose this poorly understood pathway because it represents a regulable and physiologically important sorting process (Cao, Deacon et al. 1999).

The human B2AR, is an extensively characterized mammalian GPCR that is generally considered prototypic of this large receptor family (Lefkowitz, Pitcher et al. 1998). The B2AR possesses a C-terminal PDZ ligand that is required for rapid and efficient recycling of receptors after regulated endocytosis (Cao, Deacon et al. 1999). B2AR recycling is essential for sustained functional signaling, and signaling selectivity, in response to catecholamines (Pippig, Andexinger et al. 1995; Lefkowitz, Pitcher et al. 1998; Ferguson 2001; Hanyaloglu, McCullagh et al. 2005; Wang, Lauffer et al. 2007). B2AR signaling is important to a wide variety of physiological processes, including the regulation of smooth muscle contraction and control of cardiac function (Brodde, Bruck et al. 2006). Accordingly, drugs that affect B2AR signaling are mainstays in the treatment of important pathological conditions such as asthma and heart disease (Bond, Spina et al. 2007). Therefore, elucidating the cell biological principles underlying regulation of signaling receptors, such as the B2AR, has widespread physiological and therapeutic significance.

1.4 Models for protein sorting at the endosome

Early studies of endocytosis recognized that, based on conservation of mass, the majority of the internalized membrane components must have the ability to efficiently recycle (Steinman, Brodie et al. 1976; Pearse and Bretscher 1981). Classic studies from the Maxfield group established a "geometric" model of sorting (also called the bulk flow model), which serves as a useful starting point for understanding endosomal sorting (reviewed (Maxfield and McGraw 2004)). The geometric model emerged from a study that indicated efficient separation of transmembrane nutrient receptor and soluble nutrients can happen at the endosome (Dunn, McGraw et al. 1989). In general, internalized nutrient must stay in the endosome to be delivered to the lysosome while the receptor returns to the plasma membrane in order to mediate additional rounds of nutrient uptake (Dunn and Maxfield 1992). Internalized transferrin, the iron binding protein that remains associated in the endocytic pathway with the transferrin receptor, releases its bound iron into the acidic environment of the endosome lumen and then recycles. Importantly, Maxfield's group found that internalized transferrin returned from the endosome to the surface at a similar rate to a "bulk" lipid marker. This suggested that bulk flow of membranes to the surface could provide a default recycling pathway for transmembrane receptors (Mayor, Presley et al. 1993). Dunn and Maxfield reasoned that thin tubules formed on the endosome would allow for simple partitioning to occur. These tubules, with a low volume to surface area, could maintain soluble cargo in the lumen while allowing transmembrane receptors to be selectively recycled from the tubule. Recycling of transmembrane receptors to the plasma membrane from the endosome would just be a matter of flowing with the membrane, which needs to be moving back to

the plasma membrane to maintain membrane homeostasis. While this model is capable of explaining a great deal, a major problem with it was that it could not explain why some transmembrane receptors do not efficiently recycle.

One clue to this question was the finding that transferrin receptors fail to recycle efficiently by "bulk flow" when cross-linked by sufficiently large transferrin oligomers (Marsh, Leopold et al. 1995). These oligomerized receptors appeared to be delayed in the recycling endosome, and were not delivered to lysosomes as efficiently as luminal cargo such as low density lipoprotein. This suggests that receptor oligomers may be sterically hindered from traversing the recycling pathway, and that ere might also be steric or size constraints on subsequent traffic to lysosomes.

Another clue was that not all lipids recycle efficiently after endocytosis, as modifying lipid tail lengths biases transport of endocytosed phospholipid analogues between recycling and lysosomal pathways (Mukherjee, Soe et al. 1999). Subsequent work in this area has suggested that proteins segregate with different lipids contributing to lateral segregation in the endosome membrane and differential trafficking after endocytosis (Chatterjee, Smith et al. 2001; Ceppi, Colombo et al. 2005; Sharpe, Stevens et al. 2010; Parton, Klingelhoefer et al. 2011). While biophysical properties such as transmembrane length, size, or hydrophobicity likely play roles in physiological sorting the bulk of recent research has been directed at protein-protein interactions which could prevent receptors from recycling by sorting them into the lysosomal pathway. These protein interaction based models of sorting are perhaps preferred because they allow the cell the possibility of regulating the recycling and degradative processes. Further, there is growing evidence that protein-protein interactions can alter the sorting decisions of cargo at the endosome.

For several GPCRs, non-covalent interaction with a family of cytoplasmic GPCR associating proteins (GASPs) promote sorting to lysosomes (Heydorn, Sondergaard et al. 2004; Moser, Kargl et al. 2010). Depletion of the founding member of this family, GASP1 (or GPRASP1) decreased lysosomal degradation and increased recycling of the delta opioid receptor. Similar effects have observed for several other GASP interacting GPCRs, both in cultured cells and in vivo (Martini, Waldhoer et al. 2007; Martini, Thompson et al. 2010; Thompson, Martini et al. 2010; Tschische, Moser et al. 2010; Thompson and Whistler 2011). GASP1 may have other cellular effects and it remains poorly understood how it influences receptor traffic in the endocytic pathway. For certain other GPCRs, such as PAR1 protease activated receptor, non-covalent interaction of receptors with sorting nexin 1 (SNX1) is proposed to promote endocytic trafficking to lysosomes (Wang, Zhou et al. 2002; Gullapalli, Wolfe et al. 2006). SNX1 can interact with the ESCRT0 component HRS, discussed later as a piece of lysosomal sorting machinery, but it is not known if this interaction is necessary for the lysosomal sorting of PAR1 (Chin, Raynor et al. 2001). For a number of other GPCRs, such as the CXRC4 chemokine receptor, sorting to lysosomes is thought to be induced by ubiquitination, a covalent modification which promotes the receptors interaction with the endosomal sorting complex required for transport (ESCRT). The ESCRT machinery has been carefully dissected, and its function is now thought to be well understood (Raiborg and Stenmark 2009; Wollert, Yang et al. 2009; Hurley 2010; Roxrud, Stenmark et al. 2010).

In its simplest form, the ESCRT hypothesis explains how transmembrane cargo can act like the soluble cargo (nutrients) mentioned before in the geometric sorting hypothesis. The ESCRT machinery was initially identified largely from studies of

budding yeast focused on vacuolar morphology, establishing a list of vacuolar protein sorting (VPS) mutants which contains most ESCRT components (Bryant and Stevens 1998). These yeast genes have proven to be largely conserved in mammalian cells and many play a role in generating multivesicular bodies (MVBs), a key endocytic intermediate to lysosomes. Other studies in yeast, showed that ubiquitination of cargo was required and sufficient for vacuolar localization after receptor internalization (Bankaitis, Johnson et al. 1986; Robinson, Klionsky et al. 1988; Rothman, Howald et al. 1989; Hicke 2001; Urbanowski and Piper 2001). Several VPS proteins were found to contain ubiquitin interaction motifs (UIM) and shown to be involved in the sorting of ubiquitinated cargo to the vacuole. Structural and biophysical studies have since given us great insight into how ESCRT components interact and sort ubiquitinated cargo. In general the ESCRT machinery is divided into four subcomplexes. In mammalian cells, the ESCRT-0 subcomplex binds to a clathrin associated domain on the endosome limiting membrane and UIMs on this complex bind ubiquitinated cargo. ESCRT subcomplexes I and II are then recruited to ESCRT-0. These subcomplexes aid in the cargo entrapment (more UIM) and promote inward deformation of the membrane. ESCRTIII is then thought to mediate scission of the inwardly budded membrane, trapping cargo in intraluminal vesicles (ILVs). Formation of the ILVs provide the defining morphological characteristic of MVB. Once the cargo is involuted it essentially acts as soluble cargo and the MVB can mature into a lysosome where cargo is degraded (Williams and Urbe 2007; Raiborg and Stenmark 2009; Hurley 2010; Roxrud, Stenmark et al. 2010).

While the ESCRT hypothesis provides elegant explanation for how certain transmembrane cargo are directed to the lysosomes, it is increasingly clear that this view

is insufficient to explain critical aspects of regulated endocytic trafficking of mammalian GPCRs. In particular, and as discussed further below, there is clear evidence for the existence of distinct sorting machinery that directs recycling of some cargo to the plasma membrane (Tanowitz and Von Zastrow 2002; Hislop, Marley et al. 2004; Hanyaloglu and von Zastrow 2008).

1.5 Sequence-directed protein sorting in the recycling pathway

The hypothesis of default recycling has been recognized for many years to be insufficient to explain the endocytic trafficking of membrane proteins in polarized epithelial cells (Mellman 1996). There is now a substantial body of work indicating that the default hypothesis is also insufficient to explain endocytic trafficking of various signaling receptors in nonpolarized cells. In particular, a number of sequences have been found in the C-terminal tails of particular GPCRs, which are both essential and sufficient to promote endosome to plasma-membrane recycling (Hanyaloglu and von Zastrow 2008). The first reported example of this type of "recycling sequence" was a consensus (type I) PDZ motif present in the distal C-terminal tail of the B2AR (Cao, Deacon et al. 1999). Disrupting this motif inhibits receptor recycling and promotes receptor trafficking to the lysosome, thus profoundly changing the regulated trafficking itinerary. This indicates that there is likely a protein machine necessary to bring these receptors from the endosome to the plasma membrane. In this developing field, defining interaction partners for these sequences and the endosomal machinery needed to bring receptors back to the plasma membrane is paramount to understanding the sorting process of these receptors.

While β_1 adrenergic receptor (B1AR) and B2AR have been found to have c-terminal PDZ-motifs, ESKV and DSLL respectively, the μ opiod receptor (MOR) has a distinct non-PDZ sequence of LENLEAE (Cao, Deacon et al. 1999; Gage, Kim et al. 2001; Tanowitz and von Zastrow 2003; Gage, Matveeva et al. 2005). Other receptors have even more divergent recycling sequences (Krishnamurthy, Kishi et al. 2003; Huang,

Steplock et al. 2004; Vargas and Von Zastrow 2004; Lahuna, Quellari et al. 2005). Approximately 100 other GPCRs, and scores of other transmembrane proteins, also have c-terminal PDZ ligands, making it possible that any PDZ mediated mechanism of receptor recycling may serve a large number of cargo. For this reason I chose to study the PDZ-motif mediated recycling process. At the time I started my thesis, trans-acting interaction partners for these known PDZ motifs had been found, but there was no evidence that these interaction partners had function at the endosome in the recycling process. Furthermore the different PDZ motifs had yielded different interaction partners, pointing to no common mechanism. These interaction partners were identified by column chromatography, using the isolated recycling sequence as bait against whole cell lysate. Perhaps because of the intermixing of spatially separated proteins, the interactors isolated by this means have failed to prove useful in elucidating the recycling mechanism of these receptors.

1.6 Approaches taken to identify endosomal sorting machinery

One of my initial attempts to identify the endosomal sorting machinery for B2AR recycling was through a pull down and mass spectrometry approach. I sought to improve on previously used methods for exploring binding partners of the PDZ ligand by using the whole receptor as bait and by isolating it from purified endosomes. By not adding detergent until I had purified endosomes I hoped to get rid of strong binding contaminant molecules which may displace the actual endosomal sorting machinery and to enrich the percent of receptors I am looking at that were actively in the sorting process. The purification scheme I used is depicted below (Figure 1), and the complete protocol is available in Appendices A-C (modified from (Li, Stolz et al. 2005; Cottrell, Padilla et al. 2009)). Upon purifying endosomes and receptors from endosomes, I used the modular mass spectrometry system set up by Dr. Andrew Krutchinsky to determine co-purifying proteins (Blethrow, Tang et al. 2007). The lists of proteins identified and detergent conditions are available in appendices D and E.

FIGURE 1: Receptor Purification Scheme

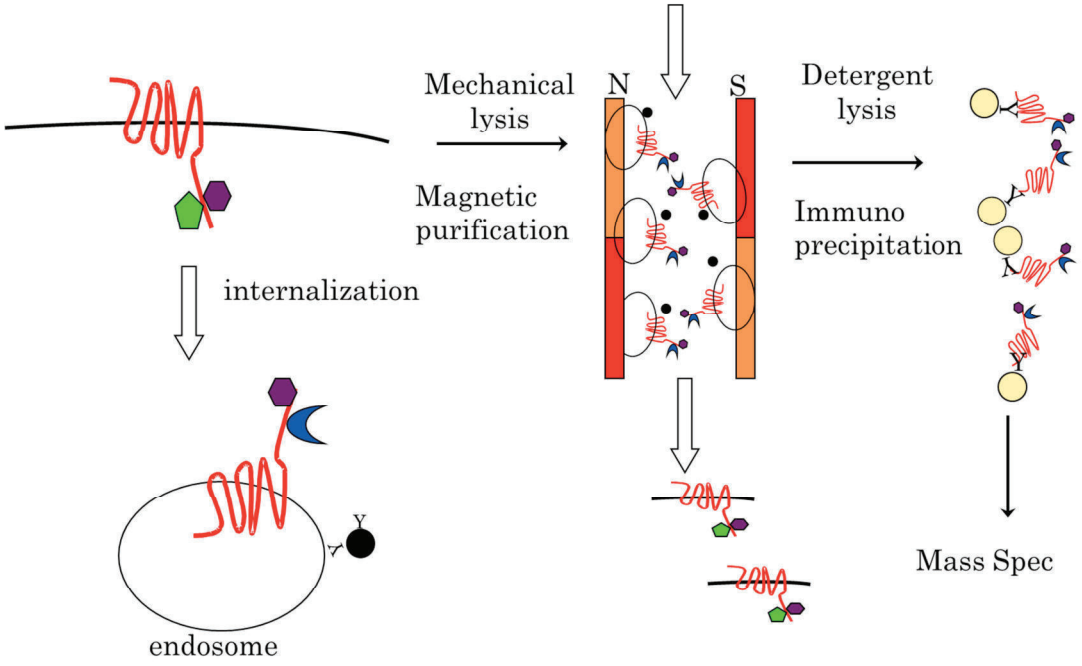

While this unbiased approach was ultimately unsuccessful at lending insight into the sorting mechanism, several candidate based approaches were successful. In one project we interrogated the ESCRT model for sorting as applied to the B2AR, making manipulations to this defined sorting machine. This data is presented in Chapter 2. A second candidate based screen investigated the role of sorting nexins in the trafficking of B2AR. Sorting nexins were chosen because their PX lipid binding motifs are believed to localize many of them to the endosome. Further, a growing literature suggests many of them are involved in protein sorting. This siRNA screen is present in Appendix?. One hit from this screen, SNX27, led to the publication presented in Chapter 4. Several other sorting nexins also had significant effects on B2AR trafficking and likely could be

followed up on as components of the B2AR specific or possibly general sorting machinery.

Visual methods for studying receptor recycling have been useful for establishing compartmental localization and trafficking kinetics but, until recently, have not been useful for looking at organelle domains (to name a few (Dunn, McGraw et al. 1989; Dunn and Maxfield 1992; Ghosh, Gelman et al. 1994; Marsh, Leopold et al. 1995)). Improvements in optical sectioning (z-resolution) and acquisition speed in fluorescence imaging have made it possible to take a closer look at endosomal sorting then was previously possible. Using spinning disk microscopy on living cells I sought to determine the point on the endosome at which the sorting sequence acts, and to identify sorting molecules present at this point. This approach primarily drove the advances reported in Chapters 3 and 5.

1.7 References

Allen, J. A. and B. L. Roth (2011). "Strategies to discover unexpected targets for drugs active at G protein-coupled receptors." Annu Rev Pharmacol Toxicol 51: 117-44.

Babst, M., G. Odorizzi, et al. (2000). "Mammalian tumor susceptibility gene 101 (TSG101) and the yeast homologue, Vps23p, both function in late endosomal trafficking." Traffic 1(3): 248-58.

Bankaitis, V. A., L. M. Johnson, et al. (1986). "Isolation of yeast mutants defective in protein targeting to the vacuole." Proc Natl Acad Sci U S A 83(23): 9075-9.

Blethrow, J. D., C. Tang, et al. (2007). "Modular mass spectrometric tool for analysis of composition and phosphorylation of protein complexes." PLoS One 2(4): e358.

Bond, R. A., D. Spina, et al. (2007). "Getting to the heart of asthma: can "beta blockers" be useful to treat asthma?" Pharmacol Ther 115(3): 360-74.

Brodde, O. E., H. Bruck, et al. (2006). "Cardiac adrenoceptors: physiological and pathophysiological relevance." J Pharmacol Sci 100(5): 323-37.

Bryant, N. J. and T. H. Stevens (1998). "Vacuole biogenesis in Saccharomyces cerevisiae: protein transport pathways to the yeast vacuole." Microbiol Mol Biol Rev 62(1): 230-47.

Cao, T. T., H. W. Deacon, et al. (1999). "A kinase-regulated PDZ-domain interaction controls endocytic sorting of the beta2-adrenergic receptor." Nature 401(6750): 286-90.

Castro-Fernandez, C., G. Maya-Nunez, et al. (2005). "Beyond the signal sequence: protein routing in health and disease." Endocr Rev 26(4): 479-503.

Ceppi, P., S. Colombo, et al. (2005). "Two tail-anchored protein variants, differing in transmembrane domain length and intracellular sorting, interact differently with lipids." Proc Natl Acad Sci U S A 102(45): 16269-74.

Chatterjee, S., E. R. Smith, et al. (2001). "GPI anchoring leads to sphingolipid-dependent retention of endocytosed proteins in the recycling endosomal compartment." Embo J 20(7): 1583-92.

Chin, L. S., M. C. Raynor, et al. (2001). "Hrs interacts with sorting nexin 1 and regulates degradation of epidermal growth factor receptor." J Biol Chem 276(10): 7069-78.

Cottrell, G. S., B. E. Padilla, et al. (2009). "Endosomal endothelin-converting enzyme-1: a regulator of beta-arrestin-dependent ERK signaling." J Biol Chem 284(33): 22411-25.

Devuyst, O. (2004). "Chloride channels and endocytosis: new insights from Dent's disease and CLC-5 knockout mice." Bull Mem Acad R Med Belg 159(Pt 2): 212-7.

Downes, G. B. and N. Gautam (1999). "The G protein subunit gene families." Genomics 62(3): 544-52.

Dunn, K. W. and F. R. Maxfield (1992). "Delivery of ligands from sorting endosomes to late endosomes occurs by maturation of sorting endosomes." J Cell Biol 117(2): 301-10.

Dunn, K. W., T. E. McGraw, et al. (1989). "Iterative fractionation of recycling receptors from lysosomally destined ligands in an early sorting endosome." J Cell Biol 109(6 Pt 2): 3303-14.

Feinstein, T. N., V. L. Wehbi, et al. (2011). "Retromer terminates the generation of cAMP by internalized PTH receptors." Nat Chem Biol 7(5): 278-84.

Ferguson, S. S. (2001). "Evolving concepts in G protein-coupled receptor endocytosis: the role in receptor desensitization and signaling." Pharmacol Rev 53(1): 1-24.

Gage, R. M., K. A. Kim, et al. (2001). "A transplantable sorting signal that is sufficient to mediate rapid recycling of G protein-coupled receptors." J Biol Chem 276(48): 44712-20.

Gage, R. M., E. A. Matveeva, et al. (2005). "Type I PDZ ligands are sufficient to promote rapid recycling of G Protein-coupled receptors independent of binding to N-ethylmaleimide-sensitive factor." J Biol Chem 280(5): 3305-13.

Ghosh, R. N., D. L. Gelman, et al. (1994). "Quantification of low density lipoprotein and transferrin endocytic sorting HEp2 cells using confocal microscopy." J Cell Sci 107 (Pt 8): 2177-89.

Grandal, M. V. and I. H. Madshus (2008). "Epidermal growth factor receptor and cancer: control of oncogenic signalling by endocytosis." J Cell Mol Med 12(5A): 1527-34.

Gruenberg, J. and H. Stenmark (2004). "The biogenesis of multivesicular endosomes." Nat Rev Mol Cell Biol 5(4): 317-23.

Gullapalli, A., B. L. Wolfe, et al. (2006). "An essential role for SNX1 in lysosomal sorting of protease-activated receptor-1: evidence for retromer-, Hrs-, and Tsg101-independent functions of sorting nexins." Mol Biol Cell 17(3): 1228-38.

Hanyaloglu, A. C., E. McCullagh, et al. (2005). "Essential role of Hrs in a recycling mechanism mediating functional resensitization of cell signaling." Embo J 24(13): 2265-83.

Hanyaloglu, A. C. and M. von Zastrow (2008). "Regulation of GPCRs by endocytic membrane trafficking and its potential implications." Annu Rev Pharmacol Toxicol 48: 537-68.

Heydorn, A., B. P. Sondergaard, et al. (2004). "A library of 7TM receptor C-terminal tails. Interactions with the proposed post-endocytic sorting proteins ERM-binding phosphoprotein 50 (EBP50), N-ethylmaleimide-sensitive factor (NSF), sorting nexin 1

(SNX1), and G protein-coupled receptor-associated sorting protein (GASP)." J Biol Chem 279(52): 54291-303.

Hicke, L. (2001). "A new ticket for entry into budding vesicles-ubiquitin." Cell 106(5): 527-30.

Hislop, J. N., A. Marley, et al. (2004). "Role of mammalian vacuolar protein-sorting proteins in endocytic trafficking of a non-ubiquitinated G protein-coupled receptor to lysosomes." J Biol Chem 279(21): 22522-31.

Huang, P., D. Steplock, et al. (2004). "kappa Opioid receptor interacts with Na(+)/H(+)-exchanger regulatory factor-1/Ezrin-radixin-moesin-binding phosphoprotein-50 (NHERF-1/EBP50) to stimulate Na(+)/H(+) exchange independent of G(i)/G(o) proteins." J Biol Chem 279(24): 25002-9.

Hupalowska, A. and M. Miaczynska (2011). "The new faces of endocytosis in signaling." Traffic.

Hurley, J. H. (2010). "The ESCRT complexes." Crit Rev Biochem Mol Biol 45(6): 463-87.

Krishnamurthy, H., H. Kishi, et al. (2003). "Postendocytotic trafficking of the follicle-stimulating hormone (FSH)-FSH receptor complex." Mol Endocrinol 17(11): 2162-76.

Lahuna, O., M. Quellari, et al. (2005). "Thyrotropin receptor trafficking relies on the hScrib-betaPIX-GIT1-ARF6 pathway." Embo J 24(7): 1364-74.

Lefkowitz, R. J., J. Pitcher, et al. (1998). "Mechanisms of beta-adrenergic receptor desensitization and resensitization." Adv Pharmacol 42: 416-20.

Li, H. S., D. B. Stolz, et al. (2005). "Characterization of endocytic vesicles using magnetic microbeads coated with signalling ligands." Traffic 6(4): 324-34.

Marsh, E. W., P. L. Leopold, et al. (1995). "Oligomerized transferrin receptors are selectively retained by a lumenal sorting signal in a long-lived endocytic recycling compartment." J Cell Biol 129(6): 1509-22.

Martini, L., D. Thompson, et al. (2010). "Differential regulation of behavioral tolerance to WIN55,212-2 by GASP1." Neuropsychopharmacology 35(6): 1363-73.

Martini, L., M. Waldhoer, et al. (2007). "Ligand-induced down-regulation of the cannabinoid 1 receptor is mediated by the G-protein-coupled receptor-associated sorting protein GASP1." Faseb J 21(3): 802-11.

Maxfield, F. R. and T. E. McGraw (2004). "Endocytic recycling." Nat Rev Mol Cell Biol 5(2): 121-32.

Mayor, S., J. F. Presley, et al. (1993). "Sorting of membrane components from endosomes and subsequent recycling to the cell surface occurs by a bulk flow process." J Cell Biol 121(6): 1257-69.

Mellman, I. (1996). "Endocytosis and molecular sorting." Annu Rev Cell Dev Biol 12: 575-625.

Moser, E., J. Kargl, et al. (2010). "G protein-coupled receptor-associated sorting protein 1 regulates the postendocytic sorting of seven-transmembrane-spanning G protein-coupled receptors." Pharmacology 86(1): 22-9.

Mukherjee, S., T. T. Soe, et al. (1999). "Endocytic sorting of lipid analogues differing solely in the chemistry of their hydrophobic tails." J Cell Biol 144(6): 1271-84.

Oldham, W. M. and H. E. Hamm (2008). "Heterotrimeric G protein activation by G-protein-coupled receptors." Nat Rev Mol Cell Biol 9(1): 60-71.

Parton, D. L., J. W. Klingelhoefer, et al. (2011). "Aggregation of model membrane proteins, modulated by hydrophobic mismatch, membrane curvature, and protein class." Biophys J 101(3): 691-9.

Pearse, B. M. and M. S. Bretscher (1981). "Membrane recycling by coated vesicles." Annu Rev Biochem 50: 85-101.

Pippig, S., S. Andexinger, et al. (1995). "Sequestration and recycling of beta 2-adrenergic receptors permit receptor resensitization." Mol Pharmacol 47(4): 666-76.

Purvanov, V., A. Koval, et al. (2010). "A direct and functional interaction between Go and Rab5 during G protein-coupled receptor signaling." Sci Signal 3(136): ra65.

Puthenveedu, M. A., B. Lauffer, et al. (2010). "Sequence-dependent sorting of recycling proteins by actin-stabilized endosomal microdomains." Cell 143(5): 761-73.

Raiborg, C. and H. Stenmark (2009). "The ESCRT machinery in endosomal sorting of ubiquitylated membrane proteins." Nature 458(7237): 445-52.

Rasmussen, S. G., B. T. Devree, et al. (2011). "Crystal structure of the beta(2) adrenergic receptor-Gs protein complex." Nature.

Robinson, J. S., D. J. Klionsky, et al. (1988). "Protein sorting in Saccharomyces cerevisiae: isolation of mutants defective in the delivery and processing of multiple vacuolar hydrolases." Mol Cell Biol 8(11): 4936-48.

Rosenbaum, D. M., S. G. Rasmussen, et al. (2009). "The structure and function of G-protein-coupled receptors." Nature 459(7245): 356-63.

Rothman, J. H., I. Howald, et al. (1989). "Characterization of genes required for protein sorting and vacuolar function in the yeast Saccharomyces cerevisiae." Embo J 8(7): 2057-65.

Roxrud, I., H. Stenmark, et al. (2010). "ESCRT & Co." Biol Cell 102(5): 293-318.

Sharpe, H. J., T. J. Stevens, et al. (2010). "A comprehensive comparison of transmembrane domains reveals organelle-specific properties." Cell 142(1): 158-69.

Sorkin, A. and L. K. Goh (2009). "Endocytosis and intracellular trafficking of ErbBs." Exp Cell Res 315(4): 683-96.

Steinman, R. M., S. E. Brodie, et al. (1976). "Membrane flow during pinocytosis. A stereologic analysis." J Cell Biol 68(3): 665-87.

Tanowitz, M. and M. Von Zastrow (2002). "Ubiquitination-independent trafficking of G protein-coupled receptors to lysosomes." J Biol Chem 277(52): 50219-22.

Tanowitz, M. and M. von Zastrow (2003). "A novel endocytic recycling signal that distinguishes the membrane trafficking of naturally occurring opioid receptors." J Biol Chem 278(46): 45978-86.

Thompson, D., L. Martini, et al. (2010). "Altered ratio of D1 and D2 dopamine receptors in mouse striatum is associated with behavioral sensitization to cocaine." PLoS One 5(6): e11038.

Thompson, D. and J. L. Whistler (2011). "Dopamine D(3) receptors are down-regulated following heterologous endocytosis by a specific interaction with G protein-coupled receptor-associated sorting protein-1." J Biol Chem 286(2): 1598-608.

Tsao, P. I. and M. von Zastrow (2000). "Type-specific sorting of G protein-coupled receptors after endocytosis." J Biol Chem 275(15): 11130-40.

Tschische, P., E. Moser, et al. (2010). "The G-protein coupled receptor associated sorting protein GASP-1 regulates the signalling and trafficking of the viral chemokine receptor US28." Traffic 11(5): 660-74.

Urbanowski, J. L. and R. C. Piper (2001). "Ubiquitin sorts proteins into the intralumenal degradative compartment of the late-endosome/vacuole." Traffic 2(9): 622-30.

Vargas, G. A. and M. Von Zastrow (2004). "Identification of a novel endocytic recycling signal in the D1 dopamine receptor." J Biol Chem 279(36): 37461-9.

Wang, Y., B. Lauffer, et al. (2007). "N-ethylmaleimide-sensitive factor regulates beta2 adrenoceptor trafficking and signaling in cardiomyocytes." Mol Pharmacol 72(2): 429-39.

Wang, Y., Y. Zhou, et al. (2002). "Down-regulation of protease-activated receptor-1 is regulated by sorting nexin 1." Mol Biol Cell 13(6): 1965-76.

Williams, R. L. and S. Urbe (2007). "The emerging shape of the ESCRT machinery." Nat Rev Mol Cell Biol 8(5): 355-68.

Wollert, T., D. Yang, et al. (2009). "The ESCRT machinery at a glance." J Cell Sci 122(Pt 13): 2163-6.

Chapter 2:

ESCRT-Mediated Lysosomal Trafficking of β2-Adrenergic Receptors is determined by the C-terminal Recycling Sequence and is Independent of Receptor Ubiquitination

Paul Temkin contributed data to Figures 7 and 8. All other data was produced by James Hislop.

All experiments were conceived by James Hislop of the von Zastrow lab.

2.1 Abstract

The human beta-2 adrenergic receptor (B_2AR) is widely considered a prototypical member of the largest group (family A) of G-protein coupled signaling receptors (GPCRs) expressed in animals. B_2AR signaling is regulated by ligand-induced endocytosis, and subsequent sorting of internalized receptors between divergent recycling or lysosomal pathways; this determines whether endocytosis produces rapid recovery (resensitization) or prolonged attenuation (downregulation) of cell signaling. Previous studies have concluded that endocytic trafficking of the B_2AR to lysosomes requires covalent modification of the receptor by ubiquitination, whereas recycling is promoted by non-covalent interactions with a PDZ ligand present in the cytoplasmic tail of the receptor. We investigated the relative importance of these distinct covalent and non-covalent sorting determinants in controlling the endocytic trafficking of receptors in human cells using a mutational approach to selectively disrupt receptor ubiquitination (by lysine mutation), PDZ interaction (by C-terminal extension), or both. Disrupting B_2AR ubiquitination did not affect the ability of internalized receptors to undergo PDZ-directed sorting into the recycling pathway. Surprisingly, ubiquitination-defective mutant receptors also trafficked to lysosomes efficiently, and did so at a rate that was determined by the C-terminal PDZ ligand. However, lysosomal trafficking of the non-ubiquitinated receptor required both early (Hrs) and late (Vps4) components of the highly conserved Endosomal Sorting Complex Required for Transport (ESCRT). Our results emphasize the ability of the conserved ESCRT machinery to mediate late endocytic trafficking of non-ubiquitinated membrane cargo, and to do so for a prototypic member of the largest known family of mammalian signaling receptors.

2.2 Introduction

The beta-2 adrenergic receptor (B_2AR) is generally considered a prototypic member of the G protein-coupled receptor (GPCR) superfamily, which comprises the largest known family of signaling receptors in animals. Agonist-induced activation of G-protein coupled receptors (GPCRs) initiates signaling events within the cell that promote receptor phosphorylation by G-protein receptor kinases (GRK) and recruitment of arrestins, resulting in receptor desensitization and targeting for endocytosis via clathrin-coated pits. Following endocytosis, receptors are sorted between divergent downstream pathways that allow the receptor to be either 1) dephosphorylated and recycled back to the plasma membrane in a functionally active state that promotes recovery of signal transduction (resensitization), or 2) trafficked to the lysosome for proteolysis and prolonged attenuation of cell signaling (Ferguson, 2001; Goodman et al., 1998; Lefkowitz, 1998; Sorkin and Von Zastrow, 2002). For many GPCRs, including the B_2AR, both pathways are accessible and are functionally important under different physiological conditions. Thus, a fundamental question is how receptors are sorted between these divergent endocytic pathways.

A number of integral membrane proteins, such as constitutively endocytosed transferrin receptors, can enter the recycling pathway efficiently in the absence of any known sorting determinant (Gruenberg, 2001; Mayor et al., 1993). It is increasingly apparent that many GPCRs do not recycle efficiently by default and require a specific cytoplasmic sorting determinant for effectual entry into the recycling pathway. Efficient recycling of the B_2AR, for example, requires a PDZ-ligand sequence that is thought to

function by linking endocytosed receptors to the cortical actin cytoskeleton (Cao et al., 1999; Gage et al., 2001; Gage et al., 2005). Disruption of this interaction, either by truncation of the Carboxyl terminus or by the addition of amino acid residues to the carboxyl-tail, prevents efficient recycling of the B_2AR and promotes receptor proteolysis via endocytic trafficking to lysosomes (Cao et al., 1999).

Considerable progress has been made in elucidating a highly conserved mechanism that mediates lysosomal sorting of many integral membrane proteins, including various signaling receptors. Endocytic sorting to the vacuole/lysosomes is directed by covalent modification of cytoplasmic lysine residues with ubiquitin, and mediated by interaction with a series of endosome-associating sorting proteins containing ubiquitin interaction domains/motifs. These proteins, collectively called the ESCRT (Endosomal Sorting Complexes Required for Transport) machinery, are essential for lysosomal trafficking and proteolysis of various ubiquitinated membrane cargo (Babst, 2005; Hicke, 2001; Raiborg et al., 2003; Slagsvold et al., 2006; Williams and Urbe, 2007). Ubiquitin-directed endocytosis and vacuolar trafficking was first shown for the yeast GPCR Ste2p (Hicke and Riezman, 1996), and an increasing number of mammalian GPCRs are thought to use ubiquitination as an essential determinant for lysosomal sorting (Cottrell et al., 2006; Dupre et al., 2003; Jacob et al., 2005; Liang and Fishman, 2004; Marchese and Benovic, 2001; Marchese et al., 2003; Martin et al., 2003). Of particular interest, the B_2AR has been shown recently to undergo lysyl-ubiquitination and this modification has been proposed to function as an essential sorting signal that directs endocytic trafficking of this GPCR to lysosomes (Shenoy et al., 2001).

The present evidence thus suggests that distinct structural determinants present on the cytoplasmic surface of the B_2AR, a C-terminal PDZ ligand and ubiquitination of cytoplasmic lysine residues, control essentially the same sorting decision. This poses two fundamental questions about how endocytic sorting of this GPCR is controlled. Do PDZ- and ubiquitination- dependent signals operate independently, or is one signal required for the sorting activity of the other? Which mechanism plays the primary role in controlling receptor sorting between functionally important recycling and degradative pathways? The present study addresses these questions by specifically disrupting the C-terminal PDZ ligand and receptor ubiquitination individually or in combination, and by taking a comprehensive approach to evaluate effects on endocytic trafficking of receptors through both recycling and degradative pathways. Our results indicate that the primary sorting determinant controlling endocytic trafficking through both pathways is primarily the C-terminal PDZ ligand, and that the sorting function of this sequence does not depend on receptor ubiquitination. Furthermore, our results clearly establish the B_2AR as a prototypic GPCR for which ubiquitination is not required for endocytic trafficking to lysosomes, even though lysosomal trafficking of these receptors requires the conserved ESCRT machinery.

2.3 Results

Ligand-induced endocytosis, and PDZ-directed sorting into the recycling pathway, do not require receptor ubiquitination.

Following agonist-induced endocytosis, the B_2AR undergoes PDZ-ligand mediated recycling to promote resensitization, however, prolonged agonist treatment (24 hours) causes the receptor to undergo lysosomal proteolysis by a process apparently dependent on ubiquitination (Shenoy et al., 2001). To determine which of these processes controls the rate of proteolysis, we generated mutant versions of the human B_2AR defective in ability to either undergo ubiquitination, to engage in PDZ-dependent protein interactions, or both. Mutation of all lysine residues in the N-terminally FLAG-tagged B_2AR (F-B_2AR) to arginine (F-B_2AR-0k mutant receptor) prevents receptor ubiquitination while retaining ligand-dependent signaling and endocytosis via clathrin-coated pits. Addition of a haemagluttanin (HA) epitope tag to the carboxyl-terminal leucine residue (F-B_2AR-HA mutant receptor) selectively prevents PDZ-mediated protein interactions with receptors, also without disrupting receptor signaling or endocytosis. To disrupt both mechanisms, these mutations were combined (F-B_2AR-0k-HA mutant receptor).

To determine if these mutations operate independently of one another, we asked if disruption of the C-terminal PDZ ligand affects regulated ubiquitination of the B_2AR. FLAG-tagged B_2AR-HA (F-B_2AR-HA) was immunopurified from stably transfected HEK293 cells expressing receptors at moderate levels (~500 fmol / mg, see Methods). Immunoblotting with anti-ubiquitin antibody (P4D1, Santa Cruz) revealed the existence

of high molecular weight ubiquitinated species (fig.1a and b), which were present in small amount relative to total receptor protein (compare with receptor immmunoblot (fig.1a, far right)), consistent with sub-stoichiometric poly-ubiquitination shown previously (and confirmed by us, not shown) for the wild-type F-B_2AR. Furthermore, as shown previously for the wild-type F-B_2AR, incubation of cells with the adrenergic agonist isoproterenol produced a significant, time-dependent increase in the amount of ubiquitinated F-B_2AR–HA species recovered in cell extracts. Both effects were abolished by lysine mutation, as indicated by carrying out the corresponding experiments with cells expressing F-B_2AR-0k-HA mutant receptors at a similar level (fig.1a and b). Thus, the PDZ-dependent sorting sequence is not required either for B_2AR ubiquitination or its regulation by agonist.

We sought to determine the fate of a receptor that cannot be ubiquitinated and cannot undergo PDZ-mediated recycling. One possible fate is for the receptor to be 'forced' to recycle, possibly via the default membrane recycling pathway utilized by transferrin receptors. We therefore tested the effects of B_2AR mutations on endocytic trafficking of receptors through the recycling pathway. Fluorescence microscopy indicated that each of the mutant receptors tested localized primarily to the plasma membrane in the absence of agonist (Fig. 2A a, d, g, j). Addition of isoproterenol to the culture medium produced a rapid redistribution of all of the mutant receptors from the cell surface to intracellular membranes (b, e, h, k), consistent with agonist-induced endocytosis of receptors. Whereas antibody-labeled F-B_2AR returned almost completely to a plasma membrane localization pattern following agonist washout (Fig.2Ac), consistent with efficient recycling characteristic of the wild type receptor, recycling of

the F-B_2AR-HA mutant receptor was visibly impaired (Fig.2Ai). Essentially identical results were obtained when comparing the ubiquitination-defective mutant receptors. Labeled F-B_2AR-0k mutant receptors returned almost completely to a plasma membrane localization pattern after agonist washout, whereas PDZ binding-defective F-B_2AR-0k-HA mutant receptors were retained in endosomes (Fig.2A f and l).

These results were confirmed and quantified in a large number of cells using a previously established flow cytometry assay whereby immunoreactive receptors accessible at the cell surface are labeled with extracellular antibody. All of the mutants tested exhibited pronounced agonist-induced internalization, and there was no significant difference among mutants in the degree to which isoproterenol promoted receptor internalization (fig 2B). While recycling of both F-B_2AR and F-B_2AR-0k was essentially complete after agonist washout, the flow cytometry assay confirmed that recycling of both F-B_2AR-HA and F-B_2AR-0k-HA was greatly impaired. Together, these observations emphasize importance of the C-terminal PDZ ligand present in the B_2AR for efficient sorting of internalized receptors into the plasma membrane recycling pathway, and indicate that receptor ubiquitination is not required for receptor recycling (F-B_2AR-0k). Importantly, prevention of ubiquitination does not appear to 'force' a PDZ-disrupted receptor (F-B_2AR-0k-HA) into the default recycling pathway used by the transferrin receptor.

<u>Disruption of the C-terminal PDZ ligand promotes lysosomal proteolysis of receptors in the absence of ubiquitination.</u>

We next determined whether the non-recycling F-B_2AR-0k-HA receptor is simply retained in endosomes, or does indeed undergo trafficking to lysosomes and subsequent proteolysis without direct ubiquitination, in a process similar to that seen for the delta opioid receptor (DOR) (Hislop et al., 2004; Tanowitz and Von Zastrow, 2002). Isoproterenol promoted rapid proteolysis of the recycling-defective F-B_2AR–HA, as indicated by a rapid and pronounced loss of immunoreactive receptor detected in cell extracts by anti-FLAG following exposure of cells to isoproterenol (fig.3A). Agonist-induced proteolysis occurred with a t½ ~ 90 minutes (fig.3B), closely comparable to that observed for other PDZ binding-defective mutant B_2AR constructs shown previously to traffic to lysosomes (Cao et al., 1999). In principle this loss of immunoreactive F-B_2AR could reflect any proteolytic process, including limited cleavage of only the N-terminal ectodomain containing the FLAG epitope tag (perhaps analogous to proteolytic 'shaving' observed previously for the Ste3p GPCR in yeast (Chen and Davis, 2002)). To test this possibility, we examined the effect of isoproterenol on receptor recovery detected by immunoblotting for the C-terminal HA epitope tag (fig.3C). This analysis confirmed the ability of isoproterenol to stimulate and revealed a time-dependent 'ladder' of HA-immunoreactive bands, indicative of multiple agonist-induced proteolytic cleavages occurring during the observed time course, suggestive of extensive proteolysis and not just ‘epitope shaving’ (fig.3C). Surprisingly, the corresponding experiments conducted on cells expressing the ubiquitination-defective F-B_2AR-0k-HA construct revealed closely similar results, both in terms of rate of receptor proteolysis (fig.3D and E) and the presence of multiple proteolytic cleavages (fig.3F).

We next investigated if the observed proteolysis was indeed mediated by endocytic trafficking of receptors to lysosomes. Agonist-induced proteolysis of both F-B_2AR-HA and F-B_2AR-0k-HA was strongly impaired by Z-Phe-Ala-diazomethylketone (Z-PAD), a selective inhibitor of lysosomal proteases, but was insensitive to the proteosome inhibitor epoximicin. A representative example of primary data is show in Fig 4A and quantification of results across multiple experiments is summarized in Fig 4B. As expected, dual label confocal microscopy revealed extensive colocalization of internalized F-B_2AR-HA with the lysosomal marker LAMP2 in cells exposed to isoproterenol for 60 min (fig.4C). Essentially identical results were obtained in dual localization of the ubiquitination-defective F-B_2AR-0k-HA (fig.4D). Together, these results indicate that ubiquitination is not required for agonist-induced trafficking of recycling-defective B_2AR mutants to lysosomes. Further, because both F-B_2AR-HA and F-B_2AR-0k-HA were proteolyzed much more rapidly in the presence of isoproterenol than the corresponding receptors with functional PDZ ligands (ref and see below), these results also suggest that the PDZ ligand sequence plays a dominant role in controlling both early and late endocytic trafficking of B_2AR.

Lysosomal proteolysis of a recycling impaired B_2AR is dependent on the ESCRT machinery.

We next asked if lysosomal sorting of the non-ubiquitinated mutant receptors was mediated by a similar or different mechanism as that mediating lysosomal sorting of ubiquitinated cargo. To do so we focused on Hrs and Vps4, two essential components of the ubiquitin-directed sorting pathway that functions at distinct early (HRS) and late

stages (Vps4) in this mechanism (Raiborg et al., 2003; Williams and Urbe, 2007). Overexpression of myc-Hrs, a previously established means for producing dominant-negative inhibition of the ESCRT-mediated lysosomal sorting mechanism, was carried out in stably transfected HEK293 cells expressing either F-B_2AR-HA or F-B_2AR-0K-HA. Receptors present in the plasma membrane were then labeled by surface biotinylation prior to agonist incubation, and agonist-induced proteolysis was assessed by determining the amount of labeled receptor protein recovered from cell lysates. In control cells, not over-expressing Myc-Hrs, labeled F-B_2AR-HA (Fig 5A) and F-B_2AR-0K-HA (Fig 5C) was proteolyzed rapidly following exposure of cells to isoproterenol. Overexpression of myc-HRS (~20-fold over endogenous Hrs levels according to immunoblotting, not shown) clearly inhibited proteolysis of both F-B_2AR-HA and the F-B_2AR-0K-HA (fig. 5B and D, compare open and solid bars). Densitometric analysis reveals that for the F-B_2AR-HA, 65.8 ± 8.9% of control remained after 1 hour and 34.7 ± 4.8% of control after 3 hours. This increased to 94.8 ± 2.1% F-B_2AR-HA remaining after 1 hour and 73.8 ± 2.8% F-B_2AR-HA remaining after 3 hours in cells overexpressing myc-HRS. Similar data was obtained for the F-B_2AR-0K-HA, in control cells after 1 hours isoproterenol treatment 58.1 ± 5.4% receptor remained and 31.9 ± 5.8% receptor remained after 3 hours treatment, whereas in HRS overexpressing cells 78.7 ± 6.4% receptor remained after 1 hour and 59.9 ± 6% receptor remained after 3 hours isoproterenol.

Point mutations in the ATPase domain of Vps4 create an ATP binding deficient mutant (E228Q), or an ATP hydrolysis deficient mutant (K173Q) (Bishop and Woodman, 2000). HEK 293 cells stably expressing F-B_2AR-HA or the F-B_2AR-0K-HA

were transiently transfected with control cDNA, or cDNA either of the two mutants, before surface biotinylation and Western blot analysis with M1-anti-FLAG antibody. Control transfected cells showed the same rapid agonist-induced proteolysis as seen previously after 3 hours isoproterenol treatment (38.9 ± 7.1% for F-B_2AR-HA and 52.9 ± 8% for F-B_2AR-0k-HA), however cells expressing Vps4E228Q-GFP and Vps4K173Q-GFP all showed significantly impaired proteolysis 65 ± 4.7%, and 63.6 ± 8 % after 3 hours respectively for F-B_2AR-HA (fig.6A) and 88.2 ± 7.4% and 78.5 ± 2.1% for F-B_2AR-0k-HA (fig.6B).

Agonist-induced lysosomal proteolysis of wild type B_2AR does not require receptor ubiquitination

The above data demonstrate that B_2AR mutants defective in PDZ-binding ability undergo ESCRT-dependent endocytic sorting to lysosomes without requiring receptor ubiquitination. Although this conclusion is fully consistent with previous studies demonstrating ubiquitination-independent lysosomal sorting of DOR (Hislop et al., 2004), this neuropeptide GPCR does not contain a PDZ-dependent sorting sequence and naturally traffics to lysosomes much more rapidly than the wild-type B_2AR (Tsao and von Zastrow, 2000). Indeed, it has been previously reported that the wild type B_2AR does require ubiquitination to allow receptor downregulation following prolonged agonist treatment (Shenoy et al., 2001). Since we have shown that rapid (PDZ-independent) lysosomal proteolysis is ubiquitin-independent, we next investigated whether the slower agonist-induced proteolysis characteristic of the wild-type B_2AR can also occur without receptor ubiquitination. Immunoblot analysis confirmed that agonist-induced proteolysis

of F-B_2AR protein levels, although not evident at early time points after agonist addition, was clearly evident within 8 hours of continuous agonist exposure (Fig.7A). Remarkably, agonist-induced down-regulation of F-B_2AR-0k mutant receptor protein level was also clearly observed (Fig.7B). Quantification across multiple experiments confirmed the ability of the F-B_2AR-0k mutant receptor to undergo pronounced agonist-induced proteolysis, and failed to detect any significant difference in the extent of this reduction at either 8 or 24 hours after agonist addition(Fig.7C). These results suggest that agonist-induced proteolysis of the wild-type B_2AR occurs via a similar lysosomal sorting mechanism as that mediating faster down-regulation of other GPCRs devoid of PDZ-dependent sorting sequences, and indicate that ubiquitination of the wild-type B_2AR is not required for endocytic trafficking to lysosomes.

An alternative, and more traditional, approach for assessing lysosomal proteolysis of the B_2AR is by measuring downregulation of receptor number using radio-ligand binding. While multiple mechanisms can contribute to pharmacological downregulation of GPCRs in tissues, B_2AR downregulation measured over a 24-hour interval in HEK293 cells is mediated primarily by lysosomal trafficking of receptors (Moore et al., 1999). To assess this in our studies, the same clones of stably transfected cells as used above were incubated for up to 24 hours either in the absence or presence of isoproterenol and assayed by whole cell radioligand binding. Assays were conducted using the membrane-permeant B_2AR receptor antagonist [^{3}H]-dihydroalprenolol (see materials and methods), in order to detect both surface and internal binding sites. Neither F-B_2AR nor F-B_2AR-ala downregulated to a significant extent when radioligand binding assay was conducted following 8 hours after incubation of cells in the presence of agonist (not shown).

Following agonist exposure for 24 hours, F-B_2AR levels were reduced to 64 ± 2.7% of control (Fig.8), consistent with downregulation of wild type receptors shown previously at this time point. Surprisingly, when similar binding studies were performed on cells expressing the previously described recycling-impaired F-B_2AR-ala (Cao et al., 1999), a decrease in receptor levels to 77 ± 8.1% of control was observed. This degree of downregulation, which was verified in multiple expression-matched cell clones, is not significantly different from that observed for the wild type receptor (Fig.8). We were surprised by these results because extensive proteolysis of F-B_2AR-ala was observed much more rapidly in the same cells when analyzed by Western blotting (data not shown, see (Cao et al., 1999)), and even wild type receptors showed at least partial proteolysis within 8 hours of agonist application. Thus, while pharmacological downregulation provides a sensitive index of B_2AR destruction in lysosomes (data not shown, see (Moore et al., 1999)), loss of radioligand binding evidently requires extensive proteolytic cleavage and occurs over a prolonged time frame relative to lysosomal proteolysis detected biochemically. Further, as pharmacological downregulation was not sensitive to PDZ-dependent sorting that controls the rate of receptor trafficking to lysosomes (and receptor proteolysis detected biochemically), these results reveal a hitherto unidentified rate-limiting step in B_2AR downregulation that is PDZ-independent. Given these considerations, we hypothesized that assay of receptor degradation by pharmacological downregulation might reveal a functional consequence of B_2AR ubiquitination in this process that is not evident from biochemical analysis of receptor proteolysis. Interestingly, downregulation of the ubiquitination-defective F-B_2AR-0K measured by radioligand binding occurred to a closely similar degree (reduced to 60.9 ± 3.2% of

control) as that of the wild type receptor (Fig 7). Thus, although biochemical (Western blot) and pharmacological (radioligand binding) assays measure kinetically distinct steps in proteolytic degradation of the B_2AR promoted by lysosomal trafficking, neither assay revealed a requirement for receptor ubiquitination in this regulatory pathway.

2.4 Discussion

In the present study we set out to determine the primary mechanism controlling endocytic trafficking of the human B_2AR to lysosomes. The B_2AR is a mammalian GPCR that displays a complex endocytic trafficking itinerary, and for which lysosomal proteolysis plays an important role in attenuating cellular signaling following prolonged activation by catecholamines. Our results establish that covalent modification of the B_2AR by ubiquitination, while clearly evident under basal conditions and increased by agonist activation, plays no detectable role in the sorting of this GPCR in the endocytic pathway. We show that PDZ-dependent sorting is the major mechanism controlling the rate at which endocytosed receptors traffic to lysosomes, and show that this sorting function is fully independent of receptor ubiquitination. Despite the apparently insignificant role of ubiquitination in determining endocytic fate, we show that lysosomal trafficking of the B_2AR occurs via a similar ESCRT -dependent mechanism as that mediating endocytic sorting of ubiquitinated membrane cargo.

The role of ubiquitin tagging as a covalent determinant of endocytic sorting was first appreciated in studies of the yeast GPCR Ste2p (Hicke, 2001; Hicke and Riezman, 1996), and has since been extended to many integral membrane proteins in diverse organisms including mammals (Raiborg et al., 2003; Williams and Urbe, 2007). Several mammalian signaling receptors, including the GPCRs the vasopressin V2R; PAR2 and neurokinin NK1R (Cottrell et al., 2006; Jacob et al., 2005; Martin et al., 2003), have convincingly been shown to require ubiquitination for trafficking to lysosomes, and at least one, the CXCR4, has been shown to require the conserved ESCRT machinery for its

lysosomal trafficking (Marchese and Benovic, 2001; Marchese et al., 2003). Our interest in ubiquitination-independent sorting of GPCRs stemmed from the identification of an opioid neuropeptide receptor that undergoes ESCRT-dependent trafficking to lysosomes without requiring receptor ubiquitination (Hislop et al., 2004; Tanowitz and Von Zastrow, 2002), and our concern that it might be an isolated example for a signaling receptor that has a simple endocytic itinerary. The human B_2AR, in contrast, is capable of diverse recycling and degradative trafficking routes and is generally considered a prototype for regulation of the largest family (family A) of GPCRs expressed in mammals. Thus we believe that sorting of non-ubiquitinated cargo by the conserved ESCRT machinery is likely to be widespread, and physiologically significant, for the largest family of signaling receptors expressed in animals. Interestingly, the B_1AR and the CGRP receptor complex are both examples of GPCRs that are able to traffic to lysosomes without detectable ubiquitination, although the role of ESCRT proteins in their trafficking has not been investigated (Cottrell et al., 2007; Liang and Fishman, 2004).

We note that a previous study concluded that ubiquitination of the B_2AR is essential for endocytic trafficking to lysosomes, but not for the initial endocytosis of receptors induced by ligand-induced activation (Shenoy et al., 2001). Our results agree with the latter conclusion, and further confirm the ability of receptors to recycle efficiently to the plasma membrane in the absence of ubiquitination, but they clearly refute the former conclusion regarding the requirement of receptor ubiquitination for endocytic trafficking to lysosomes. Further, the present results establish that the moderate downregulation of radioligand binding activity, the only assay used to estimate lysosomal trafficking in the previous study, occurs too slowly to be a reliable measure of endocytic

sorting to lysosomes. This point is perhaps most clearly evident from examination of the PDZ-mutant B_2ARs, which traffic to lysosomes within one hour after agonist-induced endocytosis and are extensively proteolyzed within several hours thereafter, yet exhibit only partial (~20%) reduction in radioligand binding even after 24 hours of continuous agonist exposure. This suggests that loss of radioligand binding requires extensive proteolysis of the B_2AR, occurring over a prolonged time period after receptor delivery to lysosomes, thus making pharmacological downregulation insensitive to endocytic sorting events that occur more rapidly. The remarkable ability of the B_2AR to retain radioligand binding for a prolonged time period after delivery to lysosomes is consistent with previous studies noting the location of residues required for radioligand binding in a hydrophobic 'core' of the B_2AR that is resistant to proteolysis (Gether, 2000; Moore et al., 1999; Rands et al., 1990; Tota and Strader, 1990). In our hands the ubiquitination-defective mutant B_2AR exhibited pharmacological downregulation to a similar extent as the wild type receptor, indicating further that slower proteolytic step(s) required for loss of radioligand binding do not require receptor ubiquitination.

A remarkable feature of B_2AR sorting to lysosomes is that this process governed primarily by a C-terminal PDZ ligand, which was previously called a 'recycling signal' based on its ability to promote efficient trafficking of internalized receptors back to the plasma membrane (Cao et al., 1999). Whereas ubiquitination is generally thought to control endocytic sorting by controlling the degree to which endocytosed membrane proteins are directed to lysosomes from a 'default' recycling pathway, the B_2AR behaves oppositely- with non-covalent protein interactions effectively diverting endocytosed receptors from an apparently 'default' lysosomal fate. An increasing number of

mammalian GPCRs are recognized to require specific sorting determinants for efficient recycling, and the existence of distinct PDZ –dependent and –independent sorting determinants in individual receptors suggests the existence of a modular sorting code that specifically controls endocytic trafficking of individual GPCR family members (Gage et al., 2005; Galet et al., 2004; Li et al., 2002; Tanowitz and von Zastrow, 2003; Vargas and Von Zastrow, 2004). An important question for future studies is to define ubiquitin-independent protein interactions with mammalian GPCRs that bias endocytic trafficking to the lysosomal pathway. GASP-family proteins influence lysosomal sorting of opioid neuropeptide receptors in a ubiquitination-independent manner (Whistler et al., 2002), and it is interesting to note that GASP interacts with a number of GPCRs including the B_2AR (Heydorn et al., 2004). There may be additional proteins promoting lysosomal sorting of mammalian GPCRs, including sorting nexin 1, which has been shown to affect lysosomal trafficking of the PAR1 GPCR without requiring ubiquitination of the receptor's cytoplasmic tail (Trejo and Coughlin, 1999; Wang et al., 2002). The relevance of this protein interaction for controlling receptor sorting via the conserved ESCRT-mediated mechanism remains unclear, as PAR1 trafficking to lysosomes evidently does not require ESCRT proteins (Gullapalli et al., 2006). Thus the present results suggests an important and quite general role of an ubiquitination-independent mechanism(s) in controlling the sorting of the largest family of signaling receptors to the conserved multivesicular body (MVB) pathway. It is interesting to note that in yeast, the integral membrane protein Sna3p does not require ubiquitination to traffic to the vacuole, yet vacuolar trafficking occurs via the conserved ESCRT-dependent mechanism. In this case endocytic sorting is mediated by a direct interaction with Rsp5, which functions as a

sorting protein independent of its ubiquitin ligase activity (McNatt et al., 2007; Oestreich et al., 2007; Reggiori and Pelham, 2001; Watson and Bonifacino, 2007). Ubiquitination-independent sorting to the late endocytic pathway, which the present results argue is critical to endocytic sorting of the largest class of mammalian signaling receptors, may have even more widespread biological significance.

2.5 Materials and Methods

Cell Culture, cDNA constructs and transfection

The myc-tagged Hrs construct was a gift from Harald Stenmark (Norwegian Radium Hospital, Norway), and the Vps4-GFP, Vps4 E228Q-GFP and Vps4 K173Q-GFP constructs were a gift from Wes Sundquist (University of Utah School of Medicine, USA). HEK 293 cells were grown in Dulbeccos modified Eagles medium supplemented with 10% fetal bovine serum (University of California, San Francisco, Cell Culture Facility). The FLAG-tagged-B_2AR with all 16 lysine residues mutated to arginine (B_2AR -0K) cDNA were obtained from Brian Kobilka (University of Stanford), ((Parola et al., 1997)), and the C-terminal hexa-His tag removed by site directed mutagensis (Hanyaloglu et al., 2005). FLAG-tagged version of the cloned human B_2AR and the B_2AR-ala has been previously described (Cao et al., 1999). The C-terminal HA-epitope was added to both the wild type B_2AR and the lysine mutated B_2AR -0K by PCR incorporating the HA sequence into the reverse primer, to make recycling impaired receptors (Cao et al., 1999). All four receptor cDNAs were sub-cloned into pcDNA3 (Invitrogen) for generation of stable cell lines. Stably transfected cells expressing epitope tagged receptors were generated by selection for neomycin resistance using 500 μg/ml G418. Neomycin resistant colonies were isolated and selected based on receptor expression levels (assessed by fluorescence microscopy and Western blot of cell lysate using the M1 anti-FLAG antibody (Sigma)).

For transient expression of myc-Hrs or Vps4 constructs, cells were transfected using Lipofectamine 2000 (Invitrogen) according to manufacturers' instructions. Cells

expressing FLAG-tagged receptors were harvested by washing with EDTA and plated in 60-mm dishes at 80% confluency, before transfection with plasmid DNA. Cells were reseeded into poly-lysine coated 6-well plates and cultured for a further 24 hours before experimentation.

Western Blotting for total receptor/protein levels

Immunoblotting of total receptor levels was performed as previously described (Hislop et al., 2004). Briefly, cells were transfected using Lipofectamine 2000 according to manufacturers instructions, and stimulated before washing three times in ice-cold phosphate buffered saline (PBS) and lysed in extraction buffer (0.2% Triton X-100, 150 mM NaCl, 25 mM KCl, 25 mM Tris pH 7.4, 1 mM EDTA, plus protease inhibitor cocktail (Roche)). Extracts were clarified by centrifugation (12,000 x g for 10 minutes), and then mixed with SDS sample buffer for denaturation. The proteins were resolved by SDS-PAGE, transferred to nitrocellulose membranes, and probed for FLAG-tagged receptor (M1 antibody, Sigma) by immunoblotting using horseradish peroxidase-conjugated sheep anti-mouse IgG or donkey anti-rabbit IgG (Amersham Biosciences), and SuperSignal detection reagent (Pierce). Band intensities of unsaturated immunoblots were analyzed and quantified by densitometry using FluorChem 2.0 software (AlphaInnotech Corp.). The amount of FLAG-tagged receptor remaining at each time point was expressed as a percentage of the identically transfected, unstimulated cells.

Biotinylation-degradation assay.

A previously described cell surface biotinylation assay was used to establish FLAG tagged receptors present at the cell surface (Hislop et al., 2004; Tanowitz and Von Zastrow, 2002). Briefly, stably transfected HEK 293 cells were grown on 60-mm dishes, washed with ice-cold PBS and incubated with 300 µg/ml sulfo-N-hydroxysuccinimide-biotin (Pierce) in PBS for 30 minutes at 4^{o}C to biotinylate surface proteins. Following washing with Tris buffered saline (TBS) to quench unreacted biotin, cells were returned to 37^{o}C for incubation in media, with or without agonist, before extraction (see above). Extracts were clarified by centrifugation (12,000 x g for 10 minutes). Biotinylated proteins were isolated from cell lysate by immobilization on streptavidin-conjugated Sepherose beads (Pierce). Washed beads were eluted with SDS sample buffer before resolving by SDS-PAGE transferred to nitrocellulose membranes, and probed for FLAG-tagged receptor (M1 antibody, Sigma).

Immunoprecipitation to detect ubiquitination

To ensure the removal of any proteins that might be associated with the receptor, denaturing conditions were used as previously described (Jacob et al., 2005). Cells were lysed in 100 µl of 50 mM Tris (pH 7.4) and 1% SDS, sonicated and mixed with 400 µl RIPA buffer (150 mM NaCl, 50 mM Tris (pH 7.4), 5 mM EDTA 1% triton X-100, 0.5% Na deoxycholate, 10 mM NaF, 10mM Na2PyroPhosphate, 0.1% SDS), before centrifugation to remove membranes (14,000 rpm for 10 minutes at 4^{o}C). Sample volume was made up to 1 ml with 600 µl IP buffer (see above), and incubated overnight at 4^{o}C with 2 µg of rabbit anti-Flag antibody (Sigma). 30 µl Protein A/G agarose (Pierce) was added for 2 hours at 4^{o}C. Immunoprecipitates were pelleted by

centrifugation (3000 rpm, 1 min, 4°C), and washed 3 times with 500 µl RIPA buffer, before addition of 20 µl SDS sample buffer (Invitrogen) with β-mercaptoethanol, and analysis by Western Blotting.

Radioligand Binding

Receptor downregulation was determined by radioligand binding as previously described (Tsao and von Zastrow, 2000). Following transfection, HEK 293 cells stably expressing FLAG tagged receptors were re-plated into 12-well plates. 24 hours later 100 µM ascorbic acid was added to the media, and 10 µM Isoproterenol, added to the cells. After 24 hours, cells were washed twice with ice-cold PBS and 300 µl PBS was added to the cells and the plates frozen. Plates were thawed and cells resuspended. Binding assays were performed in triplicate in 96 well plates using 10 nM of the membrane permeable adrenergic receptor antagonist [^{3}H]-dihydroalprenolol (DHA) (Amersham, 88 Ci/mmol) and incubated for 1 hour at room temperature, to label both surface and internal receptor. Non-specific binding was determined by the addition of 10 µM unlabelled Alprenolol. Incubations were terminated by vacuum filtration through glass fiber filters (Whatman), and repeated washes with TBS. Bound radioactivity was determined by liquid scintillation counting.

Fluorescence Microscopy

HEK293 cells stably expressing the receptors were plated onto polylysine coated coverslips and surface receptors labeled by the addition of alexa-488 labeled M1 anti-FLAG antibody to the media. Cells were incubated with agonist for 30 minutes before

fixation with 4% formaldehyde (internal), or subsequent removal of agonist, incubation with antagonist for 60 minutes and then fixation, before being processed for microscopy using an inverted Nikon Diaphot microscope equipped with a Nikon 60 x NA 1.4 objective lens and epifluorescent optics. Colocalization of receptors with lysosomes was visualized using an antibody feeding method. Cells were plated onto glass coverslips, and were then incubated for 60 minutes in the presence of agonist at 37^{o}C, before fixing with 4% formaldehyde in PBS and processed for immunocytochemical staining as previously described. Receptors were localized with anti-HA-11 (Covance) and lysosomes were localized using lysosome-associated membrane protein 2 (LAMP2) monoclonal antibody obtained from the Developmental Studies Hybridoma Data Bank. Confocal fluorescence microscopy was performed using a Zeiss LSM 510 microscope fitted with a Zeiss 63 x NA1.4 objective operated in single photon mode with standard filter sets and standard (1 Airy disc) pinhole.

Flow Cytometry

Fluorescence flow cytometry was used to quantify internalization and recycling of receptors by measuring cell surface fluorescence, as previously described (Hanyaloglu and von Zastrow, 2007). Briefly, stably transfected cells were incubated with M1 anti-FLAG antibody (20 minutes, 37^{o}C) to label surface receptors. Cells were treated for 30 minutes with 10μM isoproterenol (internalization) before placing on ice or washing and returning to 37^{o}C for 60 minutes in the presence of Alprenolol (recycling). Cells were then washed and lifted with ice-cold PBS, and incubated with Alexa Fluor-488 conjugated anti-mouse antibody (Molecular Probes). Fluorescence intensity was

measured using a FACS-Calibur (BD Biosciences), counting 10,000 cells/sample in duplicate. Recycling was determined from surface fluorescence (F) as follows ($F_{alprenolol}$ - $F_{isoproterenol}$)/($F_{untreated}$ - $F_{isoproterenol}$)X100.

2.6 Acknowledgments

We thank Harald Stenmark and Wes Sundquist for generously sharing reagents and for valuable discussion. The authors would like to thank members of the von Zastrow laboratory, particularly Aylin Hanyaloglu and Michael Tanowitz, for valuable discussion and critical reading of the manuscript. These studies were supported by the American Heart Association (JNH), the National Science Foundation (PAT) and the National Institutes of Health (MvZ).

2.7 References

Babst, M. (2005) A protein's final ESCRT. *Traffic.*, **6**, 2-9.

Bishop, N. and Woodman, P. (2000) ATPase-defective mammalian VPS4 localizes to aberrant endosomes and impairs cholesterol trafficking. *Mol Biol Cell*, **11**, 227-39.

Cao, T.T., Deacon, H.W., Reczek, D., Bretscher, A. and von Zastrow, M. (1999) A kinase-regulated PDZ-domain interaction controls endocytic sorting of the beta2-adrenergic receptor. *Nature*, **401**, 286-90.

Chen, L. and Davis, N.G. (2002) Ubiquitin-independent entry into the yeast recycling pathway. *Traffic*, **3**, 110-23.

Cottrell, G.S., Padilla, B., Pikios, S., Roosterman, D., Steinhoff, M., Gehringer, D., Grady, E.F. and Bunnett, N.W. (2006) Ubiquitin-dependent down-regulation of the neurokinin-1 receptor. *J Biol Chem.*, **281**, 27773-83. Epub 2006 Jul 17.

Cottrell, G.S., Padilla, B., Pikios, S., Roosterman, D., Steinhoff, M., Grady, E.F. and Bunnett, N.W. (2007) Post-endocytic sorting of calcitonin receptor-like receptor and receptor activity-modifying protein 1. *J Biol Chem.*, **282**, 12260-71. Epub 2007 Feb 19.

Dupre, D.J., Chen, Z., Le Gouill, C., Theriault, C., Parent, J.L., Rola-Pleszczynski, M. and Stankova, J. (2003) Trafficking, ubiquitination, and down-regulation of the human platelet-activating factor receptor. *J Biol Chem.*, **278**, 48228-35. Epub 2003 Sep 18.

Ferguson, S.S. (2001) Evolving concepts in G protein-coupled receptor endocytosis: the role in receptor desensitization and signaling. *Pharmacol Rev*, **53**, 1-24.

Gage, R.M., Kim, K.A., Cao, T.T. and von Zastrow, M. (2001) A transplantable sorting signal that is sufficient to mediate rapid recycling of G protein-coupled receptors. *J Biol Chem*, **276**, 44712-20.

Gage, R.M., Matveeva, E.A., Whiteheart, S.W. and von Zastrow, M. (2005) Type I PDZ ligands are sufficient to promote rapid recycling of G Protein-coupled receptors independent of binding to N-ethylmaleimide-sensitive factor. *J Biol Chem.*, **280**, 3305-13. Epub 2004 Nov 17.

Galet, C., Hirakawa, T. and Ascoli, M. (2004) The postendocytotic trafficking of the human lutropin receptor is mediated by a transferable motif consisting of the C-terminal cysteine and an upstream leucine. *Mol Endocrinol.*, **18**, 434-46. Epub 2003 Nov 6.

Gether, U. (2000) Uncovering molecular mechanisms involved in activation of G protein-coupled receptors. *Endocr Rev.*, **21**, 90-113.

Goodman, O.B., Jr., Krupnick, J.G., Santini, F., Gurevich, V.V., Penn, R.B., Gagnon, A.W., Keen, J.H. and Benovic, J.L. (1998) Role of arrestins in G-protein-coupled receptor endocytosis. *Adv Pharmacol*, **42**, 429-33.

Gruenberg, J. (2001) The endocytic pathway: a mosaic of domains. *Nat Rev Mol Cell Biol.*, **2**, 721-30.

Gullapalli, A., Wolfe, B.L., Griffin, C.T., Magnuson, T. and Trejo, J. (2006) An essential role for SNX1 in lysosomal sorting of protease-activated receptor-1: evidence for

retromer-, Hrs-, and Tsg101-independent functions of sorting nexins. *Mol Biol Cell.*, **17**, 1228-38. Epub 2006 Jan 11.

Hanyaloglu, A.C., McCullagh, E. and von Zastrow, M. (2005) Essential role of Hrs in a recycling mechanism mediating functional resensitization of cell signaling. *Embo J.*, **24**, 2265-83. Epub 2005 Jun 9.

Hanyaloglu, A.C. and von Zastrow, M. (2007) A novel sorting sequence in the beta2-adrenergic receptor switches recycling from default to the Hrs-dependent mechanism. *J Biol Chem.*, **282**, 3095-104. Epub 2006 Nov 30.

Heydorn, A., Sondergaard, B.P., Ersboll, B., Holst, B., Nielsen, F.C., Haft, C.R., Whistler, J. and Schwartz, T.W. (2004) A library of 7TM receptor C-terminal tails. Interactions with the proposed post-endocytic sorting proteins ERM-binding phosphoprotein 50 (EBP50), N-ethylmaleimide-sensitive factor (NSF), sorting nexin 1 (SNX1), and G protein-coupled receptor-associated sorting protein (GASP). *J Biol Chem.*, **279**, 54291-303. Epub 2004 Sep 27.

Hicke, L. (2001) Protein regulation by monoubiquitin. *Nat Rev Mol Cell Biol*, **2**, 195-201.

Hicke, L. and Riezman, H. (1996) Ubiquitination of a yeast plasma membrane receptor signals its ligand-stimulated endocytosis. *Cell*, **84**, 277-87.

Hislop, J.N., Marley, A. and Von Zastrow, M. (2004) Role of mammalian vacuolar protein-sorting proteins in endocytic trafficking of a non-ubiquitinated G protein-coupled receptor to lysosomes. *J Biol Chem.*, **279**, 22522-31. Epub 2004 Mar 15.

Jacob, C., Cottrell, G.S., Gehringer, D., Schmidlin, F., Grady, E.F. and Bunnett, N.W. (2005) c-Cbl mediates ubiquitination, degradation, and down-regulation of human protease-activated receptor 2. *J Biol Chem.*, **280**, 16076-87. Epub 2005 Feb 11.

Lefkowitz, R.J. (1998) G protein-coupled receptors. III. New roles for receptor kinases and beta-arrestins in receptor signaling and desensitization. *J Biol Chem*, **273**, 18677-80.

Li, J.G., Chen, C. and Liu-Chen, L.Y. (2002) Ezrin-radixin-moesin-binding phosphoprotein-50/Na+/H+ exchanger regulatory factor (EBP50/NHERF) blocks U50,488H-induced down-regulation of the human kappa opioid receptor by enhancing its recycling rate. *J Biol Chem.*, **277**, 27545-52. Epub 2002 May 9.

Liang, W. and Fishman, P.H. (2004) Resistance of the human beta1-adrenergic receptor to agonist-induced ubiquitination: a mechanism for impaired receptor degradation. *J Biol Chem.*, **279**, 46882-9. Epub 2004 Aug 25.

Marchese, A. and Benovic, J.L. (2001) Agonist-promoted ubiquitination of the G protein-coupled receptor CXCR4 mediates lysosomal sorting. *J Biol Chem*, **276**, 45509-12.

Marchese, A., Raiborg, C., Santini, F., Keen, J.H., Stenmark, H. and Benovic, J.L. (2003) The E3 ubiquitin ligase AIP4 mediates ubiquitination and sorting of the G protein-coupled receptor CXCR4. *Dev Cell.*, **5**, 709-22.

Martin, N.P., Lefkowitz, R.J. and Shenoy, S.K. (2003) Regulation of V2 vasopressin receptor degradation by agonist-promoted ubiquitination. *J Biol Chem.*, **278**, 45954-9. Epub 2003 Sep 5.

Mayor, S., Presley, J.F. and Maxfield, F.R. (1993) Sorting of membrane components from endosomes and subsequent recycling to the cell surface occurs by a bulk flow process. *J Cell Biol.*, **121**, 1257-69.

McNatt, M.W., McKittrick, I., West, M. and Odorizzi, G. (2007) Direct binding to Rsp5 mediates ubiquitin-independent sorting of Sna3 via the multivesicular body pathway. *Mol Biol Cell.*, **18**, 697-706. Epub 2006 Dec 20.

Moore, R.H., Tuffaha, A., Millman, E.E., Dai, W., Hall, H.S., Dickey, B.F. and Knoll, B.J. (1999) Agonist-induced sorting of human beta2-adrenergic receptors to lysosomes during downregulation. *J Cell Sci.*, **112**, 329-38.

Oestreich, A.J., Aboian, M., Lee, J., Azmi, I., Payne, J., Issaka, R., Davies, B.A. and Katzmann, D.J. (2007) Characterization of multiple multivesicular body sorting determinants within Sna3: a role for the ubiquitin ligase Rsp5. *Mol Biol Cell.*, **18**, 707-20. Epub 2006 Dec 20.

Parola, A.L., Lin, S. and Kobilka, B.K. (1997) Site-specific fluorescence labeling of the beta2 adrenergic receptor amino terminus. *Anal Biochem.*, **254**, 88-95.

Raiborg, C., Rusten, T.E. and Stenmark, H. (2003) Protein sorting into multivesicular endosomes. *Curr Opin Cell Biol*, **15**, 446-55.

Rands, E., Candelore, M.R., Cheung, A.H., Hill, W.S., Strader, C.D. and Dixon, R.A. (1990) Mutational analysis of beta-adrenergic receptor glycosylation. *J Biol Chem.*, **265**, 10759-64.

Reggiori, F. and Pelham, H.R. (2001) Sorting of proteins into multivesicular bodies: ubiquitin-dependent and -independent targeting. *Embo J*, **20**, 5176-86.

Shenoy, S.K., McDonald, P.H., Kohout, T.A. and Lefkowitz, R.J. (2001) Regulation of receptor fate by ubiquitination of activated beta 2- adrenergic receptor and beta-arrestin. *Science*, **294**, 1307-13.

Slagsvold, T., Pattni, K., Malerod, L. and Stenmark, H. (2006) Endosomal and non-endosomal functions of ESCRT proteins. *Trends Cell Biol.*, **16**, 317-26. Epub 2006 May 22.

Sorkin, A. and Von Zastrow, M. (2002) Signal transduction and endocytosis: close encounters of many kinds. *Nat Rev Mol Cell Biol*, **3**, 600-14.

Tanowitz, M. and Von Zastrow, M. (2002) Ubiquitination-independent trafficking of G protein-coupled receptors to lysosomes. *J Biol Chem.*, **277**, 50219-22. Epub 2002 Oct 24.

Tanowitz, M. and von Zastrow, M. (2003) A novel endocytic recycling signal that distinguishes the membrane trafficking of naturally occurring opioid receptors. *J Biol Chem.*, **278**, 45978-86. Epub 2003 Aug 25.

Tota, M.R. and Strader, C.D. (1990) Characterization of the binding domain of the beta-adrenergic receptor with the fluorescent antagonist carazolol. Evidence for a buried ligand binding site. *J Biol Chem.*, **265**, 16891-7.

Trejo, J. and Coughlin, S.R. (1999) The cytoplasmic tails of protease-activated receptor-1 and substance P receptor specify sorting to lysosomes versus recycling. *J Biol Chem.*, **274**, 2216-24.

Tsao, P.I. and von Zastrow, M. (2000) Type-specific sorting of G protein-coupled receptors after endocytosis. *J Biol Chem*, **275**, 11130-40.

Vargas, G.A. and Von Zastrow, M. (2004) Identification of a novel endocytic recycling signal in the D1 dopamine receptor. *J Biol Chem.*, **279**, 37461-9. Epub 2004 Jun 10.

Wang, Y., Zhou, Y., Szabo, K., Haft, C.R. and Trejo, J. (2002) Down-regulation of protease-activated receptor-1 is regulated by sorting nexin 1. *Mol Biol Cell*, **13**, 1965-76.

Watson, H. and Bonifacino, J.S. (2007) Direct Binding to Rsp5p Regulates Ubiquitination-independent Vacuolar Transport of Sna3p. *Mol Biol Cell*, **1**, 1.

Whistler, J.L., Enquist, J., Marley, A., Fong, J., Gladher, F., Tsuruda, P., Murray, S.R. and Von Zastrow, M. (2002) Modulation of postendocytic sorting of G protein-coupled receptors. *Science*, **297**, 615-20.

Williams, R.L. and Urbe, S. (2007) The emerging shape of the ESCRT machinery. *Nat Rev Mol Cell Biol.*, **8**, 355-68.

2.8 Figures

Figure 1. B_2AR-HA undergoes agonist-induced ubiquitination, B_2AR-0k-HA does not.

A, HEK293 cells stably expressing F-B_2AR-HA or F-B_2AR-0k-HA were stimulated with 10μM isoproterenol for the indicated time period before extraction and Immunoprecipitation with rabbit anti-FLAG antibody, and SDS-PAGE separation. Shown is a representative anti-ubiquitin blot for the F-B_2AR-HA (left) and F-B_2AR-0k-HA (right). Also shown is the same blot stripped and reprobed with anti-FLAG (M2) – HRP to show the relative size of the major receptor species. Each lane of the ubiquitin blot was analyzed by densitometry. B, Quantification of ubiquitin immunoreactivity after agonist addition and immunopreceiptation of receptor, expressed as a ratio of untreated cells, F-B_2AR-HA (■), F-B_2AR-0k-HA (□). Data was pooled from 4 independent experiments.

Figure 2. Mutation of lysine residues does not influence internalization or recycling of B_2AR

A, Fluorescent microscopy to show recycling. HEK293 cells were plated on coverslips and fed M1-488 anti-FLAG antibody (a, d, g, j) before treatment with isoproterenol for 30 minutes (b, e, h, k) and subsequent agonist washout and treatment with alprenolol for 60 minutes (c, f, i, l). B, HEK293 cells stably expressing FLAG-tagged receptors were fed with M1 anti-FLAG antibody and stimulated for 30 minutes with 10 μM isoproterenol, before lifting and staining with Alexa-488 anti-mouse antibody, and FACS analysis to determine surface receptors remaining. Data is expressed as a percentage

internalized (100 – (percent of surface receptor in untreated cells)), n=4. C, after 30 minutes isoproterenol treatment, cells were washed in fresh media and incubated for 60 minutes with 10 μM alprenolol to allow recycling. Data shown is the percentage of internalized receptor (A) that is recycled, n=4. * = statistical difference from B_2AR, ** = statistical difference from B_2AR-0k as determined by t test.

Figure 3. Agonist induced proteolysis of B_2AR-HA and B_2AR-0k-HA in HEK293 cells

A, HEK293 cells were stimulated at 37°C with 10μM isoproterenol for the indicated time period before extraction and detection by immunoblotting. Shown is a representative anti-FLAG Western blot of F-B_2AR-HA. B, Quantification of receptor immunoreactivity at various times after agonist addition (determined by densitometry of blots exposed in the linear range) expressed as a percentage of immunoreactivity in untreated cells, data is pooled from three independent experiments. C, blots were stripped and reprobed with anti-HA antibody to determine C-terminal degradation. D-F, The corresponding experiments were performed using cells expressing F-B_2AR-0k-HA.

Figure 4. B_2AR-HA and B_2AR-0k-HA undergo agonist induced proteolysis in lysosomes

A, HEK293 cells stably expressing FLAG-tagged B_2AR-HA or FLAG-tagged B_2AR-0k-HA were biotinylated according to methods to label surface receptors and were then pretreated for 30 minutes with a lysosome inhibitor (ZPAD) or proteosome inhibitor (epoximicin), and then incubated at 37°C in the presence or absence of isoproterenol for three hours, in the continued presence of the inhibitor. Cells were lysed and lysates incubated overnight with strepavidin beads, before SDS-PAGE and immunoblotting.

Shown is a representative anti-FLAG blot. B, quantification of receptor immunoreactivity was determined by densitometry, Bars represent the fraction of FLAG-immunoreactivity remaining after 3 hours agonist treatment as compared to untreated cells (control = white bars, ZPAD = black bars, epoximicin = gray bars). C, the localization of internalized F-B_2AR-HA (i) relative to the late endosomal marker, LAMP2 (ii) visualized 60 minutes after the addition of agonist (as described under methods). The merged image is shown in iii, where colocalized structures appear yellow. D, the corresponding experiment performed using cells expressing F-B_2AR-0k-HA

Figure 5. Overexpression of myc-HRS inhibits proteolysis of both B_2AR-HA and B_2AR-0k-HA

A, HEK293 cells stably expressing FLAG-tagged B_2AR-HA were transfected with myc-HRS and cultured for a further 24 hours before biotinylation (see methods) to label surface receptors, and then incubated at 37^{o}C in the presence or absence of isoproterenol for one and three hours. Cells were lysed and lysates incubated overnight with streptavidin beads, before SDS-PAGE and immunoblotting. Shown is a representative anti-FLAG blot. B, quantification of receptor immunoreactivity was determined by densitometry, Bars represent the fraction of FLAG-immunoreactivity remaining after 1 and 3 hours agonist treatment as compared to untreated cells. C and D, the corresponding experiment performed using cells expressing F-B_2AR-0k-HA

Figure 6. Overexpression of Vps4 mutants inhibits proteolysis of both B_2AR-HA and B_2AR-0k-HA

A, HEK293 cells stably expressing FLAG-tagged B_2AR-HA were transfected with GFP, Vps4K173Q-GFP or Vps4E228Q-GFP and cultured for a further 24 hours before biotinylation (see methods) to label surface receptors, and then incubated at 37^{o}C in the presence or absence of isoproterenol for one and three hours. Cells were lysed and lysates incubated overnight with strepavidin beads, before SDS-PAGE and immunoblotting. Shown is a representative anti-FLAG blot. B, quantification of receptor immunoreactivity was determined by densitometry, Bars represent the fraction of FLAG-immunoreactivity remaining after 3 hours agonist treatment as compared to untreated cells. C and D, the corresponding experiment performed using cells expressing F-B_2AR-0k-HA

Figure 7. Agonist induced proteolysis of B_2AR and B_2AR -0k in HEK293 cells

HEK293 cells stably expressing F-B_2AR or F-B_2AR-0k were plated in 12-well plates and stimulated at 37^{o}C with 10μM isoproterenol for the indicated time period before extraction and detection by immunoblotting. Shown is a representative anti-FLAG Western blot of F-B_2AR (A) and F-B_2AR-0k (B). C, Quantification of receptor immunoreactivity at various times after agonist addition (determined by densitometry of blots exposed in the linear range) expressed as a percentage of immunoreactivity in untreated cells, data is pooled from three independent experiments.

Figure 8. Both recycling and non-recycling B_2AR downregulate at a similar rate irrespective of ubiquitination.

HEK293 cells stably expressing FLAG-tagged receptors were treated for 24 hours with 10 μM isoproterenol. Before freeze thawing and ligand binding with [^{3}H]Dihydroalprenolol to determine the amount of receptor remaining. Data is expressed as a percentage of radioligand bound to untreated cells. n=3-4

Fig.1

A

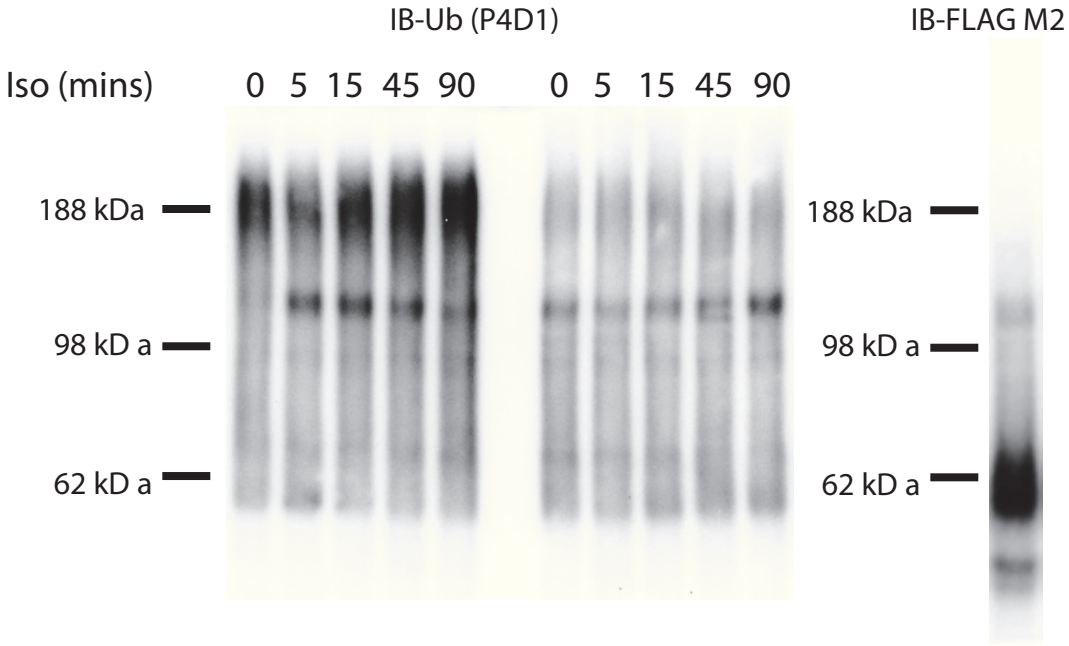
IB-Ub (P4D1)
IB-FLAG M2
Iso (mins)
0 5 15 45 90 0 5 15 45 90
188 kDa
98 kD a
62 kD a
188 kDa
98 kD a
62 kD a

B

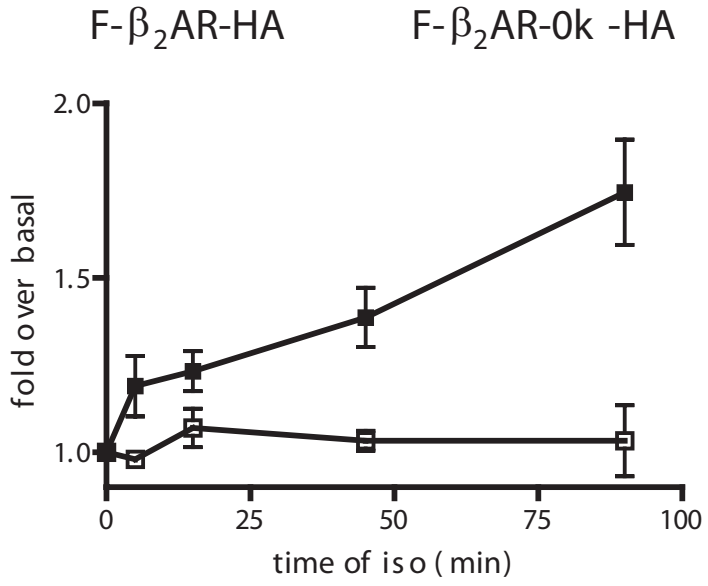
F-β2AR-HA
F-β2AR-0k -HA
2.0
1.5
1.0
fold over basal
0
25
50
75
100
time of iso (min)

Fig.2

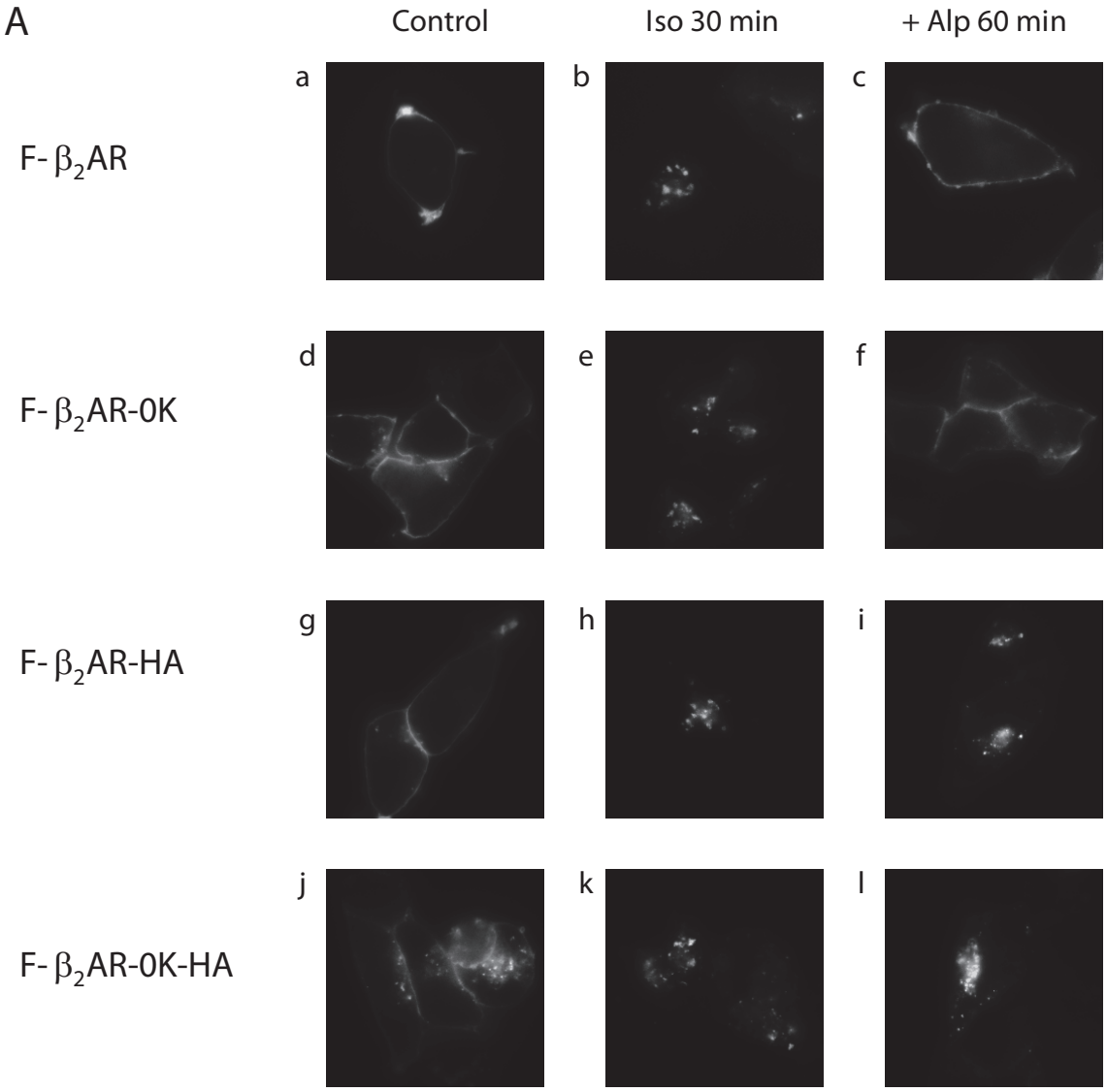
A
Control
Iso 30 min
+ Alp 60 min
a
b
c
F-β2AR
d
e
f
F-β2AR-0K
g
h
i
F-β2AR-HA
j
k
l
F-β2AR-0K-HA

B

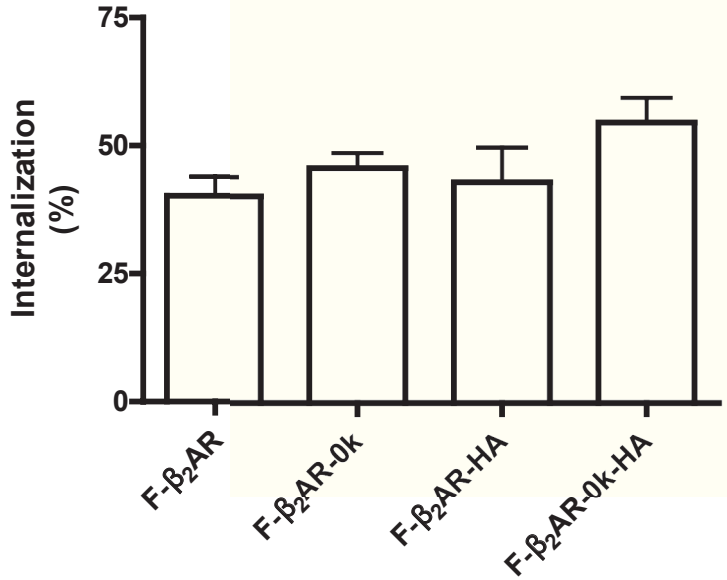
75
50
25
0
Internalization (%)
F-β2AR
F-β2AR-0k
F-β2AR-HA
F-β2AR-0k-HA

C

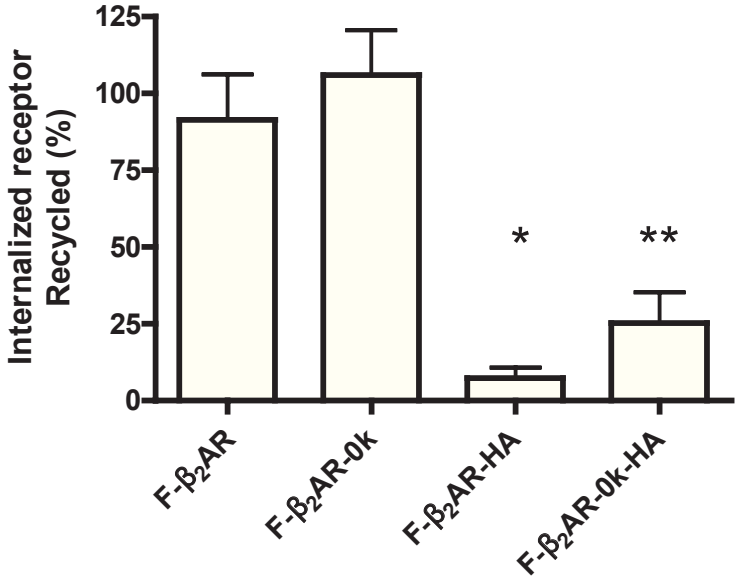
125
100
75
50
25
0
Internalized receptor Recycled (%)
*
**
F-β2AR
F-β2AR-0k
F-β2AR-HA
F-β2AR-0k-HA

Fig.3

A

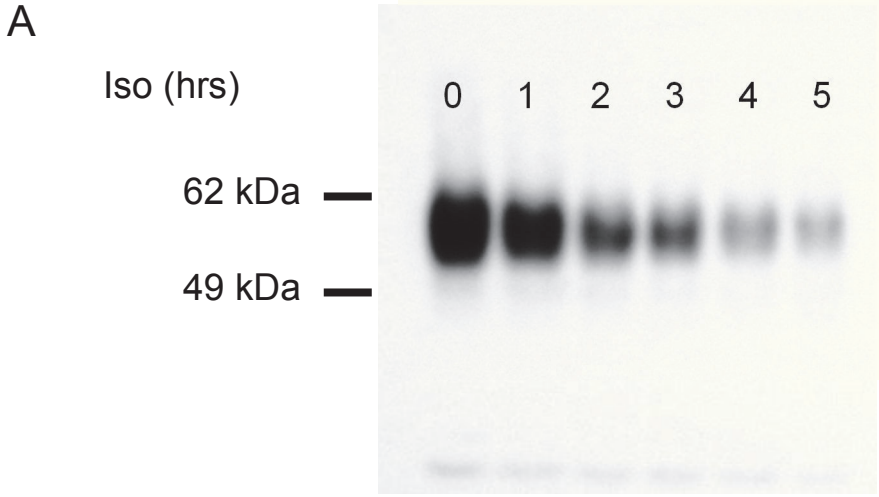
Iso (hrs)
0 1 2 3 4 5
62 kDa
49 kDa

B

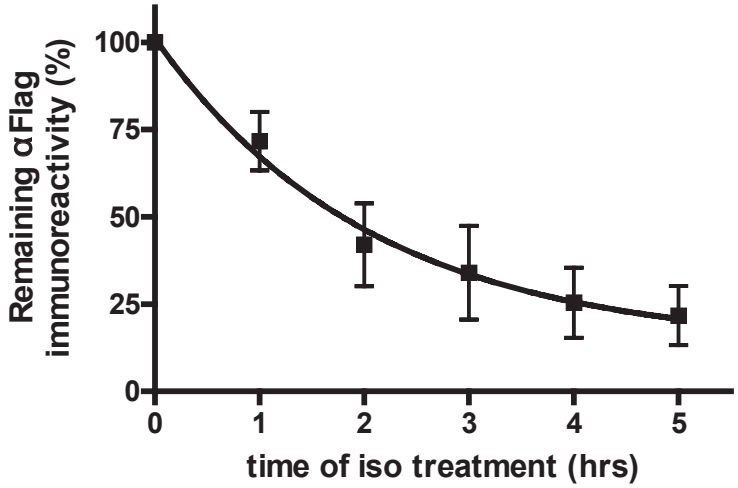
Remaining αFlag immunoreactivity (%)
100
75
50
25
0
0 1 2 3 4 5
time of iso treatment (hrs)

C

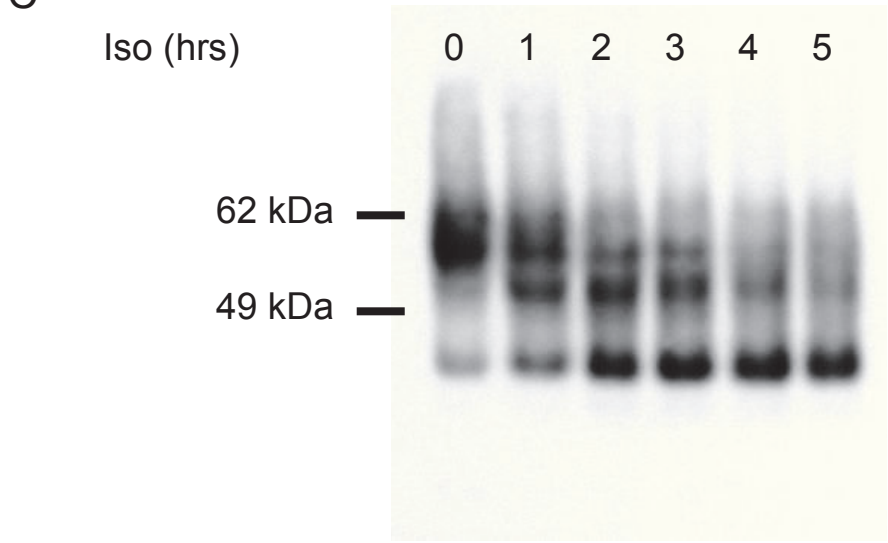
Iso (hrs)
0 1 2 3 4 5
62 kDa
49 kDa

D

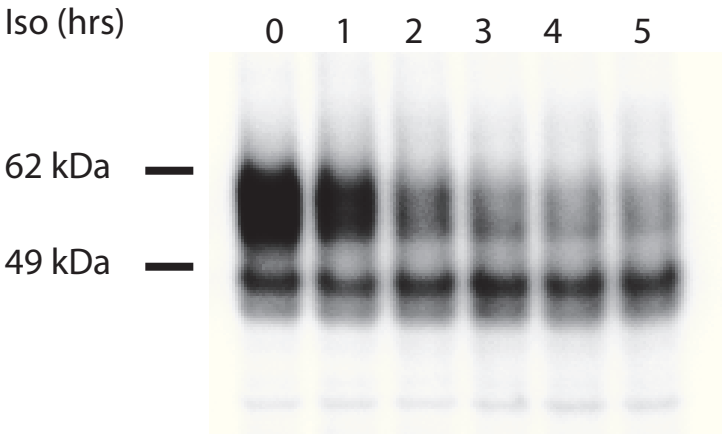
Iso (hrs)
0 1 2 3 4 5
62 kDa
49 kDa

E

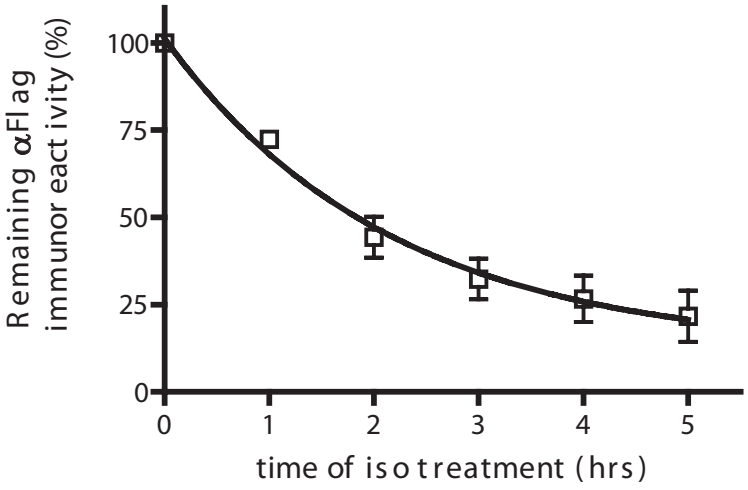
Remaining αFlag immunoreactivity (%)
100
75
50
25
0
0 1 2 3 4 5
time of iso treatment (hrs)

F

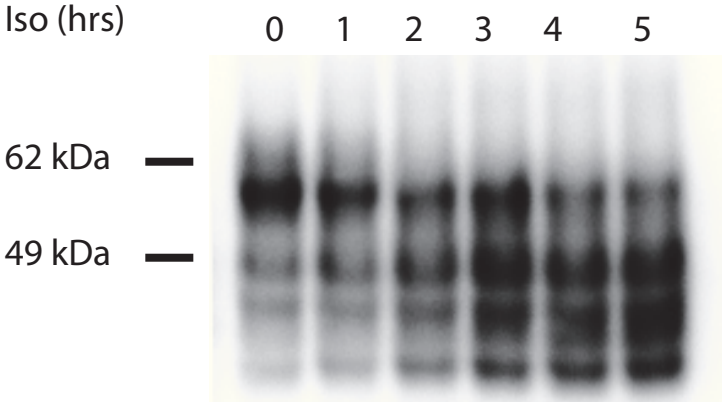
Iso (hrs)
0 1 2 3 4 5
62 kDa
49 kDa

Fig.4

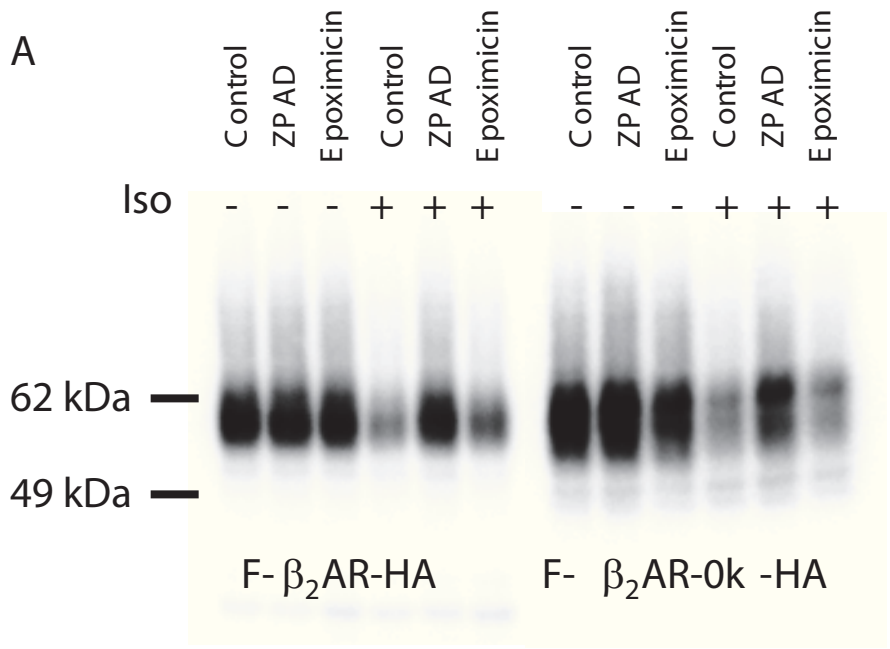
A
Control
ZPAD
Epoximicin
Control
ZPAD
Epoximicin
Control
ZPAD
Epoximicin
Control
ZPAD
Epoximicin
Iso
- - - + + + - - - + + +
62 kDa
49 kDa
F-β2AR-HA
F- β2AR-0k -HA

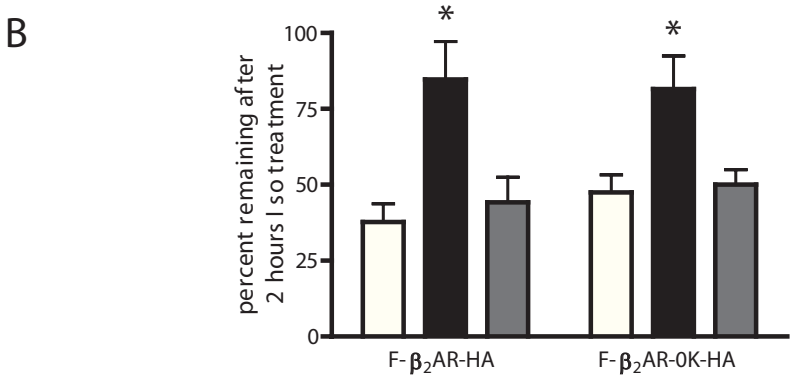
B
percent remaining after 2 hours Iso treatment
100
75
50
25
0
*
*
F-β2AR-HA
F-β2AR-0K-HA

C

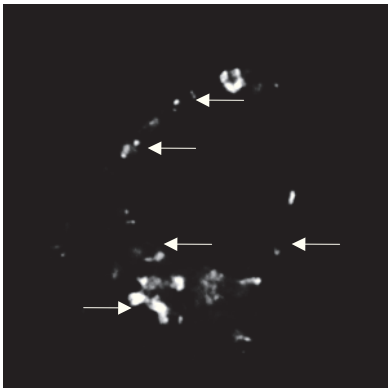

F- β_2AR-HA

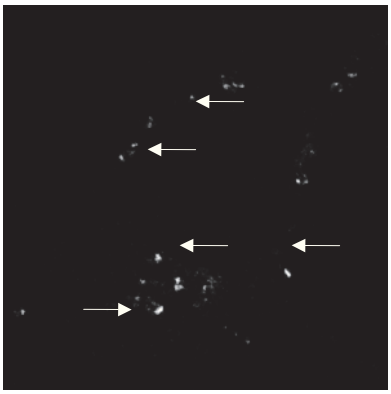

LAMP2

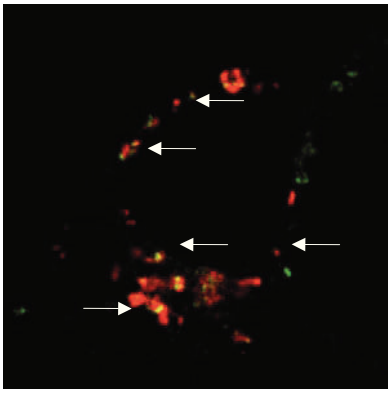

Merge

D

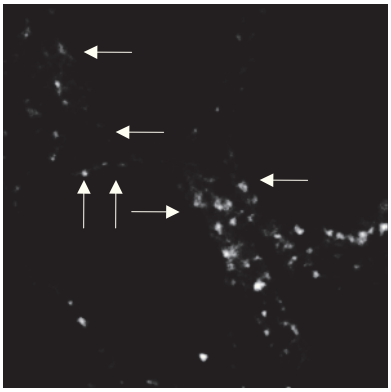

F- β_2AR-0k -HA

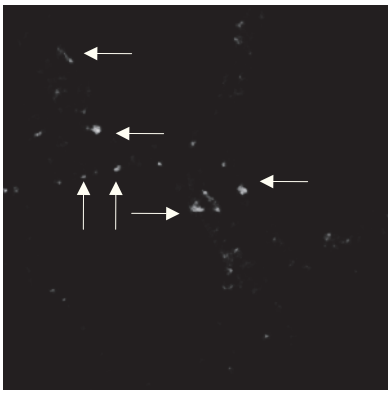

LAMP2

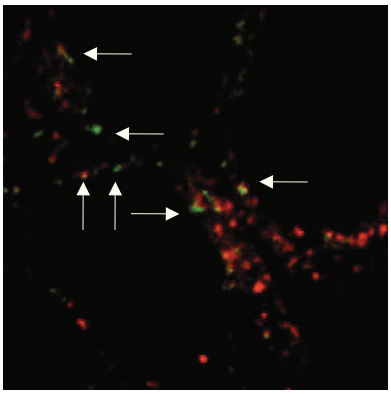

Merge

Fig.5

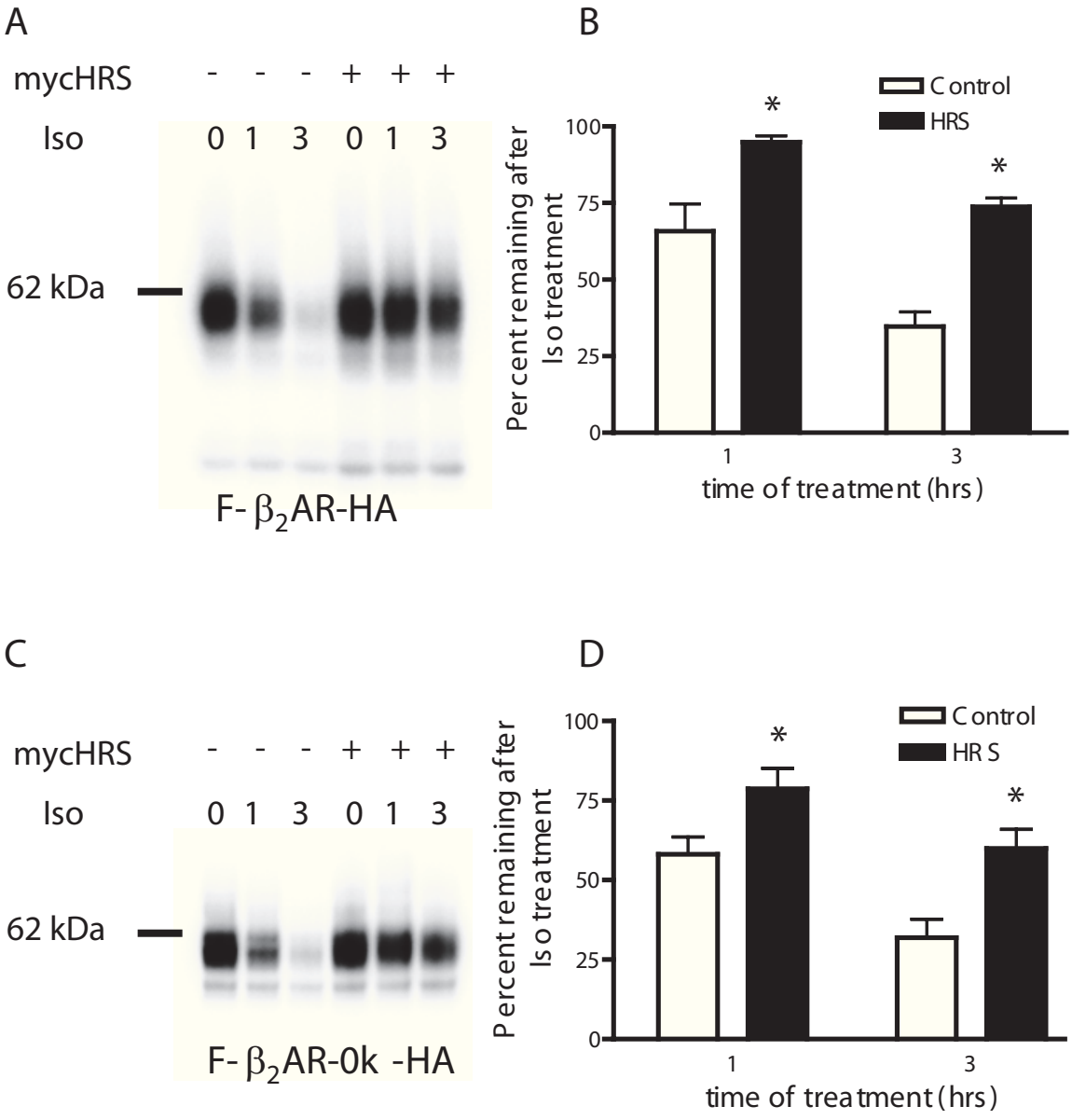
A
mycHRS - - - + + +
Iso 0 1 3 0 1 3
62 kDa
F-β2AR-HA
B
Control
HRS
Percent remaining after Iso treatment
100
75
50
25
0
*
*
1
3
time of treatment (hrs)
C
mycHRS - - - + + +
Iso 0 1 3 0 1 3
62 kDa
F-β2AR-0k -HA
D
Control
HRS
Percent remaining after Iso treatment
100
75
50
25
0
*
*
1
3
time of treatment (hrs)

Fig.6

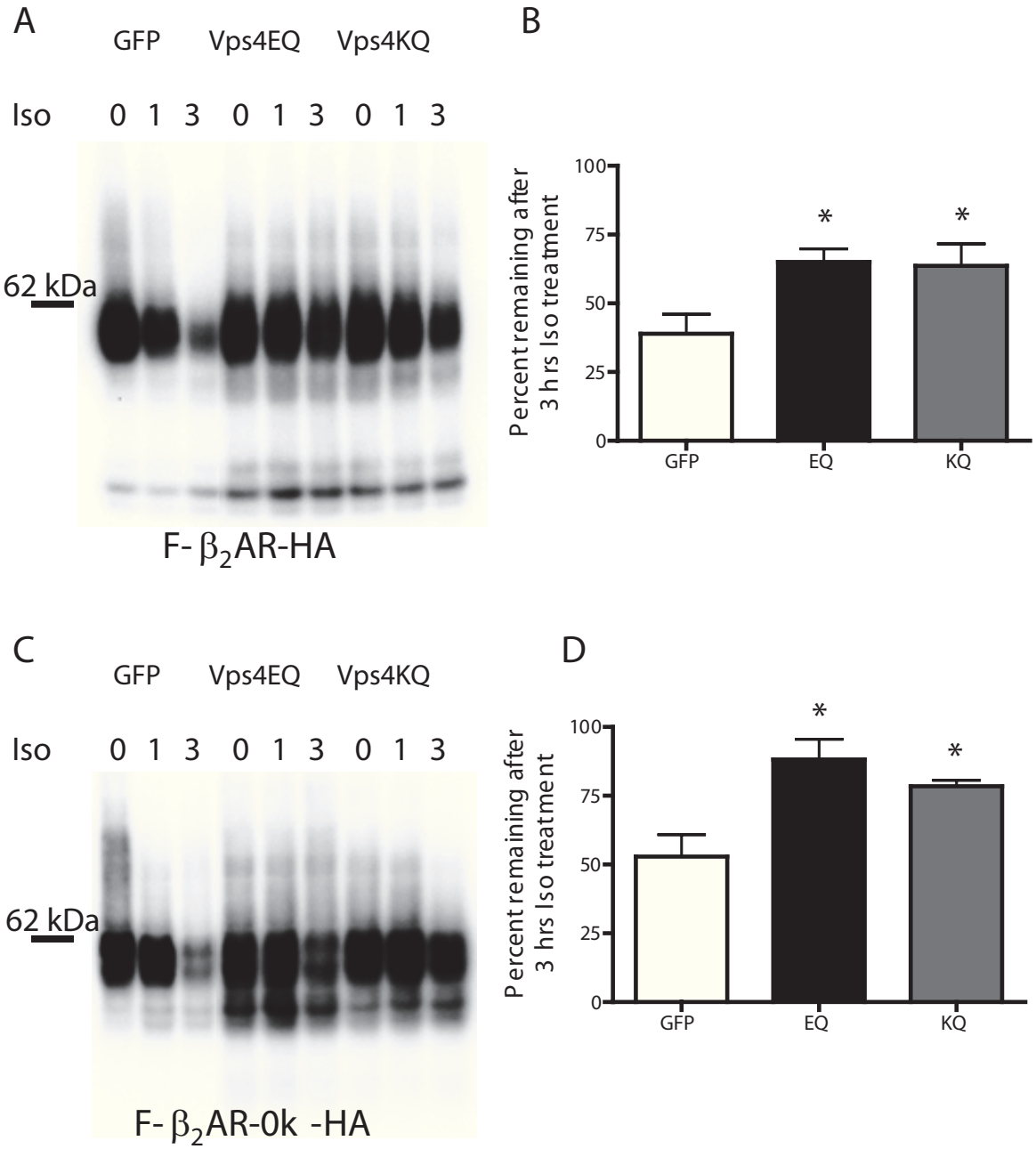
A
GFP
Vps4EQ
Vps4KQ
Iso
0 1 3 0 1 3 0 1 3
62 kDa
F-β2AR-HA
B
Percent remaining after 3 hrs Iso treatment
100
75
50
25
0
*
*
GFP
EQ
KQ
C
GFP
Vps4EQ
Vps4KQ
Iso
0 1 3 0 1 3 0 1 3
62 kDa
F-β2AR-0k -HA
D
Percent remaining after 3 hrs Iso treatment
100
75
50
25
0
*
*
GFP
EQ
KQ

Fig.7

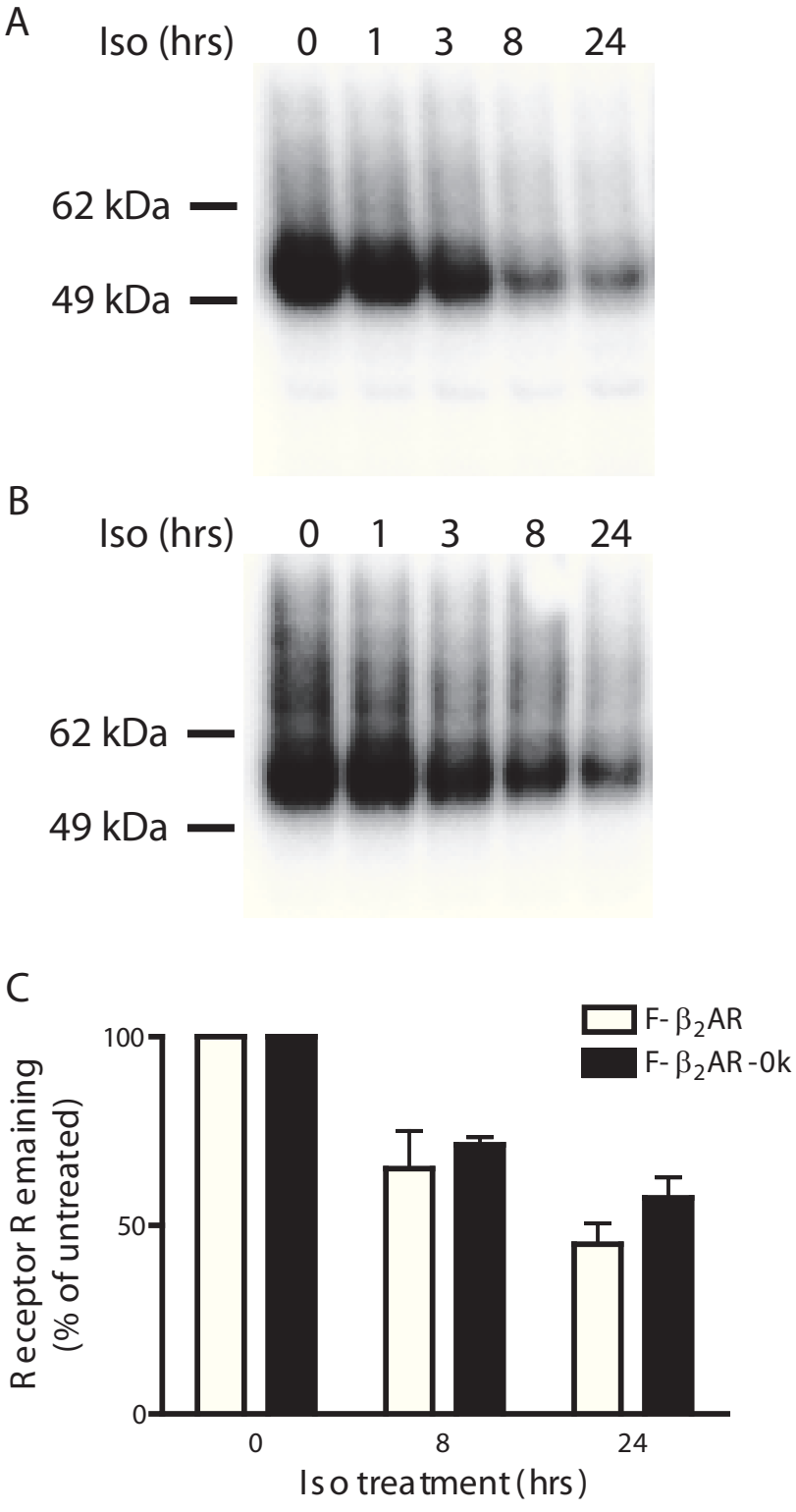
A
Iso (hrs) 0 1 3 8 24
62 kDa
49 kDa
B
Iso (hrs) 0 1 3 8 24
62 kDa
49 kDa
C
F-β2AR
F-β2AR-0k
Receptor Remaining (% of untreated)
100
50
0
0
8
24
Iso treatment (hrs)

Fig.8

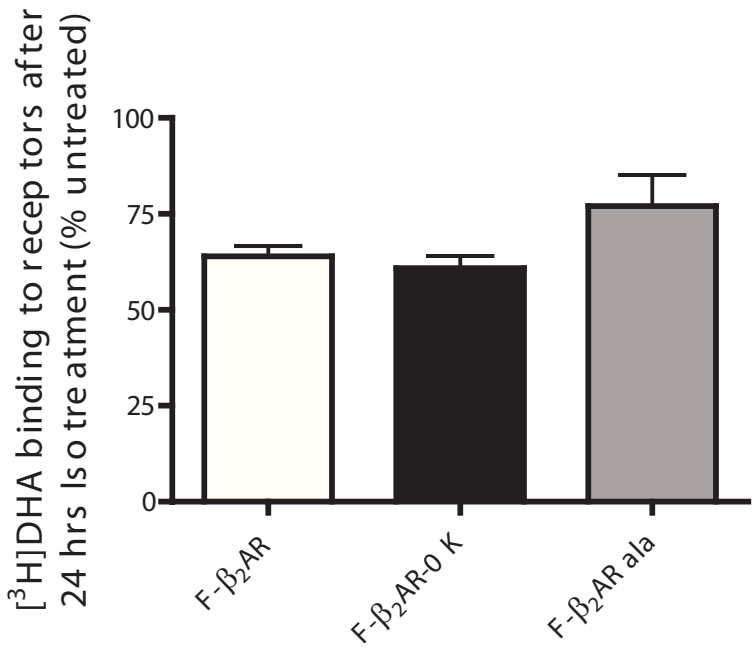
[3H]DHA binding to receptors after 24 hrs Isotreatment (% untreated)
100
75
50
25
0
F-β2AR
F-β2AR-0 K
F-β2AR ala

Chapter 3:

Sequence-Dependent Sorting of Recycling Proteins by Actin-Stabilized Endosomal Microdomains

Paul Temkin contributed data to Figure S1 and provided consultation during the experimental and writing process. The majority of other experiments were conceived and executed by Manoj Puthenveedu of the von Zastrow lab. Additional contributions were made by Benjamin Lauffer (UCSF), Rachel Vistein (Carnegie Mellon), Peter Carlton (UCSF), Kurt Thorn (UCSF), Jack Taunton (UCSF), Orion D. Weiner (UCSF), and Robert G. Parton (The University of Queensland).

3.1 Abstract

The functional consequences of signaling receptor endocytosis are determined by the endosomal sorting of receptors between degradation and recycling pathways. How receptors recycle efficiently, in a sequence-dependent manner that is distinct from bulk membrane recycling, is not known. Here, in live cells, we visualize the sorting of a prototypical sequence-dependent recycling receptor, the beta-2 adrenergic receptor, from bulk recycling proteins and the degrading delta-opioid receptor. Our results reveal a remarkable diversity in recycling routes at the level of individual endosomes, and indicate that sequence-dependent recycling is an active process mediated by distinct endosomal sub-domains distinct from those mediating bulk recycling. We identify a specialized subset of tubular microdomains on endosomes, stabilized by a highly localized but dynamic actin machinery, that mediate this sorting, and provide evidence that these actin-stabilized domains provide the physical basis for a two-step kinetic and affinity-based model for protein sorting into the sequence-dependent recycling pathway.

3.2 Introduction

Cells constantly internalize a large fraction of proteins from their surface and the extracellular environment. The fates of these internalized proteins in the endosome have a direct impact on several critical functions of the cell, including its response to environmental signals (Lefkowitz et al., 1998; Marchese et al., 2008, Sorkin and von Zastrow, 2009).

Internalized proteins have three main fates in the endosome. First, many membrane proteins, such as the transferrin receptor (TfR), are sorted away from soluble proteins, largely by bulk membrane flow back to the cell surface. This occurs via the formation and fission of narrow tubules that have a high ratio of membrane surface area (and therefore membrane proteins) to volume (soluble contents) (Mayor et al., 1993). Several proteins have been implicated in the formation of these tubules (Shinozaki-Narikawa et al., 2006; Cullen, 2008; Traer et al., 2007), which provide a geometric basis to bulk recycling and explain how nutrient receptors can recycle leaving soluble nutrients behind to be utilized in the lysosome (Dunn and Maxfield, 1992; Mayor et al., 1993; Maxfield and McGraw, 2004). Second, many membrane proteins are transported to the lysosome to be degraded. This involves a process called involution, where proteins are packaged into vesicles that bud off to the interior of the endosome and, in essence, converts these proteins into being a part of the soluble contents (Piper and Katzmann, 2007). Involution has also been studied extensively, and the machinery responsible, termed ESCRT complex, identified (Hurley, 2008; Saksena et al., 2007; Williams and Urbe, 2007). Third, several other membrane proteins, such as many signaling receptors,

escape the bulk recycling and degradation pathways, and are instead recycled in a regulated manner (Hanyaloglu and von Zastrow, 2008; Yudowski et al., 2009). This requires a specific cis-acting sorting sequence present on the receptor's cytoplasmic surface (Cao et al., 1999; Hanyaloglu and von Zastrow, 2008). How receptors use these sequences to escape the involution pathway and recycle, though they are excluded from the default recycling pathway (Maxfield and McGraw, 2004; Hanyaloglu et al., 2005), is a fundamental cell biological question that is still unanswered.

Although it is clear that different recycling cargo can travel through discrete endosomal populations (Maxfield and McGraw, 2004), endosome-to-plasma membrane recycling from a single endosome is generally thought to occur via a uniform population of tubules. Contrary to this traditional view, we identify specialized endosomal tubular domains mediating sequence-dependent recycling that are kinetically and biochemically distinct from the domains that mediate bulk recycling. These domains are stabilized by a local actin cytoskeleton that is required and sufficient for receptor recycling. We propose that such specialized actin-stabilized domains provide the physical basis for overcoming a kinetic barrier for receptor entry into endosomal tubules and for affinity-based concentration of proteins in the sequence-dependent recycling pathway.

3.3 Results

Visualization of receptor sorting in the endosomes of living cells

The beta 2-adrenergic receptor (B2AR) and the delta opioid receptor (DOR) provide excellent models for physiologically relevant proteins that are sorted from each other in the endosome. Although they share endocytic pathways, B2AR is recycled efficiently in a sequence-dependent manner while DOR is selectively degraded in the lysosome (Cao et al., 1999; Whistler et al., 2002). To study the endosomal sorting of these cargo molecules, we started by testing whether tubulation was involved in this process. Because such sorting has not been observed *in vivo,* we first attempted to visualize the dynamics of receptor sorting in live HEK293 cells expressing fluorescently labeled B2AR or DOR receptors, using high-resolution confocal microscopy. Both receptors were observed mostly on the cell surface before isoproterenol or DADLE, their respective agonists, were added. After agonist addition, both B2AR (Fig 1A) and DOR (not shown) were robustly internalized, and appeared in endosomes within 5 min (Fig 1A and movie S1). As a control, receptors did not internalize in cells not treated with agonists, but imaged for the same period of time (Fig S1A). The B2AR-containing endosomes colocalized with the early endosome markers Rab5 (Fig S1B) and EEA1 (not shown), consistent with previous data.

Internalized B2AR (Fig 1B), but not DOR (Fig 1C), also labeled tubules that extended from the main body of the receptor. When receptor fluorescence was quantified across multiple B2AR-containing tubules, we saw that receptors were enriched in these

tubules compared to the rest of the endosomal limiting membrane (Fig 1D). The bulk recycling protein TfR, in contrast, was not enriched in endosomal tubules (Fig 1D). This suggests that sequence-dependent recycling receptors are enriched by an active mechanism in these endosomal tubules.

These endosomal tubules were preferentially enriched for B2AR over DOR on the same endosome. In cells co-expressing FLAG-tagged B2AR and GFP-tagged DOR, we observed endosomes that contained both receptors within 5 min after co-applying isoproterenol and DADLE. Notably, these endosomes extruded tubules that contained B2AR but not detectable DOR (e.g. in Fig 1E, another e.g. in movie S2). Fluorescence traces across the endosome and the tubule confirmed that DOR was not detectable in these B2AR tubules, suggesting that B2AR was specifically sorted into these tubular domains (e.g. in Fig 1F). When linear pixel values from multiple sorting events were quantified, B2AR was enriched ~50% in the endosomal domains from which tubules originate, compared to the endosomal membrane outside these domains (Fig 1G). Thus, these experiments resolve, for the first time, individual events that mediate sorting of two signaling receptors in the endosomes of live cells.

B2AR-containing endosomal tubules deliver receptors to the cell surface.

To test whether these tubules mediated recycling of B2AR, we visualized direct delivery of receptors from these tubules to the cell surface. In endosomes containing internalized B2AR and DOR, these tubular domains pinched off vesicles that contained B2AR but not detectable levels of DOR (Fig 2A, and another e.g. in movie S3). To reliably assess if these vesicles traveled to the surface and fused with the plasma

membrane, we combined our current imaging with a method that we have used previously to visualize individual vesicle fusion events mediating surface receptor delivery (Yudowski et al., 2006). Briefly, we attached the pH-sensitive GFP variant superecliptic pHluorin to the extracellular domain of B2AR (SpH-B2AR) (Miesenbock et al., 1998). SpH-B2AR is highly fluorescent when exposed to the neutral pH at the cell surface, but is quenched in the acidic environments of endosomes and intracellular vesicles. This allows the detection of individual fusion events of vesicles containing B2AR at the cell surface (Yudowski et al., 2009). In cells co-expressing SpH-B2AR and B2AR labeled with a pH-insensitive fluorescent dye (Alexa-555), vesicles derived from the endosomal tubules trafficked to the cell surface and fused, as seen by a sudden increase in SpH fluorescence followed by loss of fluorescence due to diffusion (Fig 2B, and another e.g in movie S4). A fluorescence trace from movie S4 confirmed the fusion and loss of B2AR fluorescence (Fig 2C). Also, Rab4 and Rab11, which function in endosome-to-plasma membrane recycling (Zerial and McBride, 2001, Maxfield and McGraw, 2004), were localized to the domains containing B2AR (Fig S1). Together, this indicates that the B2AR-containing endosomal tubules mediate delivery of B2AR to the cell surface.

B2AR-containing tubules are marked by a highly localized actin cytoskeleton

We next examined whether the B2AR-containing microdomains were biochemically distinct from the rest of the endosomal membrane. We first focused on actin, as the actin cytoskeleton is required for efficient recycling of B2AR but not of TfR (Cao et al., 1999; Gage et al., 2005), and as it has been implicated in endosome motility

(Stamnes, 2002; Girao et al., 2008) and vesicle scission at the cell surface (Yarar et al., 2005; Perrais and Merrifield, 2005; Kaksonen et al., 2005). Strikingly, in cells co-expressing B2AR and actin-GFP, actin was concentrated on the endosome specifically on the tubular domains containing B2AR (Fig 3A). Virtually every B2AR tubule observed showed this specific actin concentration on the tubule (n=350). As with actin, coronin-GFP (Uetrecht and Bear, 2006), an F-actin binding protein, also localized specifically to the B2AR-containing tubules on endosomes (Fig 3B), confirming that this was a polymerized actin cytoskeleton. Coronin was also observed on the B2AR-containing vesicle that was generated by dynamic scission of the B2AR tubule (Fig 3B, movie S5). Fluorescence traces of the linear pixels across the tubule and the vesicle confirmed that coronin pinched off with the B2AR vesicle (Fig 3C).

We also used two separate techniques to characterize actin localization on these tubules beyond the ~250 nm resolution offered by conventional microscopy. First, we first imaged the localization of coronin on endosomes containing B2AR tubules using structured illumination microscopy (Gustafsson et al., 2008), which resolves structures at 50 - 100 nm spatial resolution. 3D stacks obtained using this high-resolution technique confirmed that coronin was specifically localized on the endosomal tubule that contained B2AR (Fig 3D, and movie S6). Second, we examined the morphology of actin on endosomal tubules at the ultrastructural level by pre-embedding immunoelectron microscopy. Actin was clearly labeled as filaments lying along tubules extruded from endosomal structures (Fig 3E).

Actin is dynamically turned over on the B2AR-containing endosomal tubules

We then tested whether the actin filaments on these tubules were a stable structure or were dynamically turned over. When cells expressing actin-GFP were exposed to latrunculin, a drug that prevents actin polymerization, endosomal actin fluorescence became indistinguishable from the 'background' cytoplasmic fluorescence within 16-18 seconds after drug exposure (e.g. in Fig 4A). When quantified across multiple cells, endosomal actin fluorescence showed an exponential loss after latrunculin exposure, with a $t_{1/2}$ of 3.5 sec (99% Confidence Interval= 3.0 to 4.1 sec) (Fig 4B), indicating that endosomal actin turned over quite rapidly. As a control, stress fibers, which are composed of relatively stable capped actin filaments, were turned over more slowly in these same cells (e.g. in Fig S2A). Endosomal actin was lost in >98% of cells within 30 seconds after latrunculin, in contrast to stress fibers, which persisted for over 2 minutes in >98% of cells (Fig S2B). Rapid turnover of endosomal actin was also independently confirmed by Fluorescence Recovery After Photobleaching (FRAP) studies. When a single endosomal actin spot was bleached, the fluorescence recovered rapidly within 20 seconds (Fig 4C). As a control for more stable actin filaments, stress fibers showed little recovery of fluorescence after bleaching in this interval (Fig 4C). Exponential curve fits yielding a $t_{1/2}$ of 8.26 sec (99% CI= 7.65 to 8.97 sec), consistent with rapid actin turnover (Fig 4D). In contrast, only part of the fluorescence (~30%) was recovered in stress fibers in the same cells by 20 sec, with curve fits yielding a $t_{1/2}$ of 50.35 sec (99% CI= 46.05 to 55.54 sec). These results indicate that actin is dynamically assembled on the B2AR recycling tubules.

Considering the rapid turnover of actin, we next explored the machinery responsible for localizing actin at the tubule. The Arp2/3 complex is a major nucleator of

dynamic actin polymerization that has been implicated in polymerization-based endosome motility (Stamnes, 2002; Girao et al., 2008; Pollard, 2007). Arp3, an integral part of the Arp2/3 complex useful for visualizing this complex in intact cells (Merrifield et al., 2004), was specifically concentrated at the base of the B2AR tubules on the endosome (e.g. in Fig 4E and fluorescence trace in Fig 4F, movie S7). Every B2AR tubule observed had a corresponding Arp3 spot at its base (n= 200). Surprisingly, however, we did not see N-WASP and WAVE-2, canonical members of the two main families of Arp2/3 activators (Millard et al., 2004), on the endosome (Fig 4G). Similarly, we did not see endosomal recruitment of activated Cdc42, as assessed by a previously characterized GFP-fusion reporter consisting of the GTPase binding domain of N-WASP (Benink and Bement, 2005) (not shown). All three proteins were readily detected at lamellipodia and filopodia as expected, indicating that the proteins were functional in these cells. While we cannot rule out a weak or transitory interaction of these activators with Arp2/3 at the endosome, the lack of enrichment prompted us to test for alternate Arp2/3 activators. Cortactin, an Arp- and actin- binding protein present on endosomes, has been proposed to be such an activator (Kaksonen et al., 2000; Millard et al., 2004; Daly, 2004). Cortactin-GFP was clearly concentrated at the base of the B2AR tubule on the endosome (Fig 4G), in a pattern identical to Arp2/3. When quantified (>200 endosomes each), every B2AR tubule was marked by cortactin, while none of the endosomes showed detectable N-WASP, WAVE-2, or Cdc42. Similarly, the WASH protein complex, which has been recently implicated in trafficking from the endosome (Derivery et al., 2009; Gomez and Billadeau, 2009; Duleh and Welch, 2010), was also clearly localized to B2AR tubules (Fig 4G). Together, these data suggest that an Arp2/3-,

cortactin- and WASH-based machinery mediates dynamic actin assembly on the endosome.

B2AR-containing tubules are a specialized subset of recycling tubules on the endosome

Since the traditional view is that the endosomal tubules that mediate direct recycling to the plasma membrane are a uniform population, we next tested whether these tubules were the same as those that recycle bulk cargo. When B2AR recycling was visualized along with bulk recycling of TfR, endosomes containing both cargo typically extruded three to four tubules containing TfR. Strikingly, however, only one of these contained detectable amounts of B2AR (Example in Fig 5A, quantified in Fig 5B). This was consistent with fast 3D confocal live cell imaging of B2AR in endosomes, which showed that most endosomes extruded only one B2AR containing tubule, with a small fraction containing two. When quantified, only 24.4% of all TfR tubules contained detectable B2AR (n= 358 tubules).

B2AR tubules are a kinetically and biochemically distinct from bulk recycling tubules.

When the lifetimes of tubules were quantified, the majority (>80%) of B2AR tubules lasted more than 30 seconds. In contrast, the majority of TfR tubules devoid of B2AR lasted less than 30 seconds (Fig 5B and C, movie S8). Each endosome extruded several tubules containing TfR, only a subset (~30%) of which were marked by actin, coronin, or cortactin (Fig 5D and E, arrows). Time-lapse movies indicated that the highly transient TfR-containing tubules were extruded from endosomal domains that were lacking cortactin (Fig 5E, arrows), while the relatively stable B2AR containing tubules

were marked by cortactin (Fig 5E, arrowheads). Importantly, the relative stability of the subset of tubules was conferred by the actin cytoskeleton, as disruption of actin using latrunculin virtually abolished the stable fraction of TfR tubules (Fig 5B and C). Together, these results suggest that sequence-dependent recycling of B2AR is mediated by specialized tubules that are kinetically and biochemically distinct from the bulk recycling tubules containing only TfR,

A kinetic model for sorting of B2AR into a subset of endosomal tubules.

The relative stability of B2AR tubules suggested a simple model, based on kinetic sorting, for how sequence-dependent cargo was sorted into a specific subset of tubules and excluded from the transient TfR-containing bulk-recycling tubules. We hypothesized that B2AR diffuses more slowly on the endosomal membrane relative to bulk recycling cargo. The short lifetimes of the bulk-recycling tubules would then create a kinetic barrier for B2AR entry, while this barrier would be overcome in the subset of tubules stabilized by actin.

To test the key prediction of this model, that B2AR diffuses more slowly than TfR on the endosomal membrane, we directly measured the diffusion rates of B2AR and TfR using FRAP. When B2AR or TfR was bleached on a small part of the endosomal membrane, B2AR fluorescence took significantly longer to recover than TfR (Fig 5F). When quantified, the rate of recovery of fluorescence of B2AR ($t_{1/2}$= 25.77 sec, 99% CI 23.45 to 28.6 sec) was ~4 times slower than that of TfR ($t_{1/2}$= 6.21 sec, 99% CI 5.49 to 7.17 sec), indicating that B2AR diffuses significantly slower on the endosomal membrane than TfR (Fig 5F and G). Neither B2AR or TfR recovered within the time

analyzed when the whole endosome was bleached (Fig 5H), confirming that the recovery of fluorescence was due to diffusion from the un-bleached part of the endosome and not due to delivery of new receptors via trafficking. Further, B2AR on the plasma membrane diffused much faster than on the endosome ($t_{1/2}$= 6.45 sec, 99% CI 5.62 to 7.66 sec), comparable to TfR, suggesting that B2AR diffusion was slower specifically on the endosome (Fig 5H).

We next tested whether the diffusion of B2AR into endosomal tubules was slower than that of TfR, by using the rate of increase of B2AR fluorescence as an index of receptor entry into tubules. B2AR fluorescence continuously increased throughout the duration of the tubule lifetimes (Fig S3A). Further, in a single tubule containing TfR and B2AR, TfR fluorescence reached its maximum at a markedly faster rate than that of B2AR (Fig S3B). Together, these results suggest that slow diffusion of B2AR on the endosome and stabilization of recycling tubules by actin can provide a kinetic basis for specific sorting of sequence-dependent cargo into subsets of endosomal tubules.

Local actin assembly is required for B2AR entry into the subset of tubules

Because actin stabilizes the B2AR-containing subset of tubules, the model predicts that endosomal actin would be required for sequence-dependent concentration of B2AR into these tubules. Consistent with this, B2AR was no longer concentrated in endosomal tubules when endosomal actin was acutely removed using latrunculin (e.g. in Fig 6A). When the pixel fluorescence along the limiting membrane of multiple endosomes was quantified, B2AR was distributed more uniformly along the endosomal membrane in the absence of actin (Fig 6B-C). We further confirmed this by comparing

the variance in B2AR fluorescence along the endosomal perimeter, irrespective of their orientation. B2AR fluorescence was significantly more uniform in endosomes without actin (Fig 6D), indicating that actin was required for endosomes to concentrate B2AR in microdomains. Less than 20% of endosomes showed B2AR-containing tubules in the absence of endosomal actin, in contrast to control cells where over 75% of endosomes showed B2AR-containing tubules (Fig 6E). Further, cytochalasin D, a barbed-end capping drug that prevents further actin polymerization but does not actively cause depolymerization, also inhibited B2AR entry into tubules (Fig 6E) and B2AR surface recycling (Fig S4A). Neither TfR tubules on endosomes (Fig 6E) nor TfR recycling (Fig S4B) was inhibited by actin depolymerization, consistent with a role for actin specifically in sequence-dependent recycling of B2AR (Cao et al., 1999). Further, depletion of cortactin using siRNA (Fig 6F) also inhibited B2AR entry into tubules (Fig 6G and H). This inhibition was specific to cortactin depletion, as it was rescued by exogenous expression of cortactin (Fig 6H). Together, these results indicate that a localized actin cytoskeleton concentrates sequence-dependent recycling cargo into a specific subset of recycling tubules on the endosome.

B2AR sorting into the recycling subdomains is mediated by its C-terminal PDZ-interacting domain.

We next asked whether this actin-dependent concentration of receptors into endosomal tubules depended on the PDZ-interacting sequence present in the B2AR cytoplasmic tail that mediates sequence-dependent recycling (Cao et al., 1999; Gage et al., 2005). To test if the sequence was required, we used a mutant B2AR (B2AR-ala) in

which the recycling sequence was specifically disrupted by the addition of a single alanine (Cao et al., 1999). Unlike B2AR, internalized B2AR-ala was not able to enter the tubular domains in the endosome (e.g. in Fig 6I, quantified in Fig 6J), or recycle to the cell surface (Fig S4). To test if this sequence was sufficient, we used a chimeric DOR construct with the B2AR-derived recycling sequence fused to its cytoplasmic tail, termed DOR-B2 (Gage et al., 2005), which recycles much more efficiently than DOR (Fig S4). In contrast to DOR, which showed little concentration in endosomal tubules, DOR-B2 entered tubules (Fig 6I and J) and recycled in an actin-dependent manner similar to B2AR (Fig S4D). Together, these results indicate that the PDZ-interacting recycling sequence on B2AR was both required and sufficient to mediate concentration of receptors in the actin-stabilized endosomal tubular domains.

As PDZ-domain interactions have been established to indirectly link various integral membrane proteins to cortical actin (Fehon et al., 2010), we tested whether linking DOR to actin was sufficient to drive receptor entry into endosomal tubules. Remarkably, fusion of the actin-binding domain of the ERM protein ezrin (Turunen et al., 1994) to the C-terminus of DOR was sufficient to localize the receptor (termed DOR-ABD) to endosomal tubules (Fig 6J). The surface recycling of B2AR, DOR-B2, and DOR-ABD were dependent on the presence of an intact actin cytoskeleton (Fig S4), consistent with previous publications (Cao et al., 1999; Gage et al., 2005; Lauffer et al., 2009). Further, transplantation of the actin-binding domain was also sufficient to specifically confer recycling to a version of B2AR lacking its native recycling signal (Fig S4F). These results indicate that the concentration of B2AR in the actin-stabilized recycling tubules is mediated by linking receptors to the local actin cytoskeleton through

PDZ interactions.

3.4 Discussion

Even though endocytic receptor sorting was first appreciated over two decades ago (e.g., Brown et al., 1983; Farquhar, 1983; Steinman et al., 1983), our understanding of the principles of this process has been limited. A major reason for this has been the lack of direct assays to visualize signaling receptor sorting in the endosome. Here we directly visualized, in living cells, endosomal sorting between two prototypic members of the largest known family of signaling receptors for which sequence-specific recycling is critical for physiological regulation of cell signaling (Pippig et al., 1995; Lefkowitz et al., 1998; Xiang and Kobilka, 2003). We resolve sorting at the level of single trafficking events on individual endosomes, and define a kinetic and affinity-based model for how sequence-dependent receptors are sorted away from bulk-recycling and degrading proteins.

By analyzing individual sorting and recycling events on single endosomes, we demonstrate a remarkable diversity in recycling pathways emanating from the same organelle (Scita and Di Fiore, 2010). The traditional view has been that recycling to the plasma membrane is mediated by a uniform set of endosomal tubules from a single endosome. In contrast to this view, we demonstrate that the recycling pathway is highly specialized, and that specific cargo can segregate into specialized subsets of tubules that are biochemically, biophysically, and functionally distinct. Receptor recycling plays a critical role in controlling the rate of cellular re-sensitization to signals (Lefkowitz et al., 1998; Sorkin and von Zastrow, 2009), and recent data suggest that the sequence-dependent recycling of signaling receptors is selectively controlled by signaling pathways

(Yudowski et al., 2009). The physical separation between bulk and sequence-dependent recycling that we demonstrate here allows for such selective control without affecting the recycling of constitutively cycling nutrient receptors. Further, such physical separation might also reflect the differences in molecular requirements that have been observed between bulk and sequence-dependent recycling (Hanyaloglu and von Zastrow, 2007).

Endosome-associated actin likely plays a dual role in endosomal sorting, both of which contribute to sequence-dependent entry of cargo selectively into special domains. First, by stabilizing the specialized endosomal tubules relative to the much more dynamic tubules that mediate bulk recycling, the local actin cytoskeleton could allow sequence-dependent cargo to overcome a kinetic barrier that limits their entry into the bulk pathway. Supporting this, we show that most endosomal tubules are highly transient, lasting less than a few seconds (Fig 5B and C), which allows enough time for entry of the fast-diffusing bulk recycling cargo, but not the slow-diffusing sequence-dependent cargo (Fig 5F and G), into these tubules. A subset of these tubules representing the sequence-dependent recycling pathway is stabilized by the presence of an actin cytoskeleton (Fig 5B and C). This stabilization allows time for B2AR to diffuse into these tubules (Fig S3), which eventually pinch off membranes that can directly fuse with the plasma membrane (Fig 2). Interestingly, inhibition of actin caused a decrease in the total number of tubules by approximately 25% (Fig 5B), suggesting that the actin cytoskeleton plays a role in maintaining the B2AR-containing subset of tubules, and not just in the sorting of B2AR into these tubules.

Second, a local actin cytoskeleton could provide the machinery for active concentration of recycling proteins like the B2AR, which interact with actin-associated sorting proteins (ERM and ERM-binding proteins) through C-terminal sequences (Weinman et al., 2006; Wheeler et al., 2007; Lauffer et al., 2009, Fehon et al., 2010), in specialized recycling tubules. Consistent with this, the C-terminal sequence on B2AR was both required and sufficient for sorting to the endosome and for recycling, and a distinct actin-binding sequence was sufficient for both receptor entry into tubules and recycling (Fig 6 and Fig S4). PDZ-interacting sequences have been identified on several signaling receptors, including multiple GPCRs, with different specificities for distinct PDZ-domain proteins (Weinman et al., 2006). Further, actin-stabilized subsets of tubules were present even in the absence of B2AR in the endosome. We propose that, using a combination of kinetic and affinity-based sorting principles, discrete Actin-Stabilized SEquence-dependent Recycling Tubule (ASSERT) domains could thus mediate efficient sorting of sequence-dependent recycling cargo away from both degradation and bulk recycling pathways that diverge from the same endosomes.

Our results, therefore, uncover an additional role for actin polymerization in endocytic sorting, separate from its role in endosome motility. It will be interesting to investigate the mechanism and signals that control the nucleation of such a spatially localized actin cytoskeleton on the endosome. The lack of obvious concentration of the canonical Arp2/3 activators, WASP and WAVE, suggests a novel mode of actin nucleation involving cortactin. Cortactin can act as a nucleation-promoting factor for Arp2/3, at least *in vitro* (Ammer and Weed, 2008), and can interact with dynamin (Schafer et al., 2002; McNiven et al., 2000), which makes it an attractive candidate for

coordinating actin dynamics on membranes. Interestingly, inhibition of WASH, a recently described Arp regulator that is present on B2AR tubules, has been reported to result in an increase in endosomal tubules (Derivery et al., 2009). Although its role in sequence-dependent recycling remains to be tested, this suggests the presence of multiple actin-associated proteins with distinct functions on the endosome.

The simple kinetic and affinity-based principle that we propose likely provides a physical basis for sequence-dependent sorting of internalized membrane proteins between essentially opposite fates in distinct endosomal domains. Proteins that bind sequence-dependent degrading receptors and are required for their degradation (Whistler et al., 2002; Marley and von Zastrow, 2010) might act as scaffolds and provide a similar kinetic barrier to prevent them from accessing the rapid bulk-recycling tubules. Entry of these receptors into the involution pathway might then be accelerated by their association with the well-characterized ESCRT-associated domains on the vacuolar portion of endosomes (Hurley, 2008; Saksena et al., 2007; Williams and Urbe, 2007), complementary to the presently identified ASSERT domains on a subset of endosomal tubules.

Such diversity at the level of individual trafficking events to the same destination from the same organelle raises the possibility that there exists yet further specialization amongst the pathways that mediate exit out of the endosome, including in the degradative pathway and the retromer-based pathway to the trans-Golgi network. Importantly, the physical separation in pathways that we report here potentially allows for cargo-mediated regulation as a mode for controlling receptor recycling to the plasma membrane. Such a mechanism can provide virtually an unlimited level of selectivity in the post-endocytic

system using minimal core trafficking machineries, as has been observed for endocytosis at the cell surface (Puthenveedu and von Zastrow, 2006). As the principles of such sorting depend critically on kinetics, the high-resolution imaging used here to analyze domain kinetics and biochemistry, and to achieve single-event resolution in living cells, provides a powerful method to elucidate biologically important sorting processes in the future.

3.5 Materials and Methods

Constructs and reagents:

Receptor constructs and stably transfected HEK293 cell lines are described previously (Gage et al., 2005, Lauffer et al., 2009) Transfections were performed using Effectene (Qiagen) according to manufacturer's instructions. For visualizing receptors, FLAG-tagged receptors were labeled with M1 antibodies (Sigma) conjugated with Alexa-555 (Invitrogen) as described (Gage et al., 2005), or fusion constructs were generated where receptors were tagged on the N-terminus with GFP. Latrunculin and Cytochalasin D (Sigma) were used at 10μM final concentration.

Live cell and fluorescence imaging:

Cells were imaged using a Nikon TE-2000E inverted microscope with a 100x 1.49 NA TIRF objective (Nikon) and a Yokagawa CSU22 confocal head (Solamere), or an Andor Revolution XD Spinning disk system on a Nikon Ti microscope. A 488nm Ar laser and a 568nm Ar/Kr laser (Melles Griot), or 488nm and 561nm solid-state lasers (Coherent) were used as light sources. Cells were imaged in Opti-MEM (Gibco) with 2% serum and 30 mM HEPES pH 7.4, maintained at 37˚C using a temperature-controlled incubation chamber. Time lapse images were acquired with a Cascade II EM-CCD camera (Photometrics) driven by MicroManager (www.micro-manager.org) or an Andor iXon+ EM-CCD camera using iQ (Andor). The same lasers were used as sources for bleaching in FRAP experiments. Structured illumination microscopy was performed as described earlier (Gustafsson et al., 2008).

Electron microscopy:

EM studies were carried out using MDCK cells because they are amenable to a previously described pre-embedding processing that facilitates detection of cytoplasmic actin filaments (Ikonen et al., 1996; Parton et al., 1991), and because they contain morphologically similar endosomes to HEK293 cells. Cells were grown on polycarbonate filters (Transwell 3412; Costar, Cambridge, MA) for 4 days as described previously (Parton et al., 1991). To allow visualization of early endosomes and any associated filaments a pre-embedding approach was employed. Cells were incubated with HRP (Sigma type II, 10mg/ml) in the apical and basolateral medium for 10min at 37°C and then washed, perforated, and immunogold labeled with a rabbit anti- actin antibody, a gift of Professor Jan de Mey (Strasbourg), followed by 9nm protein A-gold. HRP visualization and epon embedding was as described previously (Parton et al., 1991, Ikonen et al., 1996).

Image and data analysis:

Acquired image sequences were saved as 16-bit tiff stacks, and quantified using ImageJ (http://rsb.info.nih.gov/ij/). For estimating receptor enrichment, a circular mask 5 px in diameter was used to manually select the membrane at the base of the tubule or membranes derived from endosomes. Fluorescence values measured were normalized to that of the endosomal membrane devoid of tubules. An area of the coverslip lacking cells was used to estimate background fluorescence. For estimating linear pixel values along the tubules, a line selection was drawn along the tubule and across the endosome, and the Plot Profile function used to measure pixel values. For obtaining the average value plot across multiple sorting events, the linear pixels were first normalized to the diameter of

the endosome and then averaged. To generate pixel values along the endosomal limiting membranes, the Oval Profile plugin, with 60 segments, was used after manually selecting the endosomal membrane using an oval ROI. Lifetimes of tubules were calculated by manually tracking the extension and retraction of tubules over time-lapse series. Microsoft Excel was used for simple data analyses and graphing. Curve fits of data were performed using GraphPad Prism. All P-values are from two-tailed Mann-Whitney tests unless otherwise noted.

3.6 Acknowledgements

The majority of the imaging was performed at the Nikon Imaging Center at UCSF. We thank David Drubin, Matt Welch, John Sedat, Aylin Hanyaloglu, Aaron Marley, and James Hislop for essential reagents and valuable help. M.A.P was supported by a K99/R00 grant DA024698, M.v.Z by an R37 grant DA010711, and O.D.W by an RO1 grant GM084040, all from the NIH. J.T. is an investigator of the Howard Hughes Medical Institute.

3.7 References

Ammer, A.G., and Weed, S.A. (2008). Cortactin branches out: roles in regulating protrusive actin dynamics. Cell Motil Cytoskeleton *65*, 687-707.

Brown, M.S., Anderson, R.G., Goldstein, J.L. (1983). Recycling receptors: the round-trip itinerary of migrant membrane proteins. Cell *32*, 663-7.

Benink, H.A., and Bement, W.M. (2005). Concentric zones of active RhoA and Cdc42 around single cell wounds. J Cell Biol *168*, 429-39.

Cao, T.T., Deacon, H.W., Reczek, D., Bretscher, A., and von Zastrow, M. (1999). A kinase-regulated PDZ-domain interaction controls endocytic sorting of the β2-adrenergic receptor. Nature *401*, 286-290.

Cullen, P.J. (2008). Endosomal sorting and signalling: an emerging role for sorting nexins. Nat Rev Mol Cell Biol *9*, 574-82.

Daly, R.J. (2004). Cortactin signalling and dynamic actin networks. Biochem J *382*, 13-25.

Derivery, E., Sousa, C., Gautier, J.J., Lombard, B., Loew, D., and Gautreau, A. (2009). The Arp2/3 activator WASH controls the fission of endosomes through a large multiprotein complex. Dev Cell *17*, 712-23.

Duleh, S.N., and Welch, M.D. (2010). WASH and the Arp2/3 complex regulate endosome shape and trafficking. Cytoskeleton (Hoboken) *67*, 193-206.

Dunn, K.W., and Maxfield, F.R. (1992). Delivery of ligands from sorting endosomes to late endosomes occurs by maturation of sorting endosomes. Journal of Cell Biology *117*, 301-10.

Farquhar, M.G. (1983). Intracellular membrane traffic: pathways, carriers, and sorting devices. Methods Enzymol *98*, 1-13.

Fehon, R.G., McClatchey A.I., and Bretscher, A. (2010) Organizing the cell cortex: the role of ERM proteins. Nat Rev Mol Cell Biol. *11*, 276-87.

Gage, R.M., Matveeva, E.A., Whiteheart, S.W., and von Zastrow, M. (2005). Type I PDZ ligands are sufficient to promote rapid recycling of G Protein-coupled receptors independent of binding to N-ethylmaleimide-sensitive factor. J Biol Chem *280*, 3305-13.

Girao, H., Geli, M.I., and Idrissi, F.Z. (2008). Actin in the endocytic pathway: from yeast to mammals. FEBS Lett *582*, 2112-9.

Gomez, T.S., and Billadeau, D.D. (2009). A FAM21-containing WASH complex regulates retromer-dependent sorting. Dev Cell *17*, 699-711.

Gustafsson, M.G., Shao, L., Carlton, P.M., Wang, C.J., Golubovskaya, I.N., Cande, W.Z., Agard, D.A., and Sedat, J.W. (2008). Three-dimensional resolution doubling in wide-field fluorescence microscopy by structured illumination. Biophys J *94*, 4957-70.

Hanyaloglu, A.C., and von Zastrow, M. (2007). A novel sorting sequence in the beta2-adrenergic receptor switches recycling from default to the Hrs-dependent mechanism. J Biol Chem *282*, 3095-104.

Hanyaloglu, A.C., and von Zastrow, M. (2008). Regulation of GPCRs by endocytic membrane trafficking and its potential implications. Annu Rev Pharmacol Toxicol *48*, 537-68.

Hanyaloglu, A.C., McCullagh, E., and von Zastrow, M. (2005). Essential role of Hrs in a recycling mechanism mediating functional resensitization of cell signaling. Embo J *24*, 2265-83.

Hurley, J.H. (2008). ESCRT complexes and the biogenesis of multivesicular bodies. Curr Opin Cell Biol *20*, 4-11.

Ikonen, E., Parton, R.G., Lafont, F., and Simons, K. (1996). Analysis of the role of p200-containing vesicles in post-Golgi traffic. Mol Biol Cell *7*, 961-74.

Kaksonen, M., Peng, H.B., and Rauvala, H. (2000). Association of cortactin with dynamic actin in lamellipodia and on endosomal vesicles. J Cell Sci *113 Pt 24*, 4421-6.

Kaksonen, M., Toret, C.P., and Drubin, D.G. (2005). A modular design for the clathrin- and actin-mediated endocytosis machinery. Cell *123*, 305-20.

Lauffer, B.E., Chen, S., Melero, C., Kortemme, T., von Zastrow, M., and Vargas, G.A. (2009). Engineered protein connectivity to actin mimics PDZ-dependent recycling of G protein-coupled receptors but not its regulation by Hrs. J Biol Chem *284*, 2448-58.

Lefkowitz, R.J., Pitcher, J., Krueger, K., and Daaka, Y. (1998). Mechanisms of beta-adrenergic receptor desensitization and resensitization. Advances in Pharmacology *42*, 416-20.

Marchese, A., Paing, M.M., Temple, B.R., and Trejo, J. (2008). G protein-coupled receptor sorting to endosomes and lysosomes. Annu Rev Pharmacol Toxicol *48*, 601-29.

Marley, A., and von Zastrow, M. (2010). Dysbindin promotes the post-endocytic sorting of G protein-coupled receptors to lysosomes. PLoS One *5*, e9325.

Maxfield, F.R., and McGraw, T.E. (2004). Endocytic recycling. Nature reviews Molecular cell biology *5*, 121-32.

Mayor, S., Presley, J.F., and Maxfield, F.R. (1993). Sorting of membrane components from endosomes and subsequent recycling to the cell surface occurs by a bulk flow process. Journal of Cell Biology *121*, 1257-269.

McNiven, M.A., Kim, L., Krueger, E.W., Orth, J.D., Cao, H., and Wong, T.W. (2000). Regulated interactions between dynamin and the actin-binding protein cortactin modulate cell shape. J Cell Biol *151*, 187-98.

Merrifield, C.J., Qualmann, B., Kessels, M.M., and Almers, W. (2004). Neural Wiskott Aldrich Syndrome Protein (N-WASP) and the Arp2/3 complex are recruited to sites of clathrin-mediated endocytosis in cultured fibroblasts. Eur J Cell Biol *83*, 13-8.

Miesenbock, G., De Angelis, D.A., and Rothman, J.E. (1998). Visualizing secretion and synaptic transmission with pH-sensitive green fluorescent proteins. Nature *394*, 192-5.

Millard, T.H., Sharp, S.J., and Machesky, L.M. (2004). Signalling to actin assembly via the WASP (Wiskott-Aldrich syndrome protein)-family proteins and the Arp2/3 complex. Biochem J *380*, 1-17.

Parton, R.G., Dotti, C.G., Bacallao, R., Kurtz, I., Simons, K., and Prydz, K. (1991). pH-induced microtubule-dependent redistribution of late endosomes in neuronal and epithelial cells. J Cell Biol *113*, 261-74.

Perrais, D., and Merrifield, C.J. (2005). Dynamics of endocytic vesicle creation. Dev Cell *9*, 581-92.

Piper, R.C., and Katzmann, D.J. (2007). Biogenesis and function of multivesicular bodies. Annu Rev Cell Dev Biol *23*, 519-47.

Pippig, S., Andexinger, S., and Lohse, M.J. (1995). Sequestration and recycling of beta 2-adrenergic receptors permit receptor resensitization. Mol Pharmacol *47*, 666-76.

Pollard, T.D. (2007). Regulation of actin filament assembly by Arp2/3 complex and formins. Annu Rev Biophys Biomol Struct *36*, 451-77.

Puthenveedu, M.A., and von Zastrow, M. (2006). Cargo regulates clathrin-coated pit dynamics. Cell *127*, 113-24.

Saksena, S., Sun, J., Chu, T., and Emr, S.D. (2007). ESCRTing proteins in the endocytic pathway. Trends Biochem Sci *32*, 561-73.

Schafer, D.A., Weed, S.A., Binns, D., Karginov, A.V., Parsons, J.T., and Cooper, J.A. (2002). Dynamin2 and cortactin regulate actin assembly and filament organization. Curr Biol *12*, 1852-7.

Scita, G., and Di Fiore, P.P. (2010) The endocytic matrix. Nature *463*, 464-73

Shinozaki-Narikawa, N., Kodama, T., and Shibasaki, Y. (2006). Cooperation of phosphoinositides and BAR domain proteins in endosomal tubulation. Traffic *7*, 1539-50.

Sorkin, A., and von Zastrow, M. (2009). Endocytosis and signalling: intertwining molecular networks. Nat Rev Mol Cell Biol *10*, 609-22.

Stamnes, M. (2002). Regulating the actin cytoskeleton during vesicular transport. Curr Opin Cell Biol *14*, 428-33.

Steinman, R.M., Mellman, I.S., Muller, W.A., and Cohn, Z.A. (1983). Endocytosis and the recycling of plasma membrane. J Cell Biol *96*, 1-27

Traer, C.J., Rutherford, A.C., Palmer, K.J., Wassmer, T., Oakley, J., Attar, N., Carlton, J.G., Kremerskothen, J., Stephens, D.J., and Cullen, P.J. (2007). SNX4 coordinates endosomal sorting of TfnR with dynein-mediated transport into the endocytic recycling compartment. Nat Cell Biol *9*, 1370-80.

Turunen, O., Wahlström, T., and Vaheri, A. (1994). Ezrin has a COOH-terminal actin-binding site that is conserved in the ezrin protein family. J Cell Biol *126*, 1445-453.

Uetrecht, A.C., and Bear, J.E. (2006). Coronins: the return of the crown. Trends Cell Biol *16*, 421-26.

Weinman, E.J., Hall, R.A., Friedman, P.A., Liu-Chen, L.Y., and Shenolikar, S. (2006). The association of NHERF adaptor proteins with g protein-coupled receptors and receptor tyrosine kinases. Annu Rev Physiol *68*, 491-505.

Wheeler, D., Sneddon, W.B., Wang, B., Friedman, P.A., and Romero, G. (2007). NHERF-1 and the cytoskeleton regulate the traffic and membrane dynamics of G protein-coupled receptors. J Biol Chem *282*, 25076-87.

Whistler, J.L., Enquist, J., Marley, A., Fong, J., Gladher, F., Tsuruda, P., Murray, S., and von Zastrow, M. (2002). Modulation of Post-Endocytic Sorting of G Protein-Coupled Receptors. Science *297*, 615-620-.

Williams, R.L., and Urbe, S. (2007). The emerging shape of the ESCRT machinery. Nat Rev Mol Cell Biol *8*, 355-68-.

Xiang, Y., and Kobilka, B.K. (2003). Myocyte adrenoceptor signaling pathways. Science *300*, 1530-2-.

Yarar, D., Waterman-Storer, C.M., and Schmid, S.L. (2005). A dynamic actin cytoskeleton functions at multiple stages of clathrin-mediated endocytosis. Mol Biol Cell *16*, 964-75.

Yudowski, G.A., Puthenveedu, M.A., and von Zastrow, M. (2006). Distinct modes of regulated receptor insertion to the somatodendritic plasma membrane. Nat Neurosci *9*, 622-27.

Yudowski, G.A., Puthenveedu, M.A., Henry, A.G., and von Zastrow, M. (2009). Cargo-mediated regulation of a rapid Rab4-dependent recycling pathway. Mol Biol Cell *20*, 2774-784.

Zerial, M., and McBride, H. (2001). Rab proteins as membrane organizers. Nat Rev Mol Cell Biol *2*, 107-17.

3.8 Figures

Figure 1. B2AR is enriched in endosomal tubular domains devoid of DOR. A) HEK293 cells stably expressing FLAG-B2AR, labeled with fluorescently-tagged anti-FLAG antibodies, were followed by live confocal imaging before (left) and after 5 min (right) of isoproterenol treatment. Arrows show internal endosomes. B) Example endosomes showing tubular domains enriched in B2AR (arrowheads), with one enlarged in the inset. C) Examples of DOR endosomes. DOR is smoothly distributed on the endosomal membrane, and is not detected in tubules. D) Average fluorescence of B2AR (red circles) and TfR (green diamonds) calculated across multiple tubules (n= 123 for B2AR, 100 for TfR). B2AR shows a 50% enrichment over the endosomal membrane, while TfR is not enriched. Each point denotes an individual tubule, the bar denotes the mean, and the grey dotted line denotes the fluorescence of the endosomal membrane. E) An endosome containing both internalized B2AR and DOR, showing a tubule containing B2AR but no detectable DOR (arrowheads). F) Trace of linear pixel values across the same endosome, normalized to the maximum, confirms that the tubule is enriched for B2AR but not DOR. G) Linear pixel values of endosomal tubules averaged across 11 endosomes show specific enrichment of B2AR in tubules. Error bars are s.e.m. See also Fig S1 and movies S1 and S2.

Figure 2. Membranes derived from endosomal tubules deliver B2AR to the cell surface A) Frames from a representative time lapse series showing scission of a vesicle that contains B2AR but not detectable DOR, from an endosomal tubule. B) An image plane close to the plasma membrane in cells co-expressing SpH-B2AR and FLAG-B2AR

(labeled with Alexa555), exposed to isoproterenol for 5 min, and imaged by fast dual-color confocal microscopy. Arrows denote the FLAG-B2AR-containing membrane derived from the endosomal tubule that fuses. C) Fluorescence trace of the B2AR-containing membranes from the endosome in movie S4, showing the spike in SpH-B2AR fluorescence (fusion) followed by rapid loss of fluorescence. Scale bars are 1μm. See also Fig S1 and movies S3 and S4.

Figure 3. B2AR tubules are marked by a highly localized actin cytoskeleton. A) Cells co-expressing fluorescently labeled B2AR and actin-GFP exposed to isoproterenol for 5 min. The boxed area is enlarged in the inset, with arrowheads indicating specific concentration of actin on B2AR endosomal tubules. B) Time lapse series from an example endosome with B2AR and coronin-GFP. Coronin is detectable on the endosomal tubule (arrows) and on the vesicle (arrowheads) that buds off the endosome. C) A trace of linear pixel values across the same endosome, normalized to maximum fluorescence, shows coronin on the endosomal domain and the vesicle. D) Example structured illumination image of a B2AR endosome showing specific localization of coronin to a B2AR tubule (arrowheads) E) Electron micrograph of an HRP-positive endosome (arrow) showing actin filaments (labeled with 9nm gold, arrowheads) along a tubule. The right panel shows an enlarged view. See also movies S5 and S6.

Figure 4. Actin on B2AR tubules is dynamic and Arp2/3-nucleated. A) Cells expressing actin-GFP imaged live after treatment with 10 μM latrunculin for the indicated times, show rapid loss of endosomal actin. A time series of the boxed area, showing several endosomal actin loci, is shown at the lower panel. B) The change in

endosomal and cytoplasmic actin fluorescence over time after latrunculin normalized to initial endosomal actin fluorescence (n=10). One-phase exponential curve fits (solid lines) show a $t_{1/2}$ of 3.5 sec for actin loss (R^2= 0.984, d.f= 23, Sy.x= 2.1 for endosomal actin, R^2= 0.960, d.f= 23, Sy.x= 1.9 for cytoplasmic). Endosomal and cytoplasmc actin fluorescence becomes statistically identical within 15 sec after latrunculin. Error bars denote s.e.m. C) Time series showing FRAP of representative examples of endosomal actin (top) and stress fibers (bottom). D) Kinetics of FRAP of actin (mean ± s.e.m) quantified from 14 endosomes and 17 stress fibers. One-phase exponential curve fits (lines), show a $t_{1/2}$ of 8.26 sec for endosomal actin (R^2= 0.973, d.f= 34, Sy.x= 4.8) and 50.35 sec for stress fibers (R^2= 0.801, d.f= 34, Sy.x= 3.9). E) Example endosomes in live cells co-expressing B2AR and Arp3-GFP showing Arp3 at the base of B2AR tubules (arrowhead in the inset). F) Trace of linear pixel fluorescence of B2AR and Arp3 shows Arp3 specifically on the endosomal tubule. G) Example endosomes from cells co-expressing B2AR and N-WASP-, WAVE2-, cortactin-, or WASH-GFP. N-WASP and WAVE2 were not detected on endosomes, while cortactin and WASH were concentrated at the B2AR tubules (arrowheads). Scale bars are 1μm. See also Fig S2 and movie S7.

Figure 5. B2AR is enriched specifically in a subset of endosomal tubules that are stabilized by actin. A) A representative example of an endosome with two tubules containing TfR, only one of which is enriched for B2AR. B) The number of tubules with B2AR, TfR, and TfR in the presence of 10 μM latrunculin, per endosome per min, binned into lifetimes less than or more than 30 sec, quantified across 28 endosomes and 281 tubules. C) The percentages of B2AR, TfR, and TfR + latrunculin tubules with lifetimes less than or more than 30 sec, normalized to total number of tubules in each case. D) An

example endosome containing TfR and coronin, showing that coronin is present on a subset of the TfR tubules. Arrowheads indicate a TfR tubule that is marked by coronin, and arrows show a TfR tubule that is not. E) Time lapse series showing TfR-containing tubules extruding from endosomal domains without detectable cortactin. Arrowheads indicate a relatively stable TfR tubule that is marked by coronin, and arrows denote rapid transient TfR tubules without detectable cortactin. F) Frames from a representative time lapse movie showing FRAP of B2AR (top row) or TfR (bottom row). The circles mark the bleached area of the endosome. TfR fluorescence recovers rapidly, while B2AR fluorescence recovers slowly. G) Fluorescence recovery of B2AR (red circles) and TfR (green diamonds) on endosomes quantified from 11 experiments. Exponential fits (solid lines) show that B2AR fluorescence recovers with a $t_{1/2}$ of 25.77 sec (R^2= 0.83, d.f= 37, Sy.x= 6.3), while TfR fluorescence recovers with a $t_{1/2}$ of 6.21 sec (R^2= 0.91, d.f= 30, Sy.x= 7.1). H) Fluorescence recovery of B2AR (blue triangles) and TfR (green diamonds) on endosomes when the whole endosome was bleached, or of B2AR on the cell surface (red circles) quantified from 12 experiments. B2AR fluorescence on the surface recovers with a $t_{1/2}$ of 6.49 sec (R^2= 0.94, d.f= 27, Sy.x= 8.1). Error bars denote s.e.m. Scale bars are 1μm. See also Fig S3 and movie S8.

Figure 6. B2AR enrichment in tubules depends on endosomal actin and a PDZ-interacting sequence on the B2AR cytoplasmic domain. A) Representative fields from B2AR-expressing cells exposed to isoproterenol showing B2AR endosomes before (top panel) or after (bottom panel) exposure to 10 μM latrunculin for 5 min. Tubular endosomal domains enriched in B2AR (arrowheads) are lost upon exposure to latrunculin. B) Schematic of measurement of endosomal B2AR fluorescence profiles in

the limiting membrane. The profile was measured in a clockwise manner starting from the area diametrically opposite the tubule (an angle of 0˚). C) B2AR concentration along the endosomal membrane, calculated from fluorescence profiles of 20 endosomes, normalized to the average endosomal B2AR fluorescence. In the presence of latrunculin, B2AR enrichment in tubules is abolished, and B2AR fluorescence shows little variation along the endosomal membrane. D) Variance in endosomal B2AR fluorescence values measured before and after latrunculin. B2AR distribution becomes more uniform after latrunculin. E) The percentages of endosomes extruding B2AR-containing tubules, calculated before (n=246) and after (n= 106) treatment with latrunculin, or before (n=141) and after (n=168) cytochalasin-D, show a significant reduction after treatment with either drug. As a control, the percentages of endosomes extruding TfR-containing tubules before (n= 317) and after (n= 286) respectively are shown. F) Cortactin immunoblot showing reduction in protein levels after siRNA. G) Representative fields from B2AR-containing endosomes in cells treated with control and cortactin siRNA. Arrowheads denote endosomal tubules in the control siRNA-treated cells. H) Percentages of endosomes extruding B2AR tubules calculated in control siRNA-treated cells (n=210), cortactin siRNA-treated cells (n=269), and cortactin siRNA-treated cells expressing an siRNA-resistant cortactin (n=250). I) Representative examples of endosomes from agonist-exposed cells expressing B2AR, B2AR-ala, DOR, or DOR-B2. Arrowheads denote receptor-containing tubules on B2AR and DOR-B2 endosomes. J) The percentage of endosomes with tubular domains containing B2AR, B2AR-ala, DOR, DOR-B2, or DOR-ABD (n= 246, 302, 137, 200, and 245 respectively) were quantified. Scale bars are 1μm, and error bars are s.e.m. See also Fig S4.

Figure S1.

A) Cells not exposed to agonist do not show internalization over the imaging timeframe. Cells expressing B2AR were labeled and imaged by confocal microscopy without being exposed to isoproterenol. Representative images at time 0 and 5 min are shown. B–D) B2AR enters endosomes marked by Rab 5, and the B2AR tubules contain Rab 4 and Rab11. B2AR-expressing cells were transfected with Rab5Q79L-GFP, Rab 4-GFP, or Rab 11-GFP and imaged 72 hr later after exposure to isoproterenol. Colocalization of the receptor with the three Rab proteins is readily apparent in a few minutes after agonist-treatment.

Figure S2. Actin on Endosomes Is More Rapidly Turned over Than in Stress Fibers

A) Confocal section at two different planes showing endosomal actin and stress fibers in the same cell over time after latrunculin. Endosomal actin disappears within seconds, in contrast to the stable stress fibers. B) The percentage of cells (±s.e.m) showing detectable endosomal actin or stress fibers, from 5 separate experiments (n = 125, 62, 60, 68, 71, and 100 cells for each time point, respectively; the same set of cells were assessed for the presence of either endosomal actin or stress fibers).

Figure S3. B2AR Diffuses into Endosomal Recycling Tubules at a Slower Rate Than TfR

A) Trace of average B2AR fluorescence quantitated from multiple tubules (n = 8) showing a gradual increase in fluorescence over 30 s. B) Fluorescence traces of B2AR and TfR from an example stable tubule containing both. The data are normalized to the

maximum fluorescence value. Exponential curve fits (solid lines) indicate a clear difference in rate of entry of TfR and B2AR (95% confidence interval for t1/2 is 1.3 to 2.4 s for TfR and 9.4 to 21 s for B2AR) into this example tubule.

Figure S4

(A and B) Actin is required for the recycling of B2AR but not transferrin. A) HEK293 cells expressing B2AR were exposed to isoproterenol for 30 min to induce endocytosis. After washing the agonist off, the percentage of receptors recycled to the surface in 60 min in the presence of antagonist was measured using a flowcytometric assay as described previously (Lauffer et al., 2009). The presence of cytochalasin-D, like latrunculin (Cao et al., 1999), inhibited B2AR recycling. B) Cells were loaded with Alexa488-tagged transferrin, and the loss of transferrin fluorescence at two time points was measured by flow cytometry as an index of transferrin recycling. Transferrin recycling was not inhibited by disruption of actin by either cytochalasin or latrunculin. (C–F) The PDZ-interacting domain of B2AR is required and sufficient for actin-dependent receptor recycling. (A) Receptor recycling was measured in cells expressing B2AR or B2AR-ala, where the PDZ interacting domain is mutated by the addition of a single C-terminal alanine, as above. Disrupting the PDZ-interaction inhibited receptor recycling. (B and C) DOR-B2 (B), or DOR-ABD (C) were either left untreated (none) or exposed to cytochalasin-D (cytoD), latrunculin (latr), or an equivalent amount of the solvent DMSO (DMSO) as a control. Receptor recycling after agonist-induced internalization was measured as above. Addition of either the PDZ-interacting domain

or an actin-binding domain converted DOR into an actin-sensitive recycling receptor. D) Addition of an actin-binding domain to a version of the B2AR where the PDZ-interacting domain is mutated (B2-ABD) is capable of recycling as measured by flow cytometry. Truncation of the actin binding domain so that it can no longer bind actin (B2-ABDT) significantly inhibits recycling. n.s. indicates not significant.

Fig.1

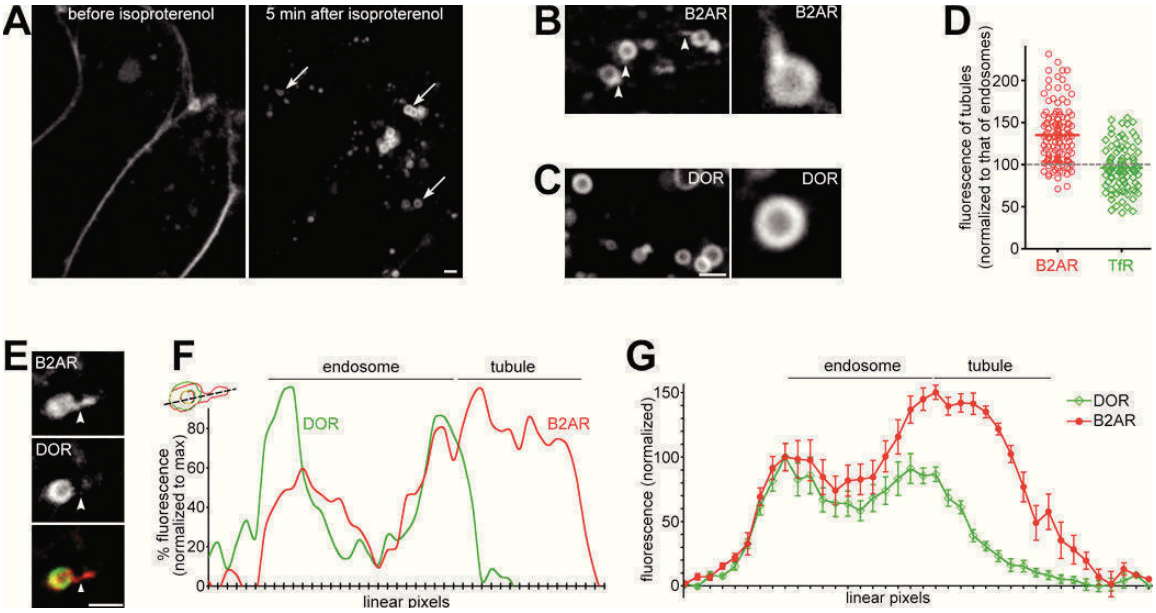
A
before isoproterenol
5 min after isoproterenol
B
B2AR
B2AR
C
DOR
DOR
D
fluorescence of tubules
(normalized to that of endosomes)
200
150
100
50
0
B2AR
TfR
E
B2AR
DOR
F
endosome
tubule
DOR
B2AR
% fluorescence
(normalized to max)
80
60
40
20
0
linear pixels
G
endosome
tubule
DOR
B2AR
fluorescence (normalized)
150
100
50
0
linear pixels

Fig.2

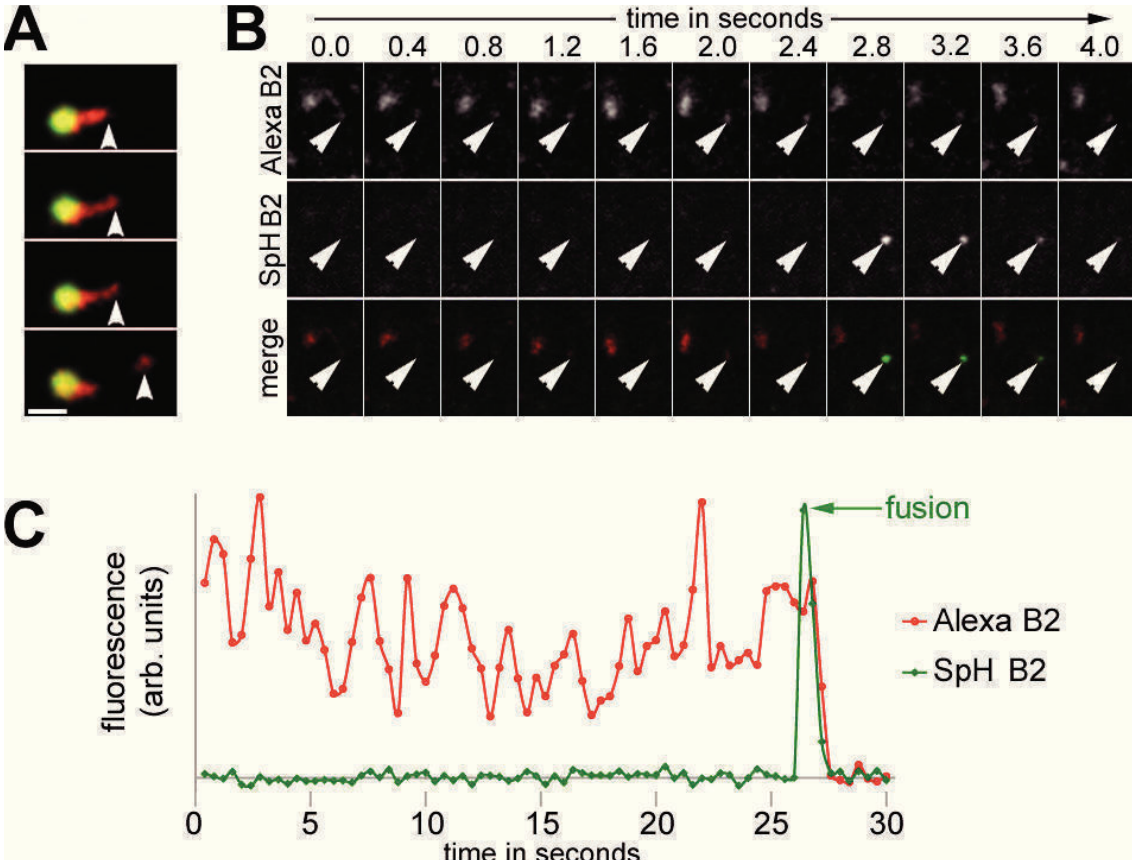
A
B
time in seconds
0.0
0.4
0.8
1.2
1.6
2.0
2.4
2.8
3.2
3.6
4.0
Alexa B2
SpH B2
merge
C
fusion
fluorescence (arb. units)
Alexa B2
SpH B2
0
5
10
15
20
25
30
time in seconds

Fig.3

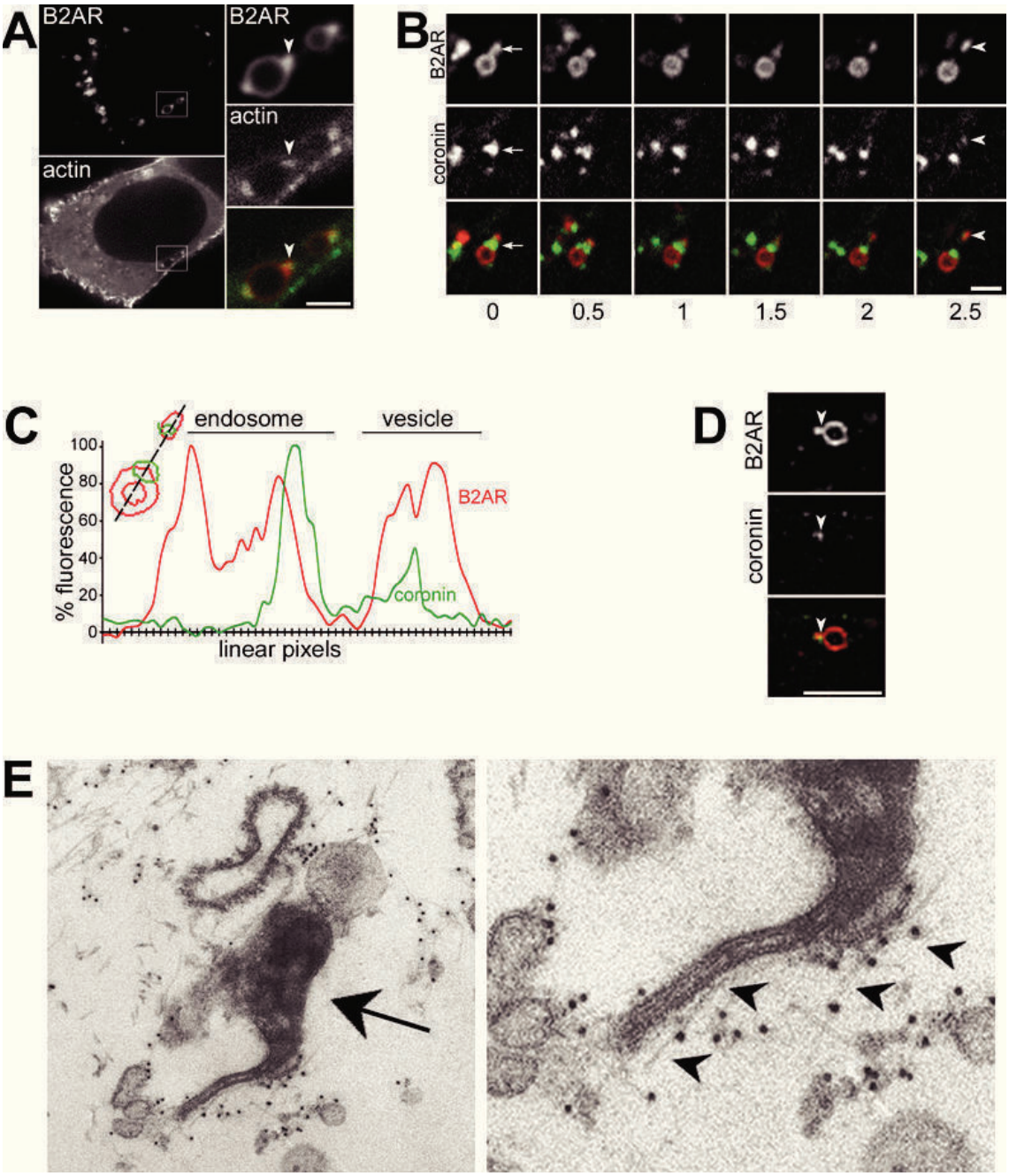
A
B2AR
actin
B2AR
actin
B
B2AR
coronin
0
0.5
1
1.5
2
2.5
C
endosome
vesicle
B2AR
coronin
% fluorescence
100
80
60
40
20
0
linear pixels
D
B2AR
coronin
E

Fig.4

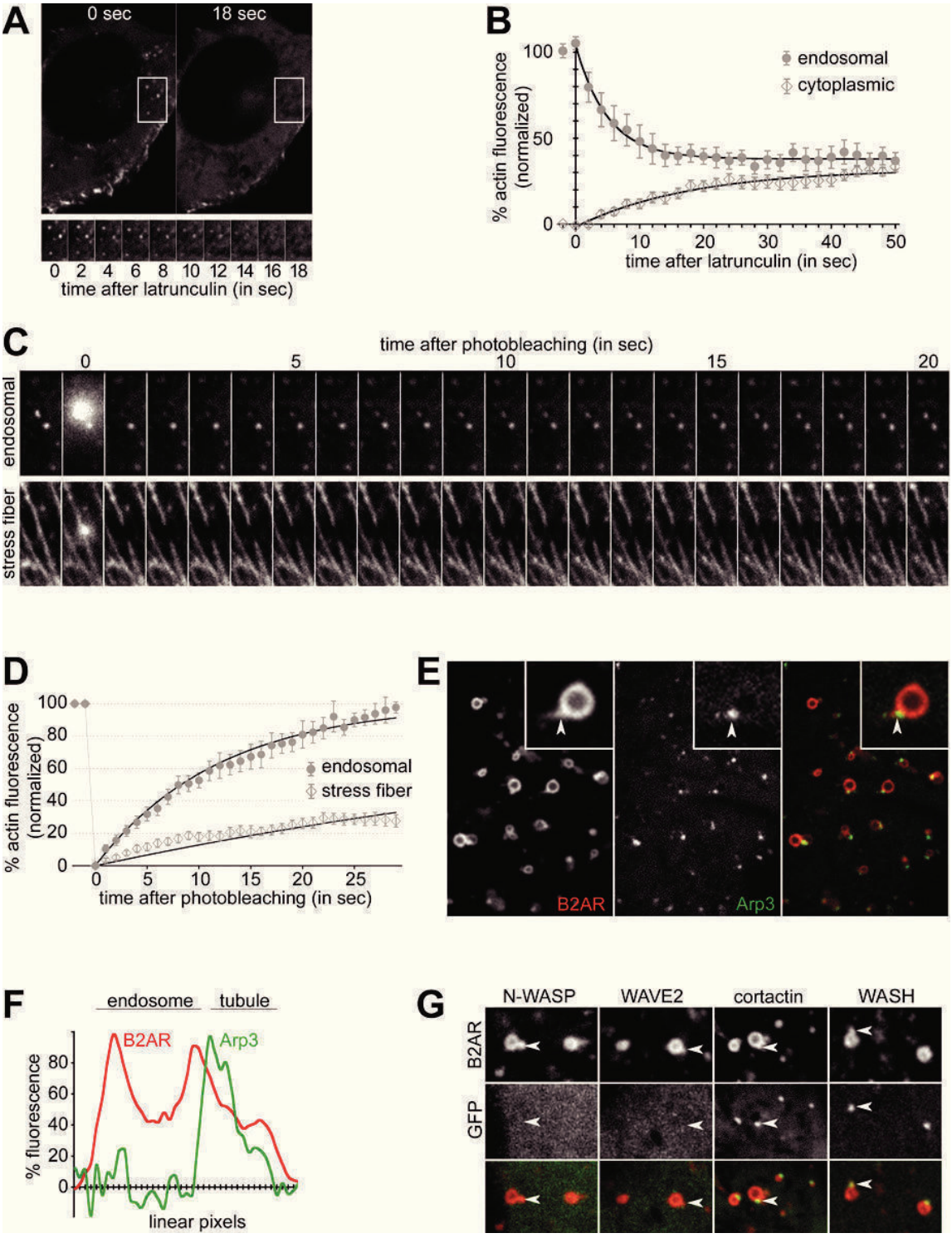
A
0 sec
18 sec
0 2 4 6 8 10 12 14 16 18
time after latrunculin (in sec)
B
100
50
0
% actin fluorescence (normalized)
endosomal
cytoplasmic
0 10 20 30 40 50
time after latrunculin (in sec)
C
time after photobleaching (in sec)
0 5 10 15 20
endosomal
stress fiber
D
100 80 60 40 20 0
% actin fluorescence (normalized)
endosomal
stress fiber
0 5 10 15 20 25
time after photobleaching (in sec)
E
B2AR
Arp3
F
endosome
tubule
B2AR
Arp3
80 60 40 20 0
% fluorescence
linear pixels
G
N-WASP
WAVE2
cortactin
WASH
B2AR
GFP

Fig.5

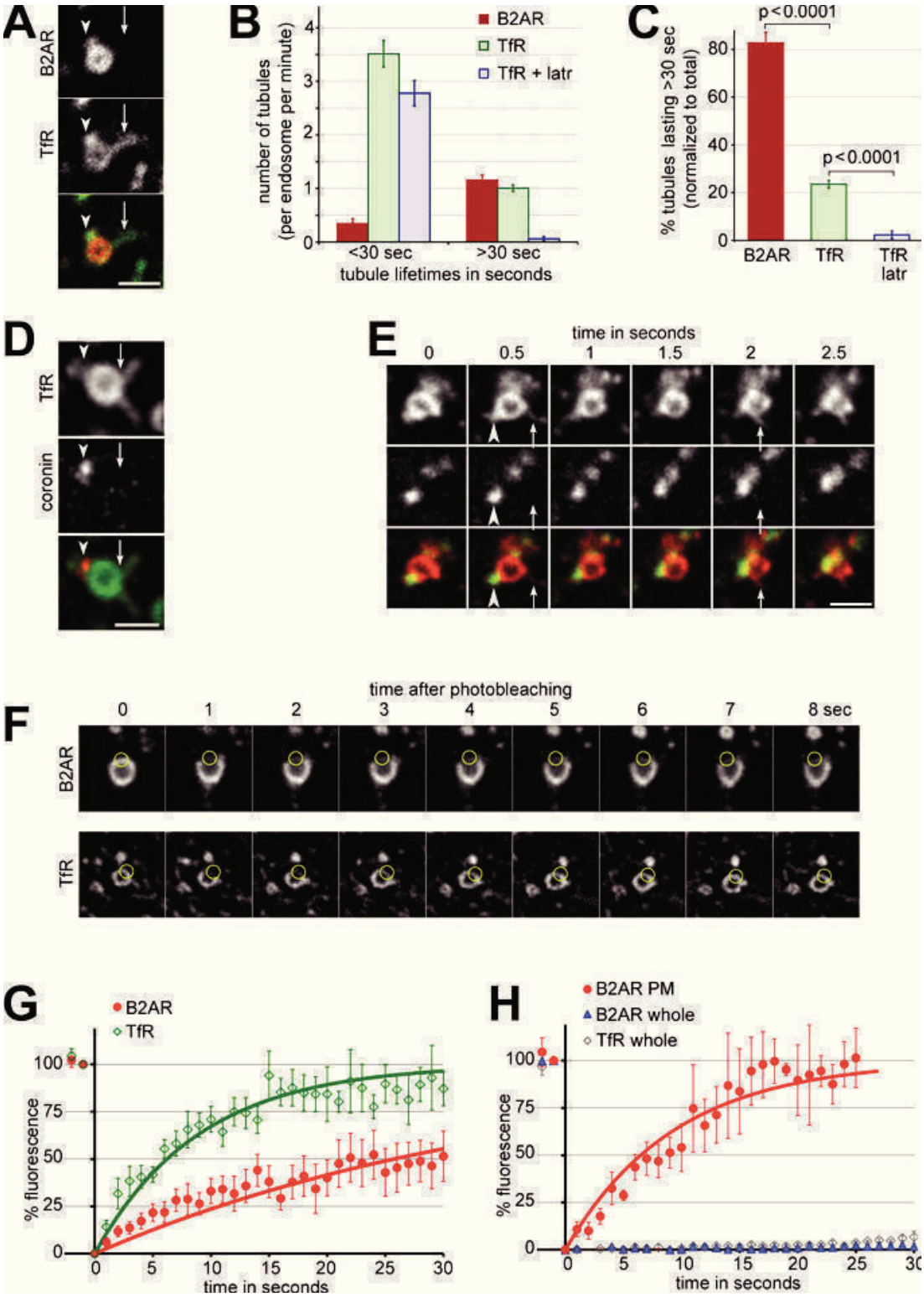
A
B2AR
TfR
B
B2AR
TfR
TfR + latr
number of tubules (per endosome per minute)
<30 sec
>30 sec
tubule lifetimes in seconds
C
p<0.0001
p<0.0001
% tubules lasting >30 sec (normalized to total)
B2AR
TfR
TfR latr
D
TfR
coronin
E
time in seconds
0
0.5
1
1.5
2
2.5
F
time after photobleaching
0
1
2
3
4
5
6
7
8 sec
B2AR
TfR
G
B2AR
TfR
% fluorescence
time in seconds
H
B2AR PM
B2AR whole
TfR whole
% fluorescence
time in seconds

Fig.6

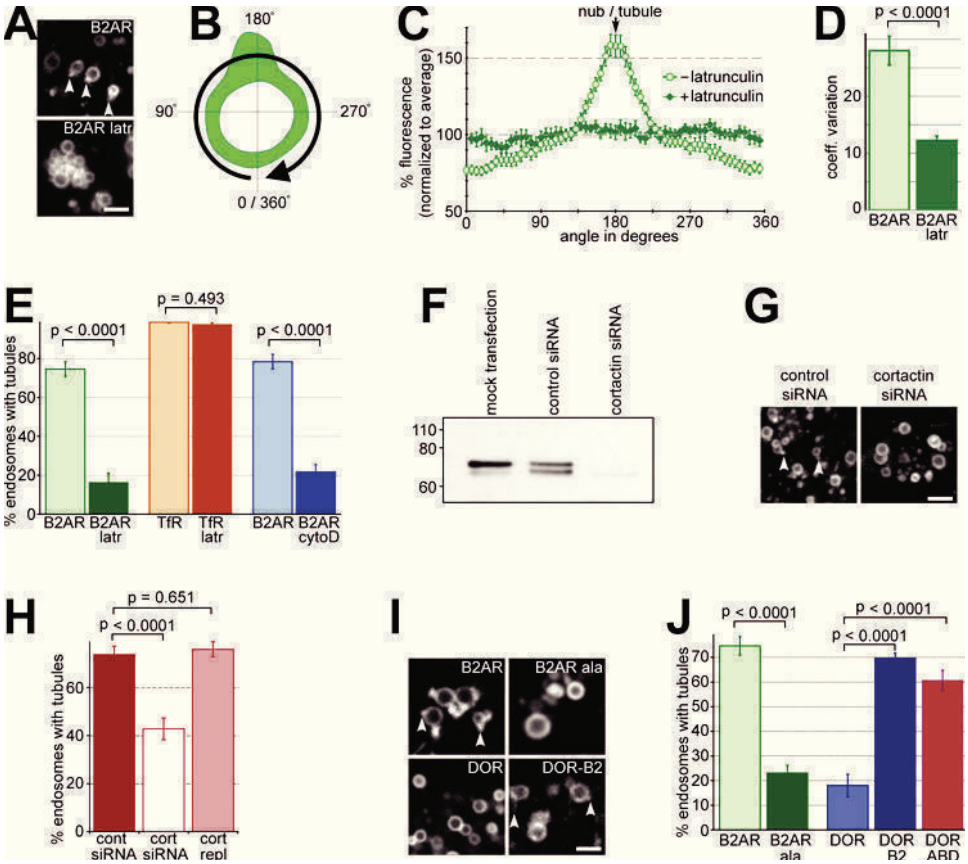
A
B2AR
B2AR latr
B
180˚
90˚
270˚
0 / 360˚
C
nub / tubule
−latrunculin
+latrunculin
% fluorescence (normalized to average)
angle in degrees
D
p < 0.0001
coeff. variation
B2AR
B2AR latr
E
p < 0.0001
p = 0.493
p < 0.0001
% endosomes with tubules
B2AR
B2AR latr
TfR
TfR latr
B2AR
B2AR cytoD
F
mock transfection
control siRNA
cortactin siRNA
110
80
60
G
control siRNA
cortactin siRNA
H
p = 0.651
p < 0.0001
% endosomes with tubules
cont siRNA
cort siRNA
cort repl
I
B2AR
B2AR ala
DOR
DOR-B2
J
p < 0.0001
p < 0.0001
p < 0.0001
% endosomes with tubules
B2AR
B2AR ala
DOR
DOR B2
DOR ABD

Fig.S1

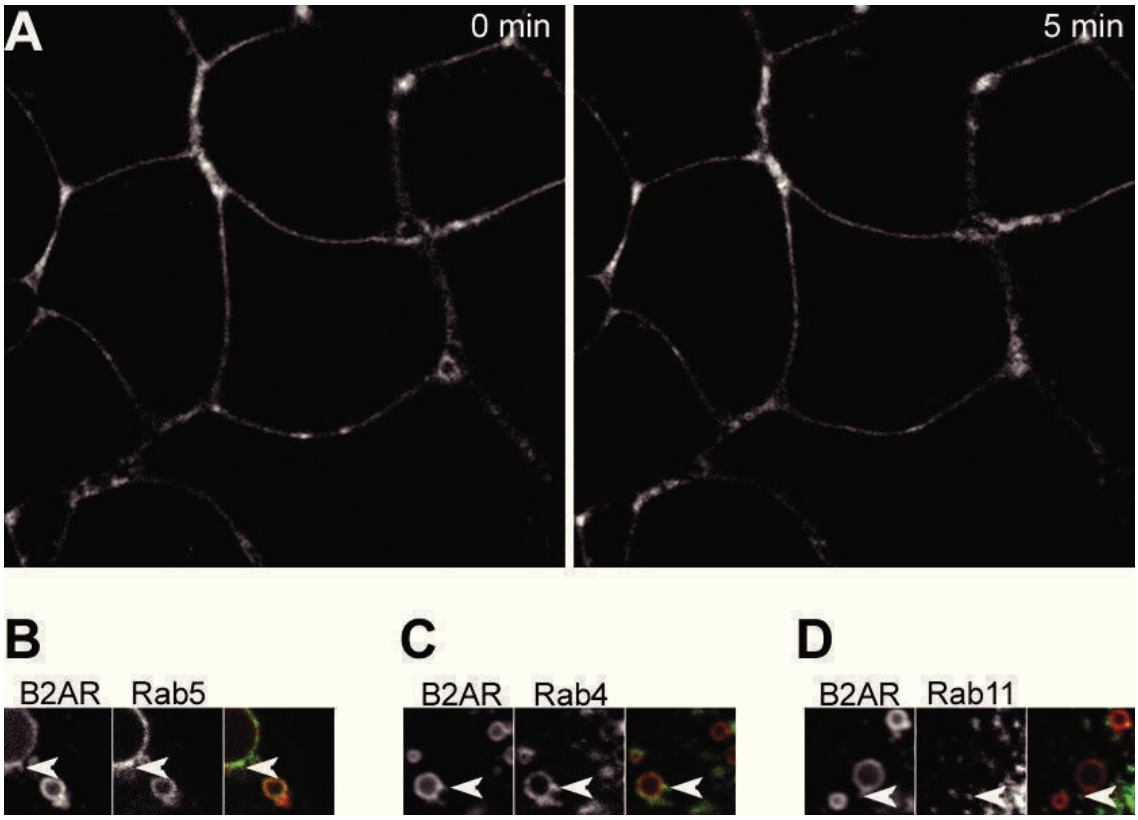

Fig.S2

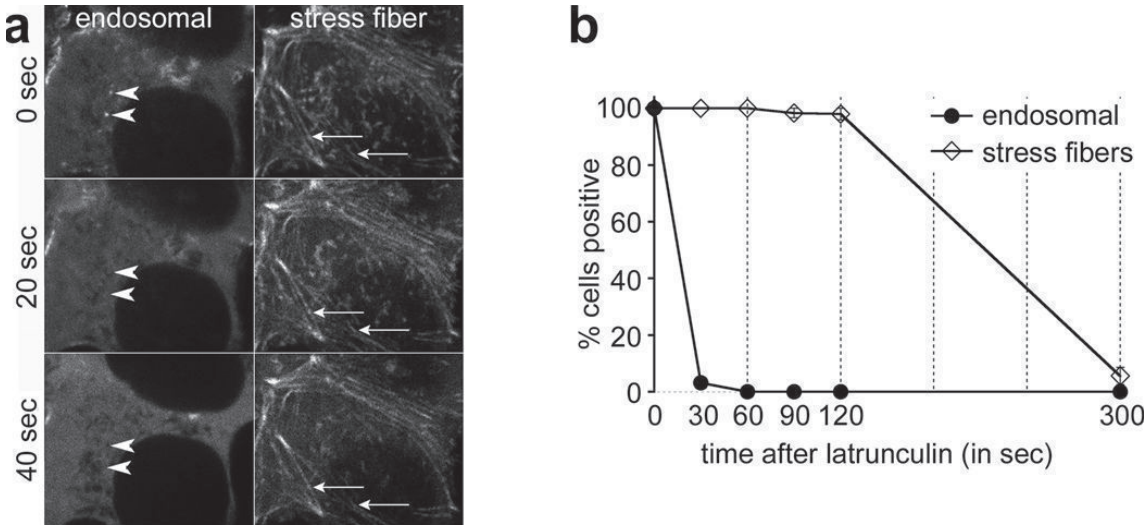
a
endosomal
stress fiber
0 sec
20 sec
40 sec
b
100
80
60
40
20
0
% cells positive
0
30
60
90
120
300
time after latrunculin (in sec)
endosomal
stress fibers

Fig.S3

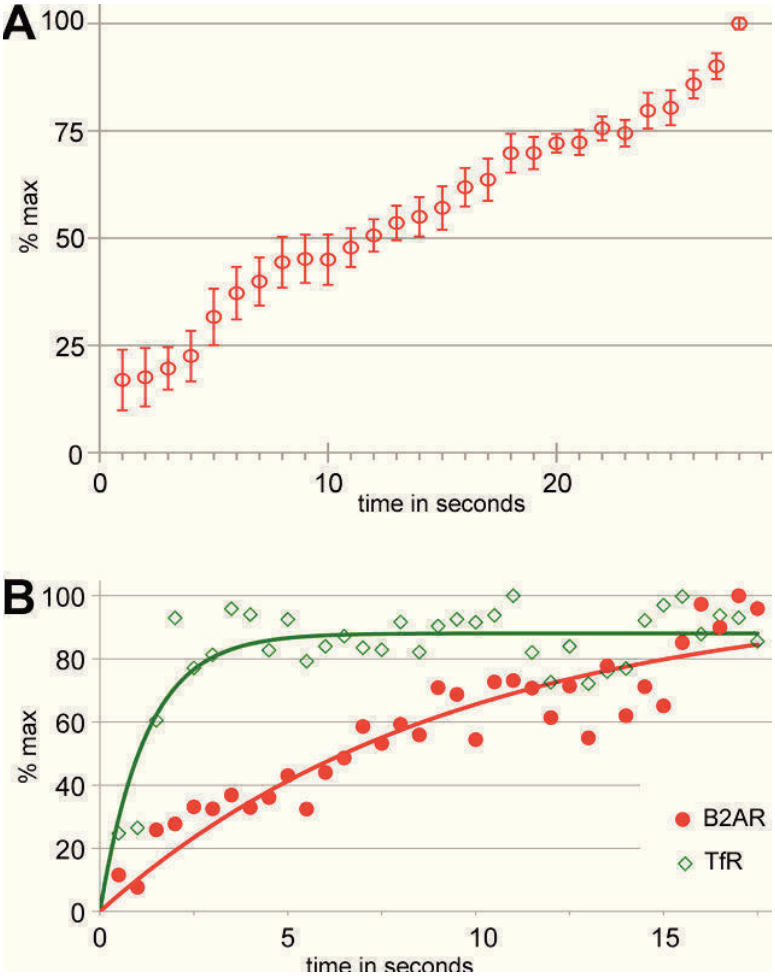
A
100
75
50
25
0
% max
0
10
20
time in seconds
B
100
80
60
40
20
0
% max
0
5
10
15
time in seconds
B2AR
TfR

Fig.S4

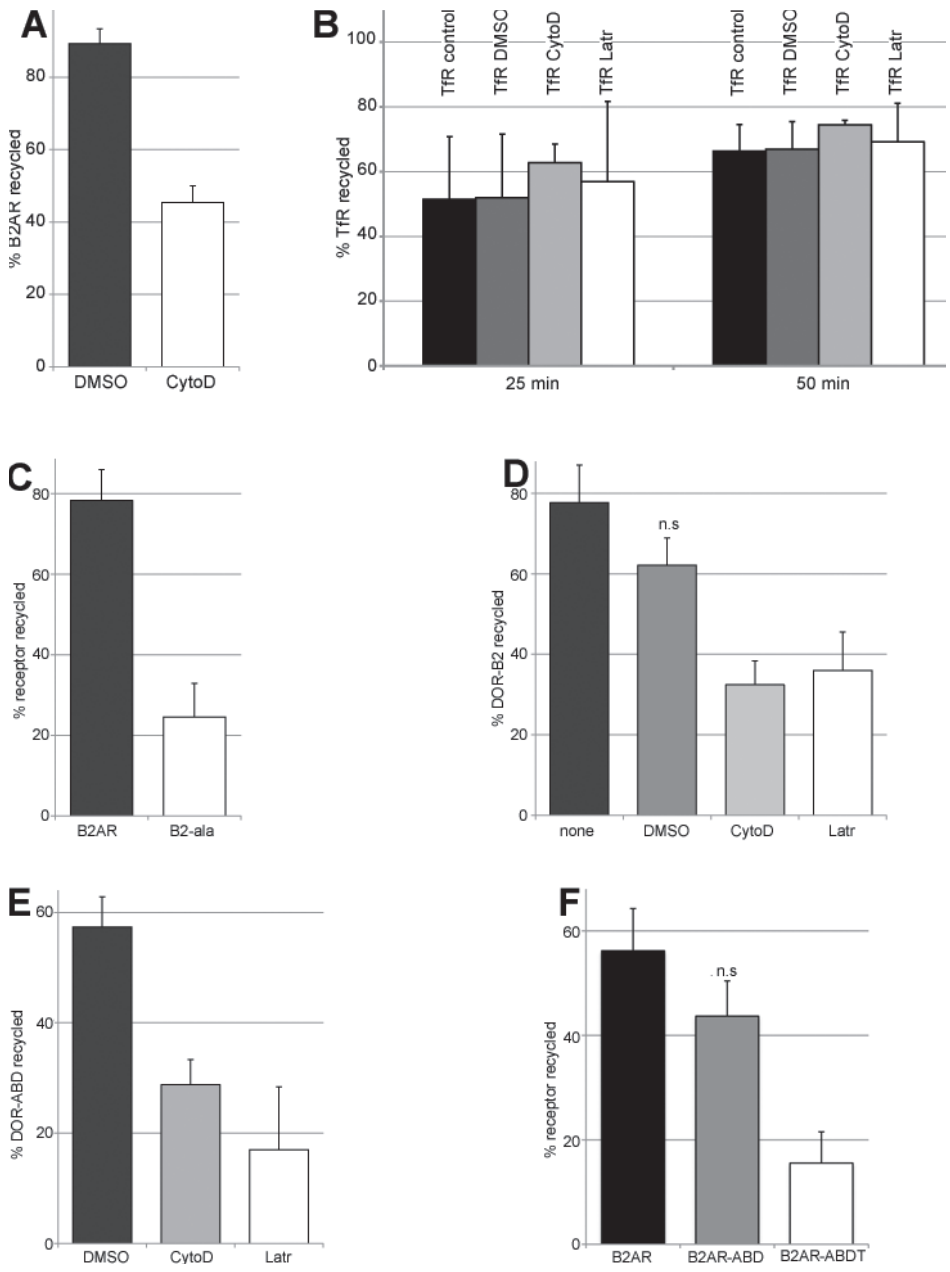
A
% B2AR recycled
0
20
40
60
80
DMSO
CytoD
B
% TfR recycled
0
20
40
60
80
100
TfR control
TfR DMSO
TfR CytoD
TfR Latr
TfR control
TfR DMSO
TfR CytoD
TfR Latr
25 min
50 min
C
% receptor recycled
0
20
40
60
80
B2AR
B2-ala
D
% DOR-B2 recycled
0
20
40
60
80
n.s
none
DMSO
CytoD
Latr
E
% DOR-ABD recycled
0
20
40
60
DMSO
CytoD
Latr
F
% receptor recycled
0
20
40
60
n.s
B2AR
B2AR-ABD
B2AR-ABDT

Chapter 4:

SNX27 mediates PDZ-directed sorting from endosomes to the plasma membrane

Paul Temkin contributed data to Figure 3 and provided consultation during the experimental and writing process. The majority of other experiments were conceived and executed by Benjamin Lauffer of the von Zastrow lab. Additional contributions were made by Cristina Melero[2], Paul Temkin[3,4], Cai Lei[7], Wanjin Hong[7], Tanja Kortemme[2] and Mark von Zastrow[3,5,6]

.

[1]Program in Pharmaceutical Sciences and Pharmacogenomics, [2]Department of Bioengineering & Therapeutic Sciences, [3]Program in Cell Biology, [4]Department of Biochemistry and Biophysics, [5]Department of Psychiatry, [6]Department of Cellular & Molecular Pharmacology , University of California, San Francisco, CA 94158; [7]Membrane and Biology Laboratory, Institute of Molecular and Cell Biology, Singapore 138673

4.1 ABSTRACT

PDZ domain-interacting motifs, in addition to their well-established roles in protein scaffolding at the cell surface, are proposed to act as *cis*-acting determinants directing the molecular sorting of transmembrane cargo from endosomes to the plasma membrane. This hypothesis requires the existence of a specific *trans*-acting PDZ protein that mediates the proposed sorting operation in the endosome membrane. Here show that SNX27 is required for efficient PDZ-directed recycling of the β_2-adrenoreceptor (β_2AR) from early endosomes. SNX27 mediates this sorting function when expressed at endogenous levels, and its recycling activity requires both PDZ domain-dependent recognition of the β_2AR cytoplasmic tail and Phox homology (PX) domain-dependent association with the endosome membrane. These results identify a discrete role of SNX27 in PDZ-directed recycling of a physiologically important signaling receptor, and extend the concept of cargo-specific molecular sorting in the recycling pathway.

4.2 INTRODUCTION

The β_2-adrenoreceptor (β_2AR) is a member of the large family of G protein-coupled signaling receptors (GPCRs), and is fundamentally regulated by ligand-induced endocytosis via clathrin-coated pits (Moore et al., 2007). The functional consequences of regulated endocytosis, specifically whether catecholamines produce sustained or transient effects, are determined by molecular sorting of internalized β_2ARs between recycling and lysosomal pathways (Hanyaloglu and von Zastrow, 2008; Marchese et al., 2008). β_2ARs recycle efficiently to the plasma membrane after endocytosis but, in contrast to the ability of some endocytic cargo to recycle essentially by bulk membrane flux, efficient recycling of the β_2AR requires a PDZ domain-interacting motif present in its distal cytoplasmic tail (Hanyaloglu et al., 2005; Maxfield and McGraw, 2004). If this motif is disrupted by phosphorylation or mutation, internalized β_2ARs traffic preferentially to lysosomes and are degraded (Cao et al., 1999; Gage et al., 2001). The β_2AR-derived recycling motif can bind to a family of PDZ proteins related to EBP50 or NHERF (Ezrin-Binding Phosphoprotein of 50KDa or Na+/H+ Exchange Regulatory Factor, respectively, henceforth referred to as NHERFs) (Cao et al., 1999; Hall et al., 1998; He et al., 2006). These observations, and results from the study of other PDZ motif-bearing GPCRs (Delhaye et al., 2007; Hanyaloglu and von Zastrow, 2008; Wente et al., 2005), have motivated the hypothesis that PDZ motifs mediate a discrete endosome-to-plasma membrane sorting operation (Gage et al., 2005; Wang et al., 2007).

A problem with the PDZ-directed recycling hypothesis is that NHERF-family PDZ proteins, while often concentrated in the cortical cytoplasm near endosomes, are not

known to localize directly to the endosome membrane when expressed at endogenous levels (Bretscher et al., 2000; Donowitz et al., 2005) and can mediate additional effects on receptors (Hall et al., 1998). It is also known that PDZ domain-mediated interactions with various membrane proteins can enhance net surface accumulation indirectly, such as by scaffold-promoted post-translational modification (Gardner et al., 2007) or physical stabilization of proteins in particular plasma membrane domains (Perego et al., 1999). A critical unresolved question, therefore, is whether there exists any *trans*-acting PDZ protein that sorts relevant motif-bearing cargo into the recycling pathway directly from the endosome membrane.

Such a *bona fide* sorting protein for the PDZ-directed recycling pathway, if it exists, would be expected to possess several key properties. First, of course, the putative sorting protein should be capable of binding the relevant *cis*-acting PDZ motif. Second, the putative sorting protein should localize to, or physically interact with, endosomes traversed by the internalized cargo. Third, the putative sorting protein should be essential for PDZ-directed recycling when expressed at endogenous levels. Fourth, and most important for establishing a direct endosome-based sorting function, the recycling activity of the putative sorting protein should require both binding to the *cis*-acting PDZ motif and localization to the relevant endosomes from which recycling occurs. Here we show that sorting nexin 27 (SNX27) meets all of these criteria, and that this PDZ protein plays an essential role regulating the β_2AR.

4.3 RESULTS AND DISCUSSION

Two NHERF-family PDZ proteins that bind the β_2AR tail, NHERF1 and NHERF2, are not known to localize to endosomes at steady state but possess a carboxyl-terminal ERM (Ezrin/Radixin/Moesin) protein-binding domain (Figure 1A) that can mediate a network of protein connectivity linking integral membrane proteins to actin (Bretscher et al., 2000). We initially proposed such indirect actin connectivity as the basis for β_2AR recycling (Cao et al., 1999). Subsequent analysis established that, while actin connectivity is sufficient to promote recycling of engineered receptors in the absence of a natural PDZ motif, this connectivity does not fully recapitulate the natural characteristics of β_2AR recycling (Lauffer et al., 2009). As such, we sought to test whether or not NHERFs 1 and/or 2 are actually the limiting factors for β_2AR recycling. To do so we utilized an established HEK293 cell clone expressing a FLAG-tagged β_2AR construct and depleted both NHERF-family proteins simultaneously using a mixture of RNA duplexes (Figure 1B). We then applied a fluorescence flow cytometric assay to measure receptor internalization occurring in response to application of the adrenergic agonist isoproterenol (10 μM), and recycling of receptors after subsequent washout of this agonist (Figure 1C). As shown previously, surface β_2AR immunoreactivity recovered nearly to control levels within 50 minutes after agonist removal (Figure 1C, solid line) (Cao et al., 1999), whereas surface recovery of an alanine-extended (PDZ binding-defective) mutant receptor construct (β_2AR-Ala) was greatly reduced (Figure 1C, dashed line). Calculation of fractional recycling (Hanyaloglu et al., 2005) confirmed this effect

across multiple experiments (Figure 1D, first and second bars from left). Strikingly, simultaneous knockdown of NHERFs 1 and 2 did not have a major effect on β_2AR recycling when compared to control levels (first and third bars). Consistent with this, we also observed PDZ motif-dependent recycling of the β_2AR in a cell line (PS120) that expresses NHERF proteins at low levels (Donowitz et al., 2005) relative to HEK293 cells (data not shown).

Thus we considered whether another PDZ protein might function alternately, or additionally, in endosome-to-plasma membrane trafficking of β_2ARs. An intriguing candidate was sorting nexin 27 (SNX27, also called Mrt1), which is widely expressed and unique among PDZ proteins because it contains a PX domain that binds specifically to PtdIns-3-P enriched on the cytoplasmic surface of early / sorting endosomes (Lunn et al., 2007; Rincon et al., 2007). SNX27 has not been shown previously to interact with the β2AR's PDZ motif, but sequence analysis suggests a close relationship between SNX27's PDZ domain and those present in NHERF-family proteins (Donowitz et al., 2005) (Figure 2A, bold residues). In particular, we noted similarity or identity at several residues thought to directly contact the PDZ motif (colored residues) (Appleton et al., 2006). Consistent with this, equilibrium binding analysis using fluorescence polarization demonstrated direct and saturable binding of this motif (a peptide corresponding to the C-terminal 6 residues of the β2AR) to the purified SNX27 PDZ domain (Figure 2B, solid line, equilibrium dissociation constant $K_d = 17 \pm 1.2$ μM). Further, binding to the SNX27 PDZ domain *in vitro* was destabilized by the alanine-extension that blocks the recycling activity of this sequence in intact cells (Figure 2B, dotted line, $K_d > 100$ μM).

We next asked if full length SNX27 associates with endosomes traversed by internalized β_2ARs. To do so, we expressed a GFP-tagged version of SNX27a in the FLAG-β_2AR -expressing HEK293 cell clone used for trafficking studies. We then exposed these cells to 10 μM isoproterenol for 25 minutes in the presence of Alexa-conjugated M1 anti-FLAG monoclonal antibody, to drive fluorescently-tagged β_2ARs to steady state throughout the recycling pathway (Gage et al., 2001). SNX27-GFP localized prominently to endosomal membranes, as shown previously (Joubert et al., 2004; Lunn et al., 2007; Rincon et al., 2007), and a large fraction of these endosomes contained internalized β2ARs (Figure 2C, top panels). We quantified this observation by counting the number of β2AR-containing endosomes colocalized with SNX27 in coded specimens (90% overlap, 8586 endosomes, 124 cells, 3 experiments). We additionally verified extensive overlap by determining Pearson's correlation coefficient between the respective image channels (0.62 ± 0.09, n = 12 images). In contrast, GFP-tagged NHERF1 was distributed throughout the cytoplasm with visible enrichment near the plasma membrane, but we did not observe or measure significant endosome localization (Figure 2C, second row of images; a different focal plane showing enrichment near the plasma membrane is shown in Supplemental Figure 1A; Pearson's coefficient = 0.33 ± 0.15 (n = 12)). GFP-NHERF2 was enriched near the plasma membrane but also localized to a fraction of β2AR-containing endosomes (Figure 2C, third row). The fluorescence intensity of GFP-NHERF2 on endosomes was not high, however (Pearson's coefficient = 0.29 ± 0.15 (n = 12)), and GFP-NHERF2 colocalization was visible only when β2ARs were also present (Supplemental Figure 1B, second row from top, compare left and right image pairs). SNX27-GFP was unique in localizing prominently to endosomes either in the absence or

presence of β2ARs (Supplemental Figure 1B, third and fourth rows from top). The SNX27-associated endosomes colocalized extensively with EEA1 (Figure 2D, top row of panels; 92% overlap, 4119 endosomes, 54 cells, 3 experiments; Pearson's coefficient = 0.60 $\pm$ 0.14 (n = 28 images)). In contrast, we observed little overlap with LAMP3 or with Rab11 (Figure 2D, middle and lower rows; Pearson's coefficient = 0.38 $\pm$ 0.16 (n = 28) and 0.25 $\pm$ 0.10 (n = 27)). These observations define the SNX27-associated membrane compartments primarily as early endosomes.

We next applied RNA interference to test the functional significance of candidate PDZ proteins when knocked down individually (Figure 3A). Consistent with the dual-knockdown results, depletion of NHERF1 did not significantly affect β_2AR recycling (Figure 3B, compare first and second bars from left). Depletion of NHERF2 produced a significant inhibition of β_2AR recycling, but the magnitude of this effect was small (third bar). Depletion of SNX27, in contrast, caused a pronounced inhibition of β_2AR recycling (fourth bar) that was similar in magnitude to the effect of disrupting the *cis*-acting PDZ motif itself (β_2AR-Ala mutant receptor, Figure 1D). Pronounced inhibition of β_2AR recycling in SNX27-depleted cells was further verified by visual inspection of epifluorescence micrographs (Supplemental Figure 1C).

SNX27 knockdown increased net receptor internalization measured at steady state, consistent with the ability of β_2ARs to repeatedly endocytose and recycle in the continuous presence of agonist (von Zastrow and Kobilka, 1992). Kinetic analysis indicated that increased net receptor internalization was accounted for by the reduced fractional recycling of receptors (F_r) produced by SNX27 depletion (Figure 3C and Supplemental Figure 2C). Also supporting this interpretation, surface biotinylation and

immunoblot analysis established that SNX27 knockdown increased agonist-induced proteolysis of the β_2AR (Figure 3D and E). Further, SNX27 depletion produced a net down-regulation of surface and total cellular receptor number measured by fluorescence flow cytometry and radioligand binding assay, respectively, in cells maintained in the absence of agonist (Supplemental Figure 2A and B). All of these observations are consistent with the hypothesis that SNX27, by mediating PDZ-directed sorting of internalized β_2ARs into the rapid recycling pathway, effectively prevents receptors from trafficking to lysosomes following both basal and agonist-stimulated endocytosis.

To further verify the specificity of the SNX27 knockdown effect, we investigated rescue using rat-derived SNX27 constructs not targeted by the human-specific siRNA duplexes. Selective knockdown and replacement were confirmed by anti-SNX27 immunoblot (Figure 4A). Both a and b isoforms of SNX27, which differ by alternative splicing affecting the carboxyl-terminal 15 residues (Kajii et al., 2003), effectively rescued β_2AR recycling while control expression of GFP did not (Figure 4B). We also verified rescue of net surface receptor immunoreactivity when measured at steady state in the absence of agonist (not shown). Gating the flow cytometric analysis according to GFP signal (Figure 4C) further verified transgenic rescue of β_2AR recycling by both SNX27 isoforms over a range of expression levels (Figure 4D).

We next asked if the recycling activity of SNX27 requires its ability to bind the PDZ motif present in the β_2AR tail. To do so we mutated a single conserved histidine residue present in the second alpha helix of the SNX27 PDZ domain (position 112 in rat SNX27 corresponds to position 114 in human, highlighted in red in Figure 2A), which is predicted to form a critical hydrogen bond with the Ser/Thr residue located at the -2

position of the PDZ-interacting motif (Doyle et al., 1996; Tonikian et al., 2008) (corresponding to S411 of the human β_2AR). This point mutation destabilized binding of SNX27 to the β_2AR-derived sorting motif (Figure 5A), and did so to a similarly large degree as mutating the PDZ motif itself (compare to Figure 2B). Using circular dichroism and gel filtration, we ruled out changes in PDZ fold stability or oligomerization state as an explanation for this result (data not shown). Further, the H112A mutation did not detectably affect localization of the mutant SNX27 protein to early endosomes (Figure 5B, top row of images; Pearson's coefficient = 0.55 $\pm$ 0.13 (n = 29 images)). However, the H112A mutant SNX27 was unable to rescue β_2AR recycling (Figure 5C, bars 2 and 3 from left). We also asked if SNX27's sorting activity requires its association with the endosome membrane. To do so, we used a mutant version of SNX27a possessing a wild type PDZ domain but lacking the PX domain (SNX27ΔPX). SNX27ΔPX failed to localize to endocytic vesicles (Figure 5B, lower row; Pearson's coefficient = 0.19 $\pm$ 0.12 (n = 20 images)) and did not rescue the recycling defect caused by depletion of endogenous SNX27 (Figure 5C, 4th bar). Together, these results indicate that the recycling activity of SNX27 requires both PDZ motif binding and direct association with the endosome membrane.

As an independent test of the specificity of SNX27 for PDZ-directed recycling, we examined the effect of replacing the PDZ motif present in the β_2AR cytoplasmic tail with a distinct 17-residue sequence derived from the cytoplasmic tail of the μ-opioid neuropeptide receptor (Supplemental Figure 3A). This 'μ receptor-derived recycling sequence' (mrs) does not conform to a PDZ motif, and does not bind PDZ domains *in vitro*, but represents a 'PDZ-independent' sorting motif that is sufficient to direct efficient

recycling when substituted for the PDZ motif present in the wild type β_2AR (Tanowitz and von Zastrow, 2003). β2-mrs recycling was insensitive to SNX27 knockdown (Figure 5D). SNX27 depletion also did not increase agonist-induced degradation of β2-mrs (Supplemental Figure 3B and C). We further verified SNX27's localization and discrete sorting activity in a physiologically relevant cell type. SNX27 colocalized extensively with β_2AR-containing endosomes in aortic smooth muscle (A10) cells (Figure 5E, Pearson's coefficient = 0.58 ± 0.10 (n = 6)). Knockdown of endogenous SNX27 in these cells inhibited recycling of the β_2AR, but not the β2-mrs engineered receptor. Finally, this specific knockdown effect was rescued by recombinant SNX27 (Figure 5F).

Together, we believe that the present results provide several lines of evidence indicating that SNX27 is a critical sorting protein for PDZ motif-directed endosome-to-plasma membrane traffic, and that it mediates this sorting function directly from the endosome membrane. We note that the presently described function of SNX27 in PDZ-directed recycling is fundamentally different from the previously proposed roles of SNX27 in promoting endocytosis or lysosomal delivery of PDZ motif-bearing cargo (Joubert et al., 2004; Lunn et al., 2007). These previous studies relied entirely on the effects of SNX27 over-expression and, consistent with this, we observed some agonist-independent accumulation of β_2ARs in endosomes when SNX27-GFP was over-expressed (Supplemental Figure 1B, agonist-naive condition shown in lower two rows). Depleting native SNX27 produced a much more pronounced retention of receptors in endosomes, however, which was evident under both agonist -induced (Supplemental Figure 2C) and -naive (Supplemental Figure 1C) conditions. Thus, while SNX27 over-

expression can indeed produce additional effect(s) consistent with expression-dependent differences in the functional effects of other sorting nexins (Carlton et al., 2005), we are confident that a primary function of SNX27 expressed endogenously is to promote PDZ motif-directed recycling from (rather than sequestration in) endosomes.

This function of SNX27 is also different from the roles of all other sorting nexins established previously. Sorting nexins are known to have a variety of effects on endocytic membrane organization and function, and several possess BAR domains that detect or impose membrane curvature. SNX27 lacks a recognized BAR domain, is the only known family member containing a PDZ domain and, except for its PX domain, is largely distinct from other sorting nexins. It is interesting to note that sorting nexin 17 (SNX17), while it lacks a PDZ domain, shares homology with SNX27 elsewhere (Xu et al., 2001) and has been found to promote recycling of the LDL receptor-related protein (LRP) by interacting with a tyrosine-based sequence distinct from a PDZ motif (van Kerkhof et al., 2005). SNX27 could potentially function via PDZ-dependent inhibition of receptor interaction with the lysosomal sorting machinery or, alternatively, by promoting PDZ-directed packaging of receptors into recycling vesicles. The present data cannot distinguish these possibilities, but set the essential groundwork for further mechanistic elucidation of SNX27's discrete sorting activity.

We focused here on trafficking of the β_2AR because this was the integral membrane protein for which the hypothesis of PDZ-directed recycling was first proposed (Cao et al., 1999), because endosome-to-plasma membrane trafficking of this receptor is well established to have physiologically significant effects (Moore et al., 2007), and because there is emerging evidence that the PDZ-dependent recycling mechanism is conversely

regulated by β_2AR signaling (Yudowski et al., 2009). We note that a number of other signaling receptors have been found to exhibit PDZ motif-dependent recycling (Delhaye et al., 2007; Hanyaloglu and von Zastrow, 2008; Wente et al., 2005). Further, PDZ domain-mediated protein interaction(s) are recognized to function more widely in determining the endomembrane trafficking of various membrane proteins (e.g., (Cushing et al., 2008; Lin and Huganir, 2007; Maday et al., 2008; Wieman et al., 2009)). We also note that the general concept of sequence-directed molecular sorting in the recycling pathway is now firmly established, particularly in polarized cell types (Mellman and Nelson, 2008). The molecular basis of such sorting has been studied most extensively in epithelial cells, where non-PDZ interactions of membrane cargo with AP-1B promote basolateral surface delivery involving Rab8 and components of the exocyst (Ang et al., 2003; Folsch et al., 1999; Folsch et al., 2003; Gan et al., 2002), and where such sorting has been shown to occur in recycling endosomes (Ang et al., 2004). We believe that the present study, by establishing SNX27 as a mediator of PDZ motif-directed recycling from the early endosome membrane, significantly extends the concept of molecular sorting in the recycling pathway and supports its physiological significance.

4.4 MATERIALS AND METHODS

Constructs and specialized reagents. Epitope-tagged receptor constructs were described previously (Cao et al., 1999; Tanowitz and von Zastrow, 2003; von Zastrow and Kobilka, 1992). GFP-NHERF1 was generated from a previously described HA-tagged version of human EBP50/NHERF1 (Cao et al., 1999). The coding sequence was subcloned from pcDNA3.0 (Invitrogen) into pEGFP-C3 (Clontech) using XmnI and HindIII, and the C-terminal HA-tag was removed by introduction of a stop codon using oligonucleotide site-directed mutagenesis (QuikChange, Stratagene). GFP-NHERF2 was generated by PCR from a cDNA encoding human NHERF2/E3KARP (Open Biosystems #5296143). SNX27-GFP was generated from rat SNX27/mrt1 (isoform a, accession #NM_001110151 obtained from ATCC) subcloned into pENTR.D.TOPO (Invitrogen). GFP tagging was accomplished by recombination into pcDNA-DEST47 (Gateway system, Invitrogen). The *b* isoform and the H112A mutant version were generated from SNX27-GFP using oligonucleotide site-directed mutatagenesis. The ΔPX construct (deleting residues 162-263) was constructed using stitch PCR of the flanking sequence and insertion into the pENR.D.TOPO vector followed by recombination into the pcDNA-DEST47 vector. For production of recombinant protein in E. coli, wild type or H112A mutant SNX27 PDZ domain (corresponding to residues 39-131 in the NM_001110151 coding sequence) was amplified by PCR and inserted using NcoI and XhoI sites to a pET19b-derived expression vector (pBH4) incorporating an N-terminal His_6 tag. All constructs were verified by dideoxynucleotide sequencing (Elim Biopharmaceuticals, Inc., Hayward, CA). Control (non-silencing) and silencing siRNAs were purchased from Qiagen's HP GenomeWide siRNA collection. The sense-strand,

silencing siRNA sequences are as follows: r(GAA GGA GAA CAG UCG UGA A)dTdT (NHERF1), r(GAG ACA GAU GAA CAC UUC A)dTdT (NHERF2), and r(CCA GGU AAU UGC AUU UGA A)dTdT (SNX27). SNX27 silencing in rat A10 cells was accomplished with a mix of the 4 siRNAs available for that species commercially (HP GenomeWide siRNA collection, Qiagen). To verify specific rescue in rat A10 cells, knockdown was achieved using r(GACCAAGUGUACCAGGCUA)dTdT targeting endogenous SNX27 and this target sequence was removed from the SNX27 rescue construct by synonymous mutation (GTGTAC -> GTATAT, nucleotides 1012 - 1017 of NM_001110151). Peptides corresponding to the C-terminal 6 residues of the β2AR (TNDSLL) and an alanine-extended version (TNDSLLA), labeled at the N-terminus with fluorescein (FITC), were obtained from Genemed Synthesis. Monoclonal anti-FLAG antibody (M1, Sigma) was conjugated with AlexaFluor dyes (Molecular Probes/Invitrogen) according to the manufacturer's instructions. AlexaFluor-conjugated secondary antibodies were purchased from the same vendor. The dilutions and sources of other primary antibodies used were: rabbit anti-FLAG, 1:500 (Sigma); rabbit anti-EBP50,1:1000 (ab3452 Abcam, Inc.); goat anti-NHERF2, 1:100 (sc-21117 Santa Cruz Biotechnology); mouse anti-EEA1, 1:500 (610457 BDBiosciences); mouse anti-LAMP3/CD63, 1:500 (H5C6 Developmental Studies Hybridoma Bank, University of Iowa); and rabbit anti-Rab11, 1:100 (71-5300 Invitrogen). Anti-SNX27 mouse monoclonal IgG was generated using residues 1-267 of hSNX27 (Joubert et al., 2004) and used at a 1:1000 dilution. HRP-coupled M2 antibody (Sigma) was used for receptor Westerns. HRP-coupled secondary antibodies were purchased from Amersham/GE Healthcare (anti-mouse and anti-rabbit IgG) and Pierce (anti-goat IgG).

Cell culture and Transfection. Human embryonic kidney 293 cells and A10 aortic smooth muscle cells (ATCC) were maintained in Dulbecco's modified Eagle's medium (DMEM) supplemented with 10% fetal bovine serum (University of California, San Francisco Cell Culture Facility). NHERF-deficient PS120 cells were kindly provided by Dr. Mark Donowitz (Johns Hopkins University, Baltimore MD). For siRNA transfection, cells at ~30% confluency in 6 cm dishes were transfected with Lipofectamine RNAiMax (Invitrogen) and 40 pmol of siRNA according to the manufacturer's protocol, split into 12-well plates 48 hours following transfection, and assayed at 72 hours post-transfection. For co-transfection of DNA and siRNA, Lipofectamine 2000 (Invitrogen) was used with 40 pmol siRNA and ~2 μg DNA in the same plating format and recommended protocol. DNA transfection was performed in 6-well or 12-well plates at ~50% cell confluency using Lipofectamine 2000 according to the manufacturer's protocol. Stably-transfected cells were selected in 500 μg/mL Geneticin (Life Technologies, Inc.), and cell clones expressing FLAG-tagged receptor constructs were chosen at similar levels based on average surface immunofluorescence/cell measured through flow cytometry, and found to have at least 90% of cells expressing surface immunoreactivity. Radioligand binding assay (performed as described in the next paragraph) verified that total receptor expression in each clone was in the range of 2-4 pmol/mg protein.

Radioligand Binding Assays. Single-point radioligand binding assay to estimate total

receptor expression was carried out using a minor variation of a previously described method (von Zastrow and Kobilka, 1992). Briefly, cells plated in 6-well dishes were washed with PBS, exposed to one cycle of freezing (-20˚C) and thawing, and mechanically resuspended in 200 µL PBS. Equal amounts of cell lysate (50 - 100 µg total protein as determined by Bradford assay) were aliquoted into 96-well plates and brought to a total volume of 100µL PBS including 11.5 nM [^{3}H]-dihydroalprenolol (Amersham), a saturating concentration used to estimate B_{max}. Each lysate was assayed in triplicate, and nonspecific binding was determined by including 10 µM unlabeled alprenolol (Sigma). Plates were incubated for 1 hour at room temperature with shaking, and membranes were harvested by filtration binding through glass fiber (Whatman GF/C) using a vacuum-driven harvester (Filtermate 196, Packard Instruments). Filters were washed extensively with 20 mM Tris Cl pH 7.5 and bound radioactivity was determined by liquid scintillation counting (Tri-Carb 2100TR, Packard Instruments).

Fluorescence Polarization Assays. Wild type and H112A mutant PDZ domains derived from SNX27, cloned in pBH4, were transformed into *E. coli* strain BL21(DE3) pLYS-S for expression, and recombinant proteins were purified using a Ni^{2+}-NTA (Qiagen) column. Proteins were further purified on a 16/60 Sephacryl S-100 gel filtration column (GE) run in 20mM HEPES/100mM NaCl (pH=7.4). The purified proteins were concentrated to 600-800µM, frozen in liquid nitrogen and stored at -80°C. Concentrations were determined using the Bradford method. The binding of the N-terminal fluorescein labeled peptides (TNDSLL and TNDSLLA) was monitored by following the increase in fluorescence polarization upon titration of the concentrated PDZ domain. The assay was

performed in 384-well plates containing 10nM labeled peptide in each well. The experiments were performed in 20 mM HEPES (pH=7.4), 100mM NaCl, and 20mM DTT at room temperature. Fluorescence polarization was measured using an Analyst HT Fluorometer (LJL Biosystems/Molecular devices) with excitation and emission set to 485nm and 530nm, respectively (Harris et al., 2001).

Fluorescence Microscopy. To assess localization of β_2ARs, PDZ proteins, and/or endosomal markers in HEK293 cells stably-expressing FLAG-tagged β_2AR, cells were transfected with siRNA or constructs encoding GFP-tagged PDZ protein where appropriate. 48 hours later agonist-naïve cells were incubated in the presence of AlexaFluor647-conjugated M1 anti-FLAG antibody (10 μg / ml) or rabbit anti-FLAG antibody (2 μg / mL) for 20 min to selectively label β_2ARs present in the plasma membrane. To label the internalized receptor pool, cells were subsequently incubated for 25 minutes in the presence of 10 μM isoproterenol, a condition that is sufficient to drive labeled β_2ARs to steady state in the recycling pathway. Cells were then quickly washed with cold phosphate-buffered saline and fixed in 4% formaldehyde/PBS for 10 minutes at room temperature, followed by a Tris-buffered saline quench for 5 minutes. Cells were then permeabilized where needed for 20 minutes in 0.1% Triton-X 100 and 5% FBS in PBS before primary and secondary antibody staining in the same buffer for 1 hr each. A10 cells were transfected with receptor constructs, and additional oligonucleotide as indicated, and labeled for FLAG-tagged receptors similarly. Surface-accessible AlexaFluor647-conjugated M1 antibody was further labeled with AlexaFluor555-conjugated anti-mouse IgG at 4°C before fixation. Fixed specimens were mounted to

glass slides in Fluormount-G (Southern Biotech) and examined at room temperature. Laser-scanning confocal microscopy was carried out using a Zeiss LSM510 microscope fitted with a 63X/NA1.4 oil objective. Wide field (epifluorescence) microscopy was carried out using a Nikon Diaphot microscope equipped with a 60X/NA1.4 oil objective, mercury arc lamp, standard dichroic filter sets (Chroma), and a 12 bit cooled CCD camera (MicroMax, Princeton Instruments) interfaced to a PC running MetaMorph acquisition and analysis software (Molecular Devices). Widefield images were rendered using ImageJ (http://rsb.info.nih.gov/ij/) (Collins, 2007) and confocal images were rendered using Zeiss LSM software. Illustrations were prepared using Photoshop and Illustrator software (Adobe). Background subtraction and scaling were done using non-saturated images and linear lookup tables. Colocalization analysis was assessed in confocal optical sections in two ways. First, independent scoring of positive structures in SNX27, EEA1 or receptor channels was done visually, with manual counting. Positive structures were defined by fluorescence intensity at least three standard deviations above background and encompassing contiguous pixels representing at least 500 nm. Degree of overlap was calculated from individual images and averaged over the indicated number of specimens selected at random. Second, colocalization was estimated by calculating the Pearson's correlation coefficient between the indicated image channels using the Manders_Coefficients.java plugin for ImageJ (Tony Collins and Wayne Rasband, Wright Cell Imaging Facility and NIH).

Fluorescence flow cytometry. Internalization and recycling of FLAG-tagged receptor constructs was assessed using AlexaFluor647-conjugated M1 anti-FLAG antibody and a

FACSCalibur flow cytometer (Becton Dickenson) as described previously (Hanyaloglu and von Zastrow, 2007). Internalization was determined by reduction of surface receptor immunoreactivity observed after incubation of cells in the presence of the adrenergic agonist isoproterenol (10μM) for the indicated number of minutes at 37°C. Recycling in HEK293 cells was determined by recovery of surface receptor immunoreactivity measured following a 25 minute exposure to isoproterenol and a subsequent agonist-removal incubation (50 minutes unless indicated otherwise) in the presence of the adrenergic antagonist alprenolol (10 μM) to prevent any residual agonist effects (corresponding to 'ALP' segment in Figure 1C). Analysis of recycling data according to level of recombinant SNX27 expression was carried out using dual channel flow cytometry in cells transiently transfected with the indicated version of SNX27-GFP, also as described previously (Lauffer et al., 2009). Recycling in A10 smooth muscle cells was evaluated by internalizing AlexaFluor647-conjugated M1 antibody with receptors, and determining internal receptor fluorescence loss following a 50 minute agonist withdrawal incubation and subsequent cell dissociation (TrypLE^{TM} trypsin replacement buffer, Invitrogen) at 4°C to retain internalized fluorescent antibodies while dissociating the surface-accessible fraction. Each experiment used duplicate or triplicate determinations of 2-10,000 cells each, and results shown represent the receptor recycling in cells transfected with (-)control siRNA minus that seen in cells transfected with SNX27 siRNA.

Western blot analysis. To assess knockdown efficiency, duplicate wells from the indicated analysis carried out in a 12-well plate were combined and solubilized in 200 μL

of lysis buffer: 0.1% (v/v) Triton X-100, 150 mM NaCl, 25 mM KCl, and 10 mM Tris, pH 7.4, Complete protease inhibitor cocktail (Roche). Lysates were clarified by centrifugation for 10 min at 20,000 x g in a microcentrifuge, the protein concentration of extracts was determined using the Bradford assay and equal protein loads were mixed 3:1 with 4x LDS sample buffer (Invitrogen) supplemented with 5% β-mercaptoethanol before heating to 95˚C for 5 minutes. Biotin-labeled, GPCR degradation assays have been described (Gage et al, 2001) and utilized here for isolation of mature receptor via surface protein biotinylation, streptavidin-agarose precipitation, and anti-FLAG immunoblotting. Protein samples from these experiments were reduced and denatured at 37°C for 1hr. The solubilized extracts were resolved by SDS-PAGE, transferred to nitrocellulose, and Ponceau S stained to verify equal loading before immunoblotting. Antibody incubations were carried out for 1 hr at room temperature in TBST containing 5% milk or BSA (anti-NHERF2). Immunoreactive species were identified using HRP-conjugated secondary antibodies (1:3000) or HRP-conjugated M2 antibody (1:500) followed by chemiluminescence detection (SuperSignal, Pierce). Exposures were captured using x-ray film or, for quantitative assessment, using a FluorChem 8000 luminescence imaging system (Alpha Innotech Corporation).

Statistical and kinetic analysis. In flow cytometric assays, mean fluorescence/cell of duplicate or triplicate collections of cells were used to calculate relative changes in basal surface receptor expression, agonist-induced internalization, and recycling efficiency for each independent experiment. Integrated densities of receptor-antibody-HRP luminescence in individual samples from biotin degradation immunoblots were similarly

normalized to the indicated reference for each independent experiment. Data were collected as replicates in a Prism spreadsheet for statistical and graphing analysis (Graphpad, Inc.). Replicate values were compared to the given reference using a Student's t-test or paired t-test as indicated in the figure legend. Curve-fitting of internalization and recycling time courses used replicate percentages over the multiple time points indicated to generate rate constants according to a 2-compartment endocytic recycling model. The rate of recycling was described by Recycling % = $F_r(1-e^{-k_r t})$ and the internalization kinetics were described by $F_{SR} = [F_r k_r + k_e * e^{-(k_e + F_r k_r)t}]/[k_e + F_r k_r]$ where F_r = recycling efficiency or maximum fraction recycled, k_r = recycling rate constant, t = time in minutes, F_{SR} = fraction of surface receptor remaining, and k_e = endocytic rate constant. Fitting of triplicate fluorescence polarization values of peptides to increasing concentrations of PDZ protein using a single binding site model have been described before (Harris et al., 2001).

4.5 ACKNOWLEDGEMENTS

We thank Henry Bourne, Robert Edwards, Keith Mostov and Bill Thelin for useful discussion, Mark Donowitz for providing PS120 cells and Courtni Salinas for assistance in developing critical reagents. The Laboratory for Cellular Analysis of the Hellen Diller Family Comprehensive Cancer Center at UCSF administered flow cytometry and confocal microscopy instrumentation. These studies were supported by the US National Institutes of Health (NIH DA012864 and DA010711 to MvZ) and the NIH Roadmap for Medical Research (PN2 EY016546 to TK).

4.6 REFERENCES

Ang, A.L., H. Folsch, U.M. Koivisto, M. Pypaert, and I. Mellman. 2003. The Rab8 GTPase selectively regulates AP-1B-dependent basolateral transport in polarized Madin-Darby canine kidney cells. *J Cell Biol*. 163:339-50.

Ang, A.L., T. Taguchi, S. Francis, H. Folsch, L.J. Murrells, M. Pypaert, G. Warren, and I. Mellman. 2004. Recycling endosomes can serve as intermediates during transport from the Golgi to the plasma membrane of MDCK cells. *J Cell Biol*. 167:531-43.

Appleton, B.A., Y. Zhang, P. Wu, J.P. Yin, W. Hunziker, N.J. Skelton, S.S. Sidhu, and C. Wiesmann. 2006. Comparative Structural Analysis of the Erbin PDZ Domain and the First PDZ Domain of ZO-1: Insights into determinants of PDZ domain specificity. *J. Biol. Chem.* 281:22312-22320.

Bretscher, A., D. Chambers, R. Nguyen, and D. Reczek. 2000. ERM-Merlin and EBP50 protein families in plasma membrane organization and function. *Annu Rev Cell Dev Biol*. 16:113-43.

Cao, T.T., H.W. Deacon, D. Reczek, A. Bretscher, and M. von Zastrow. 1999. A kinase-regulated PDZ-domain interaction controls endocytic sorting of the beta2-adrenergic receptor. *Nature*. 401:286-90.

Carlton, J., M. Bujny, A. Rutherford, and P. Cullen. 2005. Sorting Nexins – Unifying Trends and New Perspectives. *Traffic*. 6:75-82.

Collins, T.J. 2007. ImageJ for microscopy. *Biotechniques*. 43:25-30.

Cushing, P.R., A. Fellows, D. Villone, P. Boisguerin, and D.R. Madden. 2008. The Relative Binding Affinities of PDZ Partners for CFTR: A Biochemical Basis for Efficient Endocytic Recycling. *Biochemistry*. 47:10084-10098.

Delhaye, M., A. Gravot, D. Ayinde, F. Niedergang, M. Alizon, and A. Brelot. 2007. Identification of a Postendocytic Sorting Sequence in CCR5. *Mol Pharmacol*. 72:1497-1507.

Donowitz, M., B. Cha, N.C. Zachos, C.L. Brett, A. Sharma, C.M. Tse, and X. Li. 2005. NHERF family and NHE3 regulation. *J Physiol*. 567:3-11.

Doyle, D.A., A. Lee, J. Lewis, E. Kim, M. Sheng, and R. MacKinnon. 1996. Crystal Structures of a Complexed and Peptide-Free Membrane Protein-Binding Domain: Molecular Basis of Peptide Recognition by PDZ. *Cell*. 85:1067-1076.

Folsch, H., H. Ohno, J.S. Bonifacino, and I. Mellman. 1999. A novel clathrin adaptor complex mediates basolateral targeting in polarized epithelial cells. *Cell*. 99:189-98.

Folsch, H., M. Pypaert, S. Maday, L. Pelletier, and I. Mellman. 2003. The AP-1A and AP-1B clathrin adaptor complexes define biochemically and functionally distinct membrane domains. *J Cell Biol*. 163:351-62.

Gage, R.M., K.A. Kim, T.T. Cao, and M. von Zastrow. 2001. A transplantable sorting signal that is sufficient to mediate rapid recycling of G protein-coupled receptors. *J Biol Chem*. 276:44712-20.

Gage, R.M., E.A. Matveeva, S.W. Whiteheart, and M. von Zastrow. 2005. Type I PDZ ligands are sufficient to promote rapid recycling of G Protein-coupled receptors independent of binding to N-ethylmaleimide-sensitive factor. *J Biol Chem*. 280:3305-13.

Gan, Y., T.E. McGraw, and E. Rodriguez-Boulan. 2002. The epithelial-specific adaptor AP1B mediates post-endocytic recycling to the basolateral membrane. *Nat Cell Biol*. 4:605-9.

Gardner, L.A., A.P. Naren, and S.W. Bahouth. 2007. Assembly of an SAP97-AKAP79-cAMP-dependent Protein Kinase Scaffold at the Type 1 PSD-95/DLG/ZO1 Motif of the Human beta1-Adrenergic Receptor Generates a Receptosome Involved in Receptor Recycling and Networking. *J. Biol. Chem.* 282:5085-5099.

Gouet, P., E. Courcelle, D. Stuart, and F. Metoz. 1999. ESPript: analysis of multiple sequence alignments in PostScript. *Bioinformatics*. 15:305-308.

Hall, R.A., R.T. Premont, C.W. Chow, J.T. Blitzer, J.A. Pitcher, A. Claing, R.H. Stoffel, L.S. Barak, S. Shenolikar, E.J. Weinman, S. Grinstein, and R.J. Lefkowitz. 1998. The beta2-adrenergic receptor interacts with the Na+/H+-exchanger regulatory factor to control Na+/H+ exchange. *Nature*. 392:626-30.

Hanyaloglu, A.C., E. McCullagh, and M. von Zastrow. 2005. Essential role of Hrs in a recycling mechanism mediating functional resensitization of cell signaling. *Embo J*. 24:2265-83.

Hanyaloglu, A.C., and M. von Zastrow. 2007. A Novel Sorting Sequence in the beta2-Adrenergic Receptor Switches Recycling from Default to the Hrs-dependent Mechanism. *J. Biol. Chem.* 282:3095-3104.

Hanyaloglu, A.C., and M. von Zastrow. 2008. Regulation of GPCRs by endocytic membrane trafficking and its potential implications. *Annu Rev Pharmacol Toxicol*. 48:537-68.

Harris, B.Z., B.J. Hillier, and W.A. Lim. 2001. Energetic Determinants of Internal Motif Recognition by PDZ Domains. *Biochemistry*. 40:5921-5930.

He, J., M. Bellini, H. Inuzuka, J. Xu, Y. Xiong, X. Yang, A.M. Castleberry, and R.A. Hall. 2006. Proteomic analysis of beta1-adrenergic receptor interactions with PDZ scaffold proteins. *J Biol Chem*. 281:2820-7.

Joubert, L., B. Hanson, G. Barthet, M. Sebben, S. Claeysen, W. Hong, P. Marin, A. Dumuis, and J. Bockaert. 2004. New sorting nexin (SNX27) and NHERF specifically interact with the 5-HT4(a) receptor splice variant: roles in receptor targeting. *J Cell Sci*. 117:5367-5379.

Kajii, Y., S. Muraoka, S. Hiraoka, K. Fujiyama, A. Umino, and T. Nishikawa. 2003. A developmentally regulated and psychostimulant-inducible novel rat gene mrt1 encoding PDZ-PX proteins isolated in the neocortex. *Mol Psychiatry*. 8:434-444.

Lauffer, B.E., S. Chen, C. Melero, T. Kortemme, M. von Zastrow, and G.A. Vargas. 2009. Engineered Protein Connectivity to Actin Mimics PDZ-dependent

Recycling of G Protein-coupled Receptors but Not Its Regulation by Hrs. *J Biol Chem*. 284:2448-58.

Lin, D.-T., and R.L. Huganir. 2007. PICK1 and Phosphorylation of the Glutamate Receptor 2 (GluR2) AMPA Receptor Subunit Regulates GluR2 Recycling after NMDA Receptor-Induced Internalization. *J. Neurosci.* 27:13903-13908.

Lunn, M.-L., R. Nassirpour, C. Arrabit, J. Tan, I. Mcleod, C.M. Arias, P.E. Sawchenko, J.R. Yates, and P.A. Slesinger. 2007. A unique sorting nexin regulates trafficking of potassium channels via a PDZ domain interaction. *Nat Neurosci*. 10:1249-1259.

Maday, S., E. Anderson, H.C. Chang, J. Shorter, A. Satoh, J. Sfakianos, H. Folsch, J.M. Anderson, Z. Walther, and I. Mellman. 2008. A PDZ-binding motif controls basolateral targeting of syndecan-1 along the biosynthetic pathway in polarized epithelial cells. *Traffic*. 9:1915-24.

Marchese, A., M.M. Paing, B.R.S. Temple, and J. Trejo. 2008. G Protein-Coupled Receptor Sorting to Endosomes and Lysosomes. *Annual Review of Pharmacology and Toxicology*. 48:601-629.

Maxfield, F.R., and T.E. McGraw. 2004. Endocytic recycling. *Nat Rev Mol Cell Biol*. 5:121-32.

Mellman, I., and W.J. Nelson. 2008. Coordinated protein sorting, targeting and distribution in polarized cells. *Nat Rev Mol Cell Biol*. 9:833-45.

Moore, C.A.C., S.K. Milano, and J.L. Benovic. 2007. Regulation of Receptor Trafficking by GRKs and Arrestins. *Annual Review of Physiology*. 69:451-482.

Perego, C., C. Vanoni, A. Villa, R. Longhi, S.M. Kaech, E. Frohli, A. Hajnal, S.K. Kim, and G. Pietrini. 1999. PDZ-mediated interactions retain the epithelial GABA transporter on the basolateral surface of polarized epithelial cells. *EMBO J.* 18:2384-2393.

Rincon, E., T. Santos, A. Avila-Flores, J.P. Albar, V. Lalioti, C. Lei, W. Hong, and I. Merida. 2007. Proteomics Identification of Sorting Nexin 27 as a Diacylglycerol Kinase {zeta}-associated Protein: New Diacylglycerol Kinase Roles in Endocytic Recycling. *Mol Cell Proteomics*. 6:1073-1087.

Tanowitz, M., and M. von Zastrow. 2003. A novel endocytic recycling signal that distinguishes the membrane trafficking of naturally occurring opioid receptors. *J. Biol. Chem.* 278:45978-45986.

Thompson, J.D., D.G. Higgins, and T.J. Gibson. 1994. CLUSTAL W: improving the sensitivity of progressive multiple sequence alignment through sequence weighting, position-specific gap penalties and weight matrix choice. *Nucleic Acids Res*. 22:4673-80.

Tonikian, R., Y. Zhang, S.L. Sazinsky, B. Currell, J.-H. Yeh, B. Reva, H.A. Held, B.A. Appleton, M. Evangelista, Y. Wu, X. Xin, A.C. Chan, S. Seshagiri, L.A. Lasky, C. Sander, C. Boone, G.D. Bader, and S.S. Sidhu. 2008. A Specificity Map for the PDZ Domain Family. *PLoS Biology*. 6:e239.

van Kerkhof, P., J. Lee, L. McCormick, E. Tetrault, W. Lu, M. Schoenfish, V. Oorschot, G.J. Strous, J. Klumperman, and G. Bu. 2005. Sorting nexin 17 facilitates LRP recycling in the early endosome. *Embo J*. 24:2851-61.

von Zastrow, M., and B.K. Kobilka. 1992. Ligand-regulated internalization and recycling of human beta 2-adrenergic receptors between the plasma membrane and endosomes containing transferrin receptors. *J Biol Chem*. 267:3530-8.

Wang, Y., B. Lauffer, M. Von Zastrow, B.K. Kobilka, and Y. Xiang. 2007. N-Ethylmaleimide-Sensitive Factor Regulates beta2 Adrenoceptor Trafficking and Signaling in Cardiomyocytes. *Mol Pharmacol*. 72:429-439.

Wente, W., T. Stroh, A. Beaudet, D. Richter, and H.-J. Kreienkamp. 2005. Interactions with PDZ Domain Proteins PIST/GOPC and PDZK1 Regulate Intracellular Sorting of the Somatostatin Receptor Subtype 5. *J. Biol. Chem.* 280:32419-32425.

Wieman, H.L., S.R. Horn, S.R. Jacobs, B.J. Altman, S. Kornbluth, and J.C. Rathmell. 2009. An essential role for the Glut1 PDZ-binding motif in growth factor regulation of Glut1 degradation and trafficking. *Biochem J*. 418:345-367.

Xu, Y., L.F. Seet, B. Hanson, and W. Hong. 2001. The Phox homology (PX) domain, a new player in phosphoinositide signalling. *Biochem J*. 360:513-30.

Yudowski, G.A., M.A. Puthenveedu, A.G. Henry, and M. von Zastrow. 2009. Cargo-mediated regulation of a rapid Rab4-dependent recycling pathway. *Mol Biol Cell*. 20:2774-84.

4.7 Figures

Figure 1. Efficient internalization and recycling of the β_2AR in HEK293 cells simultaneously depleted of NHERFs 1 and 2. (A) Schematic of NHERF1 (also called EBP50) and NHERF2 (also called E3KARP) domain organization, showing PDZ (Post-synaptic density 95, Discs large, ZO-1) domains and ERM protein-binding domain (EBD). **(B)** Verification of dual NHERF1 + 2 knockdown by immunoblot. Arrows indicate specific bands; nonspecific bands (NS) verify equal loading between the indicated samples. Molecular mass markers (in kD) are indicated. Images shown are representative of 3 experiments. **(C)** Flow cytometric assessment of receptor internalization and recycling. HEK293 cells stably expressing either a FLAG-tagged, wild-type β_2AR or the FLAG- β_2AR-Ala PDZ mutant were transfected with the indicated siRNAs and assayed for surface receptor immunoreactivity before and after an agonist pretreatment and washout using fluorescence flow cytometry. **(D)** Recycling efficiency calculated from data shown in (C), as described in *Materials and Methods*. All error bars: SEM, p values: Student's t-test with the (–)Control condition, n=3 or 4.

Figure 2. SNX27 is a distinct NHERF-related PDZ protein that interacts with the β_2AR in early endosomes. (A) Schematic of SNX27 domain organization showing PDZ domain, Phox homology (PX) domain and the alternatively spliced C-terminal region that distinguishes a and b isoforms of SNX27 (a/b). Expanded box shows sequence comparison of the SNX27 PDZ domain (residues 43-133) with the first PDZ domain of

NHERF1 (residues 14-91) and NHERF2 (residues11-88). Sequences obtained from the SWISS/UNIPROT database were aligned with CLUSTAL-W (Thompson et al., 1994) and displayed with ESPript (Gouet et al., 1999). Secondary structure elements of the first PDZ domain of NHERF1 (Protein Data Bank code 1g9o) are indicated above the alignment. Conserved residues in the three PDZ domains are in bold. Residues critical for recognition of peptide side chains at positions P_0, P_{-1}, P_{-2}, and P_{-3} are shown in cyan, yellow, red and blue respectively (Appleton et al., 2006). **(B)** Interaction of the β2AR-derived tail sequence with the SNX27-derived PDZ domain. Purified, recombinant PDZ domain was mixed in increasing concentration with FITC-labeled peptides corresponding to the 6 C-terminal residues of the wild type β_2AR (a transplantable recycling sequence, solid line), or an alanine-extended version that lacks detectable recycling activity (dotted line). K_d was estimated by single site fit. The plots shown are representative of three independent experiments, error bars reflecting a representative SD of triplicate samples. **(C)** FLAG- β_2AR- expressing HEK293 cells were transfected with the indicated GFP-tagged PDZ protein. Following internalization of antibody-labeled receptors stimulated by 10 uM isoproterenol for 25 minutes, cells were fixed and imaged using dual-channel, laser-scanning confocal microscopy to reveal subcellular localization of the indicated protein. **(D)** FLAG- β_2AR and SNX27-GFP-transfected cells were further stained for endocytic markers detected a third fluorescent channel. All images show a middle z section and are representative of at least 3 independent experiments. Scale bar in lower right panel, 5 μm. Merged images contain boxed insets enlarged 2x from the indicated regions.

Figure 3. Depletion of endogenous SNX27 prevents PDZ-directed recycling of β2ARs and accelerates downregulation. (A) Representative immunoblot analysis (n = 4) of siRNA-mediated knockdown of the indicated PDZ protein in β_2AR-expressing HEK293 cells. NHERF2 (arrow) resolves above a nonspecific band that verifies equal loading. Apparent molecular masses are indicated in parentheses. **(B)** Effect of knockdowns on FLAG- β_2AR recycling assessed by fluorescence flow cytometry 50 minutes after agonist removal from the culture medium. Error bars: SEM, p values: Student's t-test with (-) Control results, n=4-6. **(C)** Time course of FLAG- β_2AR recycling in cells transfected with control (solid line) compared to SNX27 siRNA (dotted line). Error Bars: SEM, n=4. **(D)** Effect of SNX27 depletion on turnover of surface-biotinylated FLAG- β_2AR (top row) and FLAG- β_2AR-Ala (bottom rows) after incubation of cells for the indicated time period with 10 μM isoproterenol. **(E)** Quantification of the loss of biotinylated, FLAG-tagged receptors after the 5 hour exposure to 10 μM isoproterenol. Error bars: SEM, p values: Student's t-test for the SNX27 effect on degradation for each receptor, n=3.

Figure 4. Transgenic rescue of β_2AR recycling by recombinant SNX27. (A) Immunoblot showing depletion of endogenous SNX27 by silencing relative to (-)Control siRNA (lanes 1 and 2 from left), and replacement by co-transfection of SNX27-GFP but not GFP control plasmid (lanes 3 and 4). Electrophoretic mobilities of endogenous and SNX27 and recombinant SNX27-GFP are indicated by arrows at left. **(B)** Flow cytometric analysis showing rescue of FLAG- β_2AR recycling in SNX27 knockdown cells by co-transfection of either isoform of recombinant rat SNX27, or their GFP-tagged

counterparts. **(C and D)** Verification of transgenic rescue using dual channel fluorescence flow cytometry and gating of recycling data based on recombinant SNX27 expression. Panel C shows a representative fluorescence intensity histogram of the GFP channel. The region indicated by '(+)' represents the populations used to verify transgenic rescue of recycling. Panel D shows FLAG- β2AR recycling measured specifically in the SNX27/GFP (+) population. Error bars: SEM, p values: Student's t-test with GFP control, n=4-6 experiments.

Figure 5. The recycling activity of SNX27 requires both its PDZ domain-mediated interaction with cargo and PX domain-mediated association with endosomes. (A) Fluorescence polarization analysis demonstrating the ability of the H112A mutation of the SNX27 PDZ domain to disrupt binding to the wild type β_2AR-derived PDZ motif. Representative saturation plots for the wild type PDZ domain (solid line) and H112A mutant PDZ domain (dotted line) are shown. **(B)** Representative examples of fluorescence localization patterns of PDZ-mutant (H112A) and PX-mutant (ΔPX) versions of SNX27, relative to FLAG-β_2AR and EEA1, verifying that the PX domain is specifically required for early endosome localization of SNX27 while the PDZ domain is not. **(C)** Flow cytometric analysis of FLAG-β_2AR recycling in SNX27-knockdown cells also transfected with a GFP, SNX27a-GFP or SNX27a-GFP containing a mutated PDZ domain (H112A) or deleted PX domain (ΔPX). Error bars: SEM, p values: Student's t-test comparison to the empty GFP control, n=4. **(D)** Flow cytometric analysis showing that SNX27 depletion specifically prevents PDZ motif-directed recycling of FLAG-β2AR (bars 1 and 2 from left, these data are re-plotted from Figure 3 for comparison) without

detectably affecting recycling directed by a distinct, non-PDZ sorting sequence (FLAG-β2-mrs, bars 3 and 4). The inset shows a representative immunoblot confirming efficient knockdown of SNX27 in the FLAG-β2-mrs-expressing HEK293 cells used in the recycling assays (left lane: (-) control, right lane: SNX27 siRNA transfection). **(E)** SNX27-GFP and FLAG-β_2AR were co-expressed in A10 aortic smooth muscle cells. FLAG-β_2AR present in the plasma membrane was labeled and internalized as described in *Materials and Methods*. Representative confocal images showing SNX27-GFP (top image), FLAG-β_2AR (middle image), and a merged image (bottom). Colocalization of SNX27-GFP with β_2AR-containing endosomes are enlarged in the inset (2x larger). Scale bar, 20 μm. **(F)** The effect of SNX27 depletion on FLAG-β_2AR or FLAG-β2-mrs recycling was measured in A10 cells by antibody efflux, as described in *Materials and Methods*. Bars represent the reduction of recycling efficiency produced by SNX27 knockdown, measured 50 minutes after agonist removal from the culture medium. The third bar from right shows a rescue condition, where the relative effect of SNX27 siRNA on FLAG-β_2AR recycling was assessed in the presence of recombinant SNX27. Error bars: SEM of recycling differences, p values: paired t-test of recycling % in (-)control v. SNX27 siRNA-transfected conditions, n=3-7.

Supplemental Figure 1. Subcellular localization of FLAG-β_2AR and PDZ-interacting proteins in agonist-naïve HEK293 cells, and the recycling defect of SNX27 depletion as visualized by fluorescence microscopy. (A) Representative dual

channel epifluorescence micrographs showing the localization of GFP-NHERF1 and FLAG-β_2AR in a focal plane near the base of the cell. **(B)** Representative epifluorescence micrographs showing localization of the indicated GFP-tagged PDZ proteins relative to agonist-naïve (left set of panels) and agonist-internalized (right set of panels) FLAG-β_2AR observed in a focal plane near the middle of cells. Arrowheads indicate examples of receptor-containing endosomes. **(C)** Stably transfected HEK293 cells expressing FLAG-β_2AR were transfected with non-silencing (-) Control or SNX27-silencing siRNA. FLAG-β_2AR localization in representative cells is shown, as visualized by epifluorescence microscopy using a mid-focal plane. Left panels: SNX27 depletion produced a partial but clearly visible increase in internal FLAG-β_2AR immunoreactivity in agonist-naïve cells (compare top and bottom images), consistent with a low level of constitutive (agonist-independent) endocytosis of receptors and impaired recycling in SNX27-depleted cells. Middle panels: SNX27 depletion did not detectably impair isoproterenol-induced internalization of FLAG-β_2AR. Right panels: SNX27 depletion produced a visually obvious reduction in FLAG-β_2AR recycling after agonist washout, effectively preventing the internalized receptor pool from returning to the plasma membrane and thereby further verifying the primary recycling defect established quantitatively by flow cytometry. Scale bar, 10 μm.

Supplemental Figure 2. Effects of PDZ protein knockdown on steady-state receptor expression and internalization. **(A)** Effect of the indicated PDZ protein knockdown on steady state surface expression of FLAG-β_2AR (left set of bars) and FLAG-β_2AR-Ala (right set of bars) was assessed by fluorescence flow cytometry. HEK293 cells

expressing the indicated receptor construct were transfected with the indicated siRNA and assessed for surface receptor immunoreactivity by anti-FLAG surface staining and flow cytometry 72 hours later. Data are normalized to the surface receptor measured in the same cell clone transfected with non-silencing (-) Control RNA duplex. Error bars reflect the SEM of at least 4 experiments and p values of a Student's t-test between the surface receptor to (-) Control-treated cells are shown. **(B)** Effect of SNX27 knockdown on total cellular receptor density of FLAG-β_2AR measured by radioligand binding. FLAG-β_2AR-expressing HEK293 cells were mock-transfected (left bar), transfected with non-silencing (-) control siRNA (middle bar) or transfected with SNX27 siRNA (right bar) and total cellular receptor expression was estimated by B_{max} determination using the membrane-permeant radioligand dihydroalprenolol, as described in Materials and Methods, 72 hours later. Error bars reflect SEM (n=6) and p values shown are results of a Student's t-test relative to the mock-transfected condition. **(C)** Flow cytometric analysis of isoproterenol-induced FLAG-β_2AR internalization in cells depleted of the indicated PDZ protein. Data were incorporated into a 2-compartment model reflecting simultaneous endocytosis and fractional recycling, assuming first order kinetics for each process, as specified as an equation in the figure and further described in *Materials and Methods*. The recycling rate constant (k_r) and maximum fraction of recycled receptor (F_r) were derived from experiments shown in Figure 3, in which recycling was measured in the absence of receptor endocytosis. Endocytic rate constants (k_e) were calculated by iterative best-fit analysis carried out using GraphPad Prism software. The inset table shows a summary of the kinetic parameters determined for each condition. Error bars reflect SEM of 4 experiments. This analysis indicates that SNX27 depletion primarily

affected F_r.

Supplemental Figure 3. Schematic and relative degradation of the chimeric, FLAG-β_2AR-mrs. **(A)** Schematic showing detail of the FLAG-β2-mrs, which is a previously-characterized mutant receptor construct (Tanowitz and von Zastrow, 2003) possessing a non-PDZ recycling sequence in place of the PDZ motif present in the β_2AR. **(B)** Effect of SNX27 depletion on turnover of surface-biotinylated FLAG-β2-mrs after incubation of cells for the indicated time period with 10 μM isoproterenol. A representative immunoblot is shown. **(C)** Quantification of the effect of SNX27 knockdown on anti-FLAG immunoreactivity representing biotinylated FLAG-tagged receptors, detected after exposing cells to 10 μM isoproterenol for 5 hours. Error bars reflect the SEM of 3 experiments; p values were calculated by Student's t-test. The data for SNX27 effect on FLAG-β_2AR are replotted from Figure 3 for comparison.

Fig.1

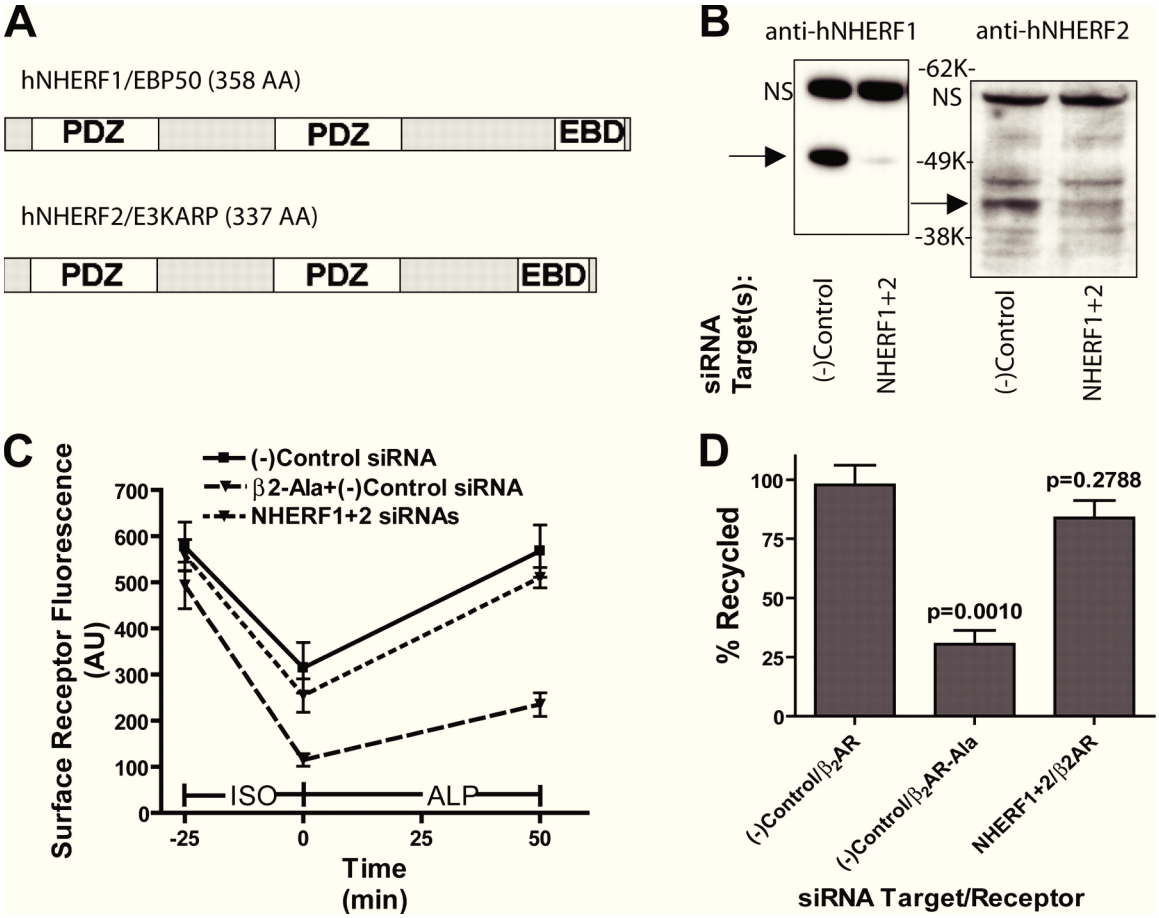
A
hNHERF1/EBP50 (358 AA)
PDZ
PDZ
EBD
hNHERF2/E3KARP (337 AA)
PDZ
PDZ
EBD
B
anti-hNHERF1
anti-hNHERF2
NS
-62K-
NS
-49K-
-38K-
siRNA Target(s):
(-)Control
NHERF1+2
(-)Control
NHERF1+2
C
(-)Control siRNA
β2-Ala+(-)Control siRNA
NHERF1+2 siRNAs
Surface Receptor Fluorescence (AU)
700
600
500
400
300
200
100
0
ISO
ALP
-25
0
25
50
Time (min)
D
% Recycled
100
75
50
25
0
p=0.0010
p=0.2788
(-)Control/β2AR
(-)Control/β2AR-Ala
NHERF1+2/β2AR
siRNA Target/Receptor

Fig.2

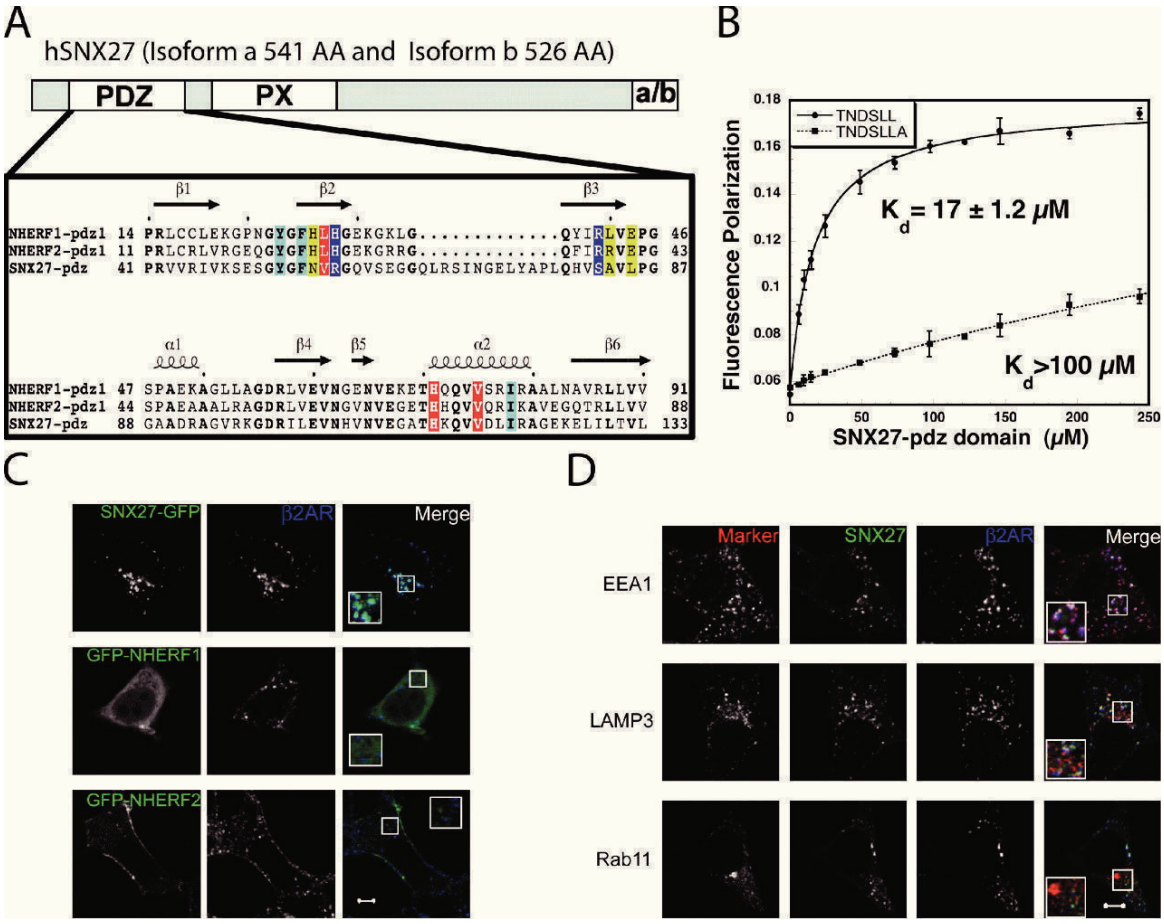
A
hSNX27 (Isoform a 541 AA and Isoform b 526 AA)
PDZ
PX
a/b
β1
β2
β3
NHERF1-pdz1 14 PRLCCLEKGPNGYGFHLHGEKGKLG.....QYIRLVEPG 46
NHERF2-pdz1 11 PRLCRLVRGEQGYGFHLHGEKGRRG.....QFIRRVEPG 43
SNX27-pdz 41 PRVVRIVKSESGYGFNVRGQVSEGGQLRSINGELYAPLQHVSAVLPG 87
α1
β4
β5
α2
β6
NHERF1-pdz1 47 SPAEKAGLLAGDRLVEVNGENVEKETHQQVVSRIRAALNAVRLLVV 91
NHERF2-pdz1 44 SPAEAAALRAGDRLVEVNGVNVEGETHHQVVQRIKAVEGQTRLLVV 88
SNX27-pdz 88 GAADRAGVRKGDRILEVNHVNVEGATHKQVVDLIRAGEKELILTVL 133
B
TNDSLL
TNDSLLA
Fluorescence Polarization
0.18
0.16
0.14
0.12
0.1
0.08
0.06
K d = 17 ± 1.2 μM
K d >100 μM
0
50
100
150
200
250
SNX27-pdz domain (μM)
C
SNX27-GFP
β2AR
Merge
GFP-NHERF1
GFP-NHERF2
D
Marker
SNX27
β2AR
Merge
EEA1
LAMP3
Rab11

Fig.3

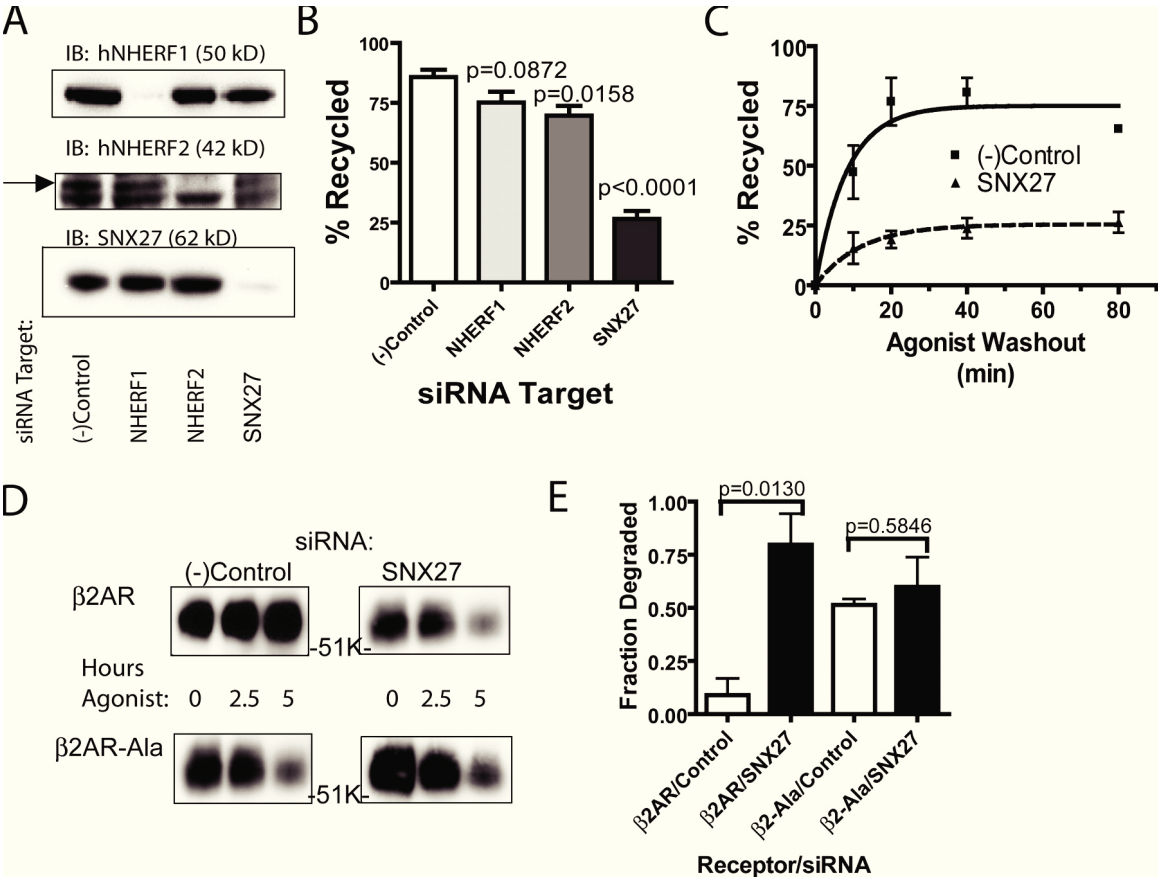
A
IB: hNHERF1 (50 kD)
IB: hNHERF2 (42 kD)
IB: SNX27 (62 kD)
siRNA Target:
(-)Control
NHERF1
NHERF2
SNX27
B
% Recycled
p=0.0872
p=0.0158
p<0.0001
(-)Control
NHERF1
NHERF2
SNX27
siRNA Target
C
% Recycled
(-)Control
SNX27
Agonist Washout
(min)
D
siRNA:
(-)Control
SNX27
β2AR
-51K-
Hours
Agonist: 0 2.5 5 0 2.5 5
β2AR-Ala
-51K-
E
Fraction Degraded
p=0.0130
p=0.5846
β2AR/Control
β2AR/SNX27
β2-Ala/Control
β2-Ala/SNX27
Receptor/siRNA

Fig.4

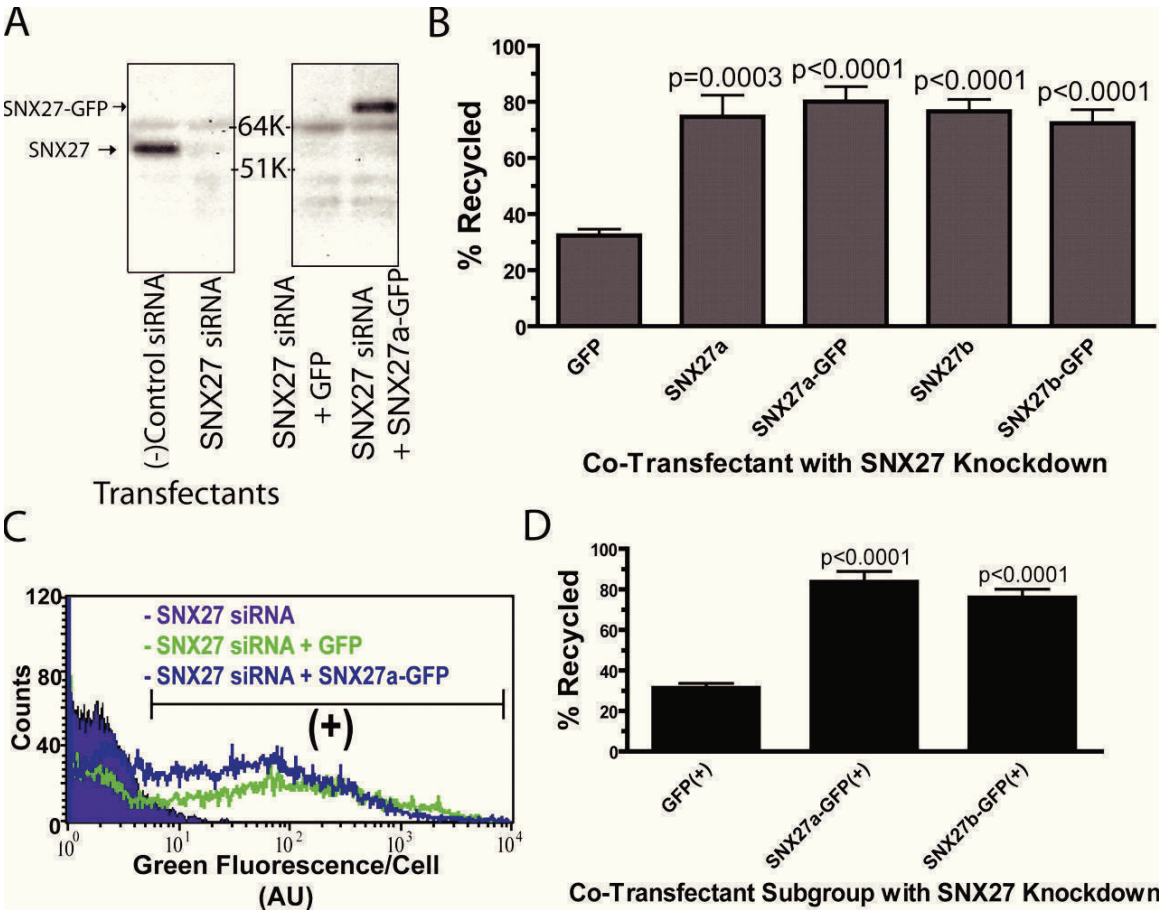
A
SNX27-GFP
SNX27
64K
51K
(-)Control siRNA
SNX27 siRNA
SNX27 siRNA + GFP
SNX27 siRNA + SNX27a-GFP
Transfectants
B
% Recycled
p=0.0003
p<0.0001
p<0.0001
p<0.0001
GFP
SNX27a
SNX27a-GFP
SNX27b
SNX27b-GFP
Co-Transfectant with SNX27 Knockdown
C
Counts
- SNX27 siRNA
- SNX27 siRNA + GFP
- SNX27 siRNA + SNX27a-GFP
(+)
Green Fluorescence/Cell (AU)
D
% Recycled
p<0.0001
p<0.0001
GFP(+)
SNX27a-GFP(+)
SNX27b-GFP(+)
Co-Transfectant Subgroup with SNX27 Knockdown

Fig.5

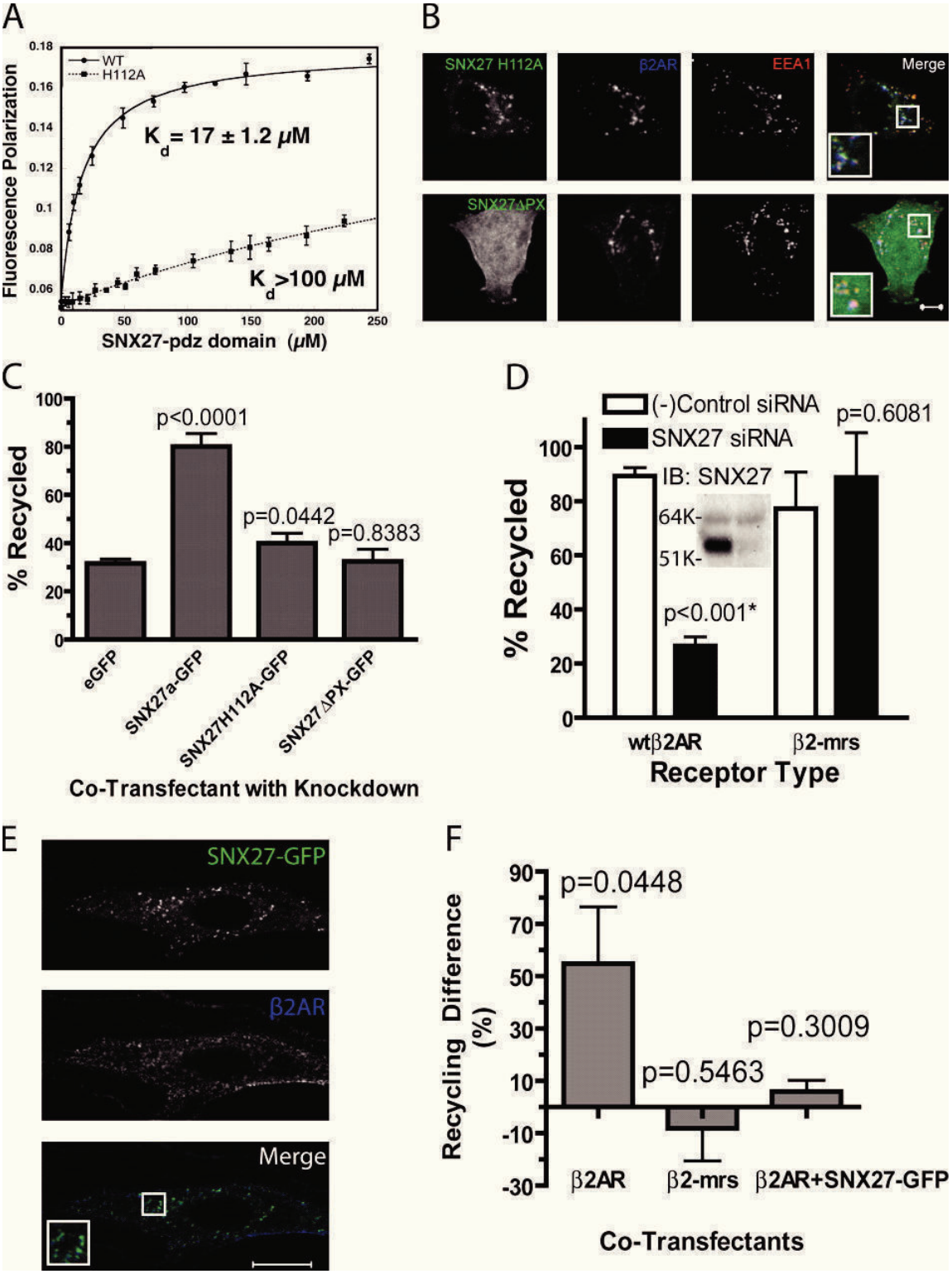
A
WT
H112A
K_d = 17 ± 1.2 μM
K_d >100 μM
Fluorescence Polarization
SNX27-pdz domain (μM)
B
SNX27 H112A
β2AR
EEA1
Merge
SNX27ΔPX
C
% Recycled
p<0.0001
p=0.0442
p=0.8383
eGFP
SNX27a-GFP
SNX27H112A-GFP
SNX27ΔPX-GFP
Co-Transfectant with Knockdown
D
(-)Control siRNA
SNX27 siRNA
IB: SNX27
64K-
51K-
p<0.001*
p=0.6081
% Recycled
wtβ2AR
β2-mrs
Receptor Type
E
SNX27-GFP
β2AR
Merge
F
Recycling Difference (%)
p=0.0448
p=0.5463
p=0.3009
β2AR
β2-mrs
β2AR+SNX27-GFP
Co-Transfectants

Fig.S1

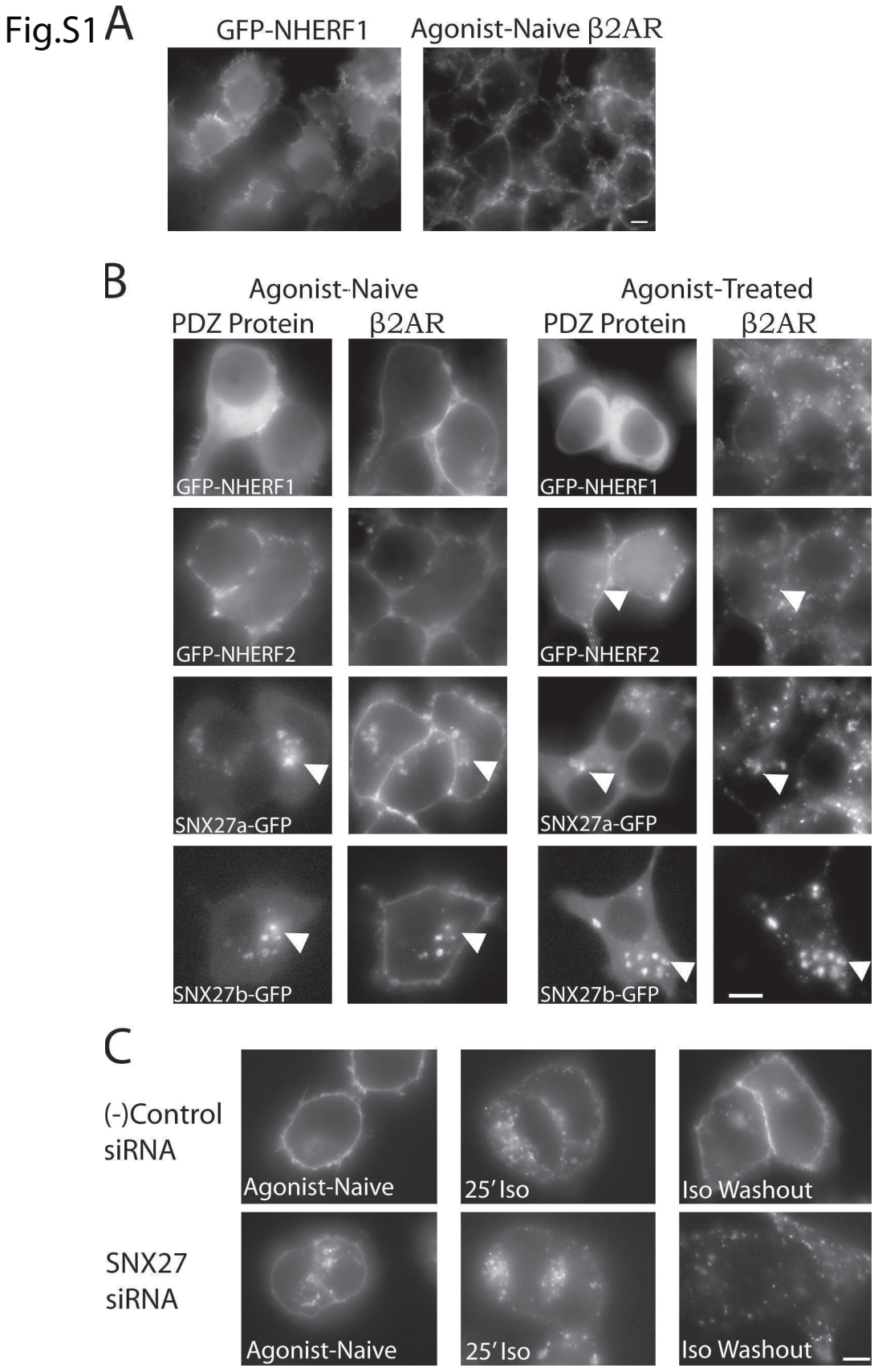
A
GFP-NHERF1
Agonist-Naive β2AR
B
Agonist-Naive
Agonist-Treated
PDZ Protein
β2AR
PDZ Protein
β2AR
GFP-NHERF1
GFP-NHERF1
GFP-NHERF2
GFP-NHERF2
SNX27a-GFP
SNX27a-GFP
SNX27b-GFP
SNX27b-GFP
C
(-)Control siRNA
SNX27 siRNA
Agonist-Naive
25' Iso
Iso Washout
Agonist-Naive
25' Iso
Iso Washout

Fig.S2

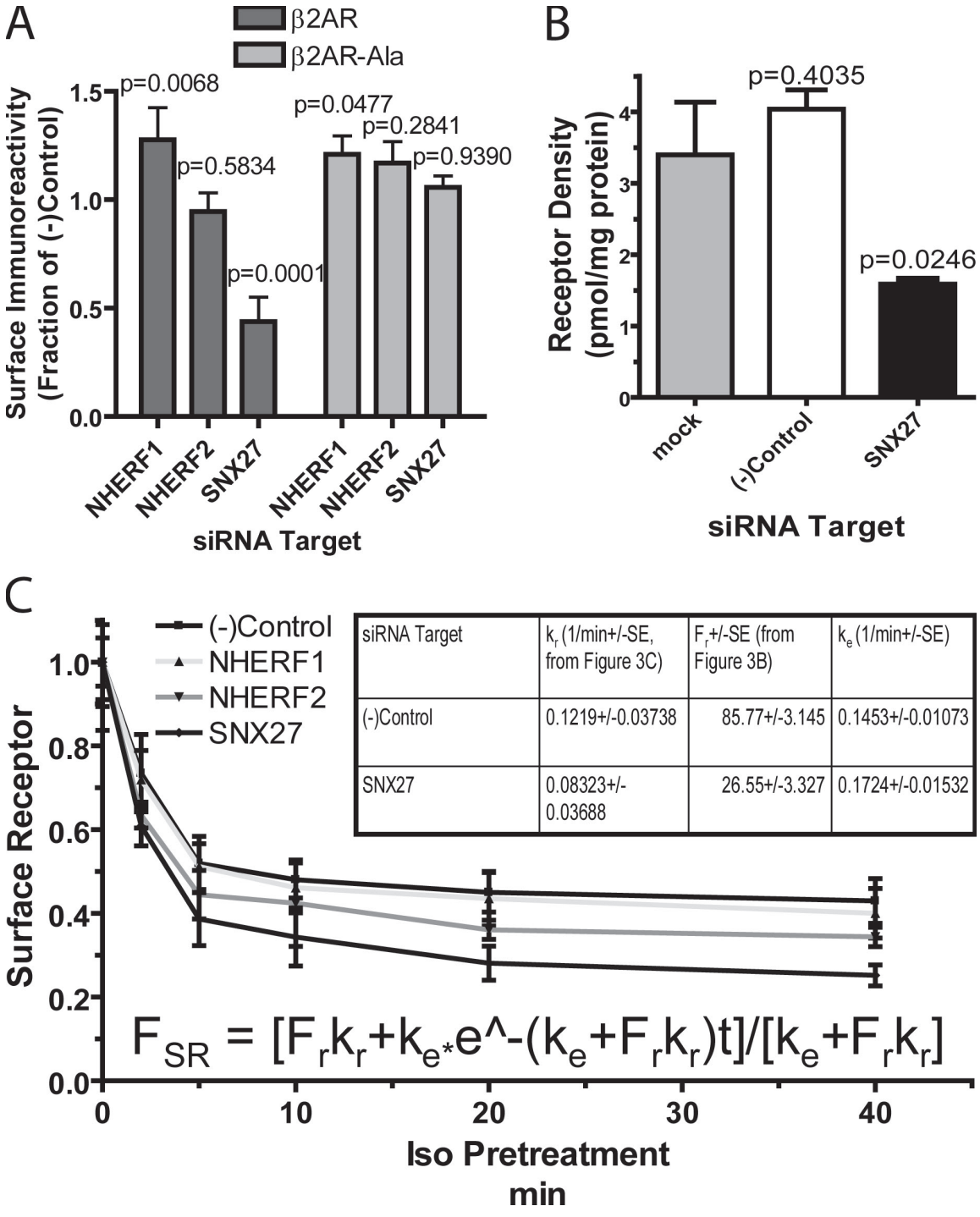

siRNA Target	k_r (1/min+/-SE, from Figure 3C)	F_r+/-SE (from Figure 3B)	k_e (1/min+/-SE)
(-)Control	0.1219+/-0.03738	85.77+/-3.145	0.1453+/-0.01073
SNX27	0.08323+/-0.03688	26.55+/-3.327	0.1724+/-0.01532

Fig.S3

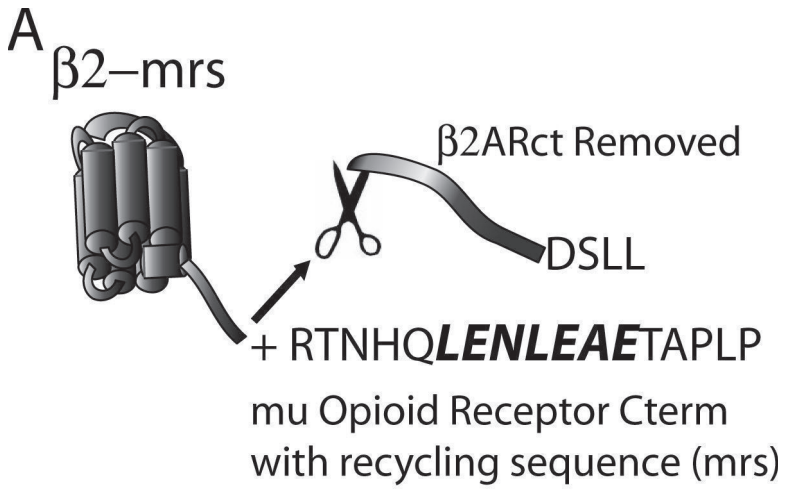
A
β2–mrs
β2ARct Removed
DSLL
+ RTNHQLENLEAETAPLP
mu Opioid Receptor Cterm
with recycling sequence (mrs)

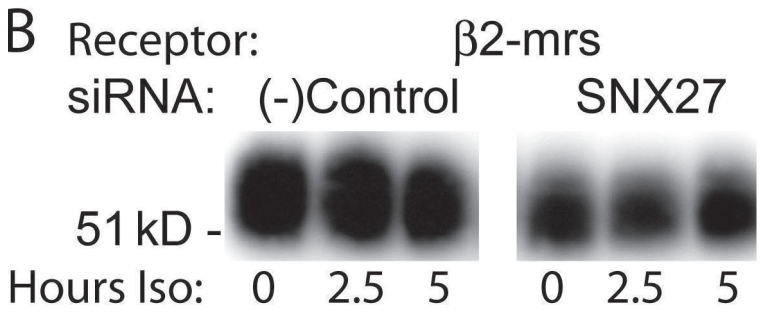
B
Receptor:
β2-mrs
siRNA:
(-)Control
SNX27
51 kD -
Hours Iso:
0
2.5
5
0
2.5
5

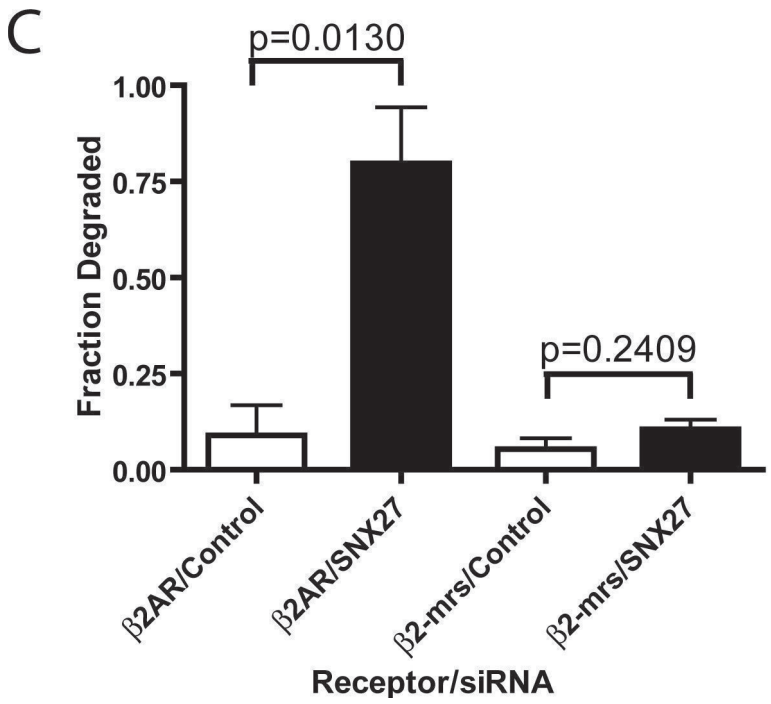
C
p=0.0130
p=0.2409
1.00
0.75
0.50
0.25
0.00
Fraction Degraded
β2AR/Control
β2AR/SNX27
β2-mrs/Control
β2-mrs/SNX27
Receptor/siRNA

Chapter 5:

SNX27 mediates retromer tubule entry and endosome-to-plasma membrane trafficking of signaling receptors

Paul Temkin conceived the project and wrote the manuscript. Paul Temkin performed most of the experiments with additional contributions from Benjamin Lauffer. Mass-Spectrometry was performed by Stefani Jager (UCSF), analyzed by Peter Cimermancic (UCSF), in the lab of Nevan Krogan (UCSF).

5.1 Abstract

Endocytic sorting of signaling receptors between recycling and degradative pathways is a key cellular process controlling the surface complement of receptors and, accordingly, the cell's ability to respond to specific extracellular stimuli. The beta-2 adrenergic receptor (β2AR) is a prototypical seven-transmembrane signaling receptor that recycles rapidly and efficiently to the plasma membrane after ligand-induced endocytosis. β2AR recycling is dependent on the receptor's C-terminal PDZ ligand and Rab4(Cao, Deacon et al. 1999; Seachrist, Anborgh et al. 2000). This active sorting process is required for functional resensitization of β2AR-mediated signaling(Wang, Lauffer et al. 2007; Hanyaloglu and von Zastrow 2008). Here we show that sequence-directed sorting occurs at the level of entry into retromer tubules and that retromer tubules are associated with Rab4. Further, we show that sorting nexin 27 (SNX27) serves as an essential adapter protein linking β2ARs to the retromer tubule. SNX27 does not appear to directly interact with the retromer core complex, but does interact with the retromer associated Wiskott-Aldrich Syndrome Protein and SCAR Homolog (WASH) complex. The present results identify a role for retromer in endocytic trafficking of signaling receptors, in regulating a receptor-linked signaling pathway, and in mediating direct endosome-to-plasma membrane traffic.

5.2 Introduction, Results, and Discussion

After treatment with agonist such as isoproterenol, β2ARs trigger a signaling cascade and undergo clathrin mediated endocytosis. β2ARs are then rapidly recycled from the early endosome antigen 1 (EEA1) compartment (Fig 1a, b, 4a) to the plasma membrane (Fig 2c), resensitizing the cell(Pippig, Andexinger et al. 1995). Internalized transmembrane proteins are generally thought to leave the endosome through tubules(Maxfield and McGraw 2004). In the case of β2AR, receptor-containing tubular endosomal protrusions can be visualized in living cells (Fig 1a, c)(Puthenveedu, Taunton et al.). β2AR recycling is sequence-dependent, requiring a C-terminal PDZ ligand(Cao, Deacon et al. 1999). When this ligand is occluded by a HA tag (β2AR-HA), mutant receptors fail to recycle efficiently and are not seen in endosomal tubules (Fig 1c)(Cao, Deacon et al. 1999). Therefore, these tubules likely represent the structure responsible for sequence-dependent recycling of β2AR.

Cargo that are capable of recycling efficiently with bulk membrane flux, such as the transferrin receptor (TFR), exit endosomes via multiple dynamic tubules(Sonnichsen, De Renzis et al. 2000). The β2AR was previously shown to enter a specific subset of these tubules(Puthenveedu, Taunton et al.). To investigate the hypothesis that β2AR-containing tubules are biochemically distinct, we took a candidate-based approach to identify specific tubule components.

Because both recycling (β2AR) and non-recycling (β2AR-HA) receptors were localized to similar endosomes but appeared to differ in lateral distribution near the highly curved neck region of endosomal tubules (Fig 1c), we asked whether curvature sensing/inducing Bin–Amphiphysin–Rvs (BAR) domain-containing proteins might be

localized there. We first considered sorting nexins, because several contain a BAR domain and an endosome-associating PX domain(Carlton, Bujny et al. 2004; Carlton and Cullen 2005). We looked at four of these BAR domain-containing sorting nexins (SNX1, SNX4, SNX5, and SNX9). We noticed striking, and nearly complete, overlap of SNX1 and SNX5 with β2AR-containing tubules (Fig 1c; data not shown for SNX5). Quantification across multiple cells verified that the vast majority (92.5%; n = 40 tubules) of endosomal tubules containing internalized β2ARs co-localized with a concentrated region of GFP-SNX1[8].

SNX1 and SNX5 have been previously associated with retromer. Retromer is composed of two distinct multi-protein subcomplexes, one containing sorting nexins and the other containing vacuolar protein sorting (VPS) proteins VPS26, VPS29, and VPS35(Bonifacino and Hurley 2008; Mari, Bujny et al. 2008). Recruitment of the VPS26/29/35 subcomplex to the endosome requires previous recruitment of the SNX-containing subcomplex and Rab7(Rojas, van Vlijmen et al. 2008). Therefore, we next visualized a component of the VPS26/29/35 retromer subcomplex to determine whether the complete retromer complex was forming on these tubules.

VPS29-GFP was also concentrated on β2AR-containing tubules (Fig 1c, Supplementary Movie); quantification across multiple examples indicated that 96.5% (n=57 tubules) of β2AR-containing endosome tubules were decorated with VPS29-GFP. These VPS29 foci extended off the edge of the endosome limiting membrane and co-localized with tubular β2AR staining. In rapid (2Hz) image series, β2AR could be seen extending distally beyond the SNX1 or VPS29 marked portion of the tubule (Fig 1c, d, Supplementary Movie). Essentially all VPS29-GFP puncta co-localized with β2AR on

vesicles (95.4%, n=177 spots) (Fig 1a). Additionally, 31.1% of these VPS29-GFP spots were tubular protrusions from an endosome with a resolvable lumen. Consistent with this co-localization, biochemical purification of EEA1 endosomes co-purified β2AR and retromer component VPS35 (Fig 1b; uncut blots for all figures are in Supplementary Figure 2). Together, this data suggests that β2ARs access the retromer marked tubular endosomal network(Bonifacino and Rojas 2006).

In contrast to β2AR, recycling-defective β2AR-HA did not extend into retromer tubules (Fig 1c). This distinction between β2AR and β2AR-HA localization was quantified by circumferential line scan analysis around the endosome limiting membrane. Whereas β2AR was enriched ~50% at the base of VPS29-GFP coated tubules relative to the rest of the endosome membrane, β2AR-HA was not (Fig 1d, e). These results indicate that β2ARs specifically enter retromer-associated tubules following endocytosis, and suggest that tubule entry is the primary sorting step required for β2AR recycling to the plasma membrane.

To investigate if retromer is required for β2AR recycling, we depleted retromer components by RNAi. We first assessed trafficking effects using fluorescence microscopy to visualize ligand-dependent redistribution of surface-labeled receptors between the plasma membrane and intracellular membranes. The β2AR agonist isoproterenol induced pronounced redistribution of antibody-labeled β2ARs from the plasma membrane to intracellular puncta, indicative of ligand-induced endocytosis. This process was not detectably inhibited by siRNA-mediated knockdown of VPS35 (Fig 2a). Subsequent recycling of receptors to the plasma membrane after agonist removal was obviously reduced in VPS35-depleted cells (Fig 2a).

We then quantified this effect of retromer depletion using a flow cytometry assay measuring changes in the internalized pool of receptors. β2AR recycling, as measured by antibody efflux following agonist removal, was strongly inhibited by multiple siRNA sequences targeting either VPS26 or VPS35 (Fig 2b). Further, retromer depletion inhibited β2AR recycling at all time points examined (Fig 2c). Consistent with this, VPS35 depletion, which prevents endosome association of VPS29-GFP, resulted in endosomes devoid of β2AR tubules (Fig 2d). Additionally, we verified that retromer is required for β2AR recycling in physiologically relevant A10 cells, a rat atrial-derived vascular smooth muscle cell line (Supplementary Figure 1).

Retromer depletion leads β2ARs to be misrouted to the lysosome and degraded (Fig 2e-g). This effect of retromer depletion on receptor degradation is fully consistent with the observed inhibition of β2AR recycling, and similar to that of disrupting the receptor's C-terminal PDZ ligand(Cao, Deacon et al. 1999).

To examine the specificity of retromer depletion effects, we tested another protein that traffics through the same endosome as β2AR. For this we used TFR, a constitutively endocytosed nutrient receptor that can recycle with bulk membrane(Mayor, Presley et al. 1993). When TFR-GFP or labeled Transferrin was imaged alongside internalized β2AR in living cells, β2AR only appeared in a subset of the TFR containing tubules projecting from the limiting membrane of individual early endosomes (Fig 3a, b), as shown previously(Puthenveedu, Taunton et al.). Additionally, only a subset of TFR tubules labeled with VPS29-mCherry (Fig 3a). As TFR can access non-retromer recycling tubules, it should be able to exit the endosome in the absence of retromer tubules. Consistent with this, retromer depletion had no effect on degradation of endogenous TFR

(Fig 3c, d) and produced only a small kinetic delay in the recycling of TFR back to the plasma membrane (Fig 3e). This second observation is consistent with the ability of a visible fraction of TFR to enter retromer tubules and further supports the ability of these tubules to mediate rapid plasma membrane recycling.

As retromer complex has not previously been implicated in recycling from endosomes to the plasma membrane, we next sought to compare β2AR localization and trafficking to that of a membrane cargo which exhibits retromer-dependent trafficking to the TGN. For this purpose we focused on the cation-independent mannose phosphate receptor (CIMPR)(Arighi, Hartnell et al. 2004; Seaman 2004). We first evaluated the localization of β2AR relative to CIMPR in fixed cells. β2AR was induced to reach a steady-state of internalization and recycling so that it populated various intermediates in endocytic and recycling pathways. Under this condition, β2AR was localized primarily in EEA1 marked endosomes and at the plasma membrane (Fig 1b, 4a)(von Zastrow and Kobilka 1992; Moore, Millman et al. 2004). CIMPR co-localized with β2AR in a large fraction of early endosomes but was also prominently localized in perinuclear endomembranes not containing β2AR (Fig 4a). This is consistent with steady state localization of CIMPR in the TGN and late endosomes(Lin, Mallet et al. 2004). Supporting this, the localization of perinuclear CIMPR was similar to, or closely adjacent to, that of the trans-Golgi / TGN marker galactosyltransferase-GFP (GalT-GFP) (Roth and Berger 1982; Cole, Smith et al. 1996). We also note that retromer cargo that traverse the TGN on the way to indirect plasma membrane delivery have shown significant colocalization with markers of the TGN region(Franch-Marro, Wendler et al. 2008). Importantly, and in marked contrast, the β2AR localization observed in these cells was

clearly distinct. β2ARs localized to peripheral early endosomes but not in the perinuclear distribution characteristic of CIMPRs (Fig 4a).

Given that β2AR and CIMPR achieve different steady state localization patterns, we next used live imaging to ask if these distinct membrane cargoes localize to the same endosomes and, if so, if they localize to the same retromer tubules. Confocal microscopy revealed that both FITC-conjugated anti-CIMPR antibody (CIMPR AB), used to detect endogenous receptor, and a GFP-tagged CIMPR construct (cCIMPR-GFP) clearly co-localized with β2AR in the same endosomes and in the same tubules (Fig 4b, f). This overlap was extensive, as >90% of the β2AR-positive tubules resolved also contained GFP-tagged CIMPR.

We next asked how the retromer tubule could support rapid endosome-to- plasma membrane traffic, evidently independent of traversing the TGN. Knowing that the small GTPase Rab4A had previously been implicated in this process we tested if it associated with β2AR containing endosomes. GFP-Rab4A localized to these compartments and was visibly enriched on the β2AR-containing retromer tubules (Fig 4c)(Puthenveedu, Taunton et al. 2010). Further, as expected, depletion of Rab4A by siRNA inhibited recycling of β2AR (data not shown)(Seachrist, Anborgh et al. 2000). In contrast, depletion of several components that function in endosome-to-TGN trafficking of CIMPR (Rab6A', Rab7b (a distinct gene from Rab7), and GCC185) failed to significantly affect β2AR recycling(Mallard, Tang et al. 2002; Utskarpen, Slagsvold et al. 2006; Derby, Lieu et al. 2007; Ganley, Espinosa et al. 2008; Progida, Cogli et al.) (Fig 4d). As a control for depletion, we established in parallel experiments that these siRNAs caused a pronounced

increase in cell surface expression of CIMPR, consistent with net disruption of normal endosome-TGN cycling of CIMPRs established previously (Fig 4e)(Seaman 2004).

Despite the co-occurrence of both membrane cargoes in a large fraction of endosomal tubules, β2AR and CIMPR were not identically localized in individual tubules imaged at high temporal resolution. Specifically, CIMPR was typically enriched near the distal end of tubules or in protrusions that extended beyond the β2AR labeled areas (Fig 4f). Apparent separation of cargo was visualized for both endogenous CIMPR and the GFP CIMPR transgenic protein (Fig 4f). These results support the previously proposed idea that an elaborated tubular endosomal network, capable of mediating the trafficking of cargoes to multiple destinations, is fed by the retromer tubule(Bonifacino and Rojas 2006). Further work will be required to investigate this, as there is also evidence that a significant fraction of CIMPRs can traffic to the plasma membrane following endosome exit(Lin, Mallet et al. 2004).

We next investigated the mechanistic basis for the role of retromer in β2AR recycling. For CIMPR, it is proposed that a direct interaction between the cytoplasmic tail and retromer complex is required for proper trafficking(Seaman 2007). β2AR trafficking is dependent on a PDZ motif present in the cytoplasmic tail that is both necessary and sufficient to mediate its plasma membrane recycling, but the core retromer complex is devoid of any recognizable PDZ domain. SNX27 contains a PDZ domain that binds the β2AR tail, and has recently been shown to be essential for PDZ-directed recycling of the β2AR(Lauffer, Melero et al. 2010). Verifying this, knockdown of SNX27 robustly inhibited recycling of β2ARs (Fig 5a). Despite this pronounced decrease in β2AR recycling, CIMPR distribution in the same cells appeared unaffected.

Furthermore, SNX27 depletion did not alter CIMPR surface expression (Fig 5b) or CIMPR turnover in the presence of cyclohexamide (data not shown).

Live imaging of SNX27 depleted cells revealed that VPS29-GFP puncta still associate with endosomes but that β2ARs no longer appear in these tubular structures (Fig 5c). Depletion of SNX27 also decreased the aggregation of β2ARs at the retromer tubule. In control siRNA treated cells there was a relative receptor density of 1.51±.061 (n=16 endosomes) at the base of the VPS29 tubule, while in SNX27 depleted cells this dropped significantly to 1.15±.055 (n=19 endosomes, p=.0002), phenocopying disruption of the PDZ motif (β2AR-HA). Together, this data suggests that SNX27 acts as a cargo adaptor to retromer, but is not a core component.

To investigate further how SNX27 was serving as a cargo adaptor to the retromer tubule, we used an affinity tagging / purification-mass spectrometry approach to determine which other proteins physically associate with it. In all 5 independent SNX27 purifications, components of the WASH actin nucleation complex were predominant hits (Supplementary Table). However, WASH complex was not detected in control purifications or in those of other bait molecules run at the same time. WASH has been shown to physically link to the retromer complex(Gomez and Billadeau 2009). Therefore this association with SNX27 supports the adaptor hypothesis by establishing protein connectivity.

Association of SNX27 with the retromer tubule was further supported by extensive colocalization between SNX27 and VPS29-GFP in fixed cells (Fig 5d). Moreover, SNX27 co-immunoprecipated endogenous VPS35 but not EEA1, an abundant protein that localizes to the same endosomes. Interestingly, VPS35 co-

immunoprecipitated with SNX27 only under crosslinking conditions, in contrast to WASH complex components that co-purified with SNX27 in the absence of crosslinking (Fig 5e). These observations suggest that SNX27 does not interact with the core retromer complex directly, but that its association with the retromer tubule is mediated by other interaction(s) including through the WASH complex. Together, these results indicate that SNX27 acts, through novel connectivity involving the WASH complex, as a specific adapter to promote PDZ-directed plasma membrane sorting through the retromer tubule (Fig 5f).

To probe the generality of the SNX27 / retromer -mediated recycling pathway we next examined two other GPCRs that are known to recycle rapidly to the plasma membrane after endocytosis. Efficient recycling of the beta-1 adrenergic receptor (β1AR) requires a class 1 PDZ motif present in its distal cytoplasmic tail, but this motif differs in primary structure and binding properties from the PDZ motif present in the β2AR tail(Gage, Matveeva et al. 2005; He, Bellini et al. 2006). The D1 dopamine receptor (D1R) recycles efficiently after endocytosis but does not contain a C-terminal PDZ motif, and truncation of its distal cytoplasmic tail does not disrupt receptor recycling(Vargas and Von Zastrow 2004). We observed a significant inhibition of β1AR recycling following knockdown of either VPS35 (33.7%±0.1 inhibition, n=9, p= 0.0013) or SNX27 (19.5%±0.1 inhibition, n=9, p= 0.0293). Recycling of FLAG-D1Rs, in contrast, was not significantly inhibited by either manipulation. Thus, retromer-dependent recycling is not unique to the β2AR and can be specified by distinct PDZ motifs. This suggests that many other membrane cargoes which contain C-terminal PDZ

ligands, including a large group of G-protein coupled receptors (GPCRs), may traffic via this SNX27 / retromer pathway(Heydorn, Sondergaard et al. 2004).

Retromer has been shown to function in trafficking of various cargo from endosomes to the TGN, and to function in transcytosis in polarized cells(Verges, Luton et al. 2004; Bonifacino and Hurley 2008). Recently several retromer cargo have been identified that traffic to the plasma membrane, though it is unclear whether they do so directly from the endosome or via the TGN(Strochlic, Setty et al. 2007; Kleine-Vehn, Leitner et al. 2008; Tabuchi, Yanatori et al.). In this paper we identify an essential role of retromer in mediating rapid recycling of a prototypical GPCR apparently directly to the plasma membrane. We also establish that β2ARs can enter the same retromer tubules as a canonical TGN-directed cargo, and identify a distinct adaptor protein that links signaling receptors specifically to the retromer-dependent plasma membrane recycling pathway. Our results support a revised view of retromer tubules as a multi-functional exit port supporting diverse membrane itineraries, including direct endosome-to-plasma membrane trafficking.

Our results have fundamental implications in the field of cell signaling because they indicate that retromer plays a critical role in mediating the sorting of a prototypical GPCR between the functionally opposing pathways of resensitization and down-regulation, the distinct physiological consequences of which are well established(Hanyaloglu and von Zastrow 2008; Marchese, Paing et al. 2008). Consistent with this, depletion of VPS35 significantly decreased isoproterenol mediated signaling from the β2AR, as measured by cellular cAMP accumulation (Fig 5g). Interestingly,

retromer depletion also affected receptor-independent activation of adenylyl cyclase by forskolin, suggesting that retromer tubules have other role(s) in cell signaling.

5. 3 Acknowledgements

We thank B. Padilla, J. Bonifacino, Y. Prabhu, N. Gulbahce, S. Duleh, M. Welch, R. Rojas, J. Hislop, M. Puthenveedu, K. Mostov, J. Weissman, K. Thorn, the Nikon Imaging Center, A. Burlingame, and the UCSF Mass Spectrometry facility for reagents, advice, technical training, and support. Lastly, we thank H. Bourne and M. Ray for critical readings of the manuscript. This work was supported by research grants from the National Institutes of Health. PT was supported by the National Science Foundation. NJK is a Searle and Keck Young Investigator Fellow.

5.4 Methods

Cell Culture, cDNA constructs, and Transfection

HEK 293 and A10 cells were grown in Dulbecco's modified Eagles medium supplemented with 10% fetal bovine serum (UCSF Cell Culture Facility, San Francisco, CA). Stably transfected HEK 293 cell clones expressing the indicated receptor constructs were created using the previously described FLAG-tagged β2AR and β2AR-HA and G418 selection at 500 μg / ml (Invitrogen)(Cao, Deacon et al. 1999).

GFP-SNX1 and VPS29-GFP were generous gifts from J. Bonifacino[25]. Vps29-mCherry was created by PCR-mediated amplification of VPS29 from the VPS29-GFP construct, inserting it into pENTR using the pENTR directional cloning kit (Invitrogen), and then into a pcDNA3 Dest53 mCherry vector using the LR clonase kit (Invitrogen). Galt-GFP was a gift from J. Lippincott-Schwartz(Cole, Smith et al. 1996). cCIMPR-GFP was created by amplifying the transmembrane and cytoplasmic domains of CIMPR from a cDNA library with the primers TATACAAAACCGGTCTGTCAGAACGGAGCCAGGCAGTCGGC and TTTGTATAGGATATCCCCCTGCAGGCACTGCGGAGTCAGATG and cloning this fragment into a N-terminal signal sequence and GFP-containing pcDNA3 vector using Age1 and EcoRV. GFP-Rab4A was a gift from S. Ferguson(Holmes, Babwah et al. 2006). Snx27-HA(Lauffer, Melero et al. 2010), FLAG-β1AR(Tang, Hu et al. 1999), and FLAG-D1R(Vargas and Von Zastrow 2004) constructs were previously described.

For transient expression of constructs, cells were transfected using Lipofectamine 2000 (Invitrogen) according to manufacturers' instructions. Cells expressing FLAG-tagged receptors were harvested with PBS EDTA and plated in 12 well plates at 80%

confluence before transfection with plasmid DNA. Cells were cultured for a further 48 h before experimentation. Target sequences for knockdown were hVPS26 (1: CTGCATAATGTTGATTATAAA, 2:CACCAAGGAATTAGAATTGAA), hVPS35 (1: CTGGACATATTTATCAATATA, 3: CAGGAAATGCATAATTAT), RnVPS35 (ACCAGGTAGATTCCATAATGA), hRab4A (AATGCAGGAACTGGCAAATCT), hRab6A (CCCACTTATTGTCACCTTGTA), hRab6A'(AACAGCTGTAGTAGTTTACGA)(Utskarpen, Slagsvold et al. 2006), hRab7B (AAGTAGCTCAAGGCTGGTGTA)(Progida, Cogli et al.), hGCC185 (AAGGAGTTGGAACAATCACAT)(Derby, Lieu et al. 2007), hSnx27-4(Lauffer, Melero et al.), and control (1027281, Qiagen). 25 picomoles of duplex RNA (Qiagen) were transfected into 30% confluent cells in a 12 well dish with Lipofectamine RNAi Max (Invitrogen) 36 h prior to experimentation.

Live Receptor Imaging and Quantification

Live imaging of FLAG-tagged receptors and the indicated GFP-labeled protein was performed using a previously described antibody feeding method(Puthenveedu, Taunton et al.). Briefly, cells expressing both constructs were plated onto glass coverslips and surface receptors were labeled by the addition of M1 anti-FLAG antibody (Sigma) conjugated to Alexa 555 (A10470, Invitrogen) to the media for 30 min. Isoproterenol was added (Sigma) and cells were imaged on a Nikon TE-2000E inverted microscope with a 100x1.49 NA TIRF objective (Nikon) and a Yokagawa CSU22 Spinning Disk confocal head (Solamere, Salt Lake City, UT). A 488nm Ar laser and a 568nm Ar/Kr laser (Melles Griot) were used as light sources for imaging GFP and FLAG

signals, respectively. Movies of endosomes were taken between 5 and 30 min after agonist addition and exported as TIF files. Each frame corresponds to 450 ms.

Analysis of receptor co-enrichment with VPS29-GFP was performed using the ImageJ (http://rsb.info.nih.gov/ij/) and the "Oval Profile" plugin. Endosomes with single VPS29-GFP spots were outlined using the oval tool. Oval Profile was used to perform a linear fluorescence intensity scan in 60 subsections of both VPS29-GFP and β2AR signals as well as background signals from an endosome free region. The data was then exported to Excel (Microsoft) where the background was subtracted and the top four consecutive points of VPS29-GFP fluorescence were determined. To determine the enrichment of receptor at the tubule as compared to the rest of the endosome, the average intensity of the four β2AR points corresponding to the four peak VPS29 points was divided by the average receptor intensity of the rest of the endosome except for the 120º centered at the VPS29 peak.

Recycling Assays

Visualization of FLAG receptors was carried out using fluorescence microscopy of stably transfected HEK 293 cells or transiently transfected A10 cells that had been plated on glass coverslips. Surface receptors were labeled by exposing intact cells to M1 anti-FLAG antibody conjugated to Alexa 555 (Sigma) for 25 min at 37 °C in the presence of 10 μM isoproterenol to promote endocytosis of labeled receptors. Cells were then either fixed or washed and further incubated in media for 45 min in the presence of the antagonist 10 μM alprenolol (Sigma) to allow for recycling. Cells were fixed using 4% formaldehyde freshly dissolved in PBS and imaged on the aforementioned spinning disk microscope.

In the flow cytometry based recycling assay, cells were plated in 12 well plates and treated as in the visual assay except that instead of fixation, HEK 293 cells were lifted in PBS EDTA, which strips the calcium dependent M1 antibody from the cell surface. When surface CIMPR was measure, CD222-FITC (BioLegend) was added to the PBS-EDTA at 1:250. Lifting of A10 cells required addition of trypsin. Fluorescence intensity profiles of cell populations (5,000 cells/sample for HEK 293 and >1500 cells/sample for A10) were measured using a FACS-Calibur instrument (BD Biosciences).

Transferrin recycling experiments involved washing cells 3 times with PBS, applying Alexa-488 labeled transferrin (Invitrogen) in serum free media for 25 minutes, and then rapid transferrin efflux occurred by switching cells to media that contained serum and no labeled transferrin. 10% serum was added to the PBS-EDTA when cells were lifted to strip all surface transferrin.

In each experiment, triplicate treatments were analyzed for each condition. All experiments were carried out on at least three separate days (number indicated in figure legends), and values reported were derived from the mean determination across experiments. The percentage of antibody recycled was calculated from internal fluorescence values as follows: % recycling = 1-("agonist→antagonist signal"/"agonist signal")

Fixed Cell Imaging

HEK 293 cells stably expressing β2AR plated onto cover slips were treated with the agonist isoproterenol for 30 min prior to fixation with 4% formaldehyde in PBS and processed for immunocytochemical staining. Staining of β2AR was done using Rabbit

anti-FLAG (Sigma) and the secondary goat anti-rabbit Alexa 594 (Invitrogen). Mouse antibodies against EEA1 (BD Biosciences) and CIMPR (Biolegend) were used in combination with donkey anti-mouse Alexa 488 (Invitrogen). Fixed cells were imaged using the aforementioned spinning disk microscope.

Degradation Assays and Western Blotting

Briefly, stably transfected HEK 293 cells expressing FLAG-β2AR were transfected with siRNA VPS35-1 or VPS35-3 as described above, and stimulated with 10 μM isoproterenol for four h before washing three times in ice-cold PBS and lysed in extraction buffer (0.2% Triton X-100, 50 mM NaCl, 5 mM EDTA, 50 mM Tris pH 7.4, Complete EDTA free protease inhibitor cocktail (Roche)). Extracts were clarified by centrifugation (21,000 x g for 10 min), and then mixed with SDS sample buffer for denaturation. The proteins were resolved by SDS-PAGE, transferred to nitrocellulose membranes, and probed for FLAG-tagged β2AR receptor (M1 antibody, Sigma), VPS35 (generously provided by C. Haft and J. Bonafacino), or GAPDH (Chemicon) by immunoblotting using horseradish peroxidase-conjugated sheep anti-mouse IgG or donkey anti-rabbit IgG (Amersham Biosciences), and SuperSignal extended duration detection reagent (Pierce). Band intensities of unsaturated immunoblots were analyzed and quantified by densitometry using a 12-bit cooled CCD camera and FluorChem 2.0 software (AlphaInnotech Corp.). The amount of FLAG-β2AR remaining at each time point was first expressed as a percentage of the amount of FLAG-β2AR in the identically transfected unstimulated cells. The lysosomal protease inhibitor ZPAD (Bachem) or the proteosomal inhibitor epoxomicin (Sigma) were added to cells 40 minutes prior to addition of isoproterenol when used at 200μM and 2μM respectively.

To compare degradation of endogenous TFR to FLAG-β2AR, stably transfected HEK 293 cells were grown in 6 well dishes, washed with ice-cold PBS and incubated with 300μg/ml sulfo-N-hydroxysuccinimide-biotin (Pierce) in PBS for 30 min at 4°C to biotinylate surface proteins. Following washing with Tris buffered saline to quench unreacted biotin, cells were returned to 37°C for incubation in media, with or without agonist, before extraction as described above. Biotinylated proteins were isolated from cell extract by immobilization on streptavidin-conjugated sepharose beads (Amersham) and washed three times with extraction buffer. Washed beads were eluted with SDS sample buffer before resolving by SDS-PAGE as above. Blotting was performed for β2AR and TFR (13-6800, Invitrogen). In each experiment, triplicate treatments were analyzed for each condition. All experiments were carried out at least in triplicate (number indicated in figure legends), and values reported were derived from the mean determination across experiments.

Immunopurification of SNX27-HA was done using HEK 293 cells three days after transient transfection. Cells were cross-linked using 0.3mM DSP (Pierce) for 30 min prior to lysis in extraction buffer and addition of mouse HA11 antibody (Covance). SNX27-HA complexes were isolated using protein A/G beads (Pierce), washed four times with extraction buffer, and eluted with Nupage LDS buffer (Invitrogen).

Mass Spectrometry

Immunopurification and mass spectrometry of SNX27-3xFLAG was performed as previously described(Jager, Gulbahce et al.).

Endosome Purification

Endosome purification was performed as previously published(Cottrell, Padilla et al. 2009). In addition to previously mentioned antibodies, Calnexin (ab22595, Abcam) and LAMP1 (H4A3, Santa Cruz) antibodies were used.

Signaling

HEK 293 cells stably expressing β2AR were treated with 10 μm isoproterenol or 1 μm forskolin (Sigma) for 20 minutes before signaling assays were performed according the manual of the Direct cAMP EIA Kit (Enzo Life Sciences, Plymouth Meeting, PA). cAMP levels were normalized to protein level using Coomasie Plus Protein Quantification Reagent (Thermo Scientific).

Statistics

Results are presented as mean ± SEM. based on data averaged across multiple independent experiments. The n value of an experiment represents experiments done on different days unless otherwise noted. To assign significance, results were compared to control experiments with an unpaired t-test using Prism (v4.03, GraphPad, La Jolla, CA). Only p-values below 0.05 are shown. Statistical comparison of knockdown effect on CD222 surface labeling (Fig 4e and 5d) and of knockdown effect on cAMP accumulation (Fig 5f) was performed using the one sampled t-test against the normalized value of one or 100%. Two-way ANOVA with Bonferonni posttest was performed on the recycling time-courses of β2AR and TFR. In these graphs * represents a $p<0.05$, ** represents $p<0.01$, and *** represents $p<0.001$ as no value is given by the program.

5.5 References

Arighi, C. N., L. M. Hartnell, et al. (2004). "Role of the mammalian retromer in sorting of the cation-independent mannose 6-phosphate receptor." J Cell Biol 165(1): 123-33.

Bonifacino, J. S. and J. H. Hurley (2008). "Retromer." Curr Opin Cell Biol 20(4): 427-36.

Bonifacino, J. S. and R. Rojas (2006). "Retrograde transport from endosomes to the trans-Golgi network." Nat Rev Mol Cell Biol 7(8): 568-79.

Cao, T. T., H. W. Deacon, et al. (1999). "A kinase-regulated PDZ-domain interaction controls endocytic sorting of the beta2-adrenergic receptor." Nature 401(6750): 286-90.

Carlton, J., M. Bujny, et al. (2004). "Sorting nexin-1 mediates tubular endosome-to-TGN transport through coincidence sensing of high- curvature membranes and 3-phosphoinositides." Curr Biol 14(20): 1791-800.

Carlton, J. G. and P. J. Cullen (2005). "Sorting nexins." Curr Biol 15(20): R819-20.

Cole, N. B., C. L. Smith, et al. (1996). "Diffusional mobility of Golgi proteins in membranes of living cells." Science 273(5276): 797-801.

Cottrell, G. S., B. E. Padilla, et al. (2009). "Endosomal endothelin-converting enzyme-1: a regulator of beta-arrestin-dependent ERK signaling." J Biol Chem 284(33): 22411-25.

Derby, M. C., Z. Z. Lieu, et al. (2007). "The trans-Golgi network golgin, GCC185, is required for endosome-to-Golgi transport and maintenance of Golgi structure." Traffic 8(6): 758-73.

Franch-Marro, X., F. Wendler, et al. (2008). "Wingless secretion requires endosome-to-Golgi retrieval of Wntless/Evi/Sprinter by the retromer complex." Nat Cell Biol 10(2): 170-7.

Gage, R. M., E. A. Matveeva, et al. (2005). "Type I PDZ ligands are sufficient to promote rapid recycling of G Protein-coupled receptors independent of binding to N-ethylmaleimide-sensitive factor." J Biol Chem 280(5): 3305-13.

Ganley, I. G., E. Espinosa, et al. (2008). "A syntaxin 10-SNARE complex distinguishes two distinct transport routes from endosomes to the trans-Golgi in human cells." J Cell Biol 180(1): 159-72.

Gomez, T. S. and D. D. Billadeau (2009). "A FAM21-containing WASH complex regulates retromer-dependent sorting." Dev Cell 17(5): 699-711.

Hanyaloglu, A. C. and M. von Zastrow (2008). "Regulation of GPCRs by endocytic membrane trafficking and its potential implications." Annu Rev Pharmacol Toxicol 48: 537-68.

He, J., M. Bellini, et al. (2006). "Proteomic analysis of beta1-adrenergic receptor interactions with PDZ scaffold proteins." J Biol Chem 281(5): 2820-7.

Heydorn, A., B. P. Sondergaard, et al. (2004). "A library of 7TM receptor C-terminal tails. Interactions with the proposed post-endocytic sorting proteins ERM-binding phosphoprotein 50 (EBP50), N-ethylmaleimide-sensitive factor (NSF), sorting nexin 1 (SNX1), and G protein-coupled receptor-associated sorting protein (GASP)." J Biol Chem 279(52): 54291-303.

Holmes, K. D., A. V. Babwah, et al. (2006). "Differential regulation of corticotropin releasing factor 1alpha receptor endocytosis and trafficking by beta-arrestins and Rab GTPases." J Neurochem 96(4): 934-49.

Jager, S., N. Gulbahce, et al. "Purification and characterization of HIV-human protein complexes." Methods 53(1): 13-9.

Kleine-Vehn, J., J. Leitner, et al. (2008). "Differential degradation of PIN2 auxin efflux carrier by retromer-dependent vacuolar targeting." Proc Natl Acad Sci U S A.

Lauffer, B. E., C. Melero, et al. (2010). "SNX27 mediates PDZ-directed sorting from endosomes to the plasma membrane." J Cell Biol 190(4): 565-74.

Lin, S. X., W. G. Mallet, et al. (2004). "Endocytosed cation-independent mannose 6-phosphate receptor traffics via the endocytic recycling compartment en route to the trans-Golgi network and a subpopulation of late endosomes." Mol Biol Cell 15(2): 721-33.

Mallard, F., B. L. Tang, et al. (2002). "Early/recycling endosomes-to-TGN transport involves two SNARE complexes and a Rab6 isoform." J Cell Biol 156(4): 653-64.

Marchese, A., M. M. Paing, et al. (2008). "G protein-coupled receptor sorting to endosomes and lysosomes." Annu Rev Pharmacol Toxicol 48: 601-29.

Mari, M., M. V. Bujny, et al. (2008). "SNX1 defines an early endosomal recycling exit for sortilin and mannose 6-phosphate receptors." Traffic 9(3): 380-93.

Maxfield, F. R. and T. E. McGraw (2004). "Endocytic recycling." Nat Rev Mol Cell Biol 5(2): 121-32.

Mayor, S., J. F. Presley, et al. (1993). "Sorting of membrane components from endosomes and subsequent recycling to the cell surface occurs by a bulk flow process." J Cell Biol 121(6): 1257-69.

Moore, R. H., E. E. Millman, et al. (2004). "Rab11 regulates the recycling and lysosome targeting of beta2-adrenergic receptors." J Cell Sci 117(Pt 15): 3107-17.

Pippig, S., S. Andexinger, et al. (1995). "Sequestration and recycling of beta 2-adrenergic receptors permit receptor resensitization." Mol Pharmacol 47(4): 666-76.

Progida, C., L. Cogli, et al. (2010). "Rab7b controls trafficking from endosomes to the TGN." J Cell Sci 123(Pt 9): 1480-91.

Puthenveedu, M. A., J. Taunton, et al. (2010). "Sequence-dependent sorting of recycling proteins by actin-stabilized endosomal microdomains." Cell 143(5): 761-73.

Rojas, R., T. van Vlijmen, et al. (2008). "Regulation of retromer recruitment to endosomes by sequential action of Rab5 and Rab7." J Cell Biol 183(3): 513-26.

Roth, J. and E. G. Berger (1982). "Immunocytochemical localization of galactosyltransferase in HeLa cells: codistribution with thiamine pyrophosphatase in trans-Golgi cisternae." J Cell Biol 93(1): 223-9.

Seachrist, J. L., P. H. Anborgh, et al. (2000). "beta 2-adrenergic receptor internalization, endosomal sorting, and plasma membrane recycling are regulated by rab GTPases." J Biol Chem 275(35): 27221-8.

Seaman, M. N. (2004). "Cargo-selective endosomal sorting for retrieval to the Golgi requires retromer." J Cell Biol 165(1): 111-22.

Seaman, M. N. (2007). "Identification of a novel conserved sorting motif required for retromer-mediated endosome-to-TGN retrieval." J Cell Sci 120(Pt 14): 2378-89.

Sonnichsen, B., S. De Renzis, et al. (2000). "Distinct membrane domains on endosomes in the recycling pathway visualized by multicolor imaging of Rab4, Rab5, and Rab11." J Cell Biol 149(4): 901-14.

Strochlic, T. I., T. G. Setty, et al. (2007). "Grd19/Snx3p functions as a cargo-specific adapter for retromer-dependent endocytic recycling." J Cell Biol 177(1): 115-25.

Tabuchi, M., I. Yanatori, et al. (2010). "Retromer-mediated direct sorting is required for proper endosomal recycling of the mammalian iron transporter DMT1." J Cell Sci 123(Pt 5): 756-66.

Tang, Y., L. A. Hu, et al. (1999). "Identification of the endophilins (SH3p4/p8/p13) as novel binding partners for the beta1-adrenergic receptor." Proc Natl Acad Sci U S A 96(22): 12559-64.

Utskarpen, A., H. H. Slagsvold, et al. (2006). "Transport of ricin from endosomes to the Golgi apparatus is regulated by Rab6A and Rab6A'." Traffic 7(6): 663-72.

Vargas, G. A. and M. Von Zastrow (2004). "Identification of a novel endocytic recycling signal in the D1 dopamine receptor." J Biol Chem 279(36): 37461-9.

Verges, M., F. Luton, et al. (2004). "The mammalian retromer regulates transcytosis of the polymeric immunoglobulin receptor." Nat Cell Biol 6(8): 763-9.

von Zastrow, M. and B. K. Kobilka (1992). "Ligand-regulated internalization and recycling of human beta 2-adrenergic receptors between the plasma membrane and endosomes containing transferrin receptors." J Biol Chem 267(5): 3530-8.

Wang, Y., B. Lauffer, et al. (2007). "N-ethylmaleimide-sensitive factor regulates beta2 adrenoceptor trafficking and signaling in cardiomyocytes." Mol Pharmacol 72(2): 429-39.

5.6 Figures

Figure 1

Rapid recycling β2ARs selectively enter retromer-associated endosomal tubules. (**a**) Representative images from a movie of a cell expressing β2AR (red) and VPS29-GFP (green). Below, the inset box is shown across multiple frames of the movie. The edges of the cell are shown as dotted lines in the merged image. The scale bar represents 4 μm. (**b**) Representative immunoblots are shown from endosomes that were immuno-purified using antibody against the early endosome component EEA1 (n=3). (**c**) Representative images of endosomes containing wild type β2AR or recycling-defective β2AR-HA receptors (red) and SNX1-GFP or VPS29-GFP (green). Images were acquired by confocal microscopy of living cells after stimulating receptor endocytosis with isoproterenol. Wild type β2ARs, but not recycling-defective β2AR-HA mutant receptors, were visible in the VPS29-associated tubule extending from the endosome body. The scale bar represents 1 μm. (**d**) Fluorescence intensity tracing of labeled β2AR (black squares) and VPS29 (red triangles) around the edge of the endosome. Each point represents average fluorescence over a six degree arc of the endosome circumference. The four points of greatest VPS29-GFP fluorescence (open triangles) were used to mark the tubule. β2AR fluorescence values were background-corrected and normalized to the average fluorescence of a portion (240º) of the endosome, excluding the 120º of circumference centered at the tubule base. The scale bar represents 1 μm. (**e**) Relative receptor enrichment (average of open squares in panel b) of β2AR (red bar) or β2AR-HA (blue bar) at the tubule base. 20 endosomes (4

independent experiments), extending a single retromer-associated tubule, per receptor type were analyzed. Data points are the mean ± standard error of the mean (SEM).

Figure 2

Knockdown of retromer by RNAi inhibits β2AR recycling and misroutes internalized β2ARs to lysosomes. (**a**) Representative images from a visual assay for β2AR trafficking are shown. Stably transfected HEK 293 cells expressing FLAG-β2AR were transfected with either control siRNA or siRNA targeting the retromer component VPS35. In the "Agonist" condition, cells were incubated in the presence of the β2AR agonist isoproterenol (10 μM) and Alexa-conjugated M1 anti-FLAG for 25 min. In the "Agonist → Antagonist" condition, cells were incubated with isoproterenol for 25 min and then for an additional 45 min in the absence of isoproterenol (and in the presence of 10 μM of the β2AR antagonist alprenelol to prevent effects of any residual agonist). The scale bar represents 20 μm. (**b**) Flow cytometric analysis of β2AR recycling by uptake and efflux of bound M1 anti-FLAG antibody (n=4). (**c**) A time-course of recycling is shown for β2AR. The experiment was performed as in (b) but the duration after agonist washout was varied (n=4). (**d**) Representative confocal image from live cell imaging showing an endosome from a VPS35-1 siRNA treated cell expressing FLAG-β2AR (red) and VPS29-GFP (green). The scale bar represents 1 μm. (**e**) A representative immunoblot assay of agonist induced FLAG-β2AR degradation. Detergent extracts were prepared from HEK 293 cells expressing FLAG-β2AR incubated in the absence of agonist or in the continuous presence of 10 μM isoproterenol for 4 h. Knockdown was verified by VPS35 immunoblot of the same lysates (middle panel), and equal loading was

verified by immunoblotting for GAPDH (bottom panel). (**f**) FLAG-β2AR immunoblots were quantified by scanning densitometry across multiple experiments (n=3), and the percent receptor remaining after 4 h isoproterenol exposure was calculated. (**g**) Representative immunoblot showing isoproterenol induced β2AR degradation in cells depleted of VPS35 and treated with the vehicle dimethyl sulfoxide (DMSO), the lysosomal cathepsin inhibitor *N*-CBZ-L-phenylalanyl-L-alanine-diazomethylketone (ZPAD), or the proteosomal inhibitor epoxomicin (EPOX) (n=3). Data points are the mean ± SEM.

Figure 3

Retromer depletion preferentially affects β2ARs over TFRs traversing the same endosomes. (**a**) Top panels show representative images of endosomes containing β2AR (red) and TFR-GFP (green). Bottom panels show localization of VPS29-mCherry (red) relative to TFR-GFP (green). Arrows point to TFR tubules lacking β2AR in the top image and lacking VPS29 labeling in the bottom image. The scale bar represents 1 μm. (**b**) Fluorescence intensity scan of labeled β2AR (red squares) and TFR (green triangles) on a circumferential path set outside of the representative endosome shown in panel (a) but crossing both TFR-labeled tubules projecting from the endosome body, as indicated on the detail merged image. Positions of the tubules are marked by the numbers 1 and 2. The scale bar represents 1 μm. (**c**) Biochemical analysis comparing degradation of surface-biotinylated β2AR (top panel) and TFR (bottom panel) in cells maintained in the absence or continuous presence of isoproterenol for 4 h. A representative immunoblot is shown. Knockdown of VPS35 using two independent siRNA targets selectively

destabilized β2AR. (**d**) Receptor immunoreactivity from the experiment shown in panel (c) was quantified by scanning densitometry and the percent receptor remaining after 4 h was calculated by dividing the 4 h agonist treatment by the untreated control. Recovery of TFR (blue bars) and β2AR (red bars) was averaged across experiments (n=3). (**e**) The graph shows efflux of labeled transferrin in HEK 293 cells treated with siRNA against a control sequence or VPS35 (n=3). Percent transferrin recycled was calculated from these flow cytometry experiments as in Fig 2b. Data points are the mean ± SEM.

Figure 4

β2AR and CIMPR follow divergent trafficking paths upon exit from the same retromer-associated tubule. (**a**) Comparative localization of CIMPR and β2AR (red) with early endosome marker EEA1 or trans-Golgi marker GalT-GFP (green). Cells were fixed and imaged following incubation with isoproterenol for 30 min to drive β2AR to steady state. Plasma membrane and nuclei (N) have been outlined with dotted lines. The arrow indicates an example of a trans-Golgi region labeled for CIMPR but not β2AR. The scale bar represents 6 μm. (**b**) Representative endosome images from live cell confocal microscopy showing β2AR (red) localization in tubules with endogenous (top panels) or recombinant (bottom panels) CIMPR (green). Arrows indicate tubules containing both β2AR and CIMPR. The scale bar represents 1 μm. (**c**) Images, as in (b), of β2AR (red) and GFP-Rab4A (green) localization on the endosome. (**d and e**) Various components of the endosome to TGN transport pathway were depleted and β2AR recycling (panel d) or CIMPR surface immunoreactivity (panel e) was quantified by flow cytometry (n=4 experiments) to assess integrity of β2AR and CIMPR trafficking. (**f**)

Representative images from live confocal imaging showing differential enrichment of CIMPR (green) relative to β2AR (red) localization on distal regions of the same endosomal tubules. Each column represents a frame from a continuous time lapse movie (450 ms/frame). Arrows indicate distal regions of the indicated tubules on which CIMPR labeling was visibly enriched relative to β2AR. Multiple frames are shown to demonstrate that the observed difference in lateral enrichment did not occur as an artifact of tubule movement. The scale bar represents 1 μm. Data points are the mean ± SEM.

Figure 5

SNX27 serves as an adapter for β2AR, sorting it into the retromer tubule. (a) Comparative localization of β2AR (red) with the trans-Golgi marker GalT-GFP (green) and CIMPR (blue). Cells were fed anti-FLAG antibody in the presence of isoproterenol for 25 minutes prior to agonist washout with alprenelol for 45 minutes. Successful knockdown of SNX27 was judged by failure of β2AR to recycle to the plasma membrane. The scale bar represents 20 μm. (**b**) CIMPR surface immunoreactivity was quantified by fluorescence flow cytometry (n=6) to assess the integrity of CIMPR trafficking when SNX27 is depleted with siRNA. Successful depletion of SNX27 was confirmed by looking at visual recycling assays of β2AR as in (a). (**c**) Representative confocal image from live cell imaging showing an endosome from a SNX27-4 siRNA treated cell expressing FLAG-β2AR (red) and VPS29-GFP (green). The scale bar represents 1 μm. (**d**) Confocal image of transiently transfected SNX27-HA (red) and VPS29-GFP (green) in fixed cells. The scale bar represents 20 μm. (**e**) Representative immunoblot showing co-immunoprecipitation of endogenous VPS35 with transiently

transfected SNX27-HA. Lanes 1 and 3 show 2% whole cell lysate for the mock IP at left and the experiment at right. (**f**) SNX27 mediates plasma membrane recycling of PDZ motif containing cargo by linking to the retromer through an interaction with the WASH complex. SNX27 also interacts with the endosome directly through its lipid binding PX domain. (**g**) Isoproterenol or forskolin induced cAMP formation was measured in HEK 293 cells stably expressing β2AR, in the absence of IBMX, 20 minutes after agonist addition (n=6). Data points are the mean ± SEM.

Supplementary Figure 1

Retromer knockdown inhibits β2AR trafficking from the endosome to plasma membrane in A10 smooth muscle cells. (a) A representative image of endosomes exhibiting retromer tubules is shown. A10 cells were transiently transfected with FLAG-β2AR (red) and VPS29-GFP (green). Cells were imaged live by spinning disk confocal microscopy as described in Fig. 1a. The scale bar represents 1 μm. **(b)** A10 cells transiently transfected with FLAG-β2AR were assayed by flow cytometry for their ability to recycle Alexa conjugated M1 anti-FLAG antibody. This experiment was performed as in Fig. 2b (n=3). Data points are the mean ± SEM.

Supplementary Table

SNX27-3xFLAG was immunopurified from HEK 293 cells and copurifying proteins were analyzed by mass spectrometry. Components of the WASH complex were highly represented and are shown in the table. Reproducibility refers to the number of independent experiments, out of five, in which the indicated component was identified.

Figure 1

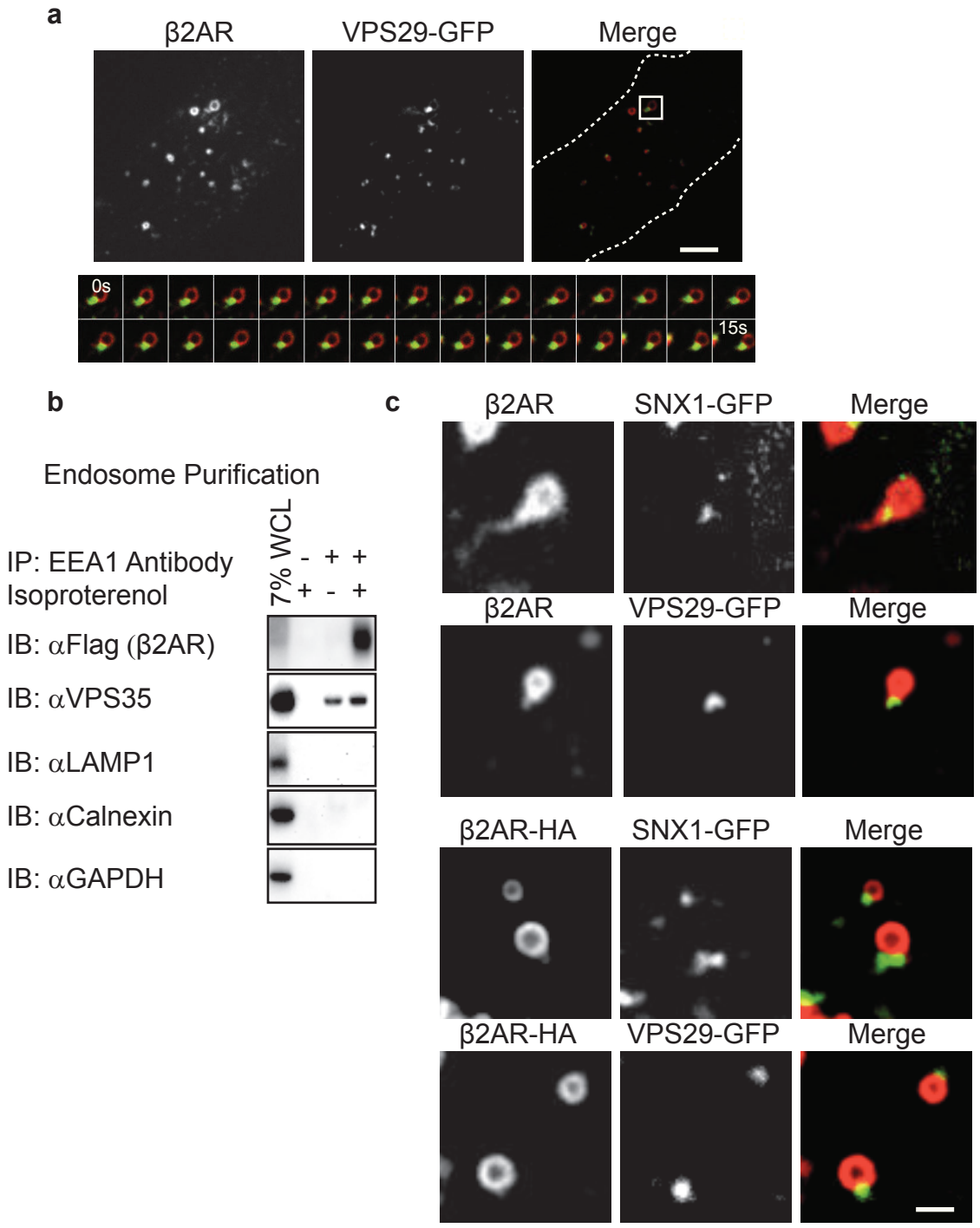
a
β2AR
VPS29-GFP
Merge
0s
15s
b
Endosome Purification
7% WCL
IP: EEA1 Antibody
Isoproterenol
- + +
+ - +
IB: αFlag (β2AR)
IB: αVPS35
IB: αLAMP1
IB: αCalnexin
IB: αGAPDH
c
β2AR
SNX1-GFP
Merge
β2AR
VPS29-GFP
Merge
β2AR-HA
SNX1-GFP
Merge
β2AR-HA
VPS29-GFP
Merge

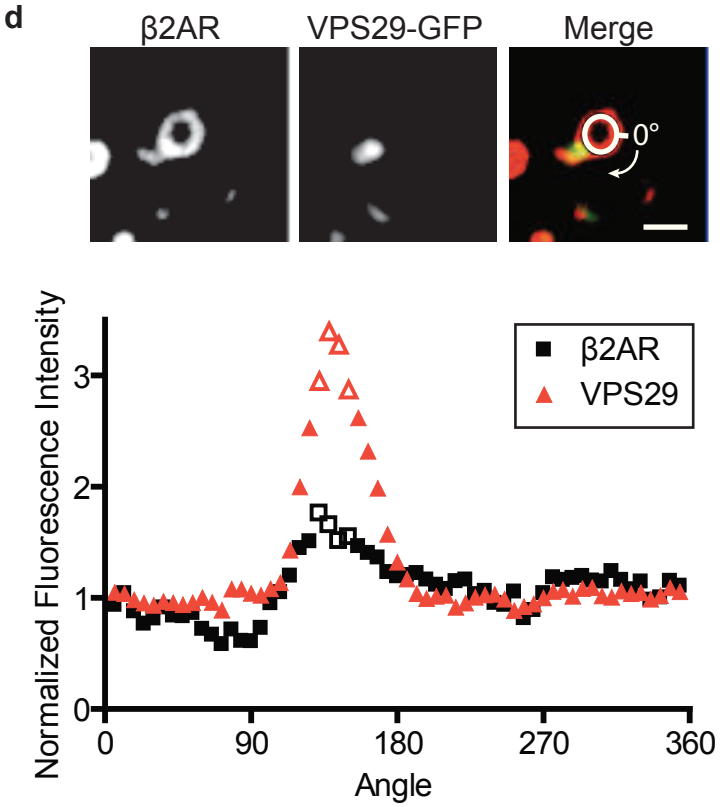
d
β2AR
VPS29-GFP
Merge
0°
Normalized Fluorescence Intensity
0
1
2
3
0
90
180
270
360
Angle
β2AR
VPS29

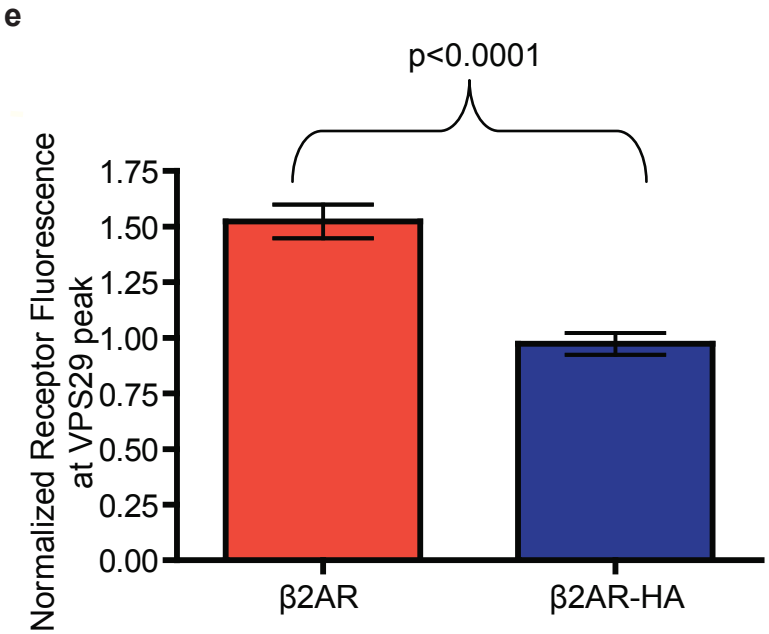
e
p<0.0001
Normalized Receptor Fluorescence at VPS29 peak
0.00
0.25
0.50
0.75
1.00
1.25
1.50
1.75
β2AR
β2AR-HA

Figure 2

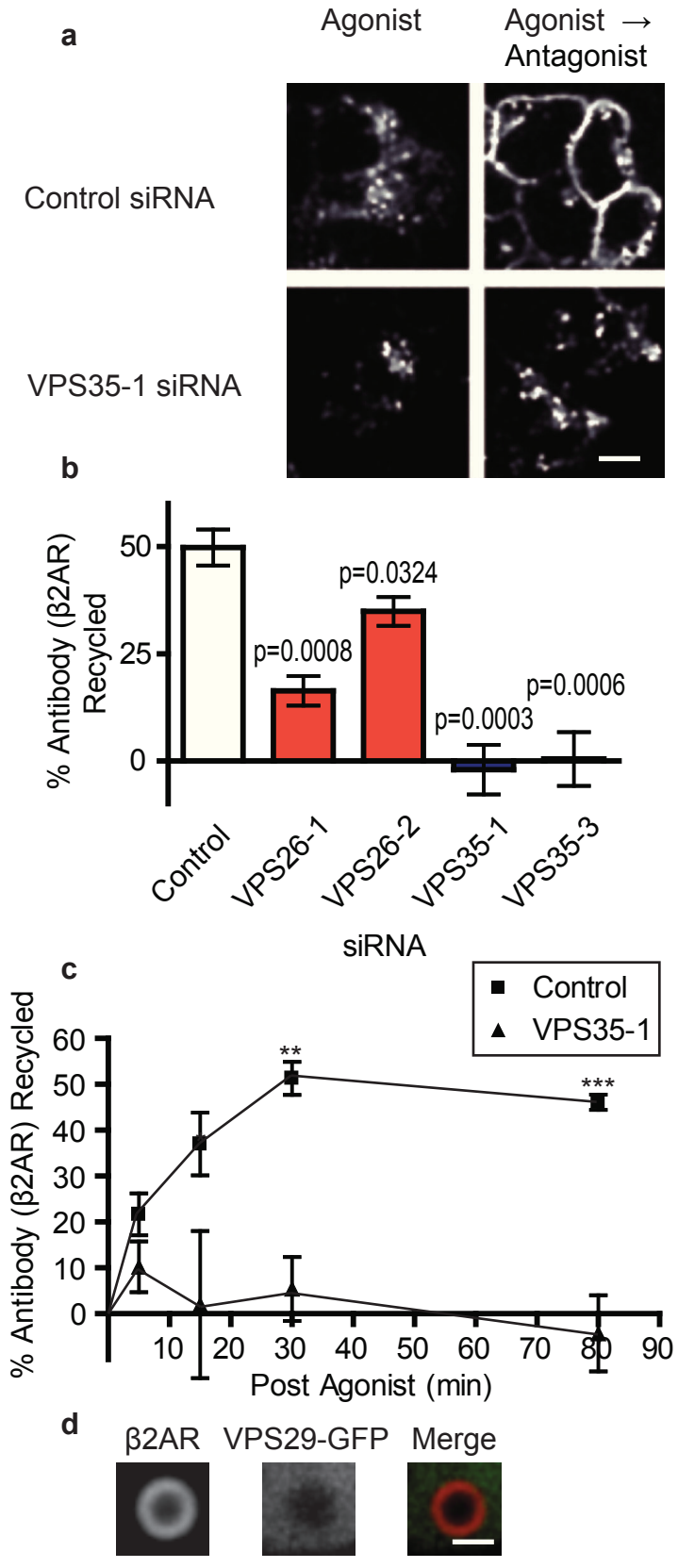
a
Agonist
Agonist → Antagonist
Control siRNA
VPS35-1 siRNA
b
% Antibody (β2AR) Recycled
50
25
0
p=0.0324
p=0.0008
p=0.0006
p=0.0003
Control
VPS26-1
VPS26-2
VPS35-1
VPS35-3
siRNA
c
Control
VPS35-1
% Antibody (β2AR) Recycled
60
50
40
30
20
10
0
**
***
10
20
30
40
50
60
70
80
90
Post Agonist (min)
d
β2AR
VPS29-GFP
Merge

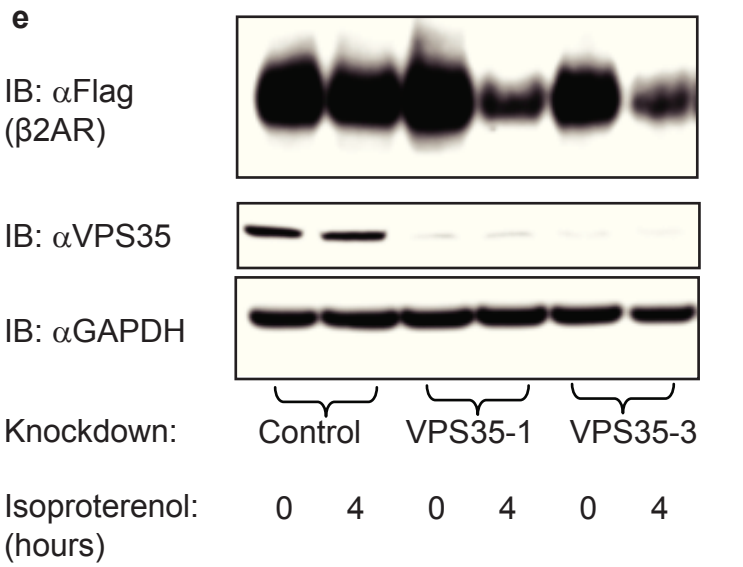
e
IB: αFlag (β2AR)
IB: αVPS35
IB: αGAPDH
Knockdown:
Control
VPS35-1
VPS35-3
Isoproterenol: (hours)
0 4 0 4 0 4

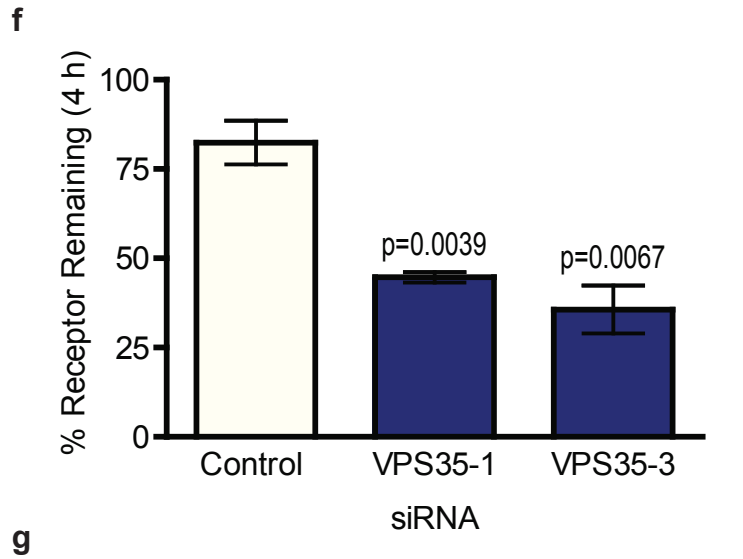
f
% Receptor Remaining (4 h)
100
75
50
25
0
p=0.0039
p=0.0067
Control
VPS35-1
VPS35-3
siRNA

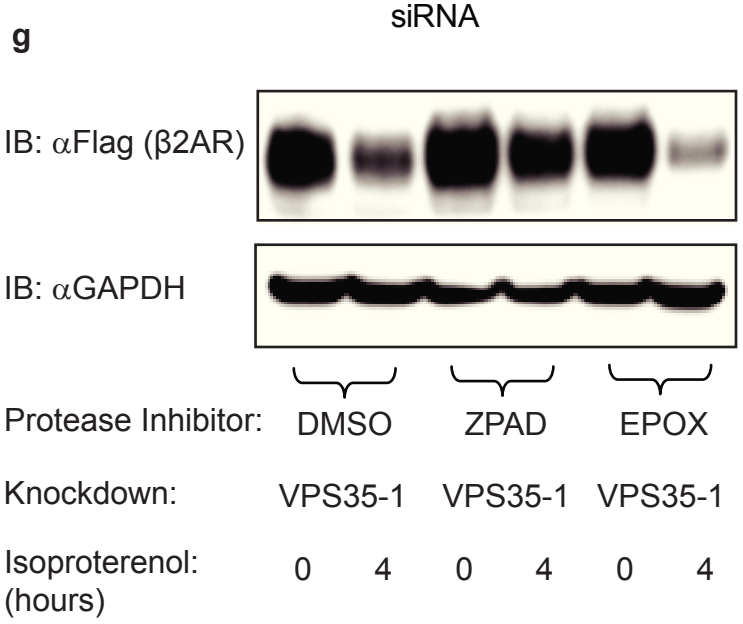
g
IB: αFlag (β2AR)
IB: αGAPDH
Protease Inhibitor:
DMSO
ZPAD
EPOX
Knockdown:
VPS35-1 VPS35-1 VPS35-1
Isoproterenol: (hours)
0 4 0 4 0 4

Figure 3

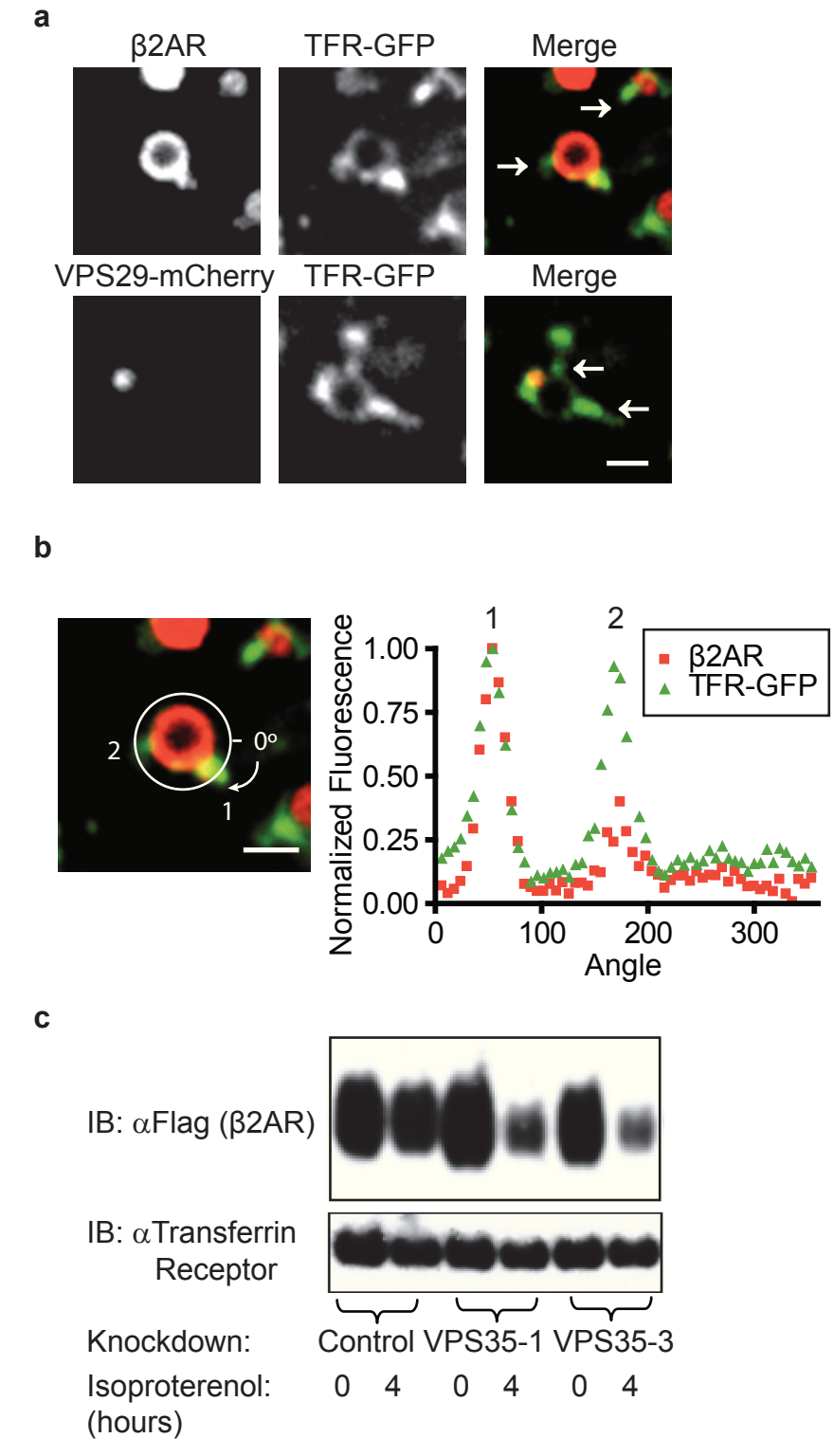
a
β2AR
TFR-GFP
Merge
VPS29-mCherry
TFR-GFP
Merge
b
2
0°
1
1
2
Normalized Fluorescence
1.00
0.75
0.50
0.25
0.00
0
100
200
300
Angle
β2AR
TFR-GFP
c
IB: αFlag (β2AR)
IB: αTransferrin Receptor
Knockdown:
Control
VPS35-1
VPS35-3
Isoproterenol: (hours)
0 4 0 4 0 4

d

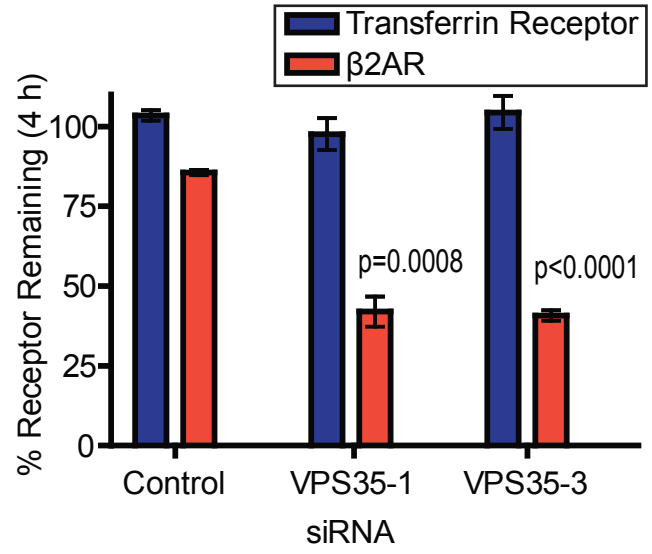
Transferrin Receptor
β2AR
% Receptor Remaining (4 h)
100
75
50
25
0
p=0.0008
p<0.0001
Control
VPS35-1
VPS35-3
siRNA

e

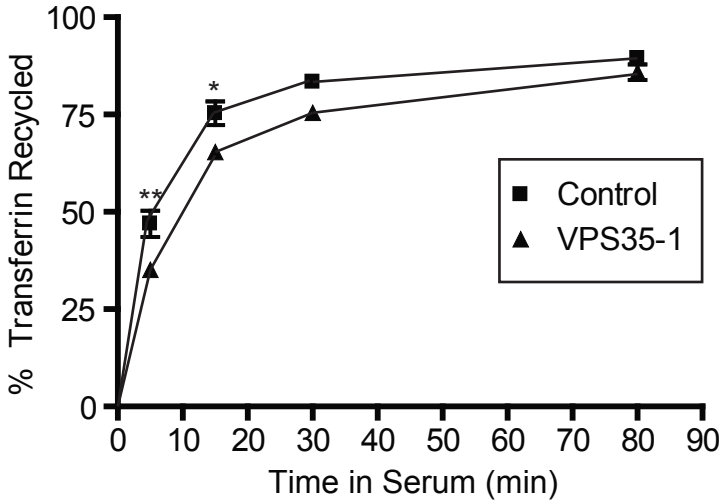
% Transferrin Recycled
100
75
50
25
0
**
*
Control
VPS35-1
0
10
20
30
40
50
60
70
80
90
Time in Serum (min)

Figure 4

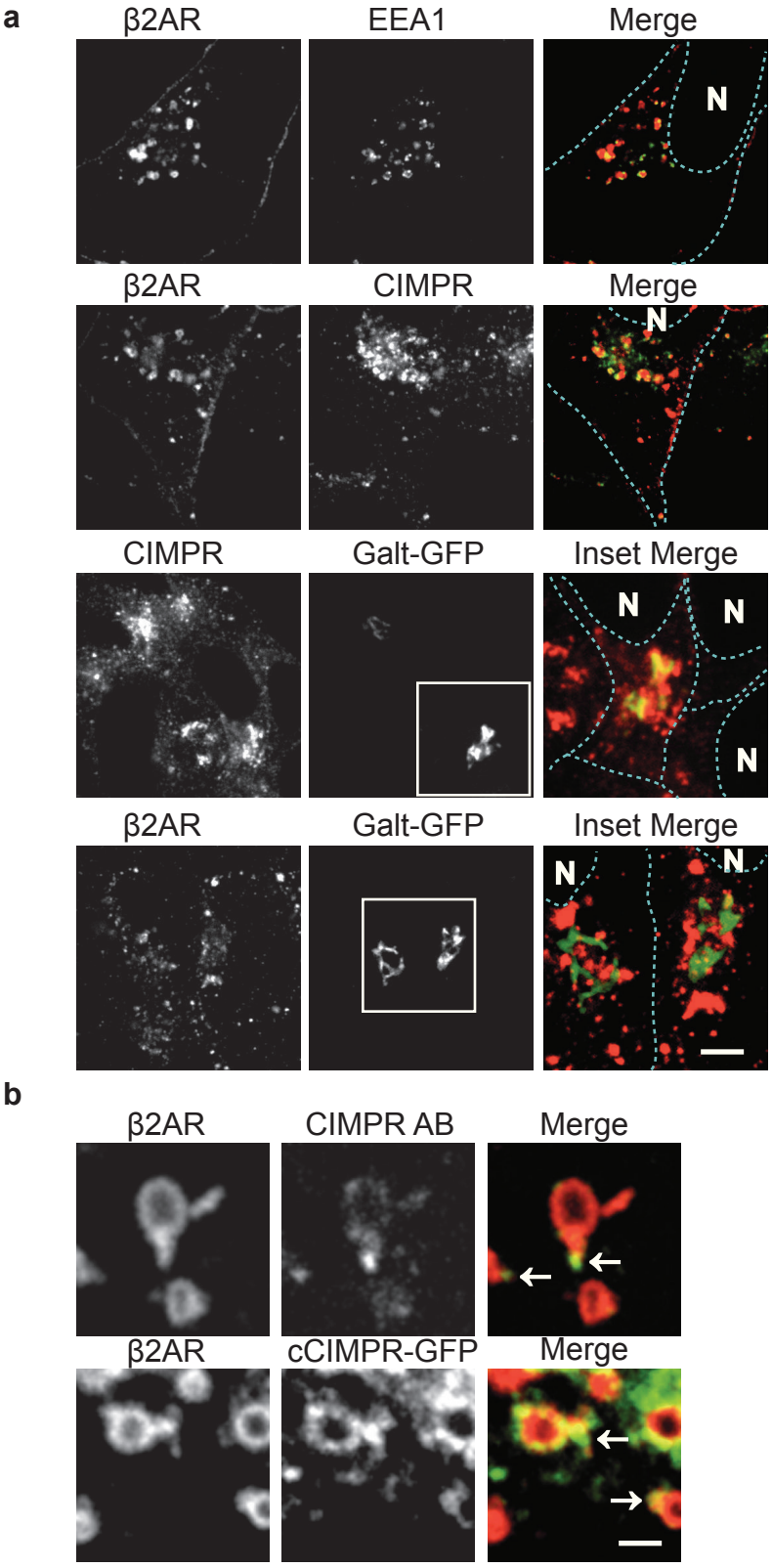
a
β2AR
EEA1
Merge
N
β2AR
CIMPR
Merge
N
CIMPR
Galt-GFP
Inset Merge
N
N
N
β2AR
Galt-GFP
Inset Merge
N
N
b
β2AR
CIMPR AB
Merge
β2AR
cCIMPR-GFP
Merge

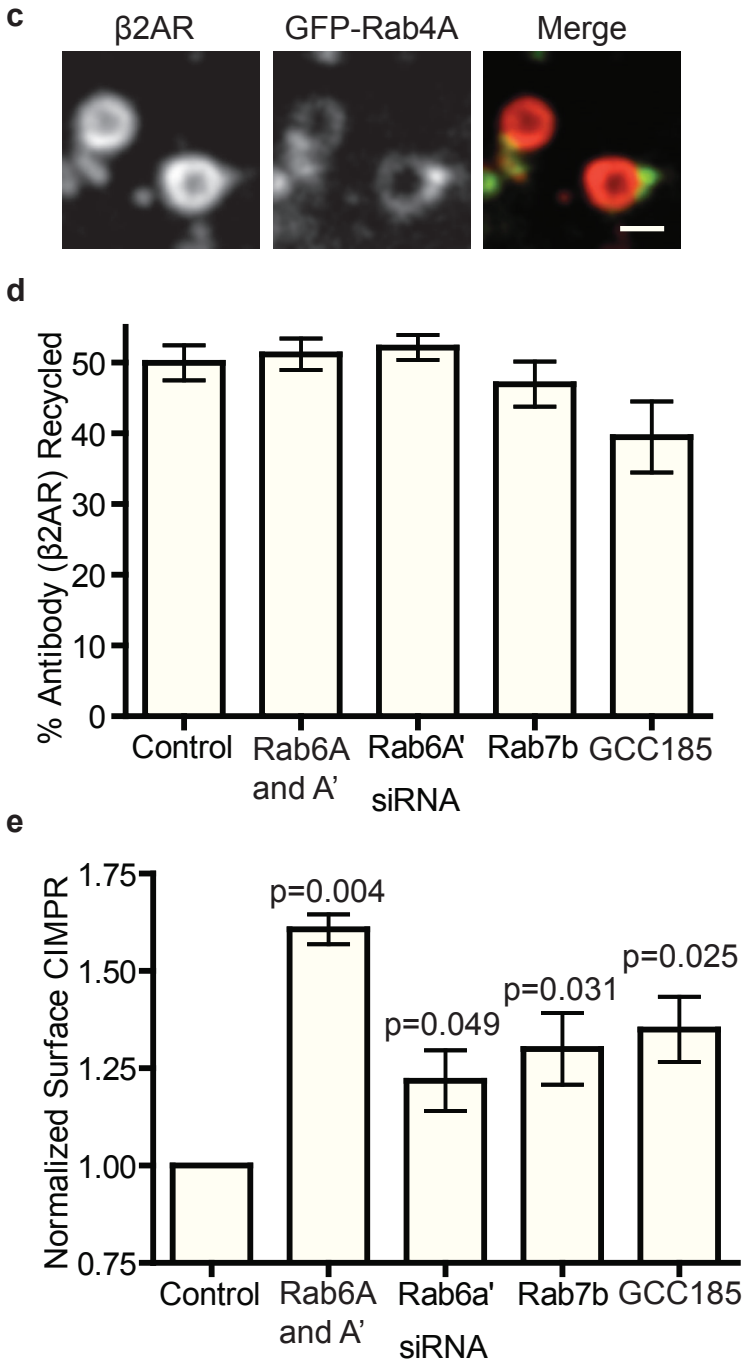
c
β2AR
GFP-Rab4A
Merge
d
% Antibody (β2AR) Recycled
0
10
20
30
40
50
Control
Rab6A and A'
Rab6A' siRNA
Rab7b
GCC185
e
Normalized Surface CIMPR
0.75
1.00
1.25
1.50
1.75
p=0.004
p=0.049
p=0.031
p=0.025
Control
Rab6A and A'
Rab6a' siRNA
Rab7b
GCC185

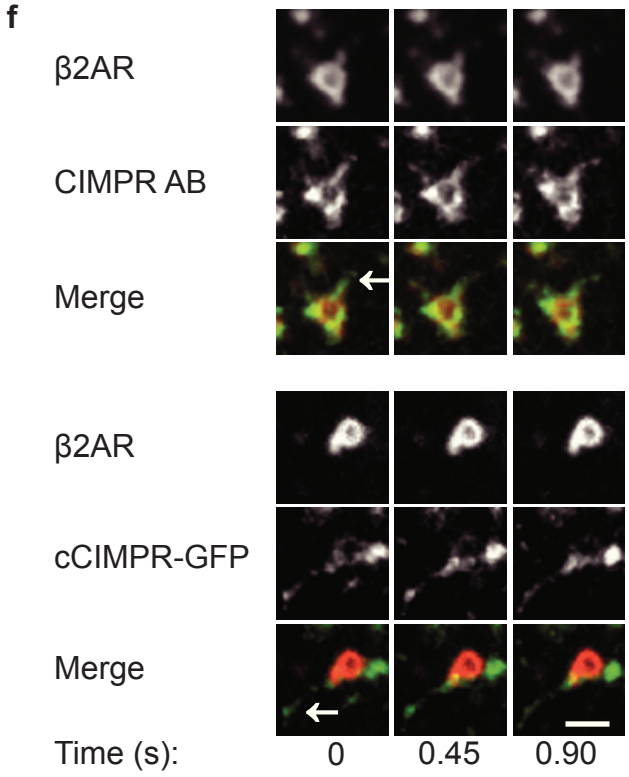
f
β2AR
CIMPR AB
Merge
β2AR
cCIMPR-GFP
Merge
Time (s):
0
0.45
0.90

Figure 5

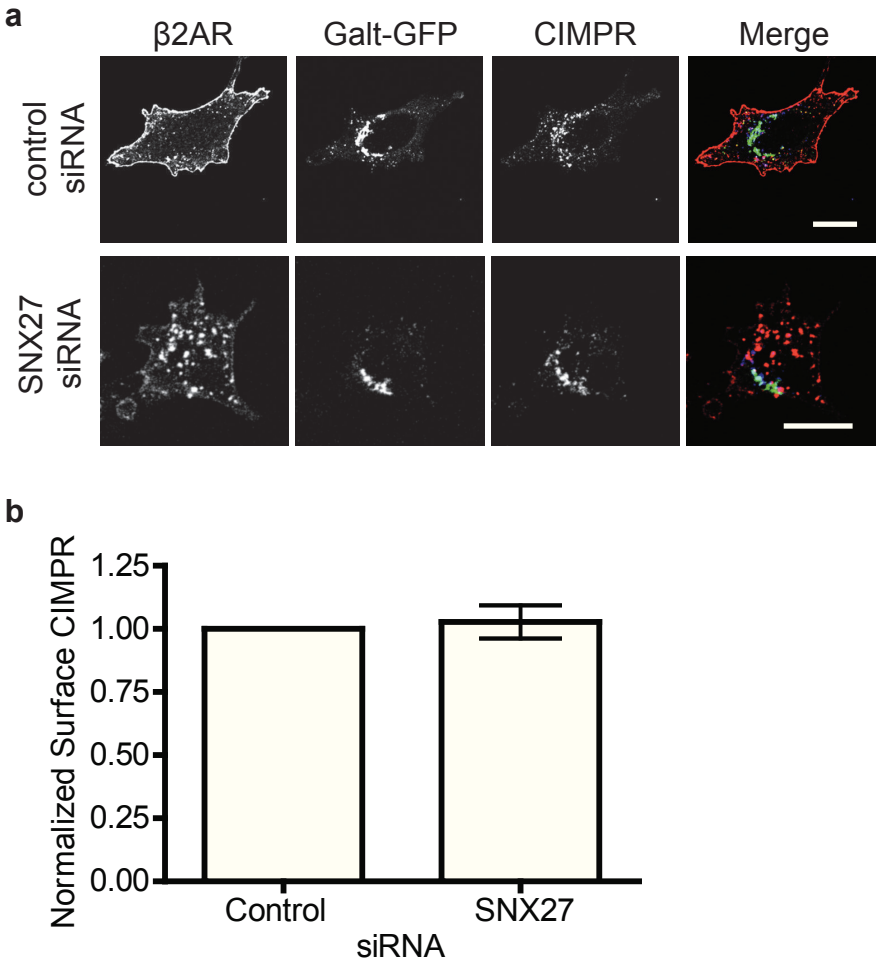
a
β2AR
Galt-GFP
CIMPR
Merge
control siRNA
SNX27 siRNA
b
Normalized Surface CIMPR
1.25
1.00
0.75
0.50
0.25
0.00
Control
SNX27
siRNA
d
SNX27
VPS29-GFP
Merge
c
β2AR
VPS29-GFP
Merge

e

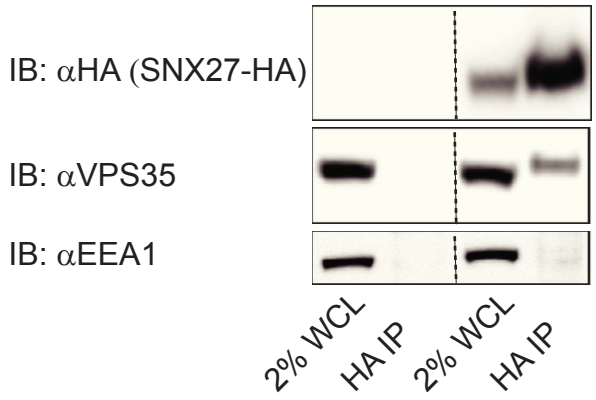
IB: αHA (SNX27-HA)
IB: αVPS35
IB: αEEA1
2% WCL
HA IP
2% WCL
HA IP

f

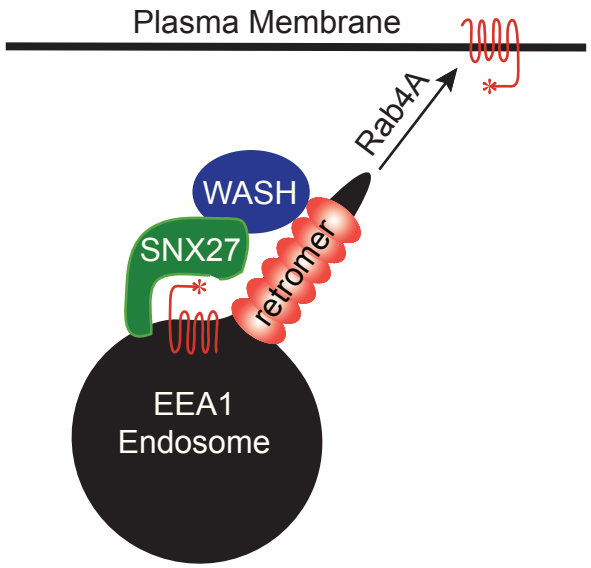
Plasma Membrane
Rab4A
WASH
SNX27
retromer
EEA1
Endosome

g

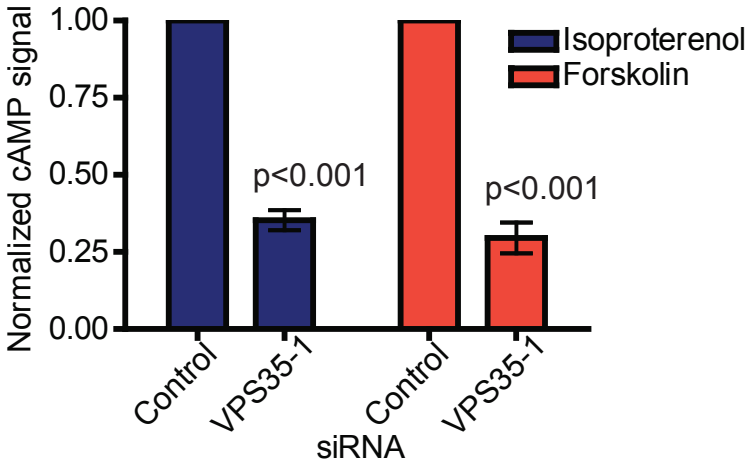
Normalized cAMP signal
1.00
0.75
0.50
0.25
0.00
p<0.001
p<0.001
Isoproterenol
Forskolin
Control
VPS35-1
Control
VPS35-1
siRNA

Supplementary Figure 1

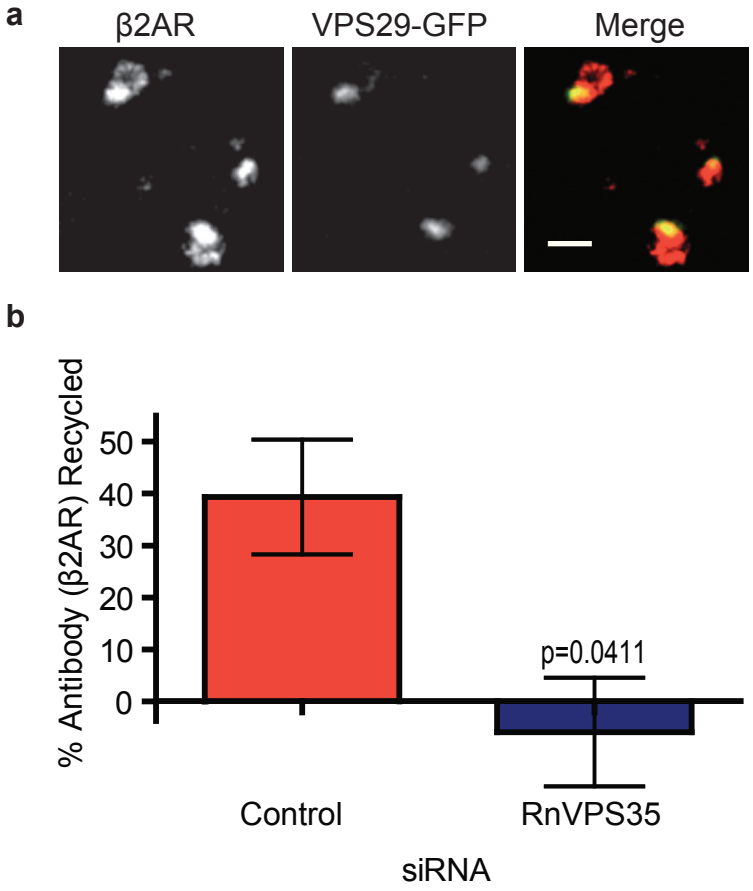

Supplementary Table

WASH Complex Component	Reproducibility	Max Peptides	Max % Coverage
CCDC53/CCD53	4/5	3	17.5
WASH2P/FAM39B	4/5	2	8.3
KIAA0592/FAM21C	5/5	13	21.4
KIAA1033/WAHS7	4/5	10	11.8
KIAA0196/Strumpellin	4/5	11	12.9

Chapter 6:

Discussion

6.1 Mass spectrometry results from B2AR purifications

Purification of B2AR from isolated endosomes yielded a list of interacting proteins that was tantalizing (Appendix 4). However, none of these leads have panned out to have unambiguously affected receptor trafficking. ATRNL1 was followed up on, as knockdown did appear to cause reliable decreases in recycling (Figure 1). This depletion effect was specific to B2AR trafficking, as transferrin recycling was unaffected (Figure 2). This protein had previously been shown to interact with another GPCR (Haqq et al., 2003) and possibly has an important role in development (Stark et al., 2010). This large transmembrane protein also contains a predicted class 1 PDZ ligand, making it possible that it engages the same recycling machinery as B2AR. However, after spending 6 months cloning this large protein, we were unable to get rescue of the depletion effect through expression of the transgene. It is possible that this large GC rich construct contains errors (4100bp) or does not express well and that this still may represent a valid target. More siRNA or shRNA sequences should be tested and the knockdown assessed by QPCR, as no good antibody exists. Possibly, other proteins identified by this method play roles in other receptor functions, such as endosomal signaling, and may be interesting to follow up on as new assays are developed to characterize B2AR.

FIGURE 1: ATRNL1 depletion on B2AR recycling

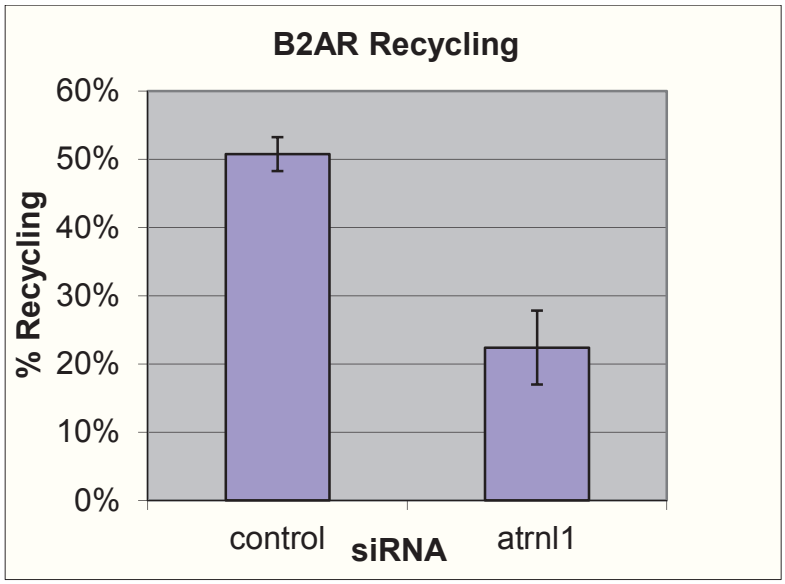

Figure legend: B2AR recycling appears to be affected by ATRNL1 depletion

Stably transfected HEK293 cells expressing FLAG-B2AR were depleted of ATRNL1 and assayed by flow cytometry for recycling by the feeding method (demonstrated in (Temkin et al., 2011)) . Bars represent mean ±SEM. N=4

FIGURE 2: ATRNL1 depletion on transferrin receptor recycling

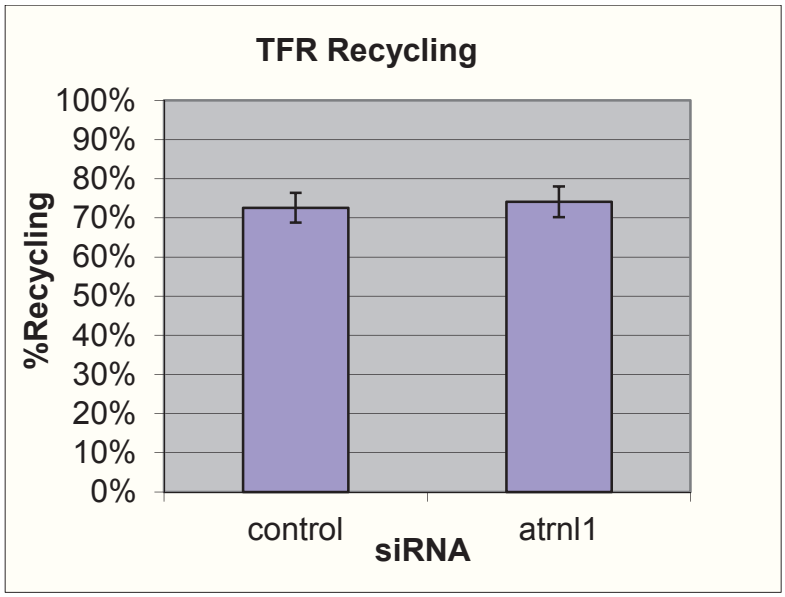

Figure legend: Transferrin receptor recycling appears to be unaffected by ATRNL1 depletion

HEK293 cells were depleted of ATRNL1 and assayed by flow cytometry for recycling or transferrin by a labeled transferrin feeding method (demonstrated in (Temkin et al., 2011)) . Bars represent mean ±SEM. N=4

It is likely that no trafficking molecules, such as the later discovered SNX27, were discovered by this mass spectrometry method because the affinities required for sorting in two dimensions (on a membrane) are very weak (Lauffer et al., 2010; Shih et al., 2002). These interactors, with μM affinity, would likely be washed away in this purification scheme. If this project were to be followed up on, it would be worth investigating crosslinking reagents to trap the receptor in the sorting process. One other possibility that this failed is that very few of the receptors are in the sorting process at any given time. NHERF2, a PDZ containing molecule, was persistently identified via this mass spectrometry approach. This suggests that a PDZ hand-off mechanisms occurs, and that

very few of the receptors are bound to sorting machinery (SNX27). Possibly, instead they bind to chaperone molecules which insulate the sorting sequence or provide some other, yet as unknown, function, until they reach the location of sorting.

6.2 The retention mechanism

The fact that a recycling sequence is needed for B2AR endosome to plasma membrane trafficking implies that there is an endosomal retention mechanism and that this receptor doesn't travel by "bulk flow." In Chapter 2 we determined that it is not a simple ubiquitin and ESCRT mediated retention, in that removal of lysines from B2AR-HA doesn't result in recycling. Despite the lack of necessity for receptor ubiquitination of the B2AR-HA mutant, perturbations of the ESCRT machinery did decrease degradation rate of this receptor in the flag loss assay. Strangely, these ESCRT perturbations (myc-HRS overexpression, VPS4KQ and EQ overexpression) did not affect the degradation rate of the wild type receptor in the flag loss assay (data not shown). This would seem to suggest that ESCRT complex can increase degradation rate of receptors that are stranded in the endosome, perhaps by a "bulk flow" involution mechanism, whereas receptors that are constantly traversing this compartment are unaffected. This could be further supported by EM data that might suggest whether there is differential involution of B2AR and B2AR-HA.

The interpretation that ubiquitin and ESCRT are not involved in the retention mechanism of B2AR is controversial as the Lefkowitz lab has performed experiments which suggest the opposite (Shenoy et al., 2001). While they perform their experiment differently, a radioligand binding measure of receptor after a 24 hr agonist treatment, they find that B2ARs missing all lysines don't degrade as rapidly as the wild type receptors. It is possible that the results in this paper represent clone bias, as having repeated these results in our lab, we get the same level of degradation for both of these receptors.

Furthermore, we get similar degradation for both B2AR and B2AR-HA receptors in the 24 hr radioligand assay, suggesting that the binding pocket for ligand is differently stable then the N-terminal FLAG epitope. Further work will need to be done to unambiguously determine, which of these measures indicates the receptor is degraded to the point it can no longer functionally couple G-proteins. They did follow up on their result and later identified Nedd4 as the E3 ubiquitin ligase responsible for the receptor degradation (Shenoy et al., 2008). In this paper they show that depletion of Nedd4 decreases receptor ubiquitination and degradation. They did not however look to see if Nedd4 affects degradation of other cargo including the lysine mutant B2AR. This control is necessary as Nedd4 is highly promiscuous and has been implicated in many processes including the recruitment of the ESCRT machinery (Blot et al., 2004).

Other possibilities for endosomal retention mechanisms include an ESCRT adapter protein, an orthogonal rafting system (possibly GASP1), or that retention is biophysically mediated (Chatterjee et al., 2001). In Chapter 3, data was presented that suggested that B2AR moved slower on the endosome then the bulk flow recycling TFR (Puthenveedu et al., 2010). It was also demonstrated in this work that recycling receptors appeared to enter a tubule, while nonrecycling receptors were evenly distributed around the endosome lumen. As the ESCRT machinery is believed to be located in a clathrin microdomain on the endosome, this uniform distribution of the non-recycling receptor doesn't make sense if the sole retention mechanism is ESCRT mediated (Raiborg et al., 2006). Instead it suggests a retention mechanism that is affecting all receptors at once. This could be a uniform protein mediated rafting (possibly due to oligomerization) or more simply that the sorting is due to a biophysical property of B2AR. We hypothesized

that the difference in diffusion rates prevents B2AR from recycling by default, however, the retromer tubule seems extremely stable, and therefore a 5 fold change in diffusion rates seems not enough to prevent recycling through this tubule. Instead it seems something is preventing the receptor from crossing over the curvature change at the base of the tubule.

The simplest sort of gating mechanism is a biophysical one, where 7 transmembrane receptors just can't bend enough to go over the curvature gradient. I attempted to test this theory in the lab of Tobias Baumgart at UPENN. Using isolated endosomes that contained tagged B2AR and TRF we pulled tubules using EEA1 antibody coated beads (modified from (Capraro et al., 2010; Tian et al., 2007)). We then sought photobleach the tubule and to measure whether these receptors could flow between the tubule and lumen. Unfortunately we found that there were extremely small mobile fractions of our receptors, precluding accurate measurement. This is consistent with other measurements made on GPCR mobility (Baker et al., 2007). Using this technique we developed, but instead using purified receptors placed into isolated liposomes, may shed light on whether retention is limited by the biophysical properties of the receptor in the membrane alone or whether protein interactions play a role.

At this point there is little evidence that any GPCR recycle by "bulk flow." It has been reported that a truncated vasopressin 2 receptor (V2R) recycles from the endosome faster than the full length receptor (Innamorati et al., 1998). However in my hands (and those of JH) this receptor doesn't recycle efficiently. Separate work from the von Zastrow lab does similarly suggest the existence of retention sequences (Hanyaloglu and von Zastrow, 2007; Hanyaloglu et al., 2005).

Dr. Hanyaloglu demonstrated that manipulations (knockdown or overexpression) of the ESCRT component HRS inhibited recycling of B2AR and MOR. This itself is not surprising as there is a lot of evidence suggesting ESCRT manipulations cause defects in receptor trafficking (Babst et al., 2000; Doyotte et al., 2005; Razi and Futter, 2006). The recycling effect was shown to be dependent on an acidic di-leucine stretch in the proximal c-terminal tail of B2AR. Appending the C-terminal portion of the B2AR containing this sequence onto the default recycling V2R362T conferred HRS sensitivity to that chimeric receptor. Additionally, mutation of that sequence EKENKLL to AKANKAA allowed the B2AR to recycle in an HRS independent manner. Most interestingly, when this mutation was made to the chimeric V2R containing the B2AR tail, this receptor could now recycle by default, without requiring the B2AR recycling sequence. This implied that this sequence was acting as a retention sequence. However, when this AKANKAA mutation is made on the B2AR-ala receptor it doesn't induce default recycling (unpublished data). Furthermore, the mutant AKANKAA B2AR receptor is still susceptible to manipulations of retromer and SNX27 (Figure XX). Together this would suggest that multiple retention sequences/mechanisms exist on the wild type B2AR receptor.

Though several endosomal retention sequences have now been identified, little is known about their mechanism of action (Hanyaloglu and von Zastrow, 2007; Innamorati et al., 1998; Johnson et al., 2001). In one case, an interaction with arrestin has been posited as the mechanism of endosomal retention (Dale et al., 2004). Further work is needed to determine if theses retention sequences effect receptor oligomerization, binding of a separate protein, or the biophysical properties of the receptors. Though these

sequences may exist, it would be compelling to survey more GPCRs to determine if endosomal retention is a general feature of all GPCRs, a further implication that it is likely a biophysical property of the receptor family. This is best addressed by a careful dissection of the trafficking of a large cohort of GPCRs, work that may lead to the discovery of more retention and recycling sequences.

Figure 3

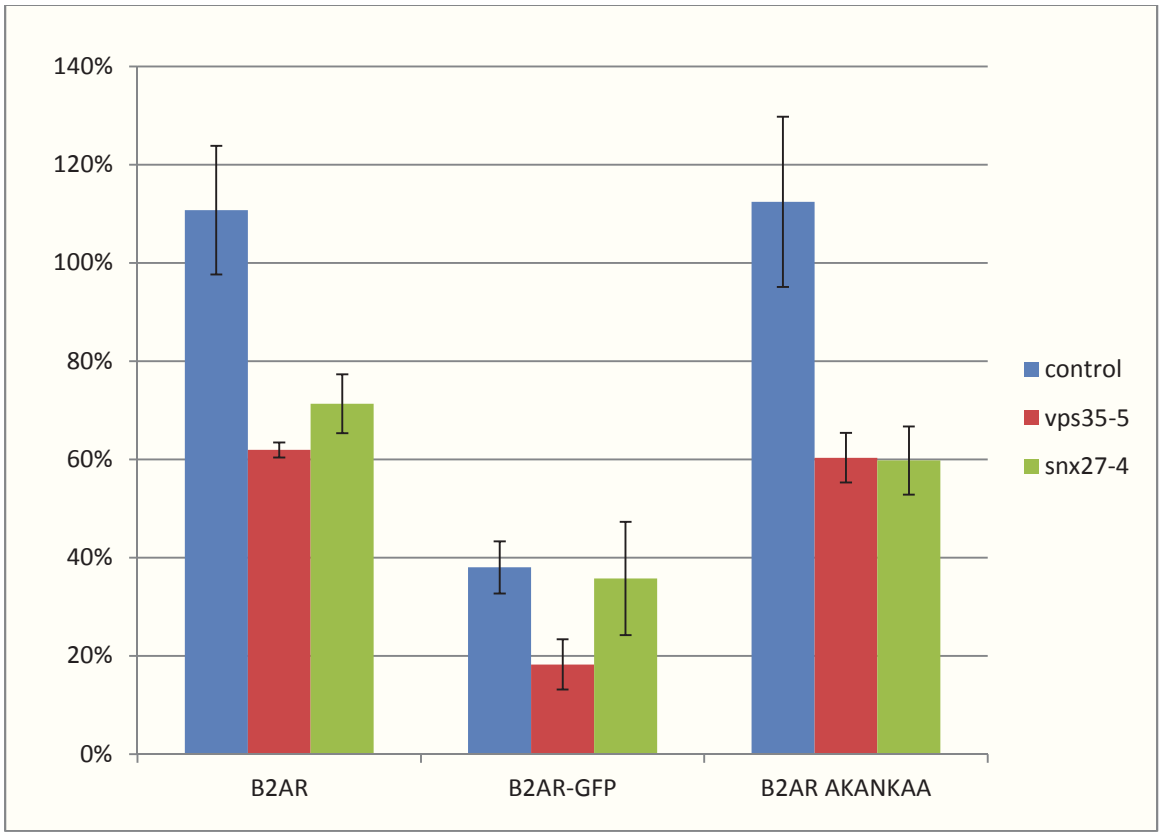

Figure legend: Receptor susceptibility to retromer and SNX27 manipulation

Transiently transfected HEK293 cells expressing FLAG-B2AR or variants were depleted of retromer component VPS35 or SNX27 and assayed by flow cytometry for recycling by the surface end label approach (Lauffer et al., 2010). Bars represent mean ±SEM. N=4

6.3 Sequence-directed recycling machinery

In the studies presented in Chapters 3 and 5 we used live cell fluorescence imaging to investigate the physical basis for PDZ-dependent endocytic sorting of B2ARs at the level of individual receptor-containing endosomes. Our results establish that this sorting process is mediated by PDZ-dependent partitioning of B2AR into a specialized subset of endosome-associated tubules. These specialized tubules are marked by actin and retromer proteins. We then showed that the retromer complex and actin are required for efficient plasma membrane recycling of B2AR. Further, we determine that SNX27 serves as a critical adapter in this recycling process, binding receptor and an actin nucleation complex. In doing so, we find two new functions for the retromer and expand our mechanistic understanding of this complex. Firstly, my results implicate the retromer in direct trafficking of receptors from endosomes to the plasma membrane. Secondly, my findings demonstrate that the retromer can regulate signaling receptors, where B2AR is considered a prototypical member of the largest known family of signaling receptors. In turn, this suggests that the retromer tubule functions as a versatile sorting platform that can support cargo transport to multiple destinations and that retromer function in the regulation of cell signaling.

The canonical retromer sorting is believed to occur through a direct interaction between cargo and retromer component VPS35, which results in sorting of cargo to the TGN. In yeast this was demonstrated through convincingly by making compensatory mutations in cargo VPS10p and retromer component VPS35p that could rescue proper sorting (Nothwehr et al., 2000). One mammalian cargo, DMT1 appears to interact

directly with the retromer complex in its sorting process (Tabuchi et al., 2010). Studies of the canonical retromer cargo CIMPR is mammalian cells have been much less clear. Though the interaction between VPS35 and CIMPR was mapped by yeast 2 hybrid, subsequent studies have found other sequences important for transport of CIMPR from the endosome to TGN (Arighi et al., 2004). A study from Seaman suggested that a 4 amino-acid aromatic motif is sufficient to mediate transport from the endosome to TGN, demonstrated by transferring this sequence onto an inert transmembrane protein and rerouting it to the TGN (Seaman, 2007). A second study from the Maxfield lab found an acidic dileucine motif in the CIMPR to be required for endosome to TGN transport (Tortorella et al., 2007). Additionally, direct interactions between CIMPR and TIP47 also seem to be required for TGN trafficking (Diaz and Pfeffer, 1998). While this data is difficult to compile into a simple model, it may suggest multiple sorting interactions exist that aid in retrieval of CIMPR from endosome to TGN. Further study will be required to determine if these are redundant interactions or represent sequential steps in trafficking. The cargo selection mechanism we discovered differs as it appears to not rely on a direct interaction with the retromer core.

This non-canonical retromer entry mechanism, whereby a SNX selects the retromer cargo, may prove more widely utilized than the canonical cargo selection method. While SNX27 selects retromer cargo via direct interactions with its PDZ domain and possibly its FERM domain, it may represent just one of many retromer adapter proteins (Ghai et al., 2011). SNX3 has also recently been shown to interact with cargo in the retromer sorting pathway (Harterink et al., 2011; Strochlic et al., 2007; Strochlic et al., 2008). Additionally, it is possible that the other SNXs involved in the

retromer may also serve as cargo adapters for different classes of cargo. SNX1 is particularly interesting as it has been shown to interact with several GPCR tail sequences (Heydorn et al., 2004).

The growing list of retromer cargo selection mechanisms and destinations served makes understanding the sorting role of the retromer less clear. Originally it was proposed to act as a coat molecule for cargo, likely determining the destination of that cargo as well. Now it is increasingly likely the same retromer tubule can serve multiple destinations. The mechanism by which cargo are sorted to the various destination will require further study. It is possible that various flavors of retromer tubule exist, capable of sorting different cargo to different destinations. For example, various VPS26 isoforms exist and little is known about how these variants bias the behavior of the retromer tubule (Haft et al., 2000; Kerr et al., 2005; Kim et al., 2008). Similarly there may be different retromer complexes which incorporate variable SNX proteins. However, in our studies we found that the same endosomal tubule seemed to support multiple cargo which appear to separate and go to different destinations. Furthermore, all retromer tubules appeared to colocalize with B2AR suggesting that it accesses all retromer tubules. Perhaps the best model to explain this data is that, instead of acting as a coat protein, the retromer acts as a passage out of the endosome into a tubular endosomal network where subsequent sorting interactions can determine the destination of the cargo. A model like this would allow the retromer tubule to support multiple sorting machineries. At least one such machine may involve actin.

Our lab has previously posited that interacting with actin is sufficient for a receptor to be recycled to the plasma membrane (Cao et al., 1999; Lauffer et al., 2009;

Puthenveedu et al., 2010). This said, experimental manipulations of actin in our lab have given inconsistent (assay dependent) answers. Adding an actin binding domain (ABD) to a GPCR induces plasma membrane recycling. It is unclear if this is an aberrant pathway as this recycling appears insensitive to HRS overexpression. We should now test whether this chimeric receptor recycles in a retromer dependent manner. While it appears clear that there is actin at the tubule, it is unclear how many roles it is playing. Work from our lab suggests that cortactin mediated actin polymerization is essential for retromer tubule stability while work from other labs suggests a role for actin in tubular scission (Derivery et al., 2009; Gomez and Billadeau, 2009). Together this data suggests multiple actin sites on the tubule are needed to perform divergent tasks of stabilization and scission. Further EM study of the actin at the retromer tubule might be useful to visualize these multiple roles of actin. As there appear to be multiple roles for actin at the tubule, determining its precise role in receptor trafficking to the plasma membrane may be difficult.

6.4 SNX27 interacting proteins

After elucidating the key role of SNX27 in B2AR recycling, many questions were left as to how SNX27 could mediate plasma membrane recycling. In order to determine what protein machinery SNX27 interacts with, a mass spectrometry approach was utilized. Immunopurification of FLAG tagged SNX27 yielded a long list of possible interacting proteins (Appendix 6) (Temkin et al., 2011). This list was then screened by siRNA depletion for defects in B2AR recycling (Appendix 7). This siRNA screen only yielded 2 siRNA sequences that significantly decreased B2AR recycling.

The first of these sequences was against the protein CRIPT, a small microtubule interacting protein that contains a c-terminal PDZ ligand (Niethammer et al., 1998; Passafaro et al., 1999). With the help of Cristina Melero of the Kortemme lab we determined that the CRIPT PDZ ligand has a ~1μM affinity towards the SNX27 PDZ domain. This is stronger than that of the B2AR PDZ ligand (17μM) (Lauffer et al., 2010). I hypothesized that CRIPT may serve to compete off SNX27 binding at specific areas on the tubules that juxtaposed microtubules. This might allow selective "release" of B2AR in areas of the tubule that are pinching of vesicles that move towards the plasma membrane. However, depletion of this protein by other siRNA sequences and viral shRNA sequences failed to confirm the functional role of this protein. Despite causing similar decreases in mRNA levels, as measured by QPCR, these other sequences did not decrease B2AR recycling.

The second of those siRNA sequences effecting B2AR trafficking was against the microtubule interacting protein, MAP4. This protein that had previously been shown to

decrease B2AR recycling when overexpressed (Cheng et al., 2005) and has been linked to the function motor proteins (Samora et al., 2010). Together these could suggest that MAP4 plays a role in recruiting SNX27, and therefore cargo, to an area on the tubule that is being actively sorted to the plasma membrane. Currently, this hypothesis, and more generally this protein are being further studied to determine if it plays a role in B2AR recycling.

SNX27 also co-purified with the whole Wiskott-Aldrich Syndrome Protein and SCAR Homolog (WASH) actin nucleation complex (Temkin et al., 2011). Though sequences against these proteins did not cause dramatic decreases in B2AR recycling, they have recently been linked to the retromer tubule function (Gomez and Billadeau, 2009). In addition to preventing CIMPR from trafficking from the endosome to TGN, manipulations of WASH proteins seemed to increase endosome size and tubule length. (Derivery et al., 2009; Duleh and Welch, 2010; Gomez and Billadeau, 2009). Together, these suggest WASH plays a role in scission of vesicles from the tubule. While the interaction between WASH and SNX27 may control localization of these proteins it is likely that they may also regulate each other's function in other ways. The first step in identifying the nature of the interaction is to map the interaction. Yeast 2 hybrid or GST pull-downs of purified proteins should be attempted to figure out the interaction surfaces. One possible mechanistic interaction is that SNX27 regulates WASH activation of ARP2/3 by controlling small GTPases through its RA domain (Liu et al., 2009). For this reason, it would be interesting to add SNX27 to a WASH mediated actin nucleation assay.

6.5 Importance in Physiology

There is no doubt that SNX27 and the retromer complex play essential physiological roles as knockout mice for either of these fail to develop properly or survive (Bachhawat et al., 1994; Cai et al., 2011). Because of the retromer and SNX27s apparent promiscuity in cargo selection it will be difficult to determine if missorting of any specific cargo is to blame or if disease phenotypes are the result of combinatorial deficiencies in cargo trafficking (Bonifacino and Hurley, 2008; Cai et al., 2011; Ghai et al., 2011; Joubert et al., 2004; Lauffer et al., 2010; Lunn et al., 2007; Temkin et al., 2011; Verges, 2008). More subtle alterations to SNX27 and retromer function likely play roles in human disease. The retromer has been suggested to play roles in Alzheimers (Muhammad et al., 2008; Sullivan et al., 2011) and Parkinsons diseases (Vilarino-Guell et al., 2011; Zimprich et al., 2011). The research into the role of retromer in Alzheimer's linked retromer depletion to increased Aβ production and neurodegeneration. It was then hypothesized this was due to improper function of gamma-secretase at the cell surface, as LTP deficits caused by retromer depletion could be rescued by a gamma-secretase inhibitor. While this mechanism needs to be explored further, it is plausible and may suggest a role for SNX27 in Alzheimer's as well. Presenilin, a component of the gamma-secretase complex contains a PDZ (Xu et al., 1999).

Phsyiological maintenance of cargo trafficking in different cell types through alteration of SNX27 levels seems a likely mechanism. In our hands A10 cells, a rat atrial derived cell, recycle B2AR poorly compared to HEK293 cells. This recycling can be increased by addition of transgenic SNX27 (Ben Lauffer, personal communication).

Careful analysis of SNX27 expression in different cell types, including neuronal populations could be highly informative. It is also likely that SNX27 levels are controlled in adaptive processes. Methamphetamine administration has been shown to increase SNX27 expression in the neocortex by ~50% (Kajii et al., 2003). As recycling endosomes juxtapose neuronal spines, SNX27 is in a location to affect neuronal circuitry via trafficking to the spine (Cooney et al., 2002). It is possible that this increase results in the neuronal adaptation that is pathogenic to chronic drug administration. Therefore it should be of great interest to determine how this increased SNX27 alters surface receptor expression. Further, measures of surface proteins under conditions of differential SNX27 expression could answer the very important question of what cargo utilize this sorting machine.

In conclusion, our results indicate that SNX27 and the retromer plays a critical role in mediating B2AR sorting between the divergent, and physiologically opposite, pathways of resensitization and down-regulation. The requirement of specialized endosomal tubules for efficient B2AR recycling indicates that there must also be an endosomal retention mechanism which keeps B2AR from flowing, like TFR, into any tubule (*i.e.* recycling by default). Thus, the fundamental role of retromer-associated tubules may be to allow endosome exit of B2AR and other membrane cargo that are unable to be recycled by the default pathway.

An advantage to this emerging endosomal sorting scheme, retention followed by selection into a recycling tubule, is that it allows for easy regulation. This regulation may be of a specific cargo or the whole system. In the case of the B2AR, for example, a simple modification to the recycling sequence could prevent selection into the retromer

tubule, recycling, and ultimately resensitization (Cao et al., 1999). B2AR recycling is indeed known to be regulable and, in future studies, it will be interesting to see if physiologically significant regulation of receptor trafficking occurs at the level of tubule entry (Yudowski et al., 2006; Yudowski et al., 2009). Alternatively, traffic through this pathway may be more directly limited by other cargo traversing it. It is easy to imagine one cargo outcompeting another for binding to SNX27. Finally, receptor oligomerization may also regulate cargo flux through this path. Combining recycling and non-recycling variants of B2AR in the same assay results in an intermediate phenotype for both receptors (Cao et al., 2005). With so many options for regulation of trafficking in this model, physiologically relevant examples need to be determined. Ideally, this will be a receptor that can be easily diverted between recycling and degradative paths through a signaling cascade.

6.6 References

Arighi, C.N., L.M. Hartnell, R.C. Aguilar, C.R. Haft, and J.S. Bonifacino. 2004. Role of the mammalian retromer in sorting of the cation-independent mannose 6-phosphate receptor. J Cell Biol 165:123-33.

Babst, M., G. Odorizzi, E.J. Estepa, and S.D. Emr. 2000. Mammalian tumor susceptibility gene 101 (TSG101) and the yeast homologue, Vps23p, both function in late endosomal trafficking. Traffic 1:248-58.

Bachhawat, A.K., J. Suhan, and E.W. Jones. 1994. The yeast homolog of H < beta > 58, a mouse gene essential for embryogenesis, performs a role in the delivery of proteins to the vacuole. Genes Dev 8:1379-87.

Baker, A., A. Sauliere, F. Dumas, C. Millot, S. Mazeres, A. Lopez, and L. Salome. 2007. Functional membrane diffusion of G-protein coupled receptors. Eur Biophys J 36:849-60.

Blot, V., F. Perugi, B. Gay, M.C. Prevost, L. Briant, F. Tangy, H. Abriel, O. Staub, M.C. Dokhelar, and C. Pique. 2004. Nedd4.1-mediated ubiquitination and subsequent recruitment of Tsg101 ensure HTLV-1 Gag trafficking towards the multivesicular body pathway prior to virus budding. J Cell Sci 117:2357-67.

Bonifacino, J.S., and J.H. Hurley. 2008. Retromer. Curr Opin Cell Biol 20:427-36.

Cai, L., L.S. Loo, V. Atlashkin, B.J. Hanson, and W. Hong. 2011. Deficiency of sorting nexin 27 (SNX27) leads to growth retardation and elevated levels of N-methyl-D-aspartate receptor 2C (NR2C). Mol Cell Biol 31:1734-47.

Cao, T.T., A. Brelot, and M. von Zastrow. 2005. The composition of the beta-2 adrenergic receptor oligomer affects its membrane trafficking after ligand-induced endocytosis. Mol Pharmacol 67:288-97.

Cao, T.T., H.W. Deacon, D. Reczek, A. Bretscher, and M. von Zastrow. 1999. A kinase-regulated PDZ-domain interaction controls endocytic sorting of the beta2-adrenergic receptor. Nature 401:286-90.

Capraro, B.R., Y. Yoon, W. Cho, and T. Baumgart. 2010. Curvature sensing by the epsin N-terminal homology domain measured on cylindrical lipid membrane tethers. J Am Chem Soc 132:1200-1.

Chatterjee, S., E.R. Smith, K. Hanada, V.L. Stevens, and S. Mayor. 2001. GPI anchoring leads to sphingolipid-dependent retention of endocytosed proteins in the recycling endosomal compartment. Embo J 20:1583-92.

Cheng, G., F. Qiao, T.N. Gallien, D. Kuppuswamy, and G.t. Cooper. 2005. Inhibition of beta-adrenergic receptor trafficking in adult cardiocytes by MAP4 decoration of microtubules. Am J Physiol Heart Circ Physiol 288:H1193-202.

Cooney, J.R., J.L. Hurlburt, D.K. Selig, K.M. Harris, and J.C. Fiala. 2002. Endosomal compartments serve multiple hippocampal dendritic spines from a widespread rather than a local store of recycling membrane. J Neurosci 22:2215-24.

Dale, L.B., J.L. Seachrist, A.V. Babwah, and S.S. Ferguson. 2004. Regulation of angiotensin II type 1A receptor intracellular retention, degradation, and recycling by Rab5, Rab7, and Rab11 GTPases. J Biol Chem 279:13110-8.

Derivery, E., C. Sousa, J.J. Gautier, B. Lombard, D. Loew, and A. Gautreau. 2009. The Arp2/3 activator WASH controls the fission of endosomes through a large multiprotein complex. Dev Cell 17:712-23.

Diaz, E., and S.R. Pfeffer. 1998. TIP47: a cargo selection device for mannose 6-phosphate receptor trafficking. Cell 93:433-43.

Doyotte, A., M.R. Russell, C.R. Hopkins, and P.G. Woodman. 2005. Depletion of TSG101 forms a mammalian "Class E" compartment: a multicisternal early endosome with multiple sorting defects. J Cell Sci 118:3003-17.

Duleh, S.N., and M.D. Welch. 2010. WASH and the Arp2/3 complex regulate endosome shape and trafficking. Cytoskeleton (Hoboken) 67:193-206.

Ghai, R., M. Mobli, S.J. Norwood, A. Bugarcic, R.D. Teasdale, G.F. King, and B.M. Collins. 2011. Phox homology band 4.1/ezrin/radixin/moesin-like proteins function as molecular scaffolds that interact with cargo receptors and Ras GTPases. Proc Natl Acad Sci U S A 108:7763-8.

Gomez, T.S., and D.D. Billadeau. 2009. A FAM21-containing WASH complex regulates retromer-dependent sorting. Dev Cell 17:699-711.

Haft, C.R., M. de la Luz Sierra, R. Bafford, M.A. Lesniak, V.A. Barr, and S.I. Taylor. 2000. Human orthologs of yeast vacuolar protein sorting proteins Vps26, 29, and 35: assembly into multimeric complexes. Mol Biol Cell 11:4105-16.

Hanyaloglu, A.C., and M. von Zastrow. 2007. A novel sorting sequence in the beta2-adrenergic receptor switches recycling from default to the Hrs-dependent mechanism. J Biol Chem 282:3095-104.

Hanyaloglu, A.C., E. McCullagh, and M. von Zastrow. 2005. Essential role of Hrs in a recycling mechanism mediating functional resensitization of cell signaling. Embo J 24:2265-83.

Haqq, A.M., P. Rene, T. Kishi, K. Khong, C.E. Lee, H. Liu, J.M. Friedman, J.K. Elmquist, and R.D. Cone. 2003. Characterization of a novel binding partner of the melanocortin-4 receptor: attractin-like protein. Biochem J 376:595-605.

Harterink, M., F. Port, M.J. Lorenowicz, I.J. McGough, M. Silhankova, M.C. Betist, J.R. van Weering, R.G. van Heesbeen, T.C. Middelkoop, K. Basler, P.J. Cullen, and H.C. Korswagen. 2011. A SNX3-dependent retromer pathway mediates retrograde transport of the Wnt sorting receptor Wntless and is required for Wnt secretion. Nat Cell Biol 13:914-23.

Heydorn, A., B.P. Sondergaard, B. Ersboll, B. Holst, F.C. Nielsen, C.R. Haft, J. Whistler, and T.W. Schwartz. 2004. A library of 7TM receptor C-terminal tails. Interactions with the proposed post-endocytic sorting proteins ERM-binding phosphoprotein 50 (EBP50), N-ethylmaleimide-sensitive factor (NSF), sorting nexin 1 (SNX1), and G protein-coupled receptor-associated sorting protein (GASP). J Biol Chem 279:54291-303.

Innamorati, G., H.M. Sadeghi, N.T. Tran, and M. Birnbaumer. 1998. A serine cluster prevents recycling of the V2 vasopressin receptor. Proc Natl Acad Sci U S A 95:2222-6.

Johnson, A.O., M.A. Lampson, and T.E. McGraw. 2001. A di-leucine sequence and a cluster of acidic amino acids are required for dynamic retention in the endosomal recycling compartment of fibroblasts. Mol Biol Cell 12:367-81.

Joubert, L., B. Hanson, G. Barthet, M. Sebben, S. Claeysen, W. Hong, P. Marin, A. Dumuis, and J. Bockaert. 2004. New sorting nexin (SNX27) and NHERF specifically interact with the 5-HT4a receptor splice variant: roles in receptor targeting. J Cell Sci 117:5367-79.

Kajii, Y., S. Muraoka, S. Hiraoka, K. Fujiyama, A. Umino, and T. Nishikawa. 2003. A developmentally regulated and psychostimulant-inducible novel rat gene mrt1 encoding PDZ-PX proteins isolated in the neocortex. Mol Psychiatry 8:434-44.

Kerr, M.C., J.S. Bennetts, F. Simpson, E.C. Thomas, C. Flegg, P.A. Gleeson, C. Wicking, and R.D. Teasdale. 2005. A novel mammalian retromer component, Vps26B. Traffic 6:991-1001.

Kim, E., J.W. Lee, D.C. Baek, S.R. Lee, M.S. Kim, S.H. Kim, K. Imakawa, and K.T. Chang. 2008. Identification of novel retromer complexes in the mouse testis. Biochem Biophys Res Commun 375:16-21.

Lauffer, B.E., S. Chen, C. Melero, T. Kortemme, M. von Zastrow, and G.A. Vargas. 2009. Engineered protein connectivity to actin mimics PDZ-dependent recycling of G protein-coupled receptors but not its regulation by Hrs. J Biol Chem 284:2448-58.

Lauffer, B.E., C. Melero, P. Temkin, C. Lei, W. Hong, T. Kortemme, and M. von Zastrow. 2010. SNX27 mediates PDZ-directed sorting from endosomes to the plasma membrane. J Cell Biol 190:565-74.

Liu, R., M.T. Abreu-Blanco, K.C. Barry, E.V. Linardopoulou, G.E. Osborn, and S.M. Parkhurst. 2009. Wash functions downstream of Rho and links linear and branched actin nucleation factors. Development 136:2849-60.

Lunn, M.L., R. Nassirpour, C. Arrabit, J. Tan, I. McLeod, C.M. Arias, P.E. Sawchenko, J.R. Yates, 3rd, and P.A. Slesinger. 2007. A unique sorting nexin regulates trafficking of potassium channels via a PDZ domain interaction. Nat Neurosci 10:1249-59.

Muhammad, A., I. Flores, H. Zhang, R. Yu, A. Staniszewski, E. Planel, M. Herman, L. Ho, R. Kreber, L.S. Honig, B. Ganetzky, K. Duff, O. Arancio, and S.A. Small. 2008. Retromer deficiency observed in Alzheimer's disease causes hippocampal dysfunction, neurodegeneration, and Abeta accumulation. Proc Natl Acad Sci U S A 105:7327-32.

Niethammer, M., J.G. Valtschanoff, T.M. Kapoor, D.W. Allison, R.J. Weinberg, A.M. Craig, and M. Sheng. 1998. CRIPT, a novel postsynaptic protein that binds to the third PDZ domain of PSD-95/SAP90. Neuron 20:693-707.

Nothwehr, S.F., S.A. Ha, and P. Bruinsma. 2000. Sorting of yeast membrane proteins into an endosome-to-Golgi pathway involves direct interaction of their cytosolic domains with Vps35p. J Cell Biol 151:297-310.

Passafaro, M., C. Sala, M. Niethammer, and M. Sheng. 1999. Microtubule binding by CRIPT and its potential role in the synaptic clustering of PSD-95. Nat Neurosci 2:1063-9.

Puthenveedu, M.A., B. Lauffer, P. Temkin, R. Vistein, P. Carlton, K. Thorn, J. Taunton, O.D. Weiner, R.G. Parton, and M. von Zastrow. 2010. Sequence-dependent sorting of recycling proteins by actin-stabilized endosomal microdomains. Cell 143:761-73.

Raiborg, C., J. Wesche, L. Malerod, and H. Stenmark. 2006. Flat clathrin coats on endosomes mediate degradative protein sorting by scaffolding Hrs in dynamic microdomains. J Cell Sci 119:2414-24.

Razi, M., and C.E. Futter. 2006. Distinct roles for Tsg101 and Hrs in multivesicular body formation and inward vesiculation. Mol Biol Cell 17:3469-83.

Samora, C.P., B. Mogessie, L. Conway, J.L. Ross, A. Straube, and A.D. McAinsh. 2010. MAP4 and CLASP1 operate as a safety mechanism to maintain a stable spindle position in mitosis. Nat Cell Biol.

Seaman, M.N. 2007. Identification of a novel conserved sorting motif required for retromer-mediated endosome-to-TGN retrieval. J Cell Sci 120:2378-89.

Shenoy, S.K., P.H. McDonald, T.A. Kohout, and R.J. Lefkowitz. 2001. Regulation of receptor fate by ubiquitination of activated beta 2-adrenergic receptor and beta-arrestin. Science 294:1307-13.

Shenoy, S.K., K. Xiao, V. Venkataramanan, P.M. Snyder, N.J. Freedman, and A.M. Weissman. 2008. Nedd4 mediates agonist-dependent ubiquitination, lysosomal targeting, and degradation of the beta2-adrenergic receptor. J Biol Chem 283:22166-76.

Shih, S.C., D.J. Katzmann, J.D. Schnell, M. Sutanto, S.D. Emr, and L. Hicke. 2002. Epsins and Vps27p/Hrs contain ubiquitin-binding domains that function in receptor endocytosis. Nat Cell Biol 4:389-93.

Stark, Z., D.L. Bruno, H. Mountford, P.J. Lockhart, and D.J. Amor. 2010. De novo 325 kb microdeletion in chromosome band 10q25.3 including ATRNL1 in a boy with

cognitive impairment, autism and dysmorphic features. Eur J Med Genet 53:337-9.

Strochlic, T.I., T.G. Setty, A. Sitaram, and C.G. Burd. 2007. Grd19/Snx3p functions as a cargo-specific adapter for retromer-dependent endocytic recycling. J Cell Biol 177:115-25.

Strochlic, T.I., B.C. Schmiedekamp, J. Lee, D.J. Katzmann, and C.G. Burd. 2008. Opposing activities of the Snx3-retromer complex and ESCRT proteins mediate regulated cargo sorting at a common endosome. Mol Biol Cell 19:4694-706.

Sullivan, C.P., A.G. Jay, E.C. Stack, M. Pakaluk, E. Wadlinger, R.E. Fine, J.M. Wells, and P.J. Morin. 2011. Retromer disruption promotes amyloidogenic APP processing. Neurobiol Dis 43:338-45.

Tabuchi, M., I. Yanatori, Y. Kawai, and F. Kishi. 2010. Retromer-mediated direct sorting is required for proper endosomal recycling of the mammalian iron transporter DMT1. J Cell Sci 123:756-66.

Temkin, P., B. Lauffer, S. Jager, P. Cimermancic, N.J. Krogan, and M. von Zastrow. 2011. SNX27 mediates retromer tubule entry and endosome-to-plasma membrane trafficking of signalling receptors. Nat Cell Biol 13:715-21.

Tian, A., C. Johnson, W. Wang, and T. Baumgart. 2007. Line tension at fluid membrane domain boundaries measured by micropipette aspiration. Phys Rev Lett 98:208102.

Tortorella, L.L., F.B. Schapiro, and F.R. Maxfield. 2007. Role of an acidic cluster/dileucine motif in cation-independent mannose 6-phosphate receptor traffic. Traffic 8:402-13.

Verges, M. 2008. Retromer: multipurpose sorting and specialization in polarized transport. Int Rev Cell Mol Biol 271:153-98.

Vilarino-Guell, C., C. Wider, O.A. Ross, J.C. Dachsel, J.M. Kachergus, S.J. Lincoln, A.I. Soto-Ortolaza, S.A. Cobb, G.J. Wilhoite, J.A. Bacon, B. Behrouz, H.L. Melrose, E. Hentati, A. Puschmann, D.M. Evans, E. Conibear, W.W. Wasserman, J.O. Aasly, P.R. Burkhard, R. Djaldetti, J. Ghika, F. Hentati, A. Krygowska-Wajs, T. Lynch, E. Melamed, A. Rajput, A.H. Rajput, A. Solida, R.M. Wu, R.J. Uitti, Z.K. Wszolek, F. Vingerhoets, and M.J. Farrer. 2011. VPS35 Mutations in Parkinson Disease. Am J Hum Genet 89:162-7.

Xu, X., Y. Shi, X. Wu, P. Gambetti, D. Sui, and M.Z. Cui. 1999. Identification of a novel PSD-95/Dlg/ZO-1 (PDZ)-like protein interacting with the C terminus of presenilin-1. J Biol Chem 274:32543-6.

Yudowski, G.A., M.A. Puthenveedu, and M. von Zastrow. 2006. Distinct modes of regulated receptor insertion to the somatodendritic plasma membrane. Nat Neurosci 9:622-7.

Yudowski, G.A., M.A. Puthenveedu, A.G. Henry, and M. von Zastrow. 2009. Cargo-mediated Regulation of a Rapid Rab4-dependent Recycling Pathway. Mol Biol Cell.

Zimprich, A., A. Benet-Pages, W. Struhal, E. Graf, S.H. Eck, M.N. Offman, D. Haubenberger, S. Spielberger, E.C. Schulte, P. Lichtner, S.C. Rossle, N. Klopp, E. Wolf, K. Seppi, W. Pirker, S. Presslauer, B. Mollenhauer, R. Katzenschlager, T. Foki, C. Hotzy, E. Reinthaler, A. Harutyunyan, R. Kralovics, A. Peters, F. Zimprich, T. Brucke, W. Poewe, E. Auff, C. Trenkwalder, B. Rost, G. Ransmayr,

J. Winkelmann, T. Meitinger, and T.M. Strom. 2011. A Mutation in VPS35, Encoding a Subunit of the Retromer Complex, Causes Late-Onset Parkinson Disease. Am J Hum Genet 89:168-75.

Appendices

Appendix 1: Protocol for iron micro-bead receptor purification

Modified from (Li et al., 2005), yielded ~25% of total cellular receptor

Done at 4 degrees

1. Adsorb antibody onto beads by mixing overnight:
    a. 2.5ul Ferrofluid (Ferrotech)
    b. 1ml Barth's saline
    c. 100ul 5mg/ml M1 anti-Flag
    d. .04% BSA
2. Purify adsorbed antibody coated iron by passing it through a mini-macs separation column (Miltenyi) in the presence of magnet (strong magnet from KJ magnetics works better than miltenyi magnet setup). Wash 2 times in the presence of magnet with Barth's saline (1ml). Remove magnet and elute with 500ul Barth's saline.
3. Incubate 100ul of adsorbed beads for 10 min on 10cm dish of cells expressing Flag tagged receptor of choice.
4. Add agonist for desired amount of time (Isoproterenol 30 min).
5. Scrape cells into 1ml endosome buffer (35mM kPipes pH=7.2, 5mM EGTA, 5mM $MgCl_2$, 0.25M sucrose, Complete protease inhibitor (Roche))
6. Homogenize cells by freeze thawing in dry ice/ethanol mixture 4 times and then 4 passages through a syringe with 22 G needle
7. Spin 3000g for 10min and transfer supernatant to fresh tube

8. Equilibrate MACs MS column by allowing .5mls endosome buffer to drip through. Run sample through MACs MS column in presence of magnet (Reserve some lysate to test for purification). Wash 3x with .5 mls endosome buffer. Remove magnet and elute with 100ul IPB (0.1% triton-x, 50mM NaCl, 50mM Tris pH=7.4, 5mM EDTA), pushing the 100ul through with the plunger.
9. See Appendix 3 for receptor purification from lysate

Appendix 2: Protocol for Miltenyi beads (EEA1 antibody) endosomal preparation

Modified from (Cottrell et al., 2009), yielded ~50% total cellular receptor

1. Plate cells in 6-well plate format and grow to 80% confluence.
2. Perform cell treatments (Isoproterenol 30 min).
3. Wash cells and scrape into 1 ml homogenization buffer (10mM HEPES, 100mM KCl, 1 mM EDTA, 25mM sucrose, Complete protease inhibitor (Roche) pH=7.2. (Optional 1mM NaVO4 and 50mM NaF))
4. Homogenize cells by freeze thawing in dry ice/ethanol mixture 4 times and then 4 passages through a syringe with 22 G needle
5. Spin (3000 g) for 10 min and transfer supernatant into fresh tubes.
6. Add anti-EEA1 antibody (1:250) and rotate O/N at 4C.
7. Add secondary antibody-magnetic beads 25 ul/tube and rotate 1 hr at 4 degrees.
8. Place column between 2 magnets and equilibrate with 1 ml homogenization buffer.
9. Allow sample to gravity filter through column on magnet.
10. Wash with 1 ml homogenization buffer x 2.
11. Remove column from magnet, add 100 ul of homogenization buffer with 0.5% triton and force through the column with the plunger collecting the final sample.
12. See Appendix 3 for receptor purification from lysate

Materials:

Mouse anti-EEA1 antibody, BD Transduction Laboratories # 610456

Goat anti-mouse IgG microbeads, Miltenyi Biotec # 130-048-402

MACS separation columns 25MS, Miltenyi Biotec # 130-042-201

K&J magnetics magnet #DC4

Appendix 3: Protocol for purification of FLAG tagged receptor from lysate

Done at 4 degrees

1. Suspend cell lysate in IPB up to 1ml (*0.1% triton-x, 50mM NaCl, 50mM Tris pH=7.4, 5mM EDTA, Complete protease inhibitor (Roche)).
2. Add 25ul M2 agarose beads (Sigma-Aldrich A2220)
3. Let rotate at 4 degrees for 3 hours
4. Add to micro-spin column (Pierce #89879). May need to spin through multiple times to add all sample.
5. Spin 1000RPM for 1min
6. Wash column 3 times with 400ul of IPB, spinning at 1000 RPM for 1 min each time
7. Elute sample with 25ul 3xFLAG peptide (Sigma F4799) dissolved in IPB to 150ng/ul and spin 1 min at 1000 RPM
8. Repeat step 7 to increase yield.

*Alternative detergents in place of triton (0.1%-0.6% DDM or CHAPS)

Appendix 4: List of Mass spectrometry hits from B2AR purification schemes

NCBI gene symbol	Gene Description	mRNA Accessions	siRNA Target Sequence
LRPPRC	leucine-rich PPR-motif containing	NM_133259	CAGGAGGTCTATGAATATAAA
LRPPRC	leucine-rich PPR-motif containing	NM_133259	CACTATAATGCTTTACTTAAA
STOML2	stomatin (EPB72)-like 2	NM_013442	AAGGACTCCAACACTATCCTA
STOML2	stomatin (EPB72)-like 2	NM_013442	CCGGGTGAAAGAGTCTATGCA
RAB14	RAB14, member RAS oncogene family	NM_016322	CACGTTAATAGAGGTAGTACA
RAB14	RAB14, member RAS oncogene family	NM_016322	TCCATTGATCCCGTATCTTAA
RAB13	RAB13, member RAS oncogene family	NM_002870	CAGGGCAAACATAAATGTAA A
MARCKSL 1	MARCKS-like 1	NM_023009	CCAGTTGAAGATGGTCCCTTA
MARCKSL 1	MARCKS-like 1	NM_023009	CCCACTGTTGTAAATAACTTT
PHB2	prohibitin 2	NM_007273	AACCCAGGAATTCTCAATAAA
PHB	prohibitin	NM_002634	AAAGCCAGCTTCCTCGCATCT
FKBP15	FK506 binding protein 15, 133kDa	NM_015258 XM_376903 XM_936355	CCGGAAACAACTGGAACTCA A
FKBP15	FK506 binding protein 15, 133kDa	NM_015258 XM_376903 XM_936355	AACCATCATGAATACGATCAA
GBAS	glioblastoma amplified sequence	NM_001483	CAAGTATTTGTCGTAAATTAA
GBAS	glioblastoma amplified sequence	NM_001483	CTGGGAGGAATTGGTATATTA
SORT1	sortilin 1	NM_002959	CAGCAGAGAATTGACTAGAT

			A
SORT1	sortilin 1	NM_002959	CTGGGTTTGGCACAATCTTTA
CMIP	c-Maf-inducing protein	NM_030629 NM_198390	CTGGCGTGTAGTACTGTATAA
CMIP	c-Maf-inducing protein	NM_030629 NM_198390	AAGATTTACAAATATAAGAA A
CKAP4	cytoskeleton-associated protein 4	NM_006825	AGGGCGCGGATTTAAAGTCCA
CKAP4	cytoskeleton-associated protein 4	NM_006825	CCAAGTGGAGGCGGACTTGA A
SEC22A	SEC22 vesicle trafficking protein homolog A (S. cerevisiae)	NM_012430	CTGCAGAAATTGGAAAGTTTA
SEC22A	SEC22 vesicle trafficking protein homolog A (S. cerevisiae)	NM_012430	AAACTGGACATTATAACATTA
HRNR	hornerin	NM_00100993 1	CTGGTTCAGGCTCGTAATAAA
HRNR	hornerin	NM_00100993 1	TCAGTGAATAATAAACATAAA
ANXA2	annexin A2	NM_00100285 7 NM_00100285 8 NM_004039	AAGTGTCGCTATTTAAGTTAA
ANXA2	annexin A2	NM_00100285 7 NM_00100285 8 NM_004039	CTGGGACTGAGCTGTACAGTA
S100A8	S100 calcium binding protein A8	NM_002964	CCACAAGTACTCCCTGATAAA
RAC1	ras-related C3 botulinum toxin substrate 1 (rho family, small GTP binding protein Rac1)	NM_006908 NM_018890 NM_198829	ATGCATTTCCTGGAGAATATA
CDC42	cell division cycle 42 (GTP binding protein, 25kDa)	NM_00103980 2 NM_001791 NM_044472	CATCAGATTTGAAATATTTAA
SYT14	synaptotagmin	NM_153262	CACCTTGTTCTTCTACCTATA

	XIV		
SYT14	synaptotagmin XIV	NM_153262	CACAGACATCCCAACATATAA
LRRC59	leucine rich repeat containing 59	NM_018509	CCGCGACAAGCTGGACGGCA A
LRRC59	leucine rich repeat containing 59	NM_018509	CTAGAACACCACGCTCAGTAA
RAP1A	RAP1A, member of RAS oncogene family	NM_001010935 NM_002884	CAGGGCCAGAATTTAGCAAG A
VIM	vimentin	NM_003380	CTGGCACGTCTTGACCTTGAA
PEX5	peroxisomal biogenesis factor 5	NM_000319	CCAGTTCACAAGACCAGTAAA
PEX5	peroxisomal biogenesis factor 5	NM_000319	ACCGATCGCTGGTATGATGAA
DNAJC13	DnaJ (Hsp40) homolog, subfamily C, member 13	NM_015268 NM_173823	TAGGTTGATTCTCTTCCTTAA
ACTN1	actinin, alpha 1	NM_001102	CCGGCCCGAGCTGATTGACTA
PLXNA3	plexin A3	NM_017514	CTGCCTATTTATTGAATCGAA
WIPF1	WAS/WASL interacting protein family, member 1	NM_001077269 NM_003387	CACGGCCAACAGGGATAATG A
SPIRE1	spire homolog 1 (Drosophila)	NM_020148	TACGAGAATCAGTCTAACAGA
OTOG	otogelin	XM_291816 XM_941002	CTGTGGGAACTTTGACTTAAA
OTOG	otogelin	XM_291816 XM_941002	CAGGAAATTTATTTCCATCAA
HRAS	v-Ha-ras Harvey rat sarcoma viral oncogene homolog	NM_005343 NM_176795	CCGGAAGCAGGTGGTCATTGA
KRAS	v-Ki-ras2 Kirsten rat sarcoma viral oncogene homolog	NM_004985 NM_033360	AAGGAGAATTTAATAAAGAT A
KRAS	v-Ki-ras2 Kirsten rat sarcoma viral oncogene	NM_004985 NM_033360	GACGATACAGCTAATTCAGAA

	homolog		
KRAS	v-Ki-ras2 Kirsten rat sarcoma viral oncogene homolog	NM_004985 NM_033360	GTGGACGAATATGATCCAACA
ATRNL1	attractin-like 1	NM_207303	CAGGGTGACAAGATATGTATA
ATRNL1	attractin-like 1	NM_207303	CAGCTTTCCGCCTAACTAGAA
LOC729144	hypothetical protein LOC729144	XM_001129457	AGGCAAGGAGGAGGAAATCCA
LOC729144	hypothetical protein LOC729144	XM_001129457	CTCGAGGGACTTTCTGCGCCA
C7orf51	chromosome 7 open reading frame 51	NM_173564	CAGGGTATTTATTTAAATTAA
C7orf51	chromosome 7 open reading frame 51	NM_173564	CTGCGTGTGCAAGGAGATCAA
CPNE6	copine VI (neuronal)	NM_006032	CCCTTTCATGGAAATCTATAA
CPNE6	copine VI (neuronal)	NM_006032	CCGAGGAGGTATCAGGCACAA
DNAJC13	DnaJ (Hsp40) homolog, subfamily C, member 13	NM_015268 NM_173823	CACGAGAAGAACTGAAAGATA
BAIAP2	BAI1-associated protein 2	NM_006340 NM_017450 NM_017451	CAGCAAGAATCCTCAGAAGTA
BAIAP2	BAI1-associated protein 2	NM_006340 NM_017450 NM_017451	CACGGGCAACCTCCTGGACAA
WIPF1	WAS/WASL interacting protein family, member 1	NM_001077269 NM_003387	CAGTATGTTATTCATGTATTA
SLC9A3R2	solute carrier family 9 (sodium/hydrogen exchanger), member 3 regulator 2	NM_004785	CGCGCTCTAAATAATTGCAAT
SLC9A3R2	solute carrier family 9 (sodium/hydroge	NM_004785	TCGAGCCATGCGAGTCAACAA

	n exchanger), member 3 regulator 2		

The proteins above were identified via the protocol shown in Appendix 3. The siRNA sequences are given that were used to screen for functional effects in B2AR trafficking. This list has been culled of proteins that showed up in control purification and those that are obvious contaminant proteins.

Appendix 5: siRNA screen of sorting nexins on B2AR trafficking

A siRNA against the following sorting nexins had a consistent effect on B2AR trafficking over 2 replicates. Experiments were done via the M1 feeding method (Temkin et al., 2011). No controls were done for effects on trafficking of other GPCR or Transferrin Receptor. The qiagen ordering number for the siRNA that showed an effect is given in parentheses. Data is not shown as it is not significant.

Decreased Internalization

SNX6 (SI02644698)

SNX9 (SI02777656)

SNX11 (SI00728658)

SNX15 (SI00728742)

SNX17 (SI00107877)

Decreased Recycling

SNX5 (SI00729015, SI00729029)

SNX10 (SI03229779)

SNX13 (SI00109655)

SNX19 (SI00728791)

SNX25 (SI00728910)

SNX27 (SI00728959, SI00728966)

Increased Internalization and Recycling

SNX24 (SI00728875, SI00728882)

Appendix 6: List of Mass spectrometry hits from SNX27 purification

UniPROT Description	comPASS	MiST	EntrezID	Gene Symbol
FA21C_HUMAN Protein FAM21C	116.601	0.6368	253725	FAM21C
GIT1_HUMAN ARF GTPase-activating protein GIT1	63.4792	0.4096	28964	GIT1
MAP4_HUMAN Microtubule-associated protein 4	60.8708	0.7398	4134	MAP4
CCD53_HUMAN Coiled-coil domain-containing protein 53	39.3901	0.9291	51019	CCDC53
CYBP_HUMAN Calcyclin-binding protein	35.6256	0.6984	27101	CACYBP
SNX27_HUMAN Sorting nexin-27	29.9841	0.6601	81609	SNX27
FA39B_HUMAN Protein FAM39B	25.5658	0.9171		
ZO2_HUMAN Tight junction protein ZO-2	20.382	0.8115	9414	TJP2
BRCC3_HUMAN BRCA1/BRCA2-containing complex subunit 3	9.3493	0.6662	79184	BRCC3
K1033_HUMAN Uncharacterized protein KIAA1033	8.1904	0.6496	23325	KIAA1033
STRUM_HUMAN Strumpellin	7.8496	0.6131	9897	
CAZA1_HUMAN F-actin-capping protein subunit alpha-1	5.8572	0.5104	829	CAPZA1
CS062_HUMAN Uncharacterized protein C19orf62	5.4417	0.4548	29086	BABAM1
K0157_HUMAN Uncharacterized protein KIAA0157	4.8139	0.5214	23172	FAM175B
BRE_HUMAN Protein BRE	4.4652	0.6175	9577	BRE
ARHG7_HUMAN Rho guanine nucleotide exchange factor 7	3.5769	0.3686	8874	ARHGEF7
CAPZB_HUMAN F-actin-capping protein subunit beta	0.9326	0.4069	832	CAPZB
GIT2_HUMAN ARF GTPase-activating protein GIT2	0.7623	0.5506	9815	GIT2
CAZA2_HUMAN F-actin-capping protein subunit alpha-2	0.6733	0.8147	830	CAPZA2
VIME_HUMAN Vimentin	0.5547	0.4284	7431	VIM
AAAT_HUMAN Neutral amino acid transporter B(0)	0.3173	0.2797	6510	SLC1A5
ACLY_HUMAN ATP-citrate synthase	0.25	0.4944	47	ACLY

CRCM_HUMAN Colorectal mutant cancer protein	0.2452	0.3217	4163	MCC
BASI_HUMAN Basigin precursor	0.1538	0.2632	682	BSG
S4A7_HUMAN Sodium bicarbonate cotransporter 3	0.138	0.2038	9497	SLC4A7
MOT1_HUMAN Monocarboxylate transporter 1	0.1226	0.215	6566	SLC16A1
RLA1_HUMAN 60S acidic ribosomal protein P1	0.0925	0.313	6176	RPLP1
RL12_HUMAN 60S ribosomal protein L12	0.0634	0.3008	6136	RPL12
RL7A_HUMAN 60S ribosomal protein L7a	0.0563	0.3204	6130	RPL7A
CRIPT_HUMAN Cysteine-rich PDZ-binding protein	0.0496	0	9419	CRIPT
RL10A_HUMAN 60S ribosomal protein L10a	0.0472	0.2519	4736	RPL10A
RL14_HUMAN 60S ribosomal protein L14	0.0462	0.3062	9045	RPL14
RS15A_HUMAN 40S ribosomal protein S15a	0.0454	0.2434	6210	RPS15A

FLAG-SNX27 was purified as described and copurifying proteins were identified by mass spectrometry (Temkin et al., 2011) (N=4). It was then ranked by the comPASS score (Sowa et al., 2009). MiST score, a new unpublished scoring system by the Krogan lab is also given .

Appendix 7: siRNA screen of SNX27 interactors on B2AR trafficking

Qiagen siRNA	Average Recycling	Standard Deviation
Hs_FAM21C_10	0.64783767	0.02897
Hs_FAM21C_11	0.578303897	0.009825
Hs_FAM21C_12	0.602816841	0.045849
Hs_KIAA1033_5	0.590638741	0.042789
Hs_KIAA1033_6	0.617940775	0.030811
Hs_KIAA1033_7	0.580316276	0.046254
Hs_GIT1_5	0.705373087	0.032632
Hs_GIT1_6	0.647659465	0.03637
Hs_CRIPT_6	0.666590662	0.034335
Hs_CRIPT_7	0.468334668	0.06498
Hs_CRIPT_8	0.55398875	0.037879
Hs_GIT2_5	0.488216946	0.080748
Hs_GIT2_6	0.576083586	0.131411
Hs_MAP4_10	0.613244795	0.06165
Hs_MAP4_11	0.615447811	0.047473
Hs_MAP4_12	0.42049103	0.133862
Hs_BRCC3_1	0.675877263	0.023263
Hs_CXorf53_1	0.663089208	0.025016
Hs_CXorf53_2	0.546306748	0.068621
Hs_KIAA0196_5	0.611868161	0.05252
Hs_KIAA0196_6	0.570056286	0.069128
Hs_KIAA0196_7	0.522698329	0.095318
Hs_KIAA0157_5	0.60167152	0.075023
Hs_KIAA0157_6	0.604464106	0.080416
Hs_KIAA0157_7	0.638703047	0.065869
Hs_TJP2_5	0.601276666	0.041262
Hs_TJP2_6	0.527009136	0.094829
AllStars Negative Control siRNA	0.633094381	0.066929
Hs_MGC52000_3	0.600809475	0.090485
Hs_WASH2P_2	0.626963043	0.07881
Hs_WASH2P_5	0.589380318	0.07626
Hs_CACYBP_4	0.520737998	0.118226
Hs_CACYBP_5	0.588679279	0.127606
Hs_CACYBP_7	0.637695817	0.042186
Hs_DLC1_10	0.589453845	0.055116
Hs_DLC1_11	0.537675382	0.076042

Hs_DLC1_12	0.627112881	0.064918
Hs_CCDC53_2	0.611941036	0.060597
Hs_CCDC53_3	0.572101227	0.072551
Hs_CCDC53_4	0.471530835	0.05417
Hs_FAM21C_9	0.487124356	0.085086
Hs_WASH2P_7	0.596980527	0.059561
Hs_SNX27_7	0.306746722	0.108138
Hs_SNX27_8	0.238141725	0.124008
Hs_VPS35_7	0.081531501	0.147622
Hs_VPS35_8	0.279602338	0.14061
Hs_ARF6_5	0.672432226	0.022544
Hs_ARF6_10	0.558886694	0.073083
Control	0.635040095	0.045988
VPS35-5	0.148005045	0.164568

Qiagen siRNA were transfected at 10 pmol siRNA per well (12 well) according to Lipofectamine RNAiMAX protocol and screened at day 3 for recycling defects by the M1 feeding method (with 25 minutes internalization and 30 minutes recycling) (Temkin et al., 2011).

Appendix References

Cottrell, G.S., B.E. Padilla, S. Amadesi, D.P. Poole, J.E. Murphy, M. Hardt, D. Roosterman, M. Steinhoff, and N.W. Bunnett. 2009. Endosomal endothelin-converting enzyme-1: a regulator of beta-arrestin-dependent ERK signaling. J Biol Chem 284:22411-25.

Li, H.S., D.B. Stolz, and G. Romero. 2005. Characterization of endocytic vesicles using magnetic microbeads coated with signalling ligands. Traffic 6:324-34.

Sowa, M.E., E.J. Bennett, S.P. Gygi, and J.W. Harper. 2009. Defining the human deubiquitinating enzyme interaction landscape. Cell 138:389-403.

Temkin, P., B. Lauffer, S. Jager, P. Cimermancic, N.J. Krogan, and M. von Zastrow. 2011. SNX27 mediates retromer tubule entry and endosome-to-plasma membrane trafficking of signalling receptors. Nat Cell Biol 13:715-21.

Publishing Agreement

It is the policy of the University to encourage the distribution of all theses, dissertations, and manuscripts. Copies of all UCSF theses, dissertations, and manuscripts will be routed to the library via the Graduate Division. The library will make all theses, dissertations, and manuscripts accessible to the public and will preserve these to the best of their abilities, in perpetuity.

I hereby grant permission to the Graduate Division of the University of California, San Francisco to release copies of my thesis, dissertation, or manuscript to the Campus Library to provide access and preservation, in whole or in part, in perpetuity.

8/24/2011

Author Signature Date